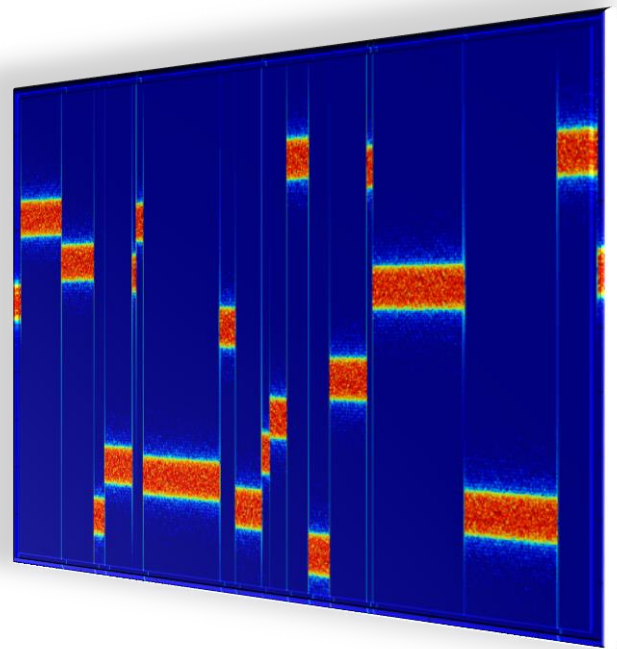




**José Pedro Mateiro  
Matias Borrego**

**Impacto do Comportamento Transitório de Sistemas  
de Radiocomunicações na Gestão do Espectro**

**Impact of the Transient Behavior of Radio  
Communication Systems on Spectrum Management**







**José Pedro Mateiro  
Matias Borrego**

**Impacto do Comportamento Transitório de Sistemas  
de Radiocomunicações na Gestão do Espectro**

**Impact of the Transient Behavior of Radio  
Communication Systems on Spectrum Management**

Tese apresentada à Universidade de Aveiro para cumprimento dos requisitos necessários à obtenção do grau de Doutor em Engenharia Eletrotécnica, realizada sob a orientação científica do **Professor Doutor Nuno Miguel Gonçalves Borges de Carvalho**, *Professor Catedrático* do Departamento de Eletrónica, Telecomunicações e Informática da Universidade de Aveiro e do **Professor Doutor José Manuel Neto Vieira**, *Professor Auxiliar* do Departamento de Eletrónica, Telecomunicações e Informática da Universidade de Aveiro.

Apoio financeiro da  
*ANACOM*  
*Autoridade Nacional de Comunicações*



*“Even the hardest problem has a solution.  
Complexity is no more than a summation of many simple things.”*

PAGE INTENTIONALLY LEFT BLANK

## **o júri / the jury**

presidente / president

### **Prof. Doutor Fernando Manuel dos Santos Ramos**

Professor Catedrático da Universidade de Aveiro, por delegação do Reitor da Universidade de Aveiro

vogais / examiners committee

### **Prof. Doutor Nuno Miguel Gonçalves Borges de Carvalho**

Professor Catedrático da Universidade de Aveiro (Orientador)

### **Prof. Doutor Roberto Gómez-García**

Professor Associado (Titular) da Universidade de Alcalá de Henares, Espanha

### **Prof. Doutor António José Castelo Branco Rodrigues**

Professor Auxiliar do Instituto Superior Técnico da Universidade de Lisboa

### **Prof. Doutor Sérgio Reis Cunha**

Professor Auxiliar da Faculdade de Engenharia da Universidade do Porto

### **Prof. Doutor Arnaldo Silva Rodrigues de Oliveira**

Professor Auxiliar da Universidade de Aveiro

PAGE INTENTIONALLY LEFT BLANK



## **agradecimentos / acknowledgements**

Gostaria de expressar os meus agradecimentos a todos aqueles que, de uma forma ou de outra, contribuíram para que esta Tese de Doutoramento possa ser hoje uma realidade.

Ao Prof. Doutor Nuno Borges de Carvalho, meu Orientador, que foi quem, pela primeira vez, me lançou o desafio de embarcar nesta enorme “aventura”, fazendo-me acreditar, desde esse instante, que este empreendimento estaria ao meu alcance. Não posso deixar de assinalar a genialidade dos seus “rasgos de criatividade” científica – *essência de um verdadeiro Engenheiro* – que, em vastas e estimulantes discussões, na mais nobre aceção da palavra, inspiraram, moldaram e ajudaram a conceber muitas das análises, abordagens e soluções propostas nesta Tese.

Ao Prof. Doutor José Neto Vieira, meu Co-Orientador, pela disponibilidade e pelo rigor nos detalhes que, tenho a certeza, fazem toda a diferença. A ele devo a forma clara e eficaz com que me ajudou a ver, pelo prisma da simplicidade, conceitos fundamentais de Processamento de Sinal, sem nunca descurar a exatidão concetual que se impunha.

Ao Eng. Sérgio Antunes, quero prestar um justo agradecimento, pelo inexcusável apoio na programação em *Labview* – área em que é exímio especialista –, e que se traduziu no incansável esforço que imprimiu na resolução de tantos e complexos problemas com que nos deparámos. Sem o seu empenho e colaboração, importantes análises e resultados fundamentais, que agora são apresentados, não teriam sido possíveis.

Ao Prof. Doutor Roberto Gómez-García, por ter aceitado o desafio de desenvolver de raiz uma solução de engenharia inovadora – filtro rejeita-banda, em circuito impresso – que pudesse dar resposta a um problema real de interferência, e que foi testado na prática, no âmbito desta Tese, com o sucesso almejado. O seu contributo foi também fundamental, sendo de louvar a sua enorme dedicação, que possibilitou uma frutuosa cooperação e um verdadeiro trabalho de equipa.

À ANACOM – Autoridade Nacional de Comunicações, quero deixar um justo reconhecimento, de apreço e gratidão, por ter acreditado no meu potencial e investido no desenvolvimento das minhas competências pessoais, criando as condições necessárias para que este desiderato pudesse um dia concretizar-se.

A todos os colegas e amigos, pela experiência e profissionalismo, demonstrados no dia a dia, e que muito contribuíram para enriquecer o trabalho aqui apresentado.

E, de uma forma muito especial, aos meus pais, irmã, e a toda a minha família.

É a todos vós que dedico esta minha Tese!

*José Pedro Borrego*

PAGE INTENTIONALLY LEFT BLANK

**palavras-chave**

Dividendo Digital, Neutralidade Tecnológica, Gestão do Espectro, Utilização Flexível do Espectro, Rádios Cognitivos, Distorção Não Linear, Regimes Transitórios, Análise Tempo-Frequência: Instrumentação e Medições, Interferência, Máscara Delimitadora de Bloco (Block Edge Mask).

**resumo**

Esta Tese de Doutorado insere-se nos domínios da engenharia do espectro e da gestão do espectro radioelétrico, e pretende abordar problemas atuais e concretos com que os reguladores se deparam. Em particular, a definição de condições técnicas a serem cumpridas pelos sistemas rádio que irão operar em determinadas faixas de frequências, selecionadas para a introdução de abordagens de gestão do espectro mais flexíveis e tecnologicamente neutras. O modelo de Máscara Delimitadora de Bloco (Block Edge Mask) foi adotado, a nível europeu, como estratégia de definição de condições técnicas de operação, nessas faixas. Contudo, este modelo, que recorre a restrições que são apenas estabelecidas no domínio da frequência, não entra em linha de conta com comportamentos transitórios ou com a variabilidade temporal de sinais inerentes aos sistemas de radiocomunicações atuais. Para além disso, a medição e validação de parâmetros técnicos associados a estes modelos, conforme definidas nas recomendações internacionais aplicáveis, levantam problemas práticos que importa escarpelizar. Nesse sentido, são exploradas, nesta tese, técnicas alternativas de processamento de sinal no domínio misto tempo-frequência, tendo em vista a sua utilização na avaliação de conformidade dos sistemas rádio em face das restrições aplicáveis.

PAGE INTENTIONALLY LEFT BLANK

**keywords**

Digital Dividend, Technological Neutrality, Spectrum Management, Spectrum Usage Flexibility, Cognitive Radio, Nonlinear Distortion, Transient Waveforms, Time-Frequency Analysis and Measurement Instrumentation, Interference, Block Edge Mask.

**abstract**

This PhD Thesis falls within the domain of spectrum engineering and spectrum management, and intends to address current and concrete problems, with which, regulators have to deal. Particularly, the definition of technical conditions to be met by radio systems, which will operate in specific bands, selected to introduce novel concepts such as flexibility and technological neutrality. The Block Edge Mask approach was adopted to define technical conditions of operation, in those bands. However, this model, based on spectral masks, which are defined in the frequency domain, do not take into account the transient behavior or time-varying characteristics of signals used by emerging radio communication systems. Furthermore, measurement methodologies developed for validation of technical parameters associated to these models, which are recommended by international bodies, potentially lead to practical issues that must be scrutinized. Thus, alternative time-frequency mixed domain signal processing techniques are explored, in this thesis, to be used for assessing the compliance of radio systems operating under such constraints.

PAGE INTENTIONALLY LEFT BLANK

# Table of Contents

<b>Table of Contents</b> .....	<b>i</b>
<b>List of Figures</b> .....	<b>v</b>
<b>List of Tables</b> .....	<b>ix</b>
<b>List of Acronyms</b> .....	<b>xi</b>
<b>1 Introduction</b> .....	<b>1</b>
1.1 Overview .....	1
1.2 Motivation.....	3
1.3 Objective.....	5
1.4 Thesis Outline .....	6
1.5 Original Contributions .....	8
<b>2 Spectrum Management: The European Regulatory Context</b> ..	<b>9</b>
2.1 Introduction .....	9
2.1.1 The European Spectrum Policy Framework, Coordination and Harmonization.....	13
2.1.1.1 The Radio Spectrum Policy Programme.....	14
2.1.1.2 The European Radio Spectrum Bodies .....	17
2.2 The Digital Dividend.....	20
2.3 New Trends in Spectrum Management in Europe: Innovative Models and Methodologies .....	22
2.3.1 Flexibility.....	23
2.3.2 WAPECS .....	25
2.3.2.1 Neutrality.....	26
2.3.2.2 Methodological Framework .....	28
2.3.3 Shared Use Models .....	40
2.3.3.1 Collective Use of Spectrum (CUS).....	41
2.3.3.2 Licensed Shared Access (LSA) .....	42
2.3.4 Dynamic Spectrum Management .....	42
2.3.4.1 White Space.....	43
2.3.4.2 Software-Defined Radio .....	43
2.3.4.3 Cognitive Radio.....	43
2.3.4.4 Likely Business Models .....	47

<b>3</b>	<b>Block Edge Mask Approach .....</b>	<b>51</b>
3.1	Concept and Definition.....	52
3.1.1	Technical Specifications (LTE 800 MHz band).....	53
3.1.1.1	Fundamentals for the Derivation of a Block Edge Mask .....	54
3.2	Drawbacks of the Block Edge Mask Approach .....	62
3.3	Practical Issues: How to Validate a Block Edge Mask.....	69
3.3.1	ECC/CEPT Block Edge Mask Measurement Methodology .....	70
3.3.1.1	EIRP Calculation for the Determination of the Applicable BEM .....	72
3.3.1.2	Measurement Prerequisites.....	76
3.3.1.3	Measurement Methods for the Assessment of BEM compliance .....	77
3.3.1.4	Major Impairments of the ECC/CEPT Methodology .....	85
<b>4</b>	<b>Interference Scenarios in the Presence of Neutral Systems .87</b>	
4.1	Case-Study 1: DVB-T reception harmed by a LTE BS emission.....	88
4.1.1	Scenario of Analysis .....	88
4.1.1.1	DVB-T Systems: Victim .....	90
4.1.2	Nonlinear Impairments .....	95
4.1.3	Innovative Band-stop Filter for LTE interference Mitigation on the DVB-T Reception .....	96
4.1.3.1	Theoretical Principles of the Proposed Band-stop Filter.....	97
4.1.3.2	Experimental Results.....	99
4.1.3.3	Comparative Analysis of Performance.....	103
4.1.4	Mitigation of the Interference on DVB-T Reception due to LTE in Portugal.....	106
4.1.5	Summary .....	111
4.2	Case-Study 2: The “Doughnut” Effect .....	112
4.2.1	Scenario of Analysis .....	112
4.2.2	Interference Analysis.....	115
4.2.3	“Doughnut” Effect Reproduction .....	119
4.2.3.1	Simulation.....	119
4.2.3.2	Laboratorial Tests.....	120
4.2.4	Summary .....	122
<b>5</b>	<b>Time-Frequency Mixed Domain Signal Processing Tools....</b>	<b>123</b>
5.1	Fourier Transform and Spectrum .....	124
5.1.1	The same Spectrum does not always represent the same Signal .....	126
5.1.1.1	Two Signals formed by two half-length “mirrored” Sinusoids of different Frequencies.....	126
5.1.1.2	Possible Transient Effects.....	128
5.1.2	The same Spectrum does not always “produce” the same Interference.....	132
5.1.2.1	Continuous and Switched Transmission of a 256-QAM Signal .....	133
5.1.2.2	Multi-sine Signal Analysis.....	137
5.2	Time-Frequency Mixed Domain Analysis.....	147
5.2.1	Windowed Fourier Transforms.....	151
5.2.1.1	Gabor Transform.....	152
5.2.1.2	Short-Time Fourier Transform .....	157
5.2.2	Quadratic Time-Frequency Transforms.....	164
5.2.2.1	Spectrogram .....	164
5.2.2.2	Wigner-Ville Transform .....	168



<b>6</b>	<b>Test and Validation of Transient Waveforms.....</b>	<b>173</b>
6.1	Overview of the Proposed Approach .....	174
6.2	Signal Acquisition .....	174
6.2.1	General Setup .....	175
6.2.1.1	The Real Time Spectrum Analyzer.....	176
6.3	Data Processing using the Waveform Validation Tool .....	182
6.3.1	General Configuration.....	182
6.3.2	Block Edge Mask Generation.....	185
6.3.2.1	STFT and Gabor Transform BEM .....	186
6.3.2.2	Generation of a Wigner-Ville BEM Equivalent.....	187
6.3.3	Output Results.....	189
6.4	Sensitivity Analysis.....	194
6.4.1	Assumptions.....	194
6.4.2	Test Signals.....	195
6.4.3	Results.....	197
6.4.3.1	Sensitivity to the STFT Window.....	197
6.4.3.2	Sensitivity to the Transform.....	204
6.4.3.3	Sensitivity of the STFT and Gabor Transform to the Window Length.....	207
6.4.3.4	Sensitivity of the STFT and Gabor Transform to the Frequency Bins .....	209
6.4.3.5	Sensitivity of the WVD to the Frequency Bins.....	211
6.4.4	Summary.....	212
<b>7</b>	<b>Conclusions.....</b>	<b>215</b>
	<b>Bibliography .....</b>	<b>221</b>
	<b>Appendices .....</b>	<b>237</b>
	Appendix A: Smoothing Windows implemented in the Software Tool and available in Labview .....	237
	Appendix B: Transient Waveform Validation, Sensitivity Analysis – Complete Results ...	243
	STFT Multiple Windows.....	243
	Frequency Bins: 32, Variable Window Length .....	243
	Frequency Bins: 64, Variable Window Length .....	245
	Frequency Bins: 128, Variable Window Length .....	246
	Frequency Bins: 256, Variable Window Length .....	247
	Frequency Bins: 512, Variable Window Length .....	248
	Frequency Bins: 1024, Variable Window Length.....	249
	Frequency Bins: 2048, Variable Window Length.....	250
	STFT Window Length: 32 samples, Variable Frequency Bins .....	251
	STFT Window Length: 64 samples, Variable Frequency Bins .....	252
	STFT Window Length: 128 samples, Variable Frequency Bins .....	253
	STFT Window Length: 256 samples, Variable Frequency Bins .....	254
	STFT Window Length: 512 samples, Variable Frequency Bins .....	255
	STFT Window Length: 1024 samples, Variable Frequency Bins .....	256
	STFT Window Length: 2048 samples, Variable Frequency Bins .....	257



# List of Figures

Fig. 1.1. Time-Frequency Representation of a Time-Varying Signal.....	2
Fig. 2.1. Spectrum Allocation in Portugal.....	11
Fig. 2.2. Radio Spectrum Policy Bodies Organogram.....	19
Fig. 2.3. UHF (800-MHz band) plan before and after the analogue TV switch off.....	21
Fig. 2.4. Illustrated Concept of WAPECS.....	24
Fig. 2.5. WAPECS Bands.....	25
Fig. 2.6. Fixed reception scenario (location may be known or unknown).....	31
Fig. 2.7. Mobile receiving scenario (unknown location).....	32
Fig. 2.8. Mobile indoor coverage scenario (provided by outdoor or indoor BS).....	32
Fig. 2.9. Radio networks <b>incompatible</b> with WAPECS (Point-to-Point and Mesh Networks).....	32
Fig. 2.10. Flowchart: General Approach applicable to the WAPECS bands.....	39
Fig. 3.1. Portuguese spectrum allocation for DTT and LTE 800 MHz band.....	52
Fig. 3.2. Illustration of the Block Edge Mask concept.....	53
Fig. 3.3. BEM for a LTE BS emission with BW: 10 MHz and In-Block EIRP: 59 dBm/10MHz.....	57
Fig. 3.4. BEMs for LTE BS emissions with BW: 10 MHz, for different In-Block EIRP's.....	58
Fig. 3.5. Full BEM for a LTE BS emission (center frequency: 806 MHz, BW: 10 MHz, In-Block EIRP: 59 dBm/10MHz).....	61
Fig. 3.6. Full Relative BEM for a LTE BS emission (BW: 10 MHz, In-Block EIRP: 59 dBm/10MHz).....	61
Fig. 3.7. Block Edge Mask and Spectrum Emission Mask for LTE FDD downlink.....	62
Fig. 3.8. Time-Frequency Analysis of a Cognitive Radio Operation.....	64
Fig. 3.9. Traditional Spectrum Analysis of the same Cognitive Radio Operation.....	65
Fig. 3.10. Field Measurement Setup to Acquire LTE Waveforms.....	67
Fig. 3.11. BEM Compliance of LTE BS Idle and Heavy Traffic Modes Emission Spectra.....	68
Fig. 3.12. CCDF of LTE BS Idle and Heavy Traffic Modes Emissions.....	68
Fig. 3.13. Flowchart for the selection of an appropriate BEM measurement approach.....	71
Fig. 3.14. Resource Block structure in a LTE downlink signal.....	72
Fig. 3.15. EIRP estimation (possible radiated measurement scenario).....	74
Fig. 3.16. LTE BS diagram.....	75
Fig. 3.17. Setup for Radiated Measurement under Normal Operating Conditions.....	77
Fig. 3.18. LTE BS Spectrum to be measured and the Notch Filter frequency response (transmission).....	80
Fig. 3.19. LTE BS Spectrum iteratively measured after the Notch Filter.....	81
Fig. 3.20. LTE BS Spectrum: measured after the Notch Filter and reconstructed compared to the BEM limits (EIRP: 59 dBm/10MHz).....	82
Fig. 3.21. Setup for Conducted Measurement under Normal Operating Conditions.....	83
Fig. 4.1. Spectrum and spectrogram of a LTE FDD downlink (800 MHz band) signal as potential interferer to the DVB-T reception.....	89
Fig. 4.2. DPX Spectrum of a LTE FDD downlink (800 MHz band) signal.....	89
Fig. 4.3. Simplified block diagram of a DVB-T receiver.....	90
Fig. 4.4. Simplified block diagram of the tuner of a DVB-T receiver.....	92
Fig. 4.5. Typical scenario of DVB-T reception affected by the proximity of a LTE BS.....	92
Fig. 4.6. Points of the DVB-T reception chain, where the MER and the BER are taken out.....	95

Fig. 4.7. Detail of the proposed band-stop transversal signal-interaction filter. ....	98
Fig. 4.8. Power transmission ( $ S_{21} $ ) and reflection ( $ S_{11} $ ) responses of the ideal synthesized band-stop filter for a broadband spectral range and the detail (inset) of the transition between the low-pass type transmission band and the stopband .....	100
Fig. 4.9. Layout of the manufactured micro-strip band-stop filter prototype (non-redundant dimensions, in mm, are indicated) .....	101
Fig. 4.10. Photo of the manufactured micro-strip band-stop filter prototype.....	101
Fig. 4.11. Simulated and measured power transmission ( $ S_{21} $ ), reflection ( $ S_{11} $ ) responses of the manufactured micro-strip band-stop filter prototype. ....	102
Fig. 4.12. Simulated and measured group-delay responses of the manufactured micro-strip band-stop filter prototype.....	103
Fig. 4.13. Comparison of the measured power transmission ( $ S_{21} $ ) responses of the manufactured micro-strip band-stop filter prototype and two commercial filter samples (filters 1 and 2). ....	104
Fig. 4.14. Comparison of the measured reflection ( $ S_{11} $ ) responses of the manufactured micro-strip band-stop filter prototype and two commercial filter samples (filters 1 and 2). ....	104
Fig. 4.15. Block Diagram: Setup to emulate the DVB-T (channel 56) reception scenario with LTE interference for filter evaluation. ....	105
Fig. 4.16. Photo: Setup to emulate the DVB-T (channel 56) reception scenario with LTE interference for filter evaluation. ....	105
Fig. 4.17. LTE BS and surrounding environment (very close to DTT aeriels). ....	107
Fig. 4.18. Relative positions of the receiver, the LTE BS and the DTT best-server transmitter.....	108
Fig. 4.19. Relative positions of the DVB-T receiver (point of analysis) and the LTE BS. ....	108
Fig. 4.20. Spectra of the DVB-T and LTE signals before filtering.....	109
Fig. 4.21. DVB-T constellation diagram with no filter before the RF front-end of the test receiver. ....	110
Fig. 4.22. Spectra the DVB-T and LTE signals after filtering. ....	110
Fig. 4.23. DVB-T constellation diagram after inserting the band-stop filter before the RF front-end of the test receiver to reject the LTE signal. ....	111
Fig. 4.24. The interferer: a damaged TV amplifier. ....	113
Fig. 4.25. The interferer tri-axial Yagi-Uda aerial.....	114
Fig. 4.26. Undesired interference-affected operation scenario. ....	114
Fig. 4.27. Conceptual block diagram of the interference scenario. ....	116
Fig. 4.28. The “doughnut” effect as a result of a rotating phasor centered at each constellation symbol. ....	119
Fig. 4.29. Simplified block diagram of the simulation process. ....	120
Fig. 4.30. Output of the simulation: “doughnut” effect on the constellation diagram.....	120
Fig. 4.31. Laboratory measurement setup used to reproduce the “doughnut” effect. ....	121
Fig. 4.32. Spectra of the QPSK and CW signals used to reproduce the “doughnut” effect. ....	121
Fig. 4.33. Constellation diagram resulting from the experimental tests to demonstrate the “doughnut” effect generation. ....	122
Fig. 5.1. Time-domain and frequency-domain independent representations of the signals $r(t)$ and $s(t)$ . ....	127
Fig. 5.2. Time-domain and time-frequency mixed domain (spectrogram) representations of the signals $r(t)$ and $s(t)$ . ....	128
Fig. 5.3. Time-domain and frequency-domain representations of $c_{orig}(t)$ and $c_{corr}(t)$ . ....	129
Fig. 5.4. Time-frequency mixed domain (spectrogram) representations of the signals $c_{orig}(t)$ and $c_{corr}(t)$ . ....	130
Fig. 5.5. Time-domain and frequency-domain representations of the original QPSK signal without any interruption and the same signal abruptly interrupted in the middle.....	131
Fig. 5.6. Time-frequency mixed domain analysis (spectrogram) of the original QPSK signal without any interruption and of the same signal abruptly interrupted in the middle.....	132
Fig. 5.7. Spectra of the Continuous and Switched 256-QAM Input Signals. ....	133
Fig. 5.8. Block diagram: nonlinearity and input and output signals’ spectra. ....	134
Fig. 5.9. Spectra of the Continuous and Switched 256-QAM Output Signals, after traversing the nonlinearity. ....	134
Fig. 5.10. Statistical behavior of the 256-QAM Input Signals (Continuous and Switched).....	135

Fig. 5.11. CCDF of the 256-QAM Input Signals (Continuous and Switched).	136
Fig. 5.12. Spectrograms of the 256-QAM Input/Output Signals (Continuous and Switched).	137
Fig. 5.13. Time waveform and Spectrum of the generated Multi-Sine Signal with Random Phases.	138
Fig. 5.14. Time waveforms and Spectra of the generated Multi-Sine Signals (Random and Constant Phases).	139
Fig. 5.15. CCDFs of the generated Multi-Sine Signals (Random and Constant Phases).	140
Fig. 5.16. Spectra of the Multi-Sine (Random and Constant Phases) Input and Output Signals.	140
Fig. 5.17. Spectra of the Multi-Sine (Random and Constant Phases) Output Signals.	141
Fig. 5.18. Spectrograms of the Multi-Sine (Random and Constant Phases) Input and Output Signals.	142
Fig. 5.19. Spectrum of the Multi-Sine and Single Tones Input Signal.	143
Fig. 5.20. Spectrogram of the Multi-Sine and Single Tones Input Signal Evolution.	144
Fig. 5.21. 3D Spectrogram of the Multi-Sine and Single Tones Input Signal Evolution.	144
Fig. 5.22. Spectrum of the Multi-Sine and Single Tones Output Signal.	145
Fig. 5.23. 3D Spectrogram of the Multi-Sine and Single Tones Output Signal Evolution.	145
Fig. 5.24. 2D Spectrogram of the Multi-Sine and Single Tones Output Signal Evolution.	146
Fig. 5.25. Linear Chirp Signal representations: Time Domain Waveform, Frequency Domain Spectrum, Instantaneous Frequency and Time-Frequency Mixed Domain Spectrogram.	149
Fig. 5.26. Gaussian Signals with several means and standard deviations.	152
Fig. 5.27. Conceptual diagram of logons over a time-frequency plane, underlying the Gabor Transform.	154
Fig. 5.28. Time-Frequency resolution as a consequence of the windows dimensions ( $t$ - $\omega$ ).	154
Fig. 5.29. Time and Frequency domains Representations of a Gaussian Window.	155
Fig. 5.30. Conceptual illustration of the Gabor Transform.	156
Fig. 5.31. Signal localization in the $t$ - $\omega$ plane.	162
Fig. 5.32. Resolution Issues: the Uncertainty Principle. Spectrograms with distinct Window Widths.	166
Fig. 5.33. Resolution Issues: the Uncertainty Problem. Trade-off between Time and Frequency Resolutions.	166
Fig. 5.34. Impact of the Type of Window on the Final Spectrogram of the Chirp Signal.	167
Fig. 5.35. Wigner-ville Time-Frequency Representations of the Chirp Signal.	169
Fig. 5.36. Cross-Term Interference of WVD of the signal $s(t)$ .	170
Fig. 5.37. Cross-Terms Interference of WVD of a Gaussian Amplitude Modulation Signal.	171
Fig. 6.1. Radiated Measurement Setup to Acquire LTE Waveforms.	175
Fig. 6.2. Conducted Measurement Setup to Acquire LTE Waveforms.	176
Fig. 6.3. Sequential Spectrum Captures and Analysis implemented by Traditional Spectrum Analyzers.	177
Fig. 6.4. Signal Capture using multiple consecutive and overlapped FFT windows.	178
Fig. 6.5. RTSA Block Diagram.	179
Fig. 6.6. Illustrated concept of the Spectrogram generated by a RTSA.	179
Fig. 6.7. Spectrogram as commonly displayed by a RTSA.	180
Fig. 6.8. RTSA Digital Processing Block Diagram.	180
Fig. 6.9. General Configuration Page.	183
Fig. 6.10. Selection and Location of Input IQ Waveforms and Output Files.	183
Fig. 6.11. STFT Parameters Configuration.	184
Fig. 6.12. Gabor Parameters Configuration.	184
Fig. 6.13. STFT Window Selection.	184
Fig. 6.14. WVD Parameter Configuration.	185
Fig. 6.15. Automatic Batch Jobs Configuration.	185
Fig. 6.16. Block Edge Mask Generation Page (Option: STFT and Gabor Analysis).	186
Fig. 6.17. BEM Parameters Configuration.	187

Fig. 6.18. BEM Configuration and Generation (EIRP = 50 dBm/10MHz).....	187
Fig. 6.19. Core BEM Multi-sine Concept (for an EIRP = 59 dBm/10MHz). ....	188
Fig. 6.20. Wigner-Ville Core BEM Equivalent (for an EIRP = 59 dBm/10MHz).....	188
Fig. 6.21. Block Edge Mask Generation Page (Option: WVD Analysis). ....	189
Fig. 6.22. Output Results Page (Option: STFT Analysis, with Hamming window). ....	190
Fig. 6.23. Spectrogram of the LTE input signal (STFT, Hamming window).....	190
Fig. 6.24. Time Waveform of the LTE input signal (STFT, Hamming window). ....	191
Fig. 6.25. BEM compliance Test with subsequent STFT Spectrum “Slices” (STFT, Hamming window). ....	191
Fig. 6.26. Spectrum of the LTE input signal (FFT applied to all acquired samples). ....	192
Fig. 6.27. Spectrum of the LTE input signal (Smoothed Trace with Moving Average).....	192
Fig. 6.28. Histogram of PAPR of the LTE input signal.....	192
Fig. 6.29. Probability Distribution Function of PAPR of the LTE input signal. ....	192
Fig. 6.30. Cumulative Distribution Function of PAPR of the LTE input signal. ....	193
Fig. 6.31. Complementary Cumulative Distribution Function of PAPR of the LTE input signal. ....	193
Fig. 6.32. Output Results Page (Option: Gabor Transform Analysis). ....	193
Fig. 6.33. Output Results Page (Option: Wigner-Ville Analysis).....	194
Fig. 6.34. PDF of Normalized Amplitude of the Test Signals. ....	196
Fig. 6.35. CCDF of PAPR of the Test Signals. ....	196
Fig. 6.36. Multiple STFT Windows, Frequency Bins: 32, Window Length: 32 samples. ....	198
Fig. 6.37. Multiple STFT Windows, Frequency Bins: 1024, Window Length: 32 samples. ....	199
Fig. 6.38. Multiple STFT Windows, Frequency Bins: 1024, Window Length: 128 samples.....	200
Fig. 6.39. Multiple STFT Windows, Frequency Bins: 1024, Window Length: 512 samples.....	200
Fig. 6.40. Multiple STFT Windows, Frequency Bins: 1024, Window Length: 2048 samples.....	201
Fig. 6.41. Multiple STFT Windows, Window Length: 512 samples, Frequency Bins: 32. ....	202
Fig. 6.42. Multiple STFT Windows, Window Length: 512 samples, Frequency Bins: 128. ....	202
Fig. 6.43. Multiple STFT Windows, Window Length: 512 samples, Frequency Bins: 256. ....	203
Fig. 6.44. Multiple STFT Windows, Window Length: 512 samples, Frequency Bins: 512. ....	203
Fig. 6.45. Multiple STFT Windows, Window Length: 512 samples, Frequency Bins: 2048.....	204
Fig. 6.46. Sensitivity Analysis: STFT, Gabor Transform and WVD (Scenario 1).....	205
Fig. 6.47. Sensitivity Analysis: STFT, Gabor Transform and WVD (Scenario 2).....	206
Fig. 6.48. Sensitivity Analysis: STFT, Gabor Transform and WVD (Scenario 3).....	206
Fig. 6.49. Sensitivity Analysis: STFT, Gabor Transform and WVD (Scenario 4).....	207
Fig. 6.50. Sensitivity Analysis of the Gabor Transform to the Window Length (Frequency Bins: 2048). ....	208
Fig. 6.51. Sensitivity Analysis of STFT (Rectangle window) to the Window Length (Frequency Bins: 2048). ....	208
Fig. 6.52. Sensitivity Analysis of STFT (Flat Top window) to the Window Length (Frequency Bins: 2048).....	209
Fig. 6.53. Sensitivity Analysis of Gabor Transform to the Frequency Bins (Window Length: 2048 samples). ....	210
Fig. 6.54. Sensitivity Analysis of STFT (Rectangle window) to the Frequency Bins (Window Length: 2048 samples). ....	210
Fig. 6.55. Sensitivity Analysis of STFT (Flat Top window) to the Frequency Bins (Window Length: 2048 samples). .	211
Fig. 6.56. Sensitivity Analysis of WVD to the Frequency Bins.....	212

# List of Tables

Table 2.1. The four basic scenarios of the WAPECS approach.....	31
Table 2.2. Models for defining Least Restrictive Technical Conditions. ....	34
Table 3.1. Baseline requirements BS BEM Out-of-Block EIRP limits (over frequencies below 790 MHz) as a function of LTE BS In-Block EIRP and local DTT deployment. ....	55
Table 3.2. Transition requirements BS BEM Out-of-Block EIRP limits (over frequencies of FDD downlink and TDD). ....	55
Table 3.3. BEM derivation for a LTE BS emission with BW: 10 MHz and In-Block EIRP: 59 dBm/10MHz. ....	56
Table 3.4. Baseline requirements BS BEM Out-of-Block EIRP limits (over frequencies of FDD uplink and TDD). ....	58
Table 3.5. Transition requirements BS BEM Out-of-Block EIRP limits (over Guard Bands).....	59
Table 3.6. Full BEM derivation for a LTE BS emission (center frequency: 806 MHz, BW: 10 MHz, In-Block EIRP: 59 dBm/10MHz).....	60
Table 3.7. Spectrum Analyzer Configuration for BEM validation. ....	79
Table 3.8. Radio Monitoring Receiver Configuration for BEM validation. ....	79
Table 3.9. Advantages and Disadvantages of the BEM Compliance Measurement Methods. ....	84
Table 4.1. Comparative Analysis of Filter Performance (Channel 56).....	106
Table 4.2. Summary of DVB-T Indicators: Comparative Analysis.....	111
Table 5.1. The most common Short-Time Fourier Transform Window Functions.....	158
Table 5.2. Time and Frequency Responses of the most common STFT Window Functions. ....	159
Table 5.3. Windows applications according to the type of signal to be analyzed. ....	160
Table 6.1. Sensitivity to the Transform – Scenarios of Analysis.....	205

PAGE INTENTIONALLY LEFT BLANK



# List of Acronyms

<b>3GPP</b>	3 <sup>rd</sup> Generation Partnership Project
<b>ACIR</b>	Adjacent Channel Interference Ratio
<b>4G</b>	4 <sup>th</sup> Generation
<b>ACLR</b>	Adjacent Channel Leakage Ratio
<b>ACPR</b>	Adjacent Channel Power Ratio
<b>ACS</b>	Adjacent Channel Selectivity
<b>ADC</b>	Analogue-to-Digital Converter
<b>AGC</b>	Automatic Gain Control
<b>ANACOM</b>	Autoridade Nacional de Comunicações (National Authority of Communications)
<b>ATPC</b>	Automatic Transmit Power Control
<b>Att</b>	Attenuation
<b>AWGN</b>	Additive White Gaussian Noise
<b>BCCH</b>	Broadcast Control Channel
<b>BEM</b>	Block Edge Mask
<b>BER</b>	Bit Error Ratio
<b>BER1</b>	(DVB-T) BER before Viterbi decoding (or Channel BER: cBER)
<b>BER2</b>	(DVB-T) BER after Viterbi decoding (or vBER), or Before Reed-Solomon decoding
<b>BER3</b>	(DVB-T) BER after Reed-Solomon decoding (or BER RS)
<b>BER RS</b>	Bit Error Rate after Reed-Solomon decoding
<b>BPF</b>	Band-Pass Filter
<b>BS</b>	Base station
<b>BW</b>	Bandwidth
<b>BWA</b>	Broadband Wireless Access
<b>cBER</b>	Channel Bit Error Rate
<b>CCDF</b>	Complementary Cumulative Distribution Function
<b>CDF</b>	Cumulative Distribution Function
<b>CDMA</b>	Code Division Multiple Access
<b>CEPT</b>	European Conference of Postal and Telecommunications
<b>CF</b>	Crest Factor
<b>C/N</b>	Carrier-to-Noise Ratio
<b>CPICH</b>	Common Pilot Channel
<b>CR</b>	Cognitive Radio
<b>CRS</b>	Cognitive Radio System
<b>CS</b>	Central Station
<b>CUS</b>	Collective Use of Spectrum
<b>CW</b>	Continuous Wave (unmodulated carrier)
<b>DAC</b>	Digital-to-Analogue Converter

<b>DAE</b>	Digital Agenda for Europe
<b>dB</b>	Decibel
<b>DB</b>	Database
<b>dBc</b>	Decibel relative to the Carrier (or Decibel below Carrier)
<b>dBd</b>	Decibel relative to a Half-Wavelength Dipole
<b>dB<sub>i</sub></b>	Decibel relative to an Isotropic Antenna
<b>dB<sub>m</sub></b>	Decibel relative to a Power of 1 milli-Watt (1 mW)
<b>dB<sub>μ</sub>V</b>	Decibel relative to a Voltage of 1 micro-Volt (1 μV)
<b>dB<sub>μ</sub>V/m</b>	Decibel relative to an Electrical Field Strength of 1 micro-Volt/meter (1 μV/m)
<b>dBW</b>	Decibel relative to a Power of 1 Watt (1 W)
<b>DC</b>	Direct Current (or Zero-Frequency)
<b>DD</b>	Digital Dividend
<b>DD1</b>	First Digital Dividend
<b>DD2</b>	Second Digital Dividend
<b>DEM<sub>OD</sub></b>	Demodulation
<b>DFT</b>	Discrete Fourier Transform
<b>DG CONNECT</b>	Directorate General for Communication Networks, Content and Technology
<b>DG – M&amp;T</b>	Directorate General for Mobility and Transport
<b>DG – R&amp;I</b>	Directorate General for Research and Innovation
<b>DL</b>	Down Link
<b>DOCSIS</b>	Data Over Cable Service Interface Specification
<b>DPX</b>	Digital Phosphor Technology (Tektronix's Trade Mark)
<b>DSM</b>	Dynamic Spectrum Management
<b>DSP</b>	Digital Signal Processor
<b>DTT</b>	Digital Terrestrial Television
<b>DUT</b>	Device Under Test
<b>DVB-C</b>	Digital Video Broadcasting – Cable
<b>DVB-H</b>	Digital Video Broadcasting – Handheld
<b>DVB-T</b>	Digital Video Broadcasting – Terrestrial
<b>DVB-T2</b>	Digital Video Broadcasting – Second Generation Terrestrial
<b>DX</b>	Long Distance Communication
<b>EIRP</b>	Equivalent Isotropic Radiated Power
<b>EC</b>	European Commission
<b>ECA</b>	European Common Allocation Table
<b>ECC</b>	Electronic Communications Committee
<b>ECN</b>	Electronic Communication Network
<b>ECN&amp;S</b>	Electronic Communication Networks and Services Directorate
<b>ECO</b>	European Communications Office
<b>ECS</b>	Electronic Communication Service
<b>E - DG</b>	Environment Directorate General
<b>E&amp;I - DG</b>	Enterprise and Industry Directorate General
<b>EEA</b>	European Economic Area

<b>EFIS</b>	European Frequency Information System
<b>EGSM</b>	Extended GSM
<b>EMC</b>	Electromagnetic Compatibility
<b>EMF</b>	Electromagnetic Field
<b>ERO</b>	European Radiocommunication Office
<b>ETSI</b>	European Telecommunications Standards Institute
<b>EU</b>	European Union
<b>EVM</b>	Error Vector Magnitude
<b>FDD</b>	Frequency Division Duplex
<b>FFT</b>	Fast Fourier Transform
<b>FH</b>	Frequency Hopping
<b>FM</b>	Frequency Modulation
<b>FPGA</b>	Field Programmable Gate Array
<b><math>f_s</math></b>	Sampling Frequency
<b>FS</b>	Fixed Service
<b>FSK</b>	Frequency Shift Keying
<b>FSS</b>	Fixed Satellite Service
<b>FT</b>	Fourier Transform
<b>FWA</b>	Fixed Wireless Access
<b>FWS</b>	Fixed Wireless Systems
<b>GI</b>	Guard Interval
<b>GPIB</b>	General Purpose Interface Bus
<b>GPS</b>	Global Positioning System
<b>GSD</b>	Geolocation Spectrum Database
<b>GSM</b>	Global System for Mobile communication
<b>GSM-R</b>	GSM 'Railways'
<b>GT</b>	Gabor Transform
<b>HD</b>	High Definition
<b>HDTV</b>	High Definition Television
<b>HEN</b>	Harmonized Standard
<b>HF</b>	High Frequency Band (Short Wave Transmission)
<b>ICAO</b>	International Civil Aviation Organization
<b>IEEE</b>	Institute of Electrical and Electronics Engineers
<b>IF</b>	Intermediate Frequency
<b>IF2</b>	Second Intermediate Frequency
<b>IIR</b>	Infinite Impulse Response
<b>IMO</b>	International Maritime Organization
<b>IMT/IMT-2000</b>	International Mobile Telecommunications/ International Mobile Telecommunications-2000
<b>IoT</b>	Internet of Things
<b>IP</b>	Internet Protocol
<b>IQ</b>	In-phase Quadrature
<b>ISI</b>	Inter-Symbol Interference

<b>ISM</b>	Industrial, Scientific and Medical
<b>ITS</b>	Intelligent Transport Systems
<b>ITU</b>	International Telecommunication Union
<b>ITU-R</b>	International Telecommunication Union – Radiocommunication Sector
<b>JTFT</b>	Joint Time-Frequency Tools
<b>LBT</b>	Listen Before Talk
<b>LNA</b>	Low-Noise Amplifier
<b>LoS</b>	Line of Sight
<b>LPD</b>	Low Power Device
<b>LSA</b>	Licensed Shared Access
<b>LTE</b>	Long Term Evolution
<b>Lvl</b>	Level
<b>MATV</b>	Master Antenna Television
<b>MER</b>	Modulation Error Rate
<b>MFN</b>	Multi-frequency Network
<b>MIMO</b>	Multiple Inputs Multiple Outputs
<b>ML</b>	Mobile Station
<b>MMDS</b>	Microwave Multipoint Distribution System
<b>MPEG</b>	Moving Picture Experts Group
<b>MS</b>	Multi-Sine
<b>M2M</b>	Machine-to-Machine
<b>MWA</b>	Mobile Wireless Access
<b>NLoS</b>	Non Light of Sight
<b>NRA</b>	National Regulatory Authority
<b>NWA</b>	Nomadic Wireless Access
<b>OA&amp;M</b>	Operations, Administration and Maintenance
<b>OFCOM</b>	Office of Communications (United Kingdom)
<b>OFDM</b>	Orthogonal Frequency Division Multiplexing
<b>OoB</b>	Out-of-Band
<b>PAMR</b>	Public Access Mobile Radio
<b>PBCH</b>	Physical Broadcast Channel
<b>PFD</b>	Power Flux Density
<b>PIM</b>	Passive Intermodulation
<b>P-MP</b>	Point-to-Multi-Point
<b>PMR</b>	Personal Mobile Radio
<b>PMR 446</b>	Personal Mobile Radio (446 MHz band)
<b>P-P</b>	Point to Point
<b>PPDR</b>	Public Protection and Disaster Relief
<b>PSD</b>	Power Spectral Density
<b>QAM</b>	Quadrature Amplitude Modulation
<b>QEF</b>	Quasi-Error Free
<b>QoS</b>	Quality of Service

<b>QPSK</b>	Quadrature Phase Shift Keying
<b>PAPR</b>	Peak-to-Average Power Ratio
<b>PDF</b>	Probability Distribution Function
<b>PMSE</b>	Programme Making and Special Events
<b>PSK</b>	Phase Shift Keying
<b>RAN</b>	Radio Access Network
<b>RAS</b>	Radio Astronomy Service
<b>RB</b>	Resource Block
<b>RBW</b>	Resolution Bandwidth
<b>Ref</b>	Reference
<b>RF</b>	Radiofrequency
<b>RFID</b>	Radiofrequency Identification
<b>RLC</b>	Resistive, Inductive and Capacitive Circuit/System
<b>RMS</b>	Root Mean Square
<b>RPC</b>	Reference Planning Configurations
<b>RR</b>	Radio Regulations
<b>RRC</b>	Regional Radiocommunication Conference
<b>RSC</b>	Radio Spectrum Committee
<b>RSD</b>	Radio Spectrum Decision
<b>RSP</b>	Radio Spectrum Policy
<b>RSPG</b>	Radio Spectrum Policy Group
<b>RSPPP</b>	Radio Spectrum Policy Programme
<b>R&amp;TTE</b>	Radio and Telecommunications Terminal Equipment
<b>RTBW</b>	Real Time Bandwidth
<b>RTSA</b>	Real Time Spectrum Analyzer
<b>SAW</b>	Surface Acoustic Wave
<b>SD</b>	Standard Definition
<b>SDR</b>	Software Defined Radio
<b>SDTV</b>	Standard Definition Television
<b>SEM</b>	Spectrum Emission Mask
<b>SFDR</b>	Spurious Free Dynamic Range
<b>SFN</b>	Single Frequency Network
<b>SIG</b>	Spectrum Interservice Group
<b>SLA</b>	Service Level Agreement
<b>S/N</b>	Signal-to-Noise Ratio
<b>SRD</b>	Short-Range Device
<b>SRR</b>	Short-Range Radar
<b>STFT</b>	Short-Time Fourier Transform
<b>SU B4</b>	Spectrum Unit B4
<b>SUR</b>	Spectrum Usage Rights
<b>SWT</b>	Sweep Time
<b>SYNC</b>	Synchronism

<b>TDD</b>	Time Division Duplex
<b>TETRA</b>	Terrestrial Trunked Radio
<b>TPS</b>	Transmission Parameter Signaling
<b>TRP</b>	Total Radiated Power
<b>TS</b>	Terminal Station
<b>TV</b>	Television
<b>TVWS</b>	Television White Space
<b>UHF</b>	Ultra High Frequency
<b>UL</b>	Up Link
<b>UMTS</b>	Universal Mobile Telecommunications System
<b>UWB</b>	Ultra Wide Band
<b>vBER</b>	Post-Viterbi Bit Error Rate
<b>VBW</b>	Video Bandwidth
<b>WAPECS</b>	Wireless Access Policy for Electronic Communications Services
<b>WBB</b>	Wireless Broadband
<b>WIFI</b>	Wireless Fidelity
<b>WiMax</b>	Worldwide Interoperability for Microwave Access
<b>WLAN</b>	Wireless Local Area Network
<b>WMO</b>	World Meteorological Organization
<b>WRC</b>	World Radiocommunication Conference
<b>WS</b>	White Space
<b>WSD</b>	White Space Device
<b>WVD</b>	Wigner-Ville Distribution (or Transform)

## 1 Introduction

### 1.1 Overview

Nowadays, the most challenging issues raised to the spectrum management authorities include: (a) the definition and validation of coexistence rules to the newcomer radio systems (e.g., Long Term Evolution (LTE) and successors, according to the principle of neutrality of technology and service), which increasingly make use of non-steady-state and/or time-varying waveforms; (b) the development of novel and adequate methodologies and techniques for the identification and resolution of the most recent radio interference problems.

These topics of research assume particular relevance in overcrowded wireless environments, in which, the radio spectrum is fully congested, typically in co-site base stations or transmitters. These kinds of scenarios are highly prone to the generation of nonlinear distortion phenomena, due to the close proximity between different systems, resulting, often and inadvertently, unwanted spurious emissions, which can overlap channels used by the neighbors. [1] Sometimes, it is not possible to filter out those components of interference, especially if they arise from Passive Intermodulation (PIM). [2] In such cases, an accurate investigation should be conducted, in order to find, not only the contributing emission sources, but also the nonlinear mechanism that origins the product of intermodulation, to be, wisely, neutralized. [3]

The base station's receiving RF front-ends of mobile communication systems, which operate with very low sensitivity levels, are frequently victims of the above problems. Consequently, the uplink channels are harmed and masked by undesired spectral components that locally are stronger than the mobile terminal emissions to be received. However, the severity of the interference depends on several factors, such as the frequency arrangements locally assigned, the radiated power levels, the physical proximity between systems, the modulation techniques, the access schemes used by each system, the adopted filtering solutions, and the linearity of the amplification stages, among many others.

Interference scenarios like these demand a complex and accurate analysis in the field. The correct identification of the involved emissions is crucial to reach the core of the problem. But, if the traditional Fourier analysis has given, so far, satisfactory responses to the most common (steady-state) radio signals, lately, the spectral analysis has revealed itself increasingly useless and "incomplete". [4] This is mainly because the modern communication signals, characterized by a dynamic (time-varying) behavior, cannot be correctly captured just by looking at the frequency domain. [5], [6] On the other hand, the Fourier Transform, when applied to a non-steady-state signal's section, with a considerable duration, tends to average the transients, smoothing or even hiding the real essence and properties of the signal. **Therefore, it is fundamental to consider both and jointly the time-frequency domains, whenever transient or non-steady-state signals are present** (Fig. 1.1). [7], [8]

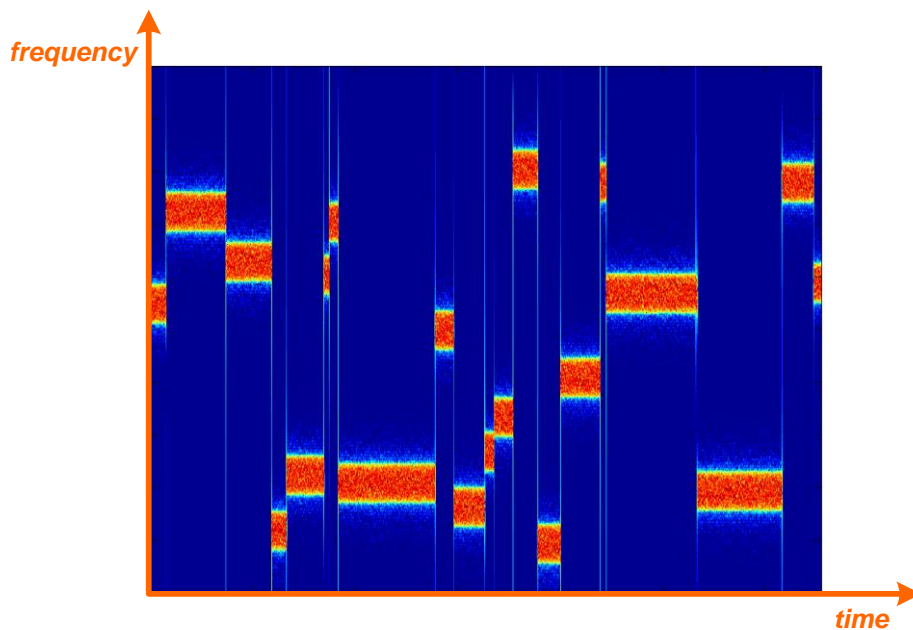


Fig. 1.1. Time-Frequency Representation of a Time-Varying Signal.



This work aims to explore alternative signal processing techniques beyond the conventional spectral analysis, which could be considered as solid candidates to give adequate responses to the current interference problems and to the existing RF signals. Naturally, the same approaches will also find application on the validation of rules, meanwhile, defined by the European regulatory bodies. The final goal of this Thesis is to build a demonstrator (software tool), integrating the most suitable Joint Time-Frequency Tools (JTFT) to analyze and validate<sup>1</sup> diverse samples of transient waveforms, acquired in the field in real situations, generated in laboratory or obtained from simulators. Aspects such as applicability, complexity, performance, implementation cost, will be taken into account and will also be carefully scrutinized for the respective proposed solution.

## 1.2 Motivation

The traditional models of spectrum management tend to classify, in a very well defined fashion, certain services and radio technologies in specific frequency bands. This homogeneous arrangement of radio services with common and invariable characteristics is intended to maximize the spectral efficiency and to ensure a proper coexistence with other services in an environment free of harmful interference. As the main technical parameters of those radio systems, which will operate in certain bands, are pre-known, it makes easier to accurately predict their behavior. This allows, if necessary, the anticipation of possible technical solutions to make these systems mutually compatible. Such a desirable compatibility scenario cannot be taken as a grant to the emerging models, which are considered more flexible.

However, the rigidity which results from the traditional approach does not always lead to the maximization of the economic return. As a result, in the last few years, new alternatives have been studied to promote original ways of using and sharing the spectrum. This encompasses not only neutral/flexible technologies and/or services, but also an ample range of scenarios involving emerging "cognitive radio" (CR) and "dynamic access" wireless communications concepts. [9]

Currently, new models of spectrum sharing by secondary users are being explored. They take advantage of the non-permanent use or reduced activity of primary systems (primary users) of some holes of the spectrum; for example, the so-called "**white spaces**" – e.g., those resulting from spectral regions assigned to military and emergency purposes which remain underutilized

---

<sup>1</sup> According to a predefined set of constraints

most of the time — , or even the bands allocated to Digital Terrestrial Television (DTT) services if their channels are not being used in a given location due to operational constraints imposed by the planning of Digital Video Broadcasting – Terrestrial (DVB-T) networks (cellular re-use factor and pattern). These specific portions of the spectrum within the Television (TV) range that are deliberately “wasted” for technical reasons are naturally known as “**TV white spaces**”. [10]

Regardless of the flexible model under consideration, it is possible to identify gains of spectral and economic efficiency. In any case, it is important to ensure the necessary radioprotection against harmful interferences, either to the primary users who share the white spaces or all other systems operating in the neighborhood and/or in adjacent bands. This impact of the coexistence between newcomers and remaining technologies should be carefully investigated from the physical layer perspective of involved RF systems.

The migration from analogue to digital television broadcasting has introduced significant improvements in terms of spectral efficiency. As a result, the number of radio channels required to ensure an equivalent coverage has been dramatically reduced. [11]

This gain of efficiency has allowed the release of a valuable portion of spectrum in the 790-862 MHz sub-band<sup>2</sup>, which was previously assigned to the analogue TV broadcasting service, usually known as “**Digital Dividend**” (**DD**). On the other hand, current dynamics of mobile communications markets and data demand for more wireless access to cope with growing trends of consumption of mobile services by their users. In this sense, this slice of 72 MHz of the spectrum is now exclusively assigned to the International Mobile Telecommunications (IMT) in line with the decisions taken in this matter. [12], [13]

Some frequency bands in Europe, including those which resulted from the digital dividend, should be ruled by the guidelines defined in the context of WAPECS<sup>3</sup>. [14] They must permit to provide electronic communications networks and services according to the principle of “**neutrality**”, either technological or of services. [15] This means that different networks could deliver the same or different services. However, by allowing a generic technology, the European Commission and the spectrum policy bodies had the necessity of introducing a set of technical requirements that should be complied by the enabling radio systems to avoid harmful interferences. These restrictions, formulated as forms of spectral masks which are commonly

---

<sup>2</sup> Channels: 61 to 69

<sup>3</sup> Wireless Access Policies for Electronic Communications Services

referred to as “**Block Edge Masks**” (**BEM**), are intended to be applied to blocks of the spectrum allocated to operators. [16]

This innovative approach aims to stimulate greater market dynamics, as well as the continuous evolution of technology, making it available more quickly to the final consumers; to streamline licensing processes of regulatory bodies; and to promote flexibility of radio spectrum usage while achieving greater economic efficiency.

Besides the conceptual aspects behind the noble principles herein invoked, such changes in paradigm require, from the technical perspective, a cautious assessment, focused on practical implementation issues, in order to ascertain the real and effective impact of the neutrality. Therefore, it is of paramount importance to ensure the coexistence and performance of other radio systems, operating in the same or in adjacent bands, by identifying unwanted physical phenomena, prescribing the best practices and resilient technological solutions to avoid harmful interference, to achieve the desired protection.

These concerns are precisely the right motto for a plenty of legitimate questions: ***Are the BEM the most appropriate way of imposing constraints to the radio systems in operation? Are the BEM universal and really effective to transient signals? How could a BEM be measured? How could a BEM be validated? Could we trust the results returned by a traditional spectrum analyzer to conclude that a BEM is being met, even if the spectrum could suggest so? Is a compliant spectrum a necessary and sufficient condition to avoid interference? Does the “same spectrum” always produce interference with the same degree of severity?*** We will try to answer all these interesting questions throughout the present Thesis.

### 1.3 Objective

The core objective of this work is **to apply time-frequency techniques to transient radio signals**, in order to extract additional and richer information, beyond that provided by the traditional spectral analysis, to be used in present and future spectrum management context.

In order to accomplish the above main goal, a sub-set of objectives was defined as follows.

- ✓ To identify the most relevant European regulatory policies and framework to the emergent radio communication systems and the future trends on the radio spectrum utilization.

- ✓ To identify, analyze and propose solutions to interference problems in the presence of “neutral” radio systems.
- ✓ To characterize the impact of transient signals on the performance of radio systems.
- ✓ To develop an alternative methodology for “Block Edge Masks” validation, using time-frequency mixed domain techniques.
- ✓ To implement a software tool, providing time-frequency techniques, to be used in the spectrum management inspections context.
- ✓ To optimize parameters of the time-frequency analysis according to the waveform to be validated.

## 1.4 Thesis Outline

Henceforth, the Thesis is organized as follows.

**Chapter 2** introduces the general European regulatory and spectrum management framework for emergent radio systems, pointing out future trends, innovative models, and new key-concepts: “neutrality” (technologies and services) and “flexibility”, as well as the emerging models of shared use of spectrum, which include the “collective use of spectrum” (CUS) and “licensed shared access” (LSA). The chapter ends with a futuristic view of the spectrum management, addressing dynamic models of spectrum allocation provided by, and based on, the conceptions of “white-space”, “software defined radio” and “cognitive radio”. In such a context, sensing mechanisms and support infrastructures of operation will be analyzed, and likely business models will be briefly explored.

**Chapter 3** describes the recently adopted model of defining technical constraints, to be applied to neutral systems, by the European regulators: the “Block Edge Mask”. This approach is conceptually detailed and materialized, in practice, with concrete examples of application. The official CEPT<sup>4</sup> methodology of measurement and validation of a BEM is analyzed and reviewed.

**Chapter 4** aims to demonstrate that, despite the above technical requirements are met, it is not taken for granted that interference does not arise. Thus, two real case-studies are presented, which provide illustrative examples of technological neutral systems as potential

---

<sup>4</sup> European Conference of Postal and Telecommunications Administrations

interferers and victims. The first one analyzes the interference caused by a LTE base station emission that inhibits the normal operation of a DVB-T receiver. The origin of such an interference problem is carefully investigated and ascertained, using factual measurement data, collected in the field. After identifying the cause, a solution – a RF band-stop filter – is proposed, engineered and successfully tested. Indeed, this device allows the desired coexistence between both systems (LTE and DVB-T). The latter case-study reports a peculiar effect detected by spectrum management teams in a real situation of interference. Specifically, a digital modulated radio signal is being harmed by a spectrally adjacent narrowband spurious emission generated by a television reception amplifier, which is oscillating in frequency due to malfunctioning. Under such non-expected operation conditions, a “doughnut” shape is observed on each symbol of the constellation diagram of the received digital signal. The problem is thoroughly analyzed from the analytical perspective (mathematical formulation), and by simulation and through laboratorial tests.

**Chapter 5** is dedicated to the Time-Frequency mixed domain analysis, but begins with the traditional Fourier methods – used, for years, to analyze radio signals, in the frequency domain –, in order to stress recurrent drawbacks, when transient or time-varying signals are evaluated with those tools. It is also demonstrated that different signals with “*the same spectrum*” may not produce interference with the same degree of severity, particularly if non-linear systems are considered. Then, the most remarkable time-frequency mixed domain signal processing transforms (*Gabor Transform*, *Short-Time Fourier Transform*, *Spectrogram* and *Wigner-Ville Distribution*) are introduced, to overcome major flaws of the conventional approaches.

**Chapter 6** proposes a more efficient and expeditious alternative methodology, to be used on the validation of the central segment of a BEM. This approach permits to capture well the dynamic/transient behavior of a LTE signal, preserving the genuine integrity of such a type of signal, even if just for a limited or partial section of a BEM. But, and above all, it ensures the necessary concurrency of the measurement procedure. Then, a general setup, for acquiring the signal, to be validated, is proposed, and a software tool for data processing and validation is prototyped as a proof of concept, developed and implemented. The chapter is concluded with a comparative analysis, using some reference LTE signals, in order to figure out how such a validation methodology is sensitive to different time-frequency techniques, parameter configuration, and types of signals.

Finally, the most relevant conclusions of this Thesis are set out in **Chapter 7**.

## 1.5 Original Contributions

1. **Borrego, J.P.**, Gomez-García, R., Carvalho, N.B., Sánchez-Soriano, M.A., Vieira, J.N., *Interference Mitigation on DVB-T Reception Caused by Neutral Systems Operating in the Digital Dividend Band*, IEEE Transactions on Broadcasting, submitted on Feb. 15<sup>th</sup>, 2014.
2. Gomez-García, R., Loeches-Sánchez, R., Muñoz-Ferreras, J.M., **Borrego, J.P.**, Magalhães, J.P., Carvalho, N.B., Vieira, J.N., Pérez-Martínez, F., *Dual-band Lowpass/Bandpass Periodic-type Microstrip Filter with Long-Term-Evolution (LTE) Service Mitigation*, LASCAS' 14 - 5th IEEE Latin American Symposium on Circuits and Systems, Santiago, Chile, Feb. 25<sup>th</sup> – 28<sup>th</sup>, 2014.
3. **Borrego, J.P.**, Carvalho, N.B., Vieira, J.N., *BEM vs. White Spaces Technologies*, Rohde & Schwarz Workshop on White Spaces Technologies, Aveiro, Portugal, Dec. 12<sup>th</sup>, 2011.
4. **Borrego, J.P.**, Carvalho, N.B., Vieira, J.N., *New Trends in Spectrum Management in Europe: How to deal with Transient Waveforms*, CETC 2011 – Conference on Electronics Telecommunications and Computers, Lisbon, Portugal, Nov. 25<sup>th</sup>, 2011.
5. **Borrego, J.P.**, Antunes, S., Postolache, O., Carvalho, N.B., Vieira, J.N., *Novos Desafios à Monitorização e Controlo do Espectro, na perspectiva dos Sistemas de Medida*, 5<sup>th</sup> Congress of the Portuguese Committee of URSI, Lisbon, Portugal, Nov. 11<sup>th</sup>, 2011.
6. **Borrego, J.P.**, N. B. Carvalho, *The State-of-the-Art of Nonlinear Transient Figures of Merit for RF*, Scientific Magazine of the Department of Electronics, Telecommunications and Informatics, 2010.
7. **Borrego, J.P.**, Carvalho, N.B., *Figures of Merit for Time-varying Radio Communication Systems*, 4<sup>th</sup> Congress of the Portuguese Committee of URSI, Lisbon, Portugal, Sep. 23<sup>rd</sup>-24<sup>th</sup>, 2010.
8. **Borrego, J.P.**, Carvalho, N.B., *Transient Nonlinear Figures of Merit for Wireless Communications*, INMMiC2010 – Workshop on Integrated Nonlinear Microwave and Millimeter-wave Circuits, Chalmers University of Technology, April 26<sup>th</sup> – 27<sup>th</sup>, 2010, Göteborg, Sweden.

---

# 2 Spectrum Management: The European Regulatory Context

## 2.1 Introduction

The radio spectrum is a scarce natural resource, which is unanimously seen as a strategic factor of competitiveness and an important driver for the present and future economic strength and development of Europe. [17] As a matter of fact, a wide range of basic activities and commodities of our daily lives are only possible because the access to radio spectrum is granted to specific systems and services. Among the vast array of likely uses of spectrum, the following are featured [18], [19]:

- a) **Communications:** *telephony, radio and TV broadcasting, wireless broadband (high-speed internet, advanced mobile communications, information and communication technologies), which are generically known as electronic communications services (ECS).*
- b) **Safety and Transport Applications:** *avionics, aircraft and maritime radio navigation aid systems, aeronautic and maritime communications, and future transport systems: vehicle communication, sensing systems for increased safety, etc.*

- c) **Research and Scientific Applications:** *radio astronomy, meteorology, engineering and academic research, industrial, scientific and medical (ISM) services and applications.*
- d) **Space Applications:** *space communications, Earth to space (and vice-versa) communications, space science, navigation (including satellite positioning systems), multi-purpose Earth observation systems (e.g., pollution, earthquakes, and ice height controlling and monitoring), among many other applications.*
- e) **Public Protection and Disaster Relief:** *emergency services (police and security forces, fire brigades, paramedics, and civil protection authorities). Particularly in extreme emergency scenarios, such as catastrophic events and serious disruptions (accidents, natural disasters, and human acts), the wireless technologies are seen as a key solution, able to respond singularly even in the presence of such adversity, showing reliability and resilience enough to ensure, not only communication capabilities, but also a wide range of multi-purpose services (location, navigation, life detection, sensing, etc.).*
- f) **Defense and Military Applications:** *military communications (voice, data and image), logistics support, surveillance, location, navigation, command and control of military operations and systems, etc.*

From the previous broad list of examples, it is by far evident that the competing demands for using this scarce resource (radio spectrum) are becoming more and more intensive. Using the common sense principle, the law of supply and demand states that, whenever the demand of a scarce asset is high, its own value soars. Therefore, the radio spectrum is seen as a valuable commodity, which must be used and managed with the utmost efficiency, in order to ensure and deliver the maximum benefit to the society. [17]

Actually, the management of radio spectrum is a complex task, which requires a fair allocation of frequencies, in order to promote the coexistence of existing and emerging services and technologies, preventing harmful interference.

Both allocation and management of radio spectrum in Europe is a competence of the national regulatory authorities of each Member State. [20], [21] The spectrum planning and engineering services of each national spectrum management agency divide the whole radio spectrum in smaller portions – bands or channels – to accommodate the different wireless services. According to the specific needs of each service, the size (bandwidth) of those portions



is variable. The Fig. 2.1 illustrates the spectrum allocation planning in Portugal, showing the distinct bands with the respective services.

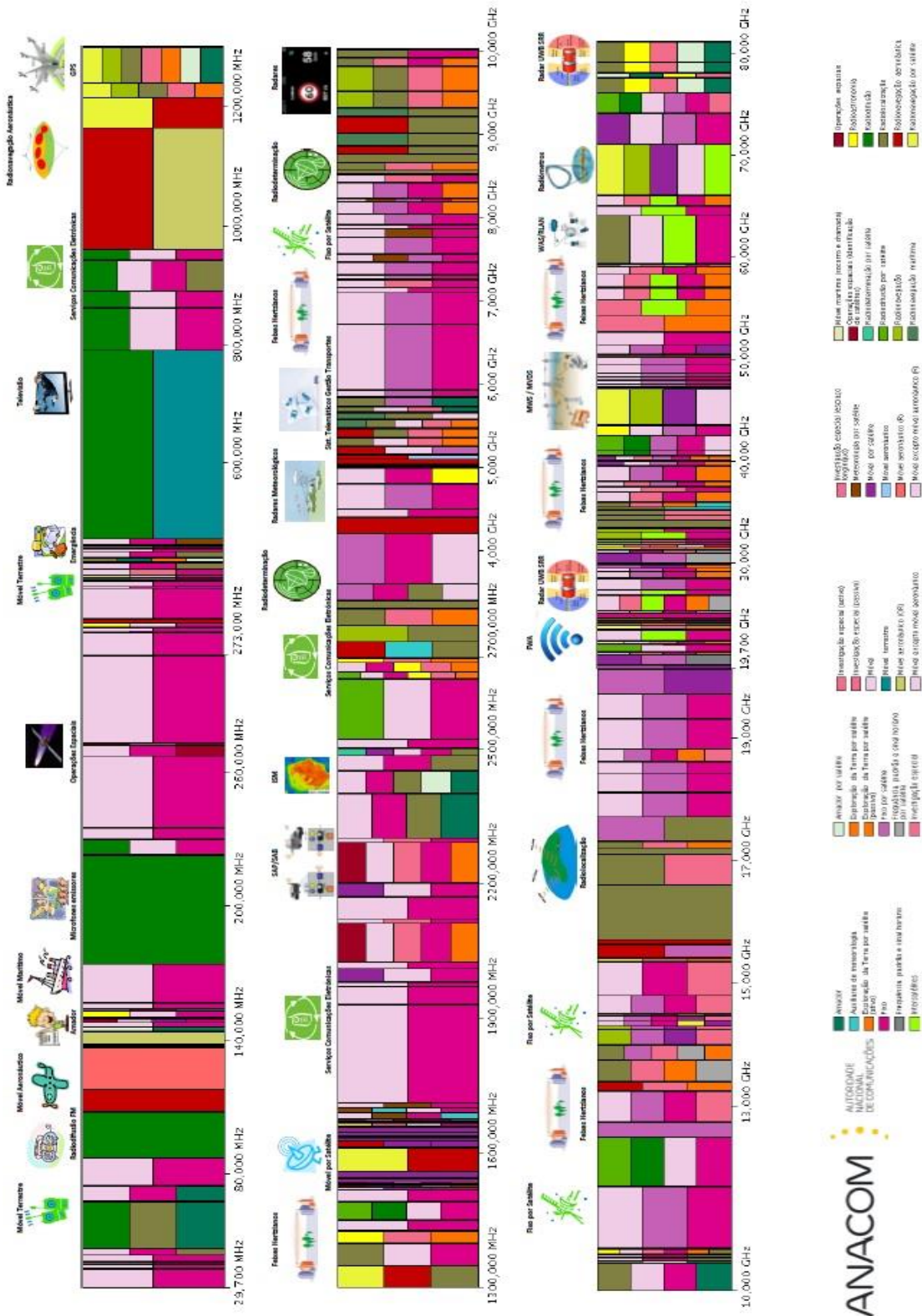


Fig. 2.1. Spectrum Allocation in Portugal.  
(Courtesy of ANACOM)

Due to physical restrictions, lower frequency bands, typically, can only offer limited bit rates, and consequently they carry little information. However, they are suitable for long distance communication (DX), for instance, using the ionosphere to refract the transmitted radio beams, such as, extra-continental coverage short-wave radio broadcasting (HF) or long distance military and amateur radio communication. The radio systems which operate in lower frequencies use, in general, high-power transmitters and very large dimension antennas (compatible with the corresponding wavelength).

On the other hand, higher frequencies provide higher capacity and they are able to carry much more information. However, the higher the frequency, the lower the coverage range. The transmitted power is typically low and the building penetration is also reduced. For the above reasons, point-to-point radio links (Fixed Service), which operate in microwave bands, demand for line-of-sight (LoS), i.e., unobstructed Fresnel's ellipsoid condition.

But there are more dimensions to be considered. In fact, the spectrum is not only shared by different services, but also by distinct users. Furthermore, the time occupancy of each channel depends on the service. For instance, the broadcasting services show typically a full time occupancy (100%), but mobile radio (trunking) services only use the spectrum according to the needs of communication of the users ( $\ll$  100%). Moreover, the spectrum tends to be more crowded in large cities than in small villages.

The aforementioned examples reveal important asymmetries and/or idiosyncrasies that should be properly weighed to assure a necessary fair spectrum allocation and the adequateness of certain frequency bands for particular services. [21]

Then, some critical factors might be identified: *coverage range, capacity (bit rate), channel occupancy, location, population density, etc.*, which could, directly or indirectly, influence the spectrum planning and consequently the assignment of licenses. Since the spectrum is not homogeneously used, even in the same country, the national governments and spectrum authorities define how that spectrum is shared by the services/applications, users, and locations; and how and whom has the right (license) to use a given channel or block of spectrum. This gives them the necessary freedom to adopt the most suitable method to grant those licenses/rights of use (tender, beauty contest, etc.), on a case-by-case basis.

**Nevertheless, this apparent heterogeneity dictated by a multiplicity of options, put into practice by every government, does not imply any lack of harmonization on the general practices followed by the European Member States.**

The European Commission does not have a direct intervention on the national spectrum management activities, but defines a common understanding (regulatory framework), relevant goals and EU policies which should be evenly achieved and implemented within Europe. However, all these decisions and options should be compliant with the common EU laws for the single market and with international radio spectrum agreements: e.g., decisions taken under the aegis of the ITU, – in particular, those which are emanated from the ITU-R, with emphasis on the Radio Regulations which join the worldwide consensus at the World Radiocommunication Conferences (WRC) –, and those resulting from other international *fora*: International Civil Aviation Organization (ICAO), International Maritime Organization (IMO), World Meteorological Organization (WMO), etc. [20], [21], [22]

### **2.1.1 The European Spectrum Policy Framework, Coordination and Harmonization**

The European Spectrum Policy aims to provide a common and solid regulatory framework, duly coordinated among all Member States, which should lead to a unified spectrum management approach; taking into account all technical and societal challenges and demands.

Some of the most recent scientific achievements have come up with new technologies and applications, which are, on the one hand, highly innovative in the way they use the radio spectrum, and on the other hand, essential for economic growth. This type of dynamics requires the most suitable framework to respond properly to the current and emerging needs for spectrum, ensuring the necessary radio protection of all users, i.e., avoiding any potential and harmful interference between applications, but stimulating innovation. [19]

Therefore, an accurate work to identify the needs for spectrum coordination should be continuously carried out. For instance, by anticipating large-scale operations, at the European level, of quite a few communication systems, some specific bands can be globally planned and reserved to serve those purposes. Complementarily, a set of policy priorities should be clearly established and ranked, in order to avoid expected conflicts between different requests for spectrum use. [20]

As a matter of fact, this fundamental instrument of the European policy has been regarded as an inductor of technologically innovative processes, not only in the cluster of wireless and electronic communications services, but in other key sectors of the European economy. At the same time, it is also seen as a catalytic agent of the global market. Regarding the context of the single internal market, all standardization efforts arise as a deciding factor of innovation and

competitiveness, which justify the desired harmonization of the spectrum usage in Europe, more and more efficient and flexible.

In order to ensure the necessary compatibility and interoperability between equipments, systems and services, the standardization efforts go beyond the spectrum allocation itself. Indeed, they also include the definition and verification (inspection) of technical requirements to which the devices must be compliant with (not only the ones that directly use the spectrum). The latter rules fall within the scope of the two following directives: *Radio and Telecommunications Terminal Equipment (R&TTE)* [23] and *Electromagnetic Compatibility (EMC)* [24].

In a nutshell, the **European Spectrum Policy Framework** has as overall goals: *the harmonization of the use of radio spectrum and the conditions to access to it, the promotion of a more efficient use of spectrum, and the improvement of the information that is provided to the stakeholders (current and future spectrum uses, availability of spectrum, etc.)*. [25] All these purposes should be consolidated by a modern regulatory environment, capable of fostering an easier and more flexible access to the radio spectrum, either by public or private entities, preserving and promoting competition. [18], [20]

Nonetheless, the social concerns are not apart from the aforementioned list of priorities; so much that is considered crucial to provide access to digital and fast broadband communication services to every European citizen, whether living in an urban or rural/remote area. Whatever the type of zone under consideration, the spectrum plays a key role in enabling the above services, breaking geographical asymmetries, and overcoming, or at least softening, the digital divide.

#### 2.1.1.1 The Radio Spectrum Policy Programme

The key policy objectives and general regulatory principles, priorities and measures - *related to radio spectrum management, internal market, innovative technologies and services, digital divide, etc.* -, and any other relevant issues with impact on the needs of the European consumer, industry and society, were compiled in a comprehensive roadmap entitled: **Radio Spectrum Policy Programme (RSPP)**. [18], [20]

The first RSPP was launched on the 14<sup>th</sup> March 2012, aligned with the *Europe 2020* strategy [26], [27] and the *Digital Agenda for Europe (DAE)* [28], and materializes the above policy goals into concrete measures to be gradually completed by the end of 2015, in order to conclude the work in progress on the internal market. [25]

Some of these **concrete actions** envisage the identification of a significant portion of spectrum (at least 1200 MHz) to tackle the growing demand for wireless data traffic, and any additional needs for harmonized bands. The “*EU’s radio spectrum inventory*”, which was considered a relevant instrument of analysis, should be finished soon. This wide repertory of information will make the band coordination and harmonization processes even more agile. The spectrum trading is also encouraged inside the EU, taking advantage of the flexibility already introduced in some specific harmonized bands.

The aim of delivering wireless broadband to sparsely populated areas<sup>5</sup>, whether using the 800 MHz band (released by the digital dividend), or the other bands where the flexibility is already possible, was set by the 1<sup>st</sup> January 2013, unless individual derogations had been approved.

In light of the defined priorities<sup>6</sup>, special attention was devoted to the innovation on wireless systems. Then, the development of more efficient techniques to use the spectrum and new sharing models are particularly fostered. On the other hand, the spectrum is also regarded as a strategic element of a broader plan: “*a low-carbon society*”, which should benefit from that innovation, in order to promote a more efficient production and distribution of energy in Europe. [29], [30]

The **first report on the implementation of the RSPP** [30] was released on the 22<sup>nd</sup> April 2014. It briefly analyzes the current status of the Programme, showing the ongoing work on the most relevant topics, the goals achieved so far, and the decisions adopted by the EC to support key EU policy areas<sup>7</sup>.

---

<sup>5</sup> The DAE assumes, as target, to deliver **30 Mbit/s** to every European citizen, by 2020.

<sup>6</sup> **Action areas:** *wireless broadband communications, audio-visual media, transport, health, research, civil protection and disaster relief, environment and energy-saving applications, besides major European Programmes: “Galileo” and “Copernicus” (European Earth Observation).*

<sup>7</sup> **Digital Agenda for Europe:** *spectrum harmonization for wireless broadband and short-range devices (SRD) for the Internet-of-Things (IoT); Single European Sky:* *spectrum harmonization for aircraft on board mobile communications; Maritime and Land Transport:* *spectrum harmonization for intelligent systems, such as tolling and automotive short-range radars (SRR).*

The quoted report covers the following issues: **spectrum inventory**<sup>8</sup>, the **wireless broadband services**<sup>9</sup> and the **implementation of the 800 MHz band**<sup>10</sup>, the **shared use**<sup>11</sup> **of spectrum: *unlicensed* and *licensed shared access (LSA)***, among **other EU policies**<sup>12</sup>, and concludes assessing the effectiveness of the implementation of the **radio spectrum decision (RSD)**.

The regulatory framework for the Radio Spectrum Policy in the EU was defined by the Radio Spectrum Decision<sup>13</sup> (RSD) [31], published in 2002, within the scope of the regulatory framework for electronic communications<sup>14</sup>. [32], [33], [34] The RSD gives to the Commission the formal legitimacy to put into practice the spectrum policies, either from the juridical, economic, or technical perspectives; allowing the creation of proper structures and bodies, interdependences, interacting and operational rules.

---

<sup>8</sup> The **spectrum inventory** aims to identify, in an integrated fashion, sharing opportunities, the actual occupancy or activity observed throughout the different regions of the radio spectrum, in order to select, wisely and properly supported, bands with potential of being allocated and reallocated to certain services, observing harmonization principles. This wellspring of data will enable the adoption of measures tending to a more efficient use of spectrum, and the optimization of the wireless services which are provided to the European citizens. Those efforts should result in an overall improvement of the necessary efficiency, innovation and competition. The Member States should keep uploading their own data, in digital format, to the European Frequency Information System (EFIS) database by the end of 2015.

<sup>9</sup> Pursuing the ambitious **objective** of reserving **at least 1200 MHz of spectrum, for future wireless broadband services**, by 2015, the measures taken so far have already identified 990 MHz to be harmonized. The Commission, spectrum bodies, a high level group of stakeholders, and Member States, are working together to get the remaining portion of spectrum. The *UHF band (470 – 790 MHz)*, the so-called “*sweet spot*”, has been quite coveted for the purpose. However, a conflict of interests between broadcasters and mobile operators is not at all desirable. This situation has to be adequately mediated.

<sup>10</sup> According to the report [30], 10 Member States, including Portugal, had assigned the **800 MHz band** in 2012 or before, 8 had assigned it in 2013, derogations (until the end of 2015 or before) were granted to 7 Member States, and the remaining 3 had not assigned yet the 800 MHz band. The above divergences and delays may suggest possible risks of fragmentation of the internal market, due to an incomplete spectrum harmonization.

<sup>11</sup> The **shared use of spectrum** is intended as a key factor to stimulate innovation and investment. The RSPP recommends the introduction of measures to promote the collective and shared use of spectrum, by adopting efficient and flexible models (alternative/emerging technologies). The harmonization of bands subjected to general authorizations (unlicensed spectrum) or individual rights of use (LSA) is regarded as a fundamental driver of innovation.

<sup>12</sup> Considering the potential of the wireless technologies, particular attention is devoted to the **energy-saving and efficient smart-grids** (*smart energy distribution grids and smart metering systems*), aiming to explore desired synergies.

<sup>13</sup> **Decision 676/2002/EC**

<sup>14</sup> The **Regulatory Framework for Electronic Communications** is in force since 2002, but was revised in 2009 to accommodate recent and future dynamics of markets and services. It establishes regulatory rules based on general principles of the EU and promotes a steady legal environment to attract investment, but flexible enough to stimulate the innovation on telecommunication technologies, products and services.

### 2.1.1.2 The European Radio Spectrum Bodies

Supported by the RSD, the Commission is assisted – for the radio spectrum issues – by two advisory bodies: the **Radio Spectrum Policy Group**<sup>15</sup> (**RSPG**) [37] and the **Radio Spectrum Committee (RSC)** [39]. They complement each other, providing policy and technical consultancy, besides supervising and monitoring the implementation of concrete measures together with the Member States. [20]

The **RSPG** is a high-level policy group, joining the Commission representatives and national governmental experts (Member State representatives), which establish a close bridge between the Commission and local communities; but other external individualities are allowed to participate as observers, including the representatives of the European Parliament, the CEPT, the European Telecommunications Standardization Institute: ETSI, candidate countries and European Economic Area (EEA) countries. The RSPG activity is guided by fair, non-discriminatory and proportional principles. Thus, the needs, requests, opinions and positions expressed by the stakeholders are taken into consideration in the RSPG consultations. [37]

The **RSC** is a technical committee, which the mission is devoted to the development of practical harmonized measures, to be implemented by each Member States, aiming efficient spectrum utilization. The European Commission chairs the RSC, which also includes a board of Member State representatives.

The Commission may issue mandates<sup>16</sup> of technical nature to the **European Conference of Postal and Telecommunications (CEPT)**. The origins of this organization date back to the late 50s of the last century. It was founded by representatives of 19 countries, which were incumbent operators controlled by state-owned national monopolies on the sector of postal and telecommunications. Presently, the CEPT has 48 member countries, and its activities include institutional and regulatory cooperation, mostly of technical and operational nature, also covering the standardization. Nowadays, the latter come within the ETSI purview; by the way, this institute of standards spun off from within the CEPT. [40]

Although the CEPT also embraces the postal sector, the matters related to the radio spectrum are concentrated on the Electronic Communications Committee (ECC) that congregates the regulatory authorities charged with the spectrum management in the CEPT

---

<sup>15</sup> The RSPG owes its origins to the **Decision 2002/622/EC** [38], following the RSD (Decision 676/2002/EC).

<sup>16</sup> A **mandate** is a formal request from the EC, via RSC, to the CEPT, to carry out technical studies on specific measures under consideration for future implementation by the Member States. [35]

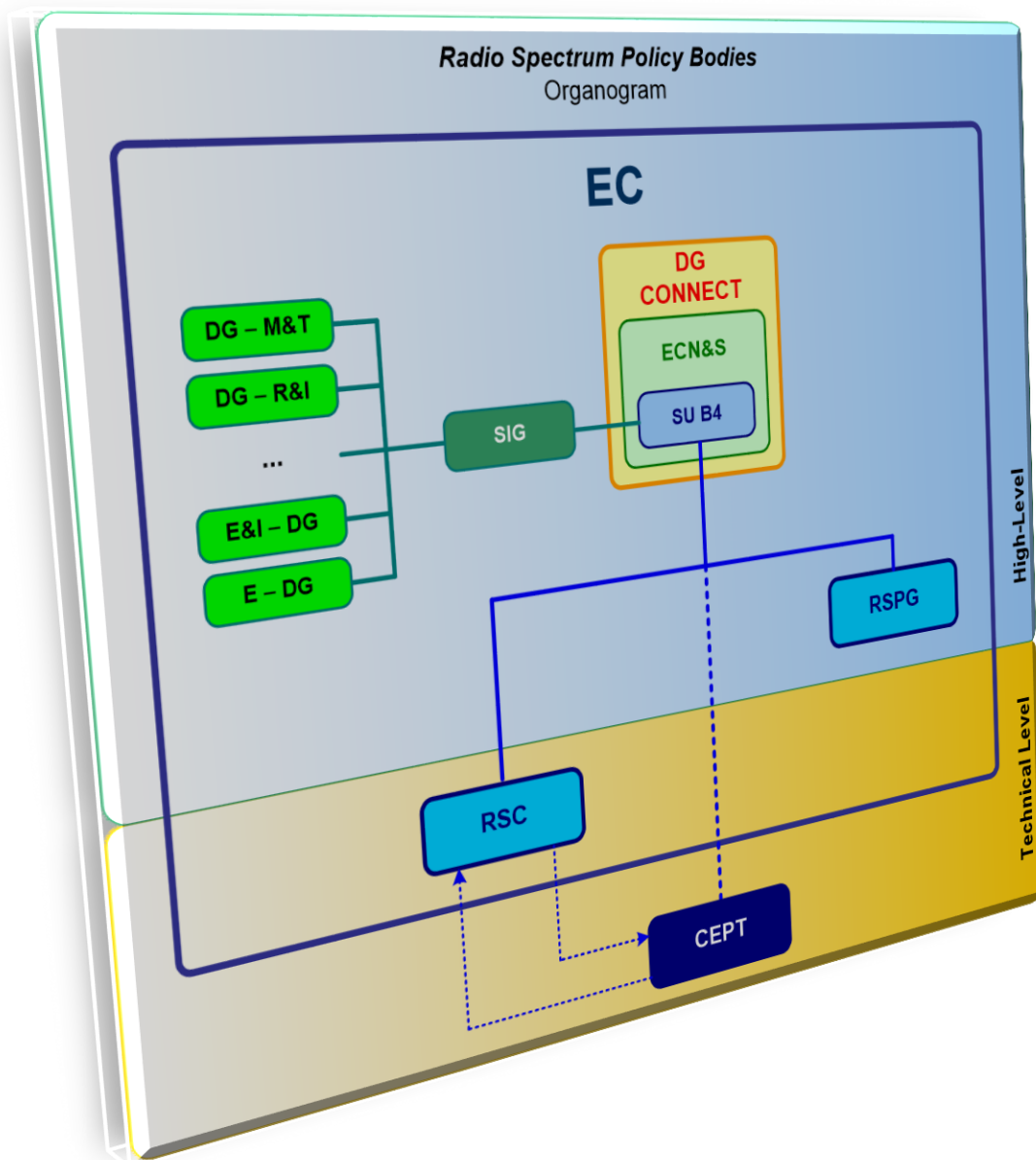
member countries. The CEPT (including the ECC) is backed by a permanent structure: the European Communications Office (ECO), based in Copenhagen, Denmark. [35]

The RSC keeps a close relationship with the CEPT. Indeed, on the technical level, there is a full cooperation between them. In response to a mandate, the CEPT provides the RSC with studies, reports, specifications or recommendations, which will support possible decisions. Nevertheless, the European Parliament scrutinizes their activities and resolutions. [36] That work may lead to further Commission Decisions or proposals, enriching the current spectrum policy framework.

Since the spectrum policies could have a direct or indirect impact on policies developed by other Directorates-General (*e.g.*, *European policies on research and innovation, mobility and transport, enterprise and industry, environment, etc.*), the Commission created the **Spectrum Interservice Group (SIG)**, which ensures the necessary coordination between departments, in order to streamline the interrelationships and processes. [20]

The Fig. 2.2 hierarchically illustrates the interdependences between the European Spectrum Bodies.





*Legend:*

**EC:** European Commission

**DG CONNECT:** Directorate General for Communication Networks, Content and Technology

**ECN&S:** Electronic Communication Networks and Services Directorate

**SU B4:** Spectrum Unit B4

**SIG:** Spectrum Interservice Group

**RSC:** Radio Spectrum Committee

**RSPG:** Radio Spectrum Policy Group

**CEPT:** European Conference of Postal and Telecommunications

**DG - M&T:** Directorate General for Mobility and Transport

**DG - R&I:** Directorate General for Research and Innovation

**E&I - DG:** Enterprise and Industry Directorate General

**E - DG:** Environment Directorate General

Fig. 2.2. Radio Spectrum Policy Bodies Organogram.

## 2.2 The Digital Dividend

An efficient spectrum management requires a permanent monitoring of the use and occupancy of the frequencies assigned to different radio services. It thus becomes possible to identify, on the one hand, the underuse of certain bands, which may indicate a potential waste, requiring the optimization of the allocated resources; and on the other hand, the overcrowding of other, suggesting the need for additional spectrum, considering the cost-benefit to the society.

The constant technological evolution is changing the way how the spectrum is being populated by the radio services, over time. The natural tendency, which is also the desirable, is that the newest and most sophisticated systems could replace the oldest and outdated technologies. These continuous optimization efforts – driven by an increasingly efficient use of spectrum – allow the release of a few slices of spectrum, often quite valuable and attractive to the stakeholders, which could accommodate, in the future, new applications or services, according to the identified needs. The latest *digital switchover*, whereby the former analogue TV system was replaced by the DTT, released a considerable portion of high quality spectrum, in the UHF band (470 – 862 MHz), and few channels in a couple of VHF bands: I (47 – 68 MHz) and III (174 – 230 MHz). This process is known as **Digital Dividend**. [41] Due to its strategic nature, it is also commonly considered the “*golden opportunity*” or the “*once in a lifetime opportunity*”.

By adopting the European DVB-T standard, with MPEG-4 video compression, the broadcasters can currently deliver, through a multiplexer, up to 8 or 9 standard definition (SD) TV channels (depending on the applied compression rates), using just one radio channel (7 or 8 MHz of bandwidth), where previously only a single analogue TV channel had fitted. This is beneficial, not only for the broadcasters – since they can provide more TV channels using much less spectrum –, but also for the mobile operators, giving them the opportunity of delivering new wireless broadband (WBB) communication services, which will contribute to enliven the economy and the social growth.

The blocks of spectrum released by the switch off of analogue TV are extremely valuable, owing to very good characteristics (*frequency response*) of the propagation channel, in this spectral region, offering a remarkable trade-off between **capacity** (*bit rate*) and **coverage** (*area*).

It is not yet fully defined the final destination for this huge amount of spectrum that became free (the DD). A part of it (up to TV channel 60, i.e., up to 790 MHz) is already being used by the

DTT, and the upper UHF sub-band – also known as the **800 MHz band**<sup>17</sup>, or *the first digital dividend (DD1)* – is already used by the 4<sup>th</sup> Generation (4G) broadband mobile communication systems, typically, Long Term Evolution (LTE), taking into account international resolutions [12] and European decisions [42]. In a medium-term time frame, it is also expected that the **700 MHz band**<sup>18</sup>, the so-called *Second Digital Dividend (DD2)*, will be allocated, on a primary basis, to IMT, for WBB service provisioning. [43] This will entail the migration of the DTT channels, currently assigned within the DD2, to lower channels (below channel 49, i.e., 694 MHz). It is hoped that this band (DD2) will be assigned across the EU before 2020.

According to the European Commission Decision 2010/267/EU [42], the above mentioned 800 MHz band, which was previously allocated to the analogue TV broadcasting service as shown in Fig. 2.3, is now exclusively assigned to electronic communications services on a basis of technological neutrality.

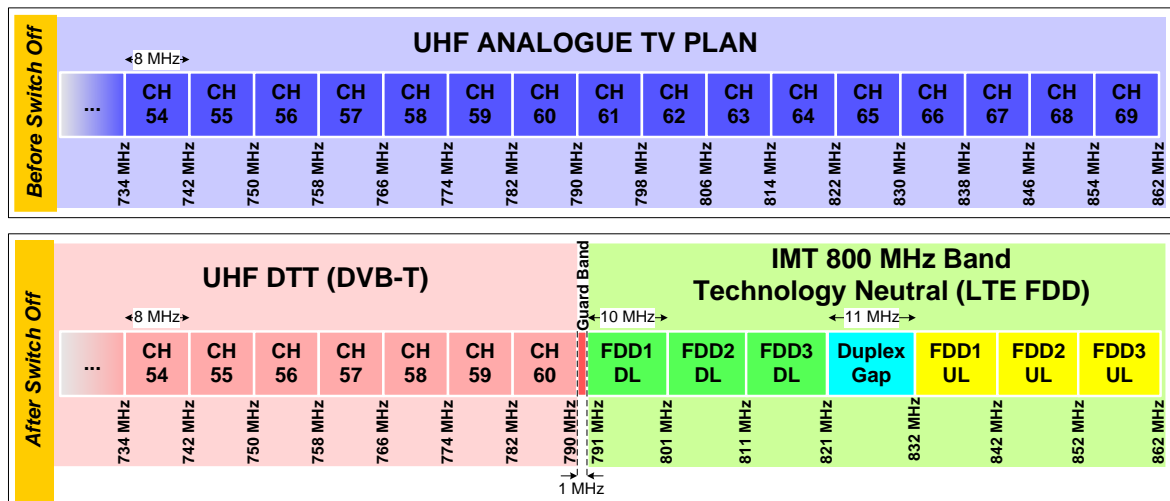


Fig. 2.3. UHF (800-MHz band) plan before and after the analogue TV switch off.

The arrangement of frequencies intended for the DD1 established by this decision consists of an allocation of two blocks of 30 MHz width, separated by a duplex gap of 11 MHz. These two 30 MHz spectral blocks are paired by channels of 5 MHz, within the upper band initially allocated to DTT. The lower limit of this 800 MHz band was left with a guard band of 1 MHz (790-791 MHz).

<sup>17</sup> The **800 MHz band** (DD1) ranges from the old TV channel 61 to the 69, i.e., from 790 to 862 MHz, a total of 72 MHz of bandwidth. Although, in practice, only 60 MHz are effectively used, since the remaining 12 MHz are reserved for guard bands.

<sup>18</sup> The **700 MHz band** (DD2) includes the current DTT channels: 49 to 60, i.e., from 694 to 790 MHz.

In Europe, after the auctions of the 800 MHz band, three paired spectrum blocks of 10 MHz width were generally assigned to different operators for the deployment of LTE networks in Frequency Division Duplex (FDD) mode [44]. In this frequency configuration, the blocks intended for the downlink (DL):  $3 \times 10$  MHz are located between 791 and 821 MHz, whereas the blocks associated with the uplink (UL):  $3 \times 10$  MHz are positioned between 832 and 862 MHz.

But the reallocation of resources does not always imply the release of spectrum. Sometimes, simply by putting other radio services in the same bands already assigned to a particular user, it is more than enough to achieve a desired optimization and, this way, drawing greater benefits for all stakeholders. These processes of reorganization of the spectrum and the consequent redefinition of radio services are generically known as “**refarming**”. [17]

However, it is necessary to create, in advance, the relevant legislation to allow such changes. With this aim, the Directive 2009/114/EC [45], which amended the Council Directive 87/372/EEC [46] (also known as “GSM Directive”), together with the Commission Decision 2009/766/EC [47] on the harmonization of the 900 MHz band, established the appropriate conditions for the “**GSM Refarming**”.

Those legal provisions introduced significant alterations to the 900 MHz and 1800 MHz bands, which were exclusively assigned to the Terrestrial Mobile Service, in accordance with the GSM specifications and standards. Since then, both bands can be used for other purposes, namely, to provide services carried by the UMTS technology or other systems, as long as they are able to coexist with GSM. The above measures have somehow contributed to add some more flexibility to the way as the spectrum had been used so far.

## **2.3 New Trends in Spectrum Management in Europe: Innovative Models and Methodologies**

The economic growth of the EU should be founded on solid technological grounds, with modern and efficient information and communication systems. The increasing development of wireless broadband technologies, and the need for narrowing the digital divide (territorial cleavages) – by delivering high speed broadband services to remote regions –, **have become even more pronounced the importance of an easier access to the radio spectrum.**

The EC believes that the traditional models of spectrum management will no longer be the most appropriate; having presented studies [48] to demonstrate a large extent of potential gains,

if greater **flexibility** would be allowed in the allocation and use of spectrum. Those reflections also point out the desirable exploitation of valuable synergies between the **secondary spectrum trading**<sup>19</sup> and its **liberalization**<sup>20</sup>, reinforcing the necessity of introducing more liberal and flexible rules, as the bottom line. [15]

### 2.3.1 Flexibility

Traditional models of spectrum management were characterized by their strong rigidity, targeting the maximization of the technical efficiency. For that reason, they offered significant predictability. Typically, a predetermined band was allocated to a specific radio service, and each service was closely related to a specific technology. Thus, the most common technical parameters, such as modulation, bandwidth, transmitted power, etc., were very well known in advance, and thus one could easily find homogeneous radio services and systems in expected bands, grouped according to some common unchangeable characteristics. [49]

If, on the one hand, this allows to predict, with a high degree of accuracy, the behavior of the radio systems and ensure the necessary compatibility between technologies and services; on the other hand, there is little room for innovation.

In addition, these models showed to be quite time consuming for the regulators. Since they were usually static, any change in the planning or in the use of the spectrum, in a given band, would demand new studies, possibly, complex or elaborate. These decisions were mostly taken by the national administrations, which did not have, neither a great margin of flexibility, nor a general overview of the constant and quick technological and economic evolution, within Europe, in order to keep pace with the latest trends and developments. The fragmentation of national policies may have influenced technological changes, which may have resulted in lost opportunities and increased costs. Therefore, the highest benefit that can be obtained from the spectrum use may not correspond to that which has been followed, based on the regulator's decision. This might be disadvantageous, particularly, if incomplete information is collected or misinterpreted. [15]

The pressures coming from the industry, claiming more flexibility, cannot also be ignored, especially, whenever innovation exists. It is considered of paramount importance to offer

---

<sup>19</sup> "Transfer of spectrum usage rights between parties in a secondary market". [48]

<sup>20</sup> "Relaxation of restrictions on the services and technologies associated with spectrum usage rights". [48]

incentives to manufacturers and operators to plan, over the course of a realistic timeframe, new investments and products.

In conclusion, the **lack of flexibility** in the use of spectrum may result in a problem of **poor economic efficiency**, and can also be **detrimental to the economic benefits**. In other words, and quoting from [15]: the “*economic efficiency requires spectrum to be used in the way that delivers highest value to society*”.

Hereupon, it is fundamental to realize ***what will have to change***, and ***how that change will work in practice***.

By capitalizing on the *golden opportunity*, created by the *digital dividend*, the European decision makers have the right chance to improve the access to the radio spectrum, and thus, to ensure a more efficient and flexible spectrum management. This can be achieved by promoting greater use of unlicensed spectrum (license exemption, under certain technical conditions), by removing the access restrictions deemed unnecessary, by allowing the effective transfer of spectrum usage rights, by implementing a more efficient and better coordinated mechanism to deploy wireless systems beyond the national frontiers, at a considerable cross-border scale within Europe.

Given the above scenario, there is a strong need for coming up with a common European approach capable of *maximizing economic and social benefits, streamlining and simplifying the access to spectrum resources*, provided that certain criteria of **interference** are met, *in order to not harm counterparts systems*. The EC has developed such targeted approach, termed **WAPECS**, which stands for *Wireless Access Policy for Electronic Communications Services*.

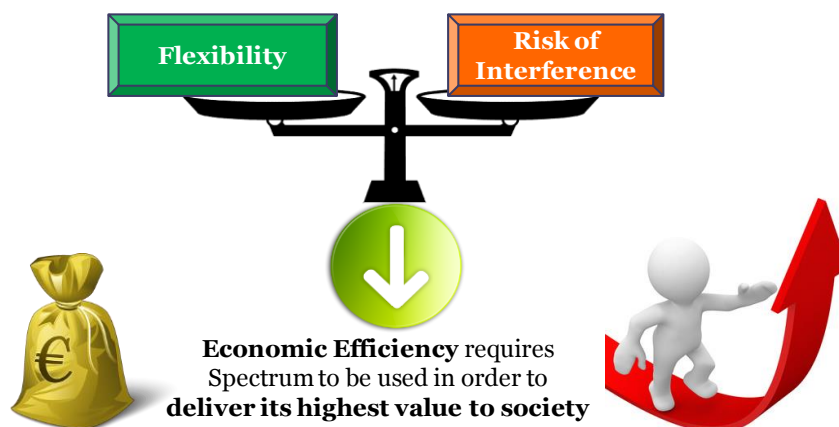


Fig. 2.4. Illustrated Concept of WAPECS.

### 2.3.2 WAPECS

The WAPECS is thus an approach or framework that is intended for the provision of Electronic Communication Services (ECS), in a limited number of frequency bands<sup>21</sup>, harmonized between the EU Member States. Using the identified bands, the operators might offer ECS, through Electronic Communication Networks (ECN), on a basis of **neutrality**, whether *technological*, or *of services*, ensuring the strict compliance with technical requirements to **avoid interference**. The WAPECS should contribute to an effective and efficient use of spectrum and the associated authorization conditions shall not distort competition. [15], [50], [51]

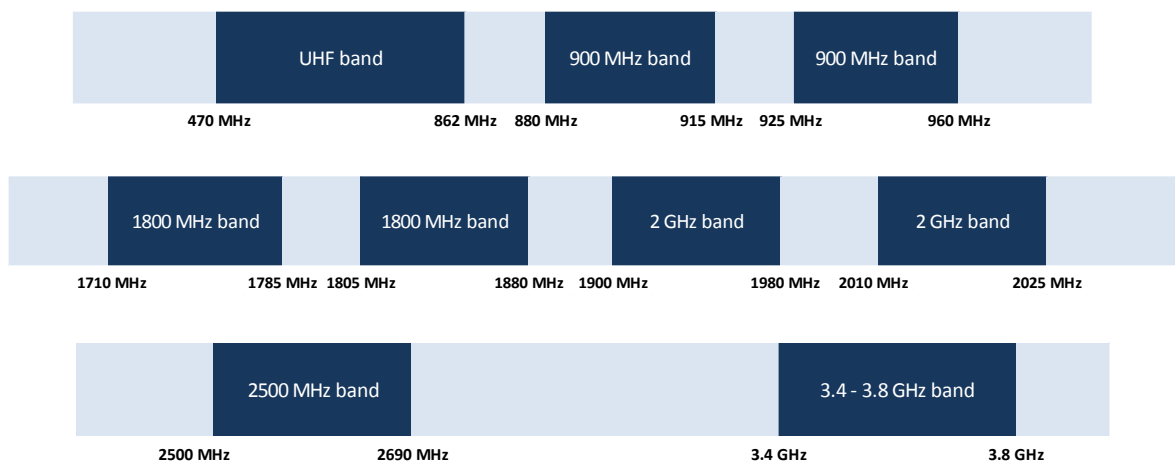


Fig. 2.5. WAPECS Bands.

The overall feasibility of WAPECS, as well as generic concepts, deployment scenarios, real earnings, economic impacts, implications of the introduction of new models in how the spectrum has been conventionally managed, including proposals of appropriate mechanisms for interference control, were initially studied by CEPT, in response to the Mandate<sup>22</sup> [14] of 5<sup>th</sup> July, 2006, issued by the EC.

<sup>21</sup> **WAPECS bands:**

[470, 862] MHz;  
 [880, 915] MHz / [925, 960] MHz, the so-called “900 MHz bands”;  
 [1710, 1785] MHz / [1805, 1880] MHz, “1800 MHz bands”;  
 [1900, 1980] MHz / [2010, 2025] MHz, “2 GHz bands”;  
 [2500, 2690] MHz;  
 [3.4, 3.8] GHz.

<sup>22</sup> Mandate to CEPT to develop *least restrictive technical conditions for frequency bands addressed in the context of WAPECS*. [14]

### 2.3.2.1 Neutrality

The WAPECS has introduced the notorious novelty of making either the technology or the final applications or services, provided by the operator, independent of the frequency band, and therefore neutral, rather than in the past. Notwithstanding the basic restrictions laid down or any other proportionate, transparent and non-discriminatory restrictions which might have resulted from public consultations or periodical revisions.

#### 2.3.2.1.1 *Technological Neutrality*

The *technological neutrality* principle gives to the operator the freedom of choice to adopt the technology that is considered as the most appropriate, according to their own criteria.

Formally, it is defined by [51] as:

*“For each WAPECS frequency band, provided that the associated electronic communications network complies with the relevant spectrum technical requirements, technological neutrality and flexibility in future use of the spectrum should be ensured. For justified reasons, in line with recital 18<sup>23</sup> of the Framework Directive, certain technological requirements may be imposed by Member States or at the EU level.”*

In the sense that is described herein, and despite the unquestionable freedom of choice that is introduced, all radio systems, working under the *technological neutrality* concept, are still subjected to a collection of minimum technical conditions.

In practice, the technical constraints will correspond to: the *boundary conditions* to be observed; the *compatible network scenarios*; the *allowed reference systems*; and last but not the least, the application of *spectral masks*, which were previously defined, the so-called “**Block Edge Mask**” (**BEM**) approach.

Besides all the above, there are some basic and generic restrictions, which must be safeguarded, in particular [53]:

- a) to avoid harmful interferences;

---

<sup>23</sup> **Recital 18 (Framework Directive 2002/21/EC):** “The requirement for Member States to ensure that national regulatory authorities take the utmost account of the desirability of making regulation technologically neutral, that is to say that it neither imposes nor discriminates in favour of the use of a particular type of technology, does not preclude the taking of proportionate steps to promote certain specific services where this is justified, for example digital television as a means for increasing spectrum efficiency.” [52]



- b) to provide adequate protection against the exposure of population to electromagnetic fields (EMF);
- c) to (technically) provide quality of service (QoS);
- d) to ensure the maximization of radio frequencies sharing;
- e) to safeguard an efficient use of spectrum;
- f) to guarantee the achievement of a specific purpose of general (public) interest in accordance with the restrictions of service neutrality.

#### 2.3.2.1.2 *Service Neutrality*

Similarly, the *service neutrality* gives the freedom to use the spectrum (within the WAPECS bands) for any electronic communication service, and it is actually stated [51] as follows:

*“Any electronic communications service (ECS) may be provided in any WAPECS band over any type of electronic communications network. No frequency band should be reserved for the exclusive use of a particular ECS. This is without prejudice to any obligation to provide some specific service in a specific band or sub-band, e.g. broadcasting and emergency services.”*

In such a context, the RSPG clarifies that different networks should be able to provide the same or differentiate ECS, in the sense of the Framework Directive [52], such as *IP based services, multimedia, multicasting, interactive broadcasting, datacasting*, using a single or multiple frequency allocations, via *mobile, portable or fixed access*, supported by *terrestrial* and/or *satellite* platforms and a plenty of technologies to seamlessly deliver the services to the end users. [51]

The basic and generic restrictions to be applied to the *service neutrality* are [53]:

- a) to safeguard the integrity and safety of human life;
- b) to promote social, regional and territorial cohesion;
- c) to prevent inefficient use of spectrum (radio frequencies);
- d) to promote cultural and linguistic diversity, as well as, the pluralism of the media, e.g., by provisioning radio (sound) and television broadcasting services.

### 2.3.2.2 Methodological Framework

The methodology [15] developed and proposed by CEPT begins by analyzing the market and likely trends to identify potential future uses of the WAPECS bands. This entails, whether the identification of candidate technologies to provide a target application or service<sup>24</sup>, or the individual frequency bands, which are available and may be used on a flexibility and neutrality basis.

In parallel, economic and technical studies are iteratively carried out, bouncing between both sides, until the convergence is satisfactory, i.e., when the optimal balance between economic profits and spectral efficiency is achieved. As the iterative process proceeds, the cost-benefit analysis to the economic potential of alternative applications/uses is being refined, taking into consideration the results provided by the compatibility studies (interference analysis). Thus, it is possible to find the most appropriate use for each band. As new most likely uses are emerging, candidate sets of technical conditions are being identified, to enable the coexistence of such technologies and systems.

When this dynamic sequence of actions tends to stabilize, in principle, a match, between the market pretensions and technical requirements, is about to be achieved. Therefore, it is considered plausible that the desired application/service can be provided using WAPECS bands.

Reaching this well thought-out stage of the overall procedure, it is crucial to enforce minimal technical conditions and a set of usage rights, which should maximize the flexibility on the spectrum allocation, minimizing the risk of interference.

This process should transparently involve, in a cooperative environment, regulatory bodies, manufacturers, potential operators and bodies of standardization.

#### 2.3.2.2.1 General Assumptions

The studies conducted by the CEPT, to investigate the feasibility of introducing *flexibility* in spectrum management, had to combine a multitude of data inputs from multidisciplinary areas (economics, statistics, spectrum engineering, law), in order to come up with realistic scenarios of analysis. These inputs are usually introduced as assumptions, and the following stand out among the fundamental principles that underpinned the WAPECS methodology [15]:

---

<sup>24</sup> In response to market demands, taking into account the willingness to pay of the users.

- **Impact of the market analysis on the technical outcomes**

The validity of the technical outcomes is conditioned by the assumptions provided by the market analysis, based on information available at the time. If meanwhile, either technology or applications evolve significantly, the initial assumptions, used to define technical constraints (to control or mitigate interference), **may no longer be appropriate** when applied to a new reality. The corollary of this is that the least restrictive conditions, to be enforced, are just right for a specific WAPECS band and for a given technology or group of applications.

- **Base stations**

If base stations are integral parts of a given technical solution under study, it is assumed that the respective networks are individually licensed, and particular technical conditions will be imposed through specific conditions enclosed in the operator's license.

- **Terminal equipment**

The way of laying down specific technical conditions for terminal equipment is not as explicit as in the previous case. Notwithstanding, the basic principles of WAPECS seem to be convergent with the relevant harmonized standards, which is strongly recommended.

- **R&TTE Directive**

The WAPECS is aligned with this important policy instrument, which seeks to establish essential requirements for radio terminal equipment, by fostering innovation and the design of radio interfaces able to provide: *increasingly better performances, an effective and efficient use of spectrum, the optimization of the spectral allocation needs* and, of course, **preventing harmful interferences**. The R&TTE directive also addresses the rules of *placing radio equipment on the market and putting it into service*, and defines the obligations, to which operators and national Administrations are bound, regarding the interconnection to compatible networks.

- **Future changes and possible negotiations between operators**

Given the flexible nature of the methodology, it is assumed that future technologies and applications will not require substantial changes to the technical conditions initially set, reducing the regulatory intervention. From this perspective of simplification, a cooperative environment is strongly stimulated, in order to facilitate negotiations between license holders, to identify alternative options or propose changes to the

conditions attached to their licenses<sup>25</sup>. Regardless, the amendment processes which may occur will be supervised, and each change will be sanctioned by the regulator.

– **Boundary conditions**

The boundary conditions to the technical analysis of the WAPECS methodology are influenced by the following key aspects, which will be addressed in the next subsections.

- i. Expected **radio network** scenarios;
- ii. Non-WAPECS **services to be protected**, both in-band and in adjacent bands;
- iii. Technical specifications of **transmitters** (*e.g., spectral efficiency, transmitted power, etc.*) and **receivers** (*e.g., selectivity and sensitivity*), which are adopted, taking into account the technological evolution and reasonable expectations;
- iv. Levels of (in-band) **interference** that license holders are willing to accept.

#### 2.3.2.2.2 *Scenarios of Application*

Generically, the network scenarios to be considered are **technological and service neutral**; and thus, as comprehensive as possible, provided that the radio network is compatible with the WAPECS approach.

There are four basic network scenarios, which result from the combination of the medium access techniques (*transmission only* or *transmission and receiving*) and the intended mobility on the user side (*fixed* or *mobile*).

– **Transmitter/Base Station (BS)**

- ✓ **Simplex** (Downstream): *e.g., broadcasting*
- ✓ **Duplex** (TDD or FDD): *e.g., mobile systems such as GSM, UMTS or LTE*

---

<sup>25</sup> This could be useful whenever an operator wishes to introduce modifications in their network, for instance, to increase the density of base stations beyond the limits set by the license. In such case, the intended collaborative relationship would allow negotiations between neighbor operators (using adjacent geographic areas and/or adjacent channels). If, after considering the impact of such changes, they are regarded as viable and universally accepted, the deployment can be undertaken. [15]

– Receiver/Terminal Station (TS)

- ✓ **Fixed:** e.g., broadcasting, Fixed Wireless Access (FWA)
- ✓ **Mobile:** e.g., mobile systems: GSM, UMTS, LTE or Digital Video Broadcasting – Handheld (DVB-H)

The four basic scenarios of the WAPECS approach are illustrated in Table 2.1, which emphasizes all possible combinations. Other more specific scenarios may be derived from therefore.

		Receiver/Terminal Station	
		Fixed	Mobile
Transmitter/ Base Station	Simplex (Downstream)	Fixed Simplex	Mobile Simplex
	Duplex (TDD or FDD)	Fixed Duplex	Mobile Duplex

Table 2.1. The four basic scenarios of the WAPECS approach.

The following illustrations present some likely basic radio scenarios.

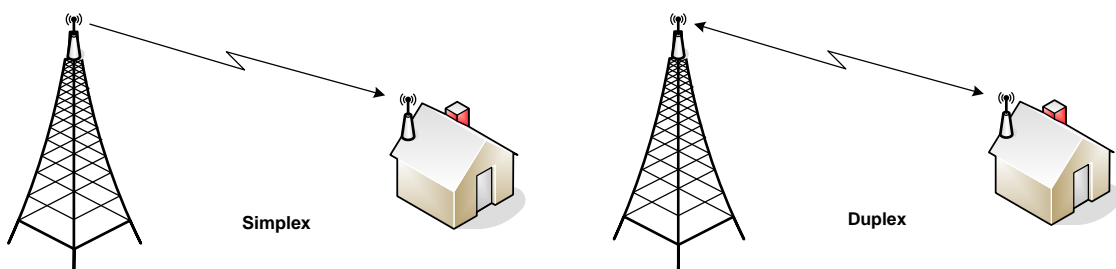


Fig. 2.6. Fixed reception scenario (location may be known or unknown).  
(e.g., using a mobile TS or a broadcasting receiver)

Source: CEPT, Report 19 [15]

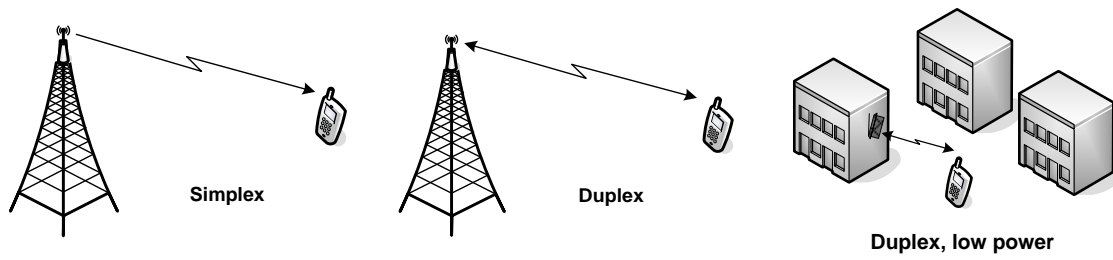


Fig. 2.7. Mobile receiving scenario (unknown location).  
 Source: CEPT, Report 19 [15]

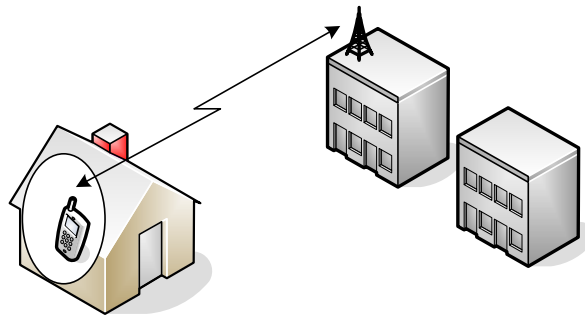


Fig. 2.8. Mobile indoor coverage scenario (provided by outdoor or indoor BS).  
 Source: CEPT, Report 19 [15]

Radio networks based on *point-to-point* topologies and *mesh networks* are **excluded** from the WAPECS scope.

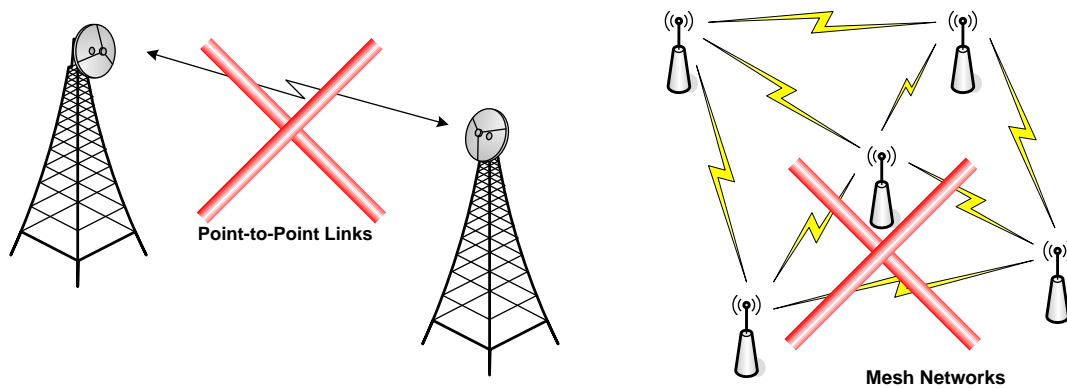


Fig. 2.9. Radio networks **incompatible** with WAPECS (Point-to-Point and Mesh Networks).

### 2.3.2.2.3 Reference Systems

The definition of compatibility criteria, to be met by legitimate systems in specific WAPECS bands, depends on the **assumptions** made, by considering likely systems and scenarios. Therefore, it should be stressed again that *all constraints thus imposed* are **very dependent** on the **set of assumptions** resulting from the *market analysis*.

In order to derive appropriate technical constraints – capable of ensuring the necessary compatibility –, both for adjacent and co-channel; some **reference systems** should be considered and detailed. The following major parameters must be taken into account for the **network scenario** under evaluation, which will also outline a given WAPECS reference system: **transmitted/radiated power levels**; **type of coverage**: *outdoor, indoor*; **terminal stations nature**: *fixed, nomadic or mobile, known or unknown location, etc.*; **density of transmitters or BS**: *dense urban, sparse rural, etc.*; **height of the stations**; **medium access scheme**: *FDD and/or TDD*. Similarly, for the **receiver's performance**, assuming reasonable expectations about future devices, the following parameters must be set: **sensitivity**, **selectivity** and **susceptibility/immunity to interference**. But there are other fundamental band sharing issues to be considered, in order to define acceptable interference levels. The peculiar **propagation characteristics** of each WAPECS band can affect the choice of a service to be provided. This influences significantly the coverage area, the density of transmitters, the bit rates to deliver to end users, etc. Moreover, if there are already other WAPECS systems in the same or in adjacent bands, suitable measures should be taken to prevent harmful interference and ensure the desired co-existence. [15]

In conclusion, a **reference system** collects and provides, among others, the above input parameters for the compatibility analysis, which will set the necessary technical conditions to be met by the final systems that will use the WAPECS bands. Those actual implemented systems may adopt **any technology**, *as long as it complies with the conditions laid out*.

### 2.3.2.2.4 Definition of Least Restrictive Technical Conditions

The technical framework for identifying least restrictive conditions to which radio systems should comply in WAPECS bands, developed by CEPT, is extensively detailed in the Report 19 [15]. It starts by studying – from comprehensive and cross-disciplinary perspectives – the applicability of 6 different models of analysis, which are summarized in Table 2.2. The purpose of considering such a wide range of models is to collect an extended set of technical restrictions – some of them, more stringent than others, depending on how they were obtained (model) – in

order to validate a final approach, capable of ensuring an optimal compromise between *flexibility* and *spectral efficiency*, preventing harmful interferences. The final option, to be adopted, should still preserve the most relevant constraints, which have resulted from all the above models.

Model		Description
Model 1	Traditional	Traditional compatibility and sharing analysis method (e.g., ACLR, ACS, ACIR)
Model 2	2A BEM (Transmit Power)	Block Edge Mask (BEM) model based on the transmit power BEM
	2B BEM (EIRP)	Block Edge Mask (BEM) model based on the EIRP BEM
Model 3	PFD	Power Flux Density (PFD) mask model based on the determination of aggregate Power Flux Density
Model 4	PSD	Power Spectral Density (PSD) transmitter masks based on the determination of aggregate PSD (transmitted power spectral density) within a specified area
Model 5	BEM-EIRP & PFD / PSD & PFD	Hybrid model based on a combination of Models: 2 and 3, or 3 and 4
Model 6	Space-Centric	Space-centric model

Table 2.2. Models for defining Least Restrictive Technical Conditions.  
*Source: CEPT, Report 19 [15]*

Each model has its own specific nature, and thus, advantages and disadvantages, as will be seen below in overview.

#### – Model 1: Traditional Compatibility and Sharing Analysis Methods

This has been the traditional model, used for years in spectrum planning. Its results are very reliable, providing good radio protection against counterpart systems operating in the same or in adjacent bands. The method relies on analytical calculations of widely disseminated figures of merit, such as: *Adjacent Channel Leakage Ratio (ACLR)*, *Adjacent Channel Selectivity (ACS)*, *Adjacent Channel Interference Ratio (ACIR)*, etc. It however requires a deep knowledge, in advance, of the involved radio systems



(transmitters and receivers). It is a well proven approach, but its main flaw is to use specific parameters of a given technology, which makes it non-neutral and inflexible. Any future change in technology could nullify its results.

– **Model 2: The Block Edge Mask (BEM) Approach**

The BEM model is the most generic approach (among the 6 considered in this study), being completely transparent in relation to the technology to be used in a given block of spectrum. It is very flexible, which gives to the operator tremendous freedom of choice; leaving the decision up to the operator, regarding the most appropriate technical solution to make use of the allotted spectrum. This is the solution of choice for assigning blocks of spectrum, without having to specify which technology should be used. In this approach, **spectral masks**<sup>26</sup> are defined, to which radio systems must comply, in order to ensure their coexistence and control interference. A BEM is derived from an initial set of assumptions made for the corresponding reference system, which is representative of the types of systems that are most likely to be deployed. This model is mostly guided by the characteristics of transmitter systems, but can also be complemented with other types of models or analysis, in order to include specific requirements of receivers (receiving conditions).

– **Model 3: Power Flux Density (PFD) Masks / Aggregate PFD Approach**

This method is particularly appropriate to define **geographical compatibility conditions**, since it is focused on the analysis of the aggregate effect of power that is received at a given user's location. By assessing the cumulative impact of different radio sources on the *victim's* side, the co-channel interference, between systems in different geographical areas, can thus properly be studied. The actual density of deployment and the geographical location of network elements must be detailed in advance, for the above purposes. Therefore, the Aggregate PFD is an entangled approach that entails very complex calculations and measurements, which makes it difficult to apply in practice. However, it defines quite well how the networks of different operators can, spectrally and geographically, coexist. If the basic conditions of interference are well defined, future changes to the networks may be facilitated, through negotiations, between licensed operators, duly submitted to regulatory approval. This model can hopefully be combined with the BEM approach.

---

<sup>26</sup> A **spectral mask** establishes the maximum allowed limit (upper boundary) of power spectral density (expressed, for example, in W/Hz units) within the radio systems must remain, whether in-band or out-of-band. If the power levels are taken out at the *output of a transmitter*, the BEM is termed “**BEM – Transmit Power Mask**” (**Model 2A**); otherwise, if they have as a reference the *power that is radiated by an isotropic antenna*, the BEM is called “**BEM – EIRP Mask**” (**Model 2B**).

– **Model 4: Aggregate Power Spectral Density (PSD) Transmitter Masks**

This approach defines a maximum aggregate level of power spectral density, which is admissible within a given geographical area, through a PSD transmitter mask. The mask limit is calculated taking into account the cumulative effect of emissions, from all transmitters confined to a specified area, concentrated within a particular radio channel (or band), and respective density of deployment. Thus, a PSD mask<sup>27</sup> is set for each individual emission (transmitter). The total allowable PSD threshold can be derived from each individual mask, by multiplying it by the expected number of transmitters. On the one hand, if spectrum usage rights are defined according to PSD transmitter masks, within a given region, the operators can, easily and flexibly, increase or decrease the density of deployment of a network, just by acting on the mask (by adjusting the scale factor). On the other hand, possible changes on the access schemes (e.g., FDD to TDD, or vice-versa) may require a reassessment of the initial restrictions. Moreover, it can be difficult to implement, since essential requirements of terminal stations may not be adequately addressed. For that very reason, this model might hopefully be combined with the Aggregate PFD approach.

– **Model 5: Hybrid Approach**

The Hybrid Approach combines some of the above models to produce interference studies with more solid grounds, covering both adjacent channel and co-channel analysis, between radio systems operating in the same or in distinct geographical areas.

Models that impose restrictions on the radiated power in adjacent bands, such as **BEM-EIRP (Model 2B)** and **Aggregate PSD Transmitter Mask (Model 4)** turn out to be more adequate to deal with adjacent channel interference than co-channel interference, for radio systems in the same geographical area. Complementarily, the **Aggregate PFD Approach (Model 3)** – fairly widespread in frequency planning – is preferable in co-channel compatibility analysis, between radio systems operating in different geographical areas.

In order to merge the best virtues of these models, two sub-models were created:

- **Hybrid Model 5A:** BEM-EIRP (Model 2B) + Aggregate PFD (Model 3)
- **Hybrid Model 5B:** Aggregate PSD Transmitter Mask (Model 4) + Aggregate PFD (Model 3)

---

<sup>27</sup> The reference power levels, to be used, may be defined, for example, at the output stage of the transmitter, i.e., the power delivered to the antenna.

### – Model 6: Space-Centric Management

The Space-Centric<sup>28</sup> model is an innovative paradigm to deal with new technologies and services, without having to constantly redefine the conditions for spectrum use. In this approach, the spectrum usage rights have indirect mechanisms – the so-called **Guard Space Isolation**<sup>29</sup> – and (practical) technical and legal instruments to ensure radio protection to the users. The set of rights explicitly limits the radiated power (maximum EIRP of the devices), implicitly defining the receiving conditions. This allows any operator or user to self-manage the interference between his new devices and the other new ones, operating under different licenses or outside that “*spectrum space*” – without negotiations, just by adjusting the necessary *guard space isolation* set by the usage right. The model assumes the existence of a centralized online device data base to support processes of coordination and interference management, between new and legacy services.

After conducting an extensive number of detailed technical studies on this field, CEPT **gave its assent to the introduction of flexibility** in the bands identified by the Mandate [14] of the EC, in the context of WAPECS.

CEPT also concludes that, among all the approaches previously contemplated, **the BEM model/concept is the best suited to define the least restrictive technical conditions** in these bands.

Notwithstanding the generic nature of the model, not always all parameters or technical restrictions, originated by the remaining models, can properly be accommodated or fully addressed by a mere BEM. However, during the validation stage of a BEM – which involves the compatibility analysis, and thus is an important part of the overall process of defining minimal technical conditions (summarized below) – these parameters are somehow considered and incorporated by the reference systems.

---

<sup>28</sup> It has been used in Australia in the last few years.

<sup>29</sup> The *guard space isolation* is a device-centric management concept, from which the necessary coordination is studied (*distance* separation, *time* and/or *frequency* separation gaps), in order to reach an interference-free condition of operation.

### 2.3.2.2.5 Summary

The definition of least restrictive technical conditions, in the WAPECS bands, is iteratively developed over various sequential steps or phases [15], as shown by the flowchart of Fig. 2.10.

Firstly, the basic radio network scenario<sup>30</sup> is defined and the best suited WAPECS reference system is therefore assumed (**Phase 1**). Then, if the mentioned reference system is going to share the same band with a non-WAPECS system, a co-channel compatibility analysis (**Phase 2**) must be carried out. According to the results, a re-evaluation of the initial assumptions (reference system) should be reconsidered or not.

In the **Phase 3**, an out-of-band compatibility analysis between WAPECS and non-WAPECS systems is conducted. Once again, if the results show evidences of interference (incompatibility), a re-evaluation of the basic assumptions (reference system) must be done.

Since the reference system is stabilized and accepted (Phase 1), the results provided by the prior compatibility (in-band and out-of-band) analysis (Phases 2 and 3) are used to derive the appropriate Block Edge Mask (BEM), taking particularly into consideration out-of-block aspects (**Phase 4**).

All the above outputs (Phases: 2, 3 and 4) are then used together to derive the appropriate BEM, by considering co-channel compatibility aspects and geographical conditions (**Phase 5**). The resulting restrictions may also resort to other complementary models (e.g., Aggregate PFD).

Finally, the BEM is fully derived and ready for an ultimate review and testing. At this point, the national regulator is provided with a flexible and generic instrument which, if considered appropriate, could be used to set spectrum usage rights (**Phase 6**).

---

<sup>30</sup> Type of deployment, simplex or duplex, medium sharing/access techniques: FDD or TDD, expected cell radii and terminal stations density, output power of transmitters, antenna gains, typical receiver sensitivity, etc.

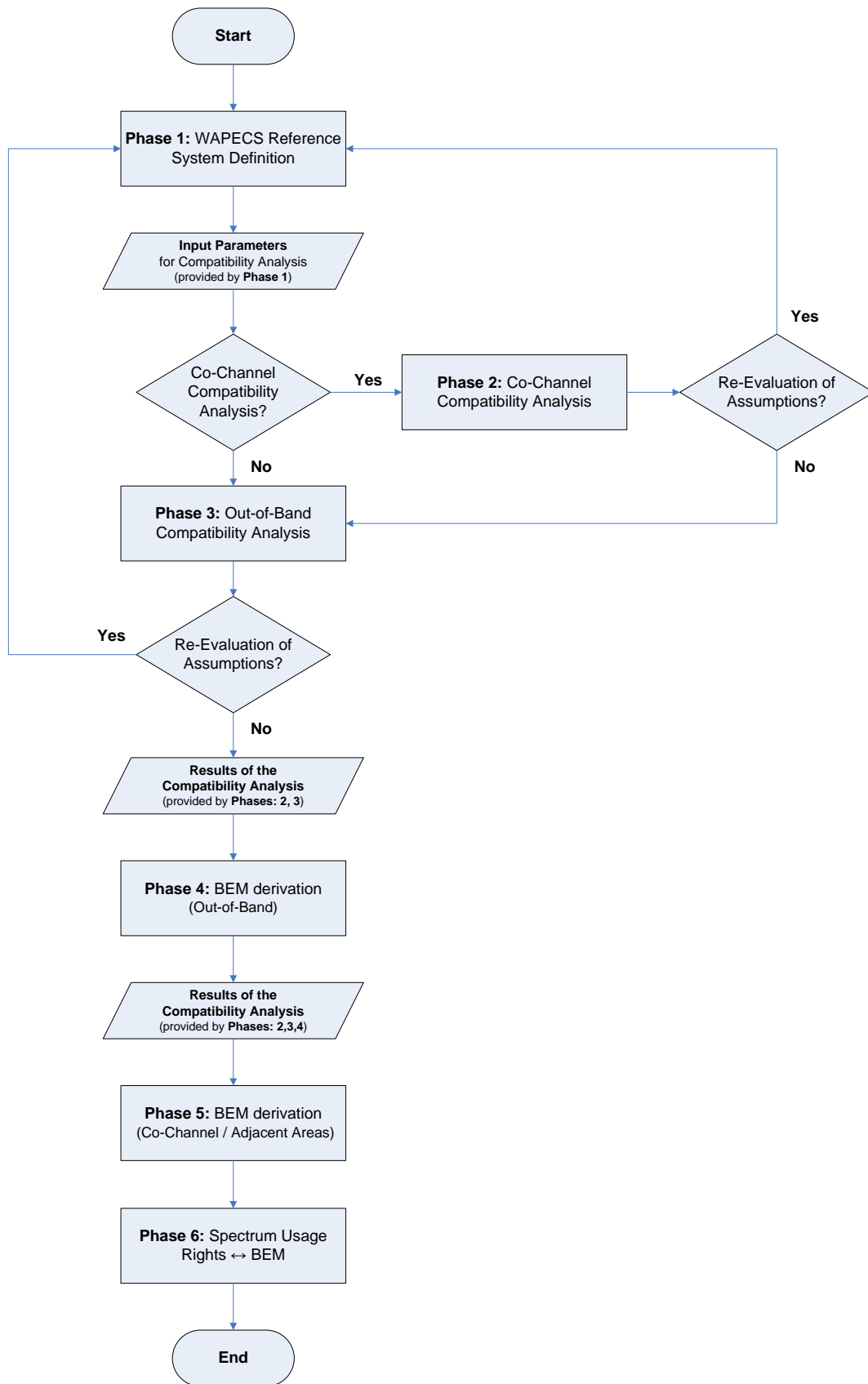


Fig. 2.10. Flowchart: General Approach applicable to the WAPECS bands.

### 2.3.3 Shared Use Models

The collective shared bands, with generalized access conditions, such as ISM bands, have been recognized as a cradle of excellence in innovation and development of promising wireless technologies. Such particular conditions, with no major barriers to forthcoming users, have vigorously encouraged the emergence of radio systems increasingly robust and resilient, even in the presence of interference in adverse environments.

Successful examples of such approach include WIFI – a widespread cluster of wireless local area networks (WLAN) technologies, based on the IEEE 802.11 standard, which has undergone successive amendments and effective improvements – but many other cases may also be pointed out.

For instance, *RFID systems, general purpose SRD*, typically license exempted low power devices (LPD), such as *radio remote controls* – for opening and closing garage gates, or for locking and unlocking car doors –, *baby monitors, wireless headphones, walkie-talkies* also known as *personal mobile radio* (PMR or PMR446), *alarm control and intrusion detection sensors, machine-to-machine* (M2M) applications, *intelligent transport systems*, such as automotive *short-range radars* (SRR) using ultra-wide band<sup>31</sup> (UWB) technologies, etc. [54], [55]

Given the track record of success, the above spectrum access models have inspired the EC to carry on with the work of promoting and fostering the introduction of new alternative technologies, even more efficient and flexible, in the way how they use the spectrum. [56] Accordingly, it was established as a *priority* the **shared use of spectrum resources** within the EU, being highlighted the important role played by innovation in developing solutions to meet the technological challenges and opportunities afforded by the proposed desideratum.

This can only be achieved collectively by involving diverse European actors (*legislators, national regulators, researchers, academics, and other stakeholders*) and engaging with them on the creation of a favorable regulatory environment to the innovation and deployment of such disruptive wireless technologies.

---

<sup>31</sup> UWB technologies are used to provide short-range wireless communications/applications, transmitting low power radio signals, which are spread across a very wide band. These systems originate a very low power spectral density, which is regarded as noise by the remaining applications. For that reason, this is considered an **underlay spectrum usage**. As the interference is kept under control, the coexistence of other applications is thus possible, above that reduced noise floor, which enables a collective or shared use of spectrum.

After identifying beneficial opportunities for spectrum sharing, some action points were put in place [54]:

- a) to create economic and legal incentives to develop and disseminate efficient spectrum sharing technologies;
- b) to authorize shared access to spectrum, with guaranteed usage rights, as a way of stimulating economies of scale very oriented towards innovative wireless technologies;
- c) to follow up and expand the harmonized license exemption regime.

Formally, from a regulatory standpoint, there are two distinct ways of spectrum sharing (detailed in the following subsections):

- **Collective Use of Spectrum (CUS)**
- **Licensed Shared Access (LSA)**

### 2.3.3.1 Collective Use of Spectrum (CUS)

The **collective use of spectrum (CUS)** or *license exempt approach* determines that a specific band can be simultaneously accessed by more than one user, in a given geographical area, and **no license is required**, as long as they respect the technical parameters dictated by the exemption conditions. [54]

The CUS regime confers, to all users, shared (or collective) access rights to a particular band, but introduces a certain degree of self-regulation in how the sharing is actually implemented. As a result, the interference management is somehow transferred to the users, who **must use the systems in accordance with the rules laid down by the regulator**, since, **only this way, an exemption is granted**. Otherwise, the users do not fulfill the exemption conditions, and thus they lose their access rights to the band. In addition, the use of such bands is allowed on a **non-interference, non-protection basis**, i.e., the systems, operating within those bands, must not cause interference to, and will not receive any protection from interference caused by, others.

If, on the one hand, the general authorization regime, underlying the CUS model, allows milder regulatory restrictions and remarkable benefits: virtually nonexistent entry barriers, assured access to the spectrum – an incentive to innovation of wireless technologies –,

streamlined licensing processes and reduced administrative burden (for regulator and user); on the other hand, it requires, from the users, increased responsibility and wisdom to use/share the spectrum as efficient as possible, and to manage interference on a best effort basis.

### 2.3.3.2 Licensed Shared Access (LSA)

The **licensed shared access** (LSA) regime concedes<sup>32</sup>, to the users, access rights to the shared spectrum, which are safeguarded by the regulator, by providing the necessary radio protection against harmful interference, which is critical to ensure an expected quality of service<sup>33</sup> (QoS).

Each user (licensee) needs a separate license – but not exclusive – to access a given band. However, the use of such band is subjected to particular sharing requirements, in accordance with the conditions articulated by the respective term of authorization. Sharing conditions should necessarily be attractive, by minimizing the risk of uncertainty, and offering a predictable and stable regulatory environment, in order to capture the interest of potential players, with willingness to invest in new operations, equipment and networks. [54]

## 2.3.4 Dynamic Spectrum Management

New and promising technologies have recently emerged [57], with great potential to shift the traditional paradigms – of spectrum sharing and access – towards opportunistic and dynamic approaches<sup>34</sup>, which take advantage of the non-permanent use or reduced activity of **primary spectrum users**<sup>35</sup> that are not always transmitting.

---

<sup>32</sup> For example, through an auction or beauty contest.

<sup>33</sup> This is a basic requirement, whenever a given user (or operator) has to honor any service level agreement (SLA) settled with a third party.

<sup>34</sup> Dynamic spectrum sharing (by secondary users) models.

<sup>35</sup> Also known as **primary systems** or **incumbent radio systems/services**.



#### 2.3.4.1 White Space

During such periods of inactivity, some frequencies are, locally and temporarily, free or vacant, which are under such circumstances termed as “**spectrum holes**” or “**white spaces**”<sup>36</sup> (WS). [9], [58], [59]

The spectrum planning of DTT multi-frequency networks (MFN) has to consider some radio channels that cannot be used locally, in certain regions, due to operational/technological constraints (interference management) and planning requirements (cell re-use factors and patterns). Those particular frequencies, which are deliberately kept unused by the DTT, are designated as “**TV white spaces**” (TVWS). [10]

With traditional and more conservative spectrum management models, the white spaces have been naturally “wasted”, and so, some spectral resources might have been unevenly used or, at least, they have not been fully exploited. The ultimate purpose of the dynamic models is precisely to overcome this “frailty”, by optimizing the use of certain frequencies, and thus, extracting from the spectrum, as much as possible, its maximum potential, but without jeopardizing the operation of primary radio services.

#### 2.3.4.2 Software-Defined Radio

The latest cutting-edge advances in **software-defined radio** (SDR) technologies have made possible the design of agile and reconfigurable radios (transmitters and/or receivers), in which, technical parameters (*e.g., frequency of operation, type of modulation, output power, filter bandwidth, selectivity, etc., and even technological standard*) can be changed (adjusted, tuned, updated), just by modifying the respective software. [57], [60] Such on-the-fly software operations enable to act dynamically on the hardware, promptly controlling the system’s final behavior and performance.

#### 2.3.4.3 Cognitive Radio

If to the above capabilities, some intelligence is added, so that the flexible radio (SDR) is aware of the surrounding environment, and if after being provided with relevant information – collected from the radio context – it is able to make its own decisions, then it becomes a “**cognitive radio**” (CR).

---

<sup>36</sup> Formally and according to [58], a “**white space**” corresponds to a given portion of spectrum, which is available, at a given time, in a particular geographical region, to be used by a radiocommunication application (system or service), *on a non-interference/non-protection basis in relation to other services with higher priority*.

Actually, a **cognitive radio system** (CRS) uses technology to learn from experience, and with that, it, autonomously and dynamically, defines its own operational state and policies. Additionally, with the gained knowledge, it also manages internal parameters and protocols to keep, in an orderly fashion, the desired coexistence/cooperation with other radio systems and networks, according to predefined rules. [60]

The flexibility – provided by such innovative features/capabilities – is fundamental, not only to dynamically address and manage interference, but also to monitor and adapt system's performance and/or QoS requirements towards contingences that can be found.

Although cognitive radio systems could find broad scenarios of use, including emergency and disaster relief situations, **they are particularly suitable for white space applications**. In this latter case, a CRS is specifically referred as a **white space device** (WSD). [59]

During the learning process, a WSD must carry out a survey, to be aware of the frequencies locally in use, to realize which ones might be potentially used (according to the activity record). This entails that **sensing capabilities** must be implemented by WSD, in order to detect the presence of protected radio services<sup>37</sup> or primary users, in each, potentially available, frequency.

#### **2.3.4.3.1 Spectrum Sensing**

If, in a particular situation, the WSD is provided with all the necessary information, which includes collected data (sensing) and a possible internal set of predefined priority/allowance rules (maybe, stored in a device database) –; in principle, it has the ability to manage its own operation. This type of sensing, which is done by the device itself, i.e., in standalone mode, is termed **independent**.

However, the above scenario might not be the general case of WS operation. For example, if the sharing rules, of the surrounding radio context, are dynamically evolving (e.g., driven by new regulatory requirements), the WSD internal database may not be prepared (updated) to get an overview of recent changes on such sharing policies. Therefore, the simple implementation of spectrum sensing mechanisms alone may not suffice to protect fundamental radio services; and thus, it is not yet taken for granted that such frequencies – identified by spectrum sensing – may be effectively utilized. Indeed, in some WS deployment models, the gathered (sensing)

---

<sup>37</sup> Passive radio services, such as **Radio Astronomy**, are not detectable by sensing, because they do not transmit. Consequently, frequency bands allocated to passive services must not be considered for WS purposes.

data must be somehow validated before the WSD is configured and ready to transmit<sup>38</sup>. Only after receiving the necessary acknowledgement, a WSD is authorized to use a specific frequency or group of frequencies.

All these command and control procedures must rely on **spectrum databases** or on alternative distributed mechanisms of authorization, such as **radio beacons**. [59], [61], [62]

The reliability of detection provided by sensing mechanisms can be considerably improved if additional information, collected by other nearby devices (WSD), is used<sup>39</sup>. The correlation of data, from multiple independent sources, dramatically increases the robustness of the solution. In such cases, where multiple nodes are involved, the sensing is called **cooperative**.

But sensing activity **does not cease** at the moment when a frequency is assigned to a WSD. As the channel may again be populated, by primary users, at any time, a WSD should keep sensing that frequency periodically (**re-sensing**), in order to identify the presence of possible emerging users.

Sensing techniques may vary according to the *principle of detection*, which is actually implemented. There are two major approaches: **energy detection** and **feature detection**. [59]

The *energy detection* technique is based on comparing a power level – which is measured in a given channel – with a reference threshold. The main advantage is to be independent of the type of radio system to be detected. However, the detector must be properly matched with the precise bandwidth of different signals. Furthermore, signals close to the noise floor are difficult to detect, by employing this technique, which requires a high sensitivity. On the other hand, noisier environments (i.e., with higher noise floor levels) may produce false positives.

Alternatively, the *feature detection* employs signal pattern recognition methods to detect channel activity (e.g., *correlation, blind source separation, cyclostationarity [63], modulation classifier, etc.*). In practice, this technique is focused on the identification of peculiar characteristics<sup>40</sup> of the signals, to detect them. The most remarkable advantage is to enable the detection of signals below the noise floor (processing gain). Nevertheless, this approach suffers

---

<sup>38</sup> Even when a radio channel is considered vacant, adjacent channels should be carefully scrutinized, in order to ascertain possible restrictions to be applied to WSD (e.g., maximum power levels).

<sup>39</sup> The exchange of information may occur directly between both WSD, or through an intermediary (e.g., database or beacon).

<sup>40</sup> Such distinct signal's signatures may include: **type of modulation** (e.g., *OFDM, BPSK, QAM, etc.*); **technology standard** (e.g., *DVB-T, LTE, GSM, UMTS, etc.*); **periodic signaling and control**, i.e., specific carriers such as **pilots** or expected **synchronism sequences/preambles** (e.g., *GSM: BCCH, UMTS: CPICH, DVB-T: TPS, DVB-T: G.I. – guard interval, etc.*).

from a heavy dependence upon specific signal characteristics, and a comprehensive internal database may be required. Even so, the adaptability to new technologies and signals – which may be implemented later by primary systems – may not be straightforward, especially if the internal database cannot be updated<sup>41</sup>. In that case, such emerging systems might go unnoticed (undetected).

#### 2.3.4.3.2 *Geolocation Spectrum Databases*

As already mentioned, spectrum databases play a key role in the functioning of WS systems. Such information systems must store *detailed, reliable, and updated* information. If, in addition, all this information is properly *geo-referenced*, a **geolocation spectrum database** (GSD) is available and ready to cooperate with WSD, managing WS fundamental operations. If so, **individual sensing** systems – embedded in WSD – **can be dispensed**. In this scenario, the database assumes all responsibility for control operations. The WSD has just to **report its position** (coordinates) to the GSD, and wait for the acknowledgement of resource allocation (frequency assignment). [59], [62]

The Major purposes of a **geolocation spectrum database** are summarized as follows:

- to support WS operations, by storing WSD activity records, which are of paramount importance to manage interference;
- to define and keep updated sharing policies and WSD working principles;
- to accept or reject additional users;
- to support individual or collective (cooperative) sensing.

This entails that a GSD must have a comprehensive set of data records about primary systems and WSD (actual and potential users); operating policies set by regulation (e.g., scheduling algorithms, restrictions in force at a given time); frequencies in use and potentially

---

<sup>41</sup> If the WSD is SDR base, this can be overcome, by updating the firmware.

usable; data regarding interference, system's performance, QoS management, load balancing (of users), etc.

#### 2.3.4.3.3 *Radio Beacons*

A **radio beacon** is a radio control signal that indicates whether a given WS may or may not be used. Thus, a WSD can only operate after having received the beacon's authorization. A control system, like this, significantly improves the performance of energy detectors, used for sensing purposes; particularly, if the signals – to be protected and detected – are near the noise floor.

Three types of beacons are considered by [59]:

- **Enable:** if the beacon is activated, the channel is ready to be used by the WS;
- **Disable:** if the beacon is activated, the channel is occupied, and thus, it cannot be used by the WS;
- **Pilot Channel:** identification of TV channels, locally, in use, based upon expected control (synchronism and signaling) information, extracted from broadcast DTT signals (typically, DVB-T or DVB-T2).

A WS operation based on such a paradigm requires a network of radio beacons with a reasonable coverage area and density, which may have considerable costs of roll-out, operations, administration and maintenance (OA&M).

#### 2.3.4.4 *Likely Business Models*

The foregoing innovative conceptions and technological solutions have demonstrated substantiated potential to pave the way for some novel dynamic spectrum management business models. This brief section intends to provide an insight into some key ideas to identify potential market niches and, at the same time, to promote a brief reflection on the most likely business models and plausible application scenarios. [64] In fact, such state-of-the-art paradigms are likely to be used to support market mechanisms able to detect, in nearly real-time or even in

real-time, the actual value of the spectrum, in a given location, at a given time, according to acceptable<sup>42</sup> levels of interference or QoS standards (to be defined/agreed). Following this line of reasoning, a spectrum band comparator (e.g., a web portal) might be deployed, in order to provide, at each instant, the current value of each assignable channel and respective interference parameters<sup>43</sup>, giving the user the opportunity to choose, from among the options available, which suit him better.

An updated information system like this might be inductor of future spectrum market transactions; but additional synergies can be reached, if combined with the LSA regime described previously. If such facilities exist, then new dynamic/flexible spectrum management models may be thought up, for instance, by considering different types of users – sharing the same band, or the same cluster of bands – with differentiated demands of interference and QoS requirements, to whom, specific channels, with customized levels of service, could be offered, taking into account the interference levels that they are willing to stand and, concomitantly, the price that they are willing to pay for that spectrum.

In a broader sense, spectrum trading operations between users might be considered under this scope, essentially when the interference conditions are not acceptable for the “owner” of a given portion of spectrum (licensee); but even so, the same conditions may be favorable for others, depending on the applications to be provided, and the QoS levels to be met. But other conceivable situations may include, for example, the underutilization of radio channels allocated to certain users, due to reduced or residual traffic demand, in specific periods or locations.

From the network operators’ perspective, the introduction of these adaptive techniques and technologies is also very interesting, since they are able to maximize the resource utilization, by employing cognitive radio sensing capabilities to detect such inactivity conditions; not only to identify/select specific channels as potential candidates to be shared or reassigned to other users, but also to dynamically dimension, in real-time, the resources of a radio access network (RAN), considering its actual behavior, determined by the traffic that is generated by the end-users. The operators, equipped with these means, can manage the current available network capacity, based on judicious guesses promptly confirmed, or not, by the sensing network, if properly deployed. This provides the operators with grounded information about the real network performance, giving them the opportunity to quickly react to sudden changes and, if necessary, to adopt counter-measures, in case of contingency situations.

---

<sup>42</sup> It will be up to the user to judge which technical conditions he is willing to accept.

<sup>43</sup> Assuming reliable, consistent, and steadfast interference management mechanisms.

As a final remark, it should be noticed that the **dynamic spectrum management models will not replace the conventional/traditional “static” models**, especially, whenever primary services have to be protected and safeguarded. However, they should be seen as a complement, with great potential to take “full” advantage of specific underused bands, which will definitely contribute to optimize the spectral resources and to dynamically value the spectrum, at every moment, in accordance with interference conditions, channel activity (occupancy), QoS, etc.





### 3 Block Edge Mask Approach

The Block Edge Mask (BEM) is the generic approach that was chosen to impose, in a flexible fashion, technical conditions to technological neutral systems which are operating in the WAPECS bands.

A **BEM** is considered **part of the authorization regime for spectrum usage**, and both types of emission, whether within (in-block), or outside (out-of-block), the block of spectrum, are equally addressed by itself, through explicit rules, properly defined. [15]

Contrary to the Spectrum Emission Mask (SEM) – which is usually defined by standardization bodies, such as ETSI, and applied to specific equipment –, a BEM is applied to the **whole block of spectrum**, which is assigned to an operator, **regardless of the number of channels occupied by the technology** to be implemented in such a block, and which was adopted by the operator.

Assuming that an operator is using the paired blocks: FDD1 DL and FDD1 UL, each one with 10 MHz of bandwidth, in accordance with the allocation plan defined for the 800 MHz band, depicted in Fig. 3.1; nothing prevents him from using, for instance, a LTE emission with only 5 MHz of bandwidth, despite having more 5 MHz at his disposal. By the way, this situation actually occurred in some cross-border regions of certain countries, which released the DD1

sooner than the neighbors. During this transition period – in which DTT networks above channel 60 coexisted, from one side of the border, with LTE on the other side –, some operators opted for using 5 MHz LTE channels, near the border, in order to avoid interference<sup>44</sup> from/to DVB-T systems. In any case, the operator still has to comply with the BEM requirements defined for the entire assigned block of 10 MHz, even when just 5 MHz are actually being used.

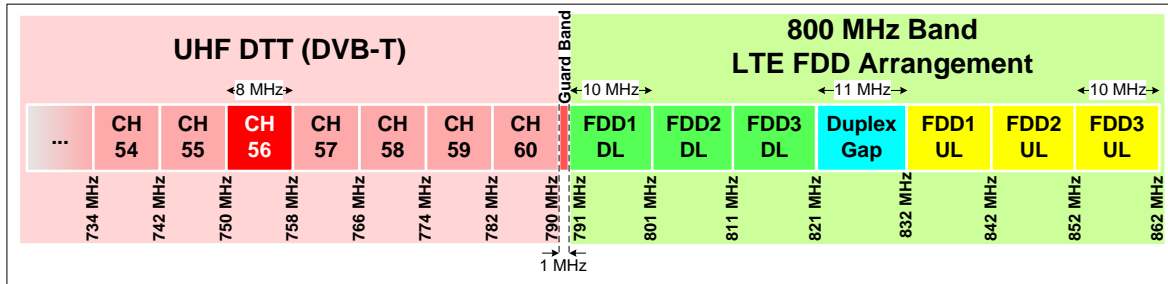


Fig. 3.1. Portuguese spectrum allocation for DTT and LTE 800 MHz band.

### 3.1 Concept and Definition

A **Block Edge Mask**, according to the formal CEPT's definition [16], is:

*“an emission mask that is defined, as a function of frequency, relative to the edge of a block of spectrum that is licensed to an operator. It consists of in-block and out-of-block components, which specify the permitted emission levels over frequencies inside and outside the licensed block of spectrum respectively. The out-of-block component of the BEM itself consists of a baseline level and, where applicable, intermediate (transition) levels, which describe the transition from the in-block level to the base-line level as a function of frequency”.*

Fig. 3.2 illustrates a generic BEM, showing the power limits for both in-block and out-of-block regions (including the transition zone).

<sup>44</sup> As an illustrative example, and supposing that the channel 61 ([790, 798] MHz) is being used by one country for DTT, but channel 62 is not. If the LTE operator, on the other side of the border, uses the upper 5 MHz of his FDD1 DL block ([797, 801] MHz), he just allows a small overlap of 1 MHz, leaving the remaining 4 MHz free of interference.

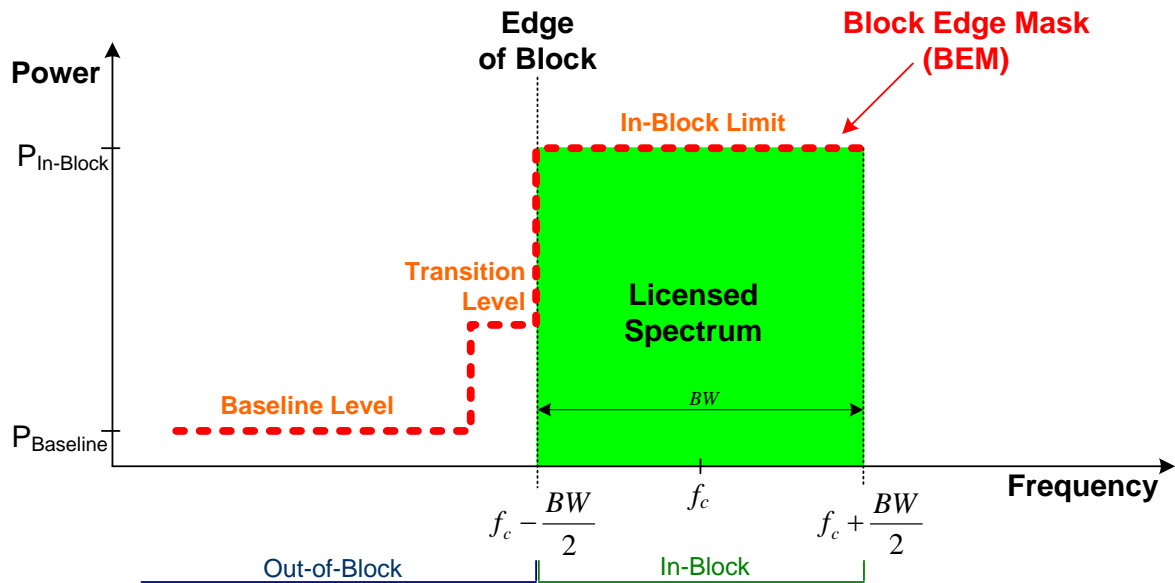


Fig. 3.2. Illustration of the Block Edge Mask concept.  
Source: CEPT, Report 19 [15]

In the above figure,  $BW$  is the total bandwidth of the assigned block of spectrum and defines the width of the *in-block region*;  $f_c$  is the center frequency of the licensed block of spectrum;  $f_c - \frac{BW}{2}$  and  $f_c + \frac{BW}{2}$  are the *lower* and *upper edges* frequencies of the block, respectively.  $P_{in-block}$  and  $P_{baseline}$  are the power levels of *in-block* and *baseline* limits, respectively.

Although the BEM approach may be applied to a multiplicity of WAPECS bands, henceforward, our analysis will be mainly focused on the **800 MHz band**, without prejudice to the major conclusions to be drawn, which will be mostly applicable and extendable to the remaining WAPECS bands, without loss of generality.

### 3.1.1 Technical Specifications (LTE 800 MHz band)

In line with the generic nature of the BEM concept, the specified technical conditions would allow, in principle, the introduction of any technology to operate on a neutrality basis. However, in Europe, the operator's choice fell unanimously on the LTE technology, to be deployed in the 800 MHz band. For that very reason, references to "LTE 800 MHz band" or "800 MHz band" will be indistinctly used, throughout this thesis, with the same meaning.

Two different types of BEM were defined for the 800 MHz band, as they are applied to the emissions of **base stations (BS)** or **terminal stations (TS)**. They are both relevant for the

regulators and spectrum management authorities. However, they are distinctly addressed. The TS BEM compliance is commonly verified by independent laboratories, which usually test equipment based on EMC and R&TTE procedures and requirements. On the other hand, the BS BEM compliance is typically investigated by spectrum control and monitoring entities, aiming the prevention or resolution of harmful interferences.

This work is focused on the **BS BEM** compliance check, and intends to contribute to explore alternative methodologies of measurement for those purposes. Thus, whenever the simplified designation “BEM” is employed, it actually means “BS BEM”.

There are legitimate concerns about the need of protection of distinct primary services, such as DTT (UHF band) and GSM and UMTS (900 MHz band). Therefore, the full BEM is extensive and combines discriminated out-of-block conditions, according to specific needs of each radio service to be protected.

#### 3.1.1.1 Fundamentals for the Derivation of a Block Edge Mask

The basics for the derivation of a Block Edge Mask will be introduced through an illustrative example. The BEM will be derived from the assigned block of spectrum (in-block region). Subsequently, the remaining constraints will be progressively added, meeting all technical specifications established by [16], [42], [67], [69], and [107].

The in-block BEM limit is critically dependent on the DTT spectrum planning, especially if channel 60 requires radio protection. This condition will influence the maximum in-block EIRP that is allowed. Table 3.1 defines such BS in-block EIRP requirements and prescribes the respective out-of-band baseline limits to be observed in the DTT band (i.e., below 790 MHz).

The adjacent (out-of-block) transition levels, which are introduced in Table 3.2, are independent of the center frequency of the block of spectrum that was assigned, but the BEM still dependent on the in-block EIRP. This means that, whatever the block that is considered (FDD1 DL, FDD2 DL or FDD3 DL), the BEM shape, within a central bandwidth of 30 MHz, is the same, **but only if the in-block EIRP is also the same**. For that reason, we will firstly derive the BEM around DC ( $f_c = 0$  Hz), taking into account only the adjacent limits mentioned so far. In order to distinguish this partial (central) section of a BEM from its full version, we will adopt the designations “core BEM” and “full BEM”, respectively.

The core BEM for a specific operator can be easily obtained just by shifting it from DC to the desired (assigned) central frequency, and all the conditions, defined so far, remain valid, **as long as the in-block EIRP is correct**.

		<i>column 1</i>	<i>column 2</i>
Case		LTE Base Station In-Block EIRP: P [dBm/10MHz]	Maximum Mean Out-of-Block EIRP [dBm/8MHz]
		(applicable to frequencies: $\left[fc - \frac{BW}{2}, fc + \frac{BW}{2}\right]$ MHz)	(applicable to frequencies below 790 MHz)
A	DTT Channel 60 (*) is locally used (Broadcasting is protected)	$P \geq 59$	0
		36	P-59
		$36 \leq P < 59$	-23
B	DTT Channel 60 (*) is used (Broadcasting is subject to an intermediate level of protection)	$P \geq 59$	10
		36	P-49
		$36 \leq P < 59$	-13
C	DTT Channel 60 is not locally used (Broadcasting is not protected)	no restrictions (all power levels are allowed) (**)	22

(\*) Channel 60: [782, 790] MHz

(\*\*) The derived conditions resulted from compatibility studies, which considered a **maximum In-Block EIRP limit** ranging from **56 dBm/5MHz** (i.e., 59 dBm/10MHz) to **64 dBm/5MHz** (i.e., 67 dBm/10MHz). However, higher In-Block EIRP levels may be authorized in specific circumstances (e.g., rural deployments). [107]

Table 3.1. Baseline requirements BS BEM Out-of-Block EIRP limits (over frequencies below 790 MHz) as a function of LTE BS In-Block EIRP and local DTT deployment.

Sources: [16], [42], [67], [69], [107]

Out-of-Block Emissions Frequency Range [MHz]	Maximum Mean Out-of-Block EIRP [dBm]	Reference Bandwidth [MHz]
$\left[fc - \frac{BW}{2} - 10, fc - \frac{BW}{2} - 5 \right[$	18	5
$\left[fc - \frac{BW}{2} - 5, fc - \frac{BW}{2} \right[$	22	5
$\left]fc + \frac{BW}{2}, fc + \frac{BW}{2} + 5 \right]$	22	5
$\left]fc + \frac{BW}{2} + 5, fc + \frac{BW}{2} + 10 \right]$	18	5
Remaining FDD downlink frequencies	11	1

Table 3.2. Transition requirements BS BEM Out-of-Block EIRP limits (over frequencies of FDD downlink and TDD).

Sources: [16], [42], [67], [69], [107]

The wanted core BEM will be finally derived under the following assumptions:

- The Portuguese DVB-T deployment – in which, the channel 60 is not being used for DTT broadcasting (see Fig. 3.1) – is considered;
- The Portuguese LTE FDD (800 MHz band) deployment – which consists of 3 paired blocks of 10 MHz allocated to 3 mobile operators (see Fig. 3.1) – is taken as a reference:
  - Block bandwidth: 10 MHz (BW = 10 MHz)
  - A maximum in-block EIRP of 59 dBm/10MHz is taken as an illustrative example.

Table 3.3 summarizes the most relevant calculations that were needed for obtaining the desired core BEM.

BEM region	Relative Frequency Band [MHz]	EIRP BEM [dBm]	EIRP BEM Ref. BW [MHz]	EIRP BEM PSD [dBm/MHz]	Normalized BEM [dBc]	Notes
Out-of-Block	[ -12.5 , -7.5 [	18	5	11	<b>-38</b>	From Table 3.2
	[ -7.5 , -2.5 [	22	5	15	<b>-34</b>	
In-Block	[ -2.5 , 2.5 ]	59	10	49	<b>0</b>	From Table 3.1, column 1, case C
Out-of-Block	] 2.5 , 7.5 ]	22	5	15	<b>-34</b>	From Table 3.2
	] 7.5 , 12.5 ]	18	5	11	<b>-38</b>	

Table 3.3. BEM derivation for a LTE BS emission with BW: 10 MHz and In-Block EIRP: 59 dBm/10MHz.

Since the diverse source tables specify EIRP levels using different reference bandwidth values, it was necessary to convert all of them to the same reference. In this case, 1 MHz was considered as reference bandwidth. For that purpose, a PSD, in dBm/MHz, was calculated by applying the Eq. 3.1.

$$PSD_{[dBm/MHz]} = EIRP\ BEM_{[dBm]} - 10 \times \log_{10} \left( \frac{EIRP\ BEM\ Ref.\ BW_{[MHz]}}{1\ MHz} \right) \quad \text{Eq. 3.1}$$

Then, all the individual PSD levels were normalized to the maximum (in-block PSD, i.e., 49 dBm/MHz), in order to obtain the relative core BEM depicted in Fig. 3.3.

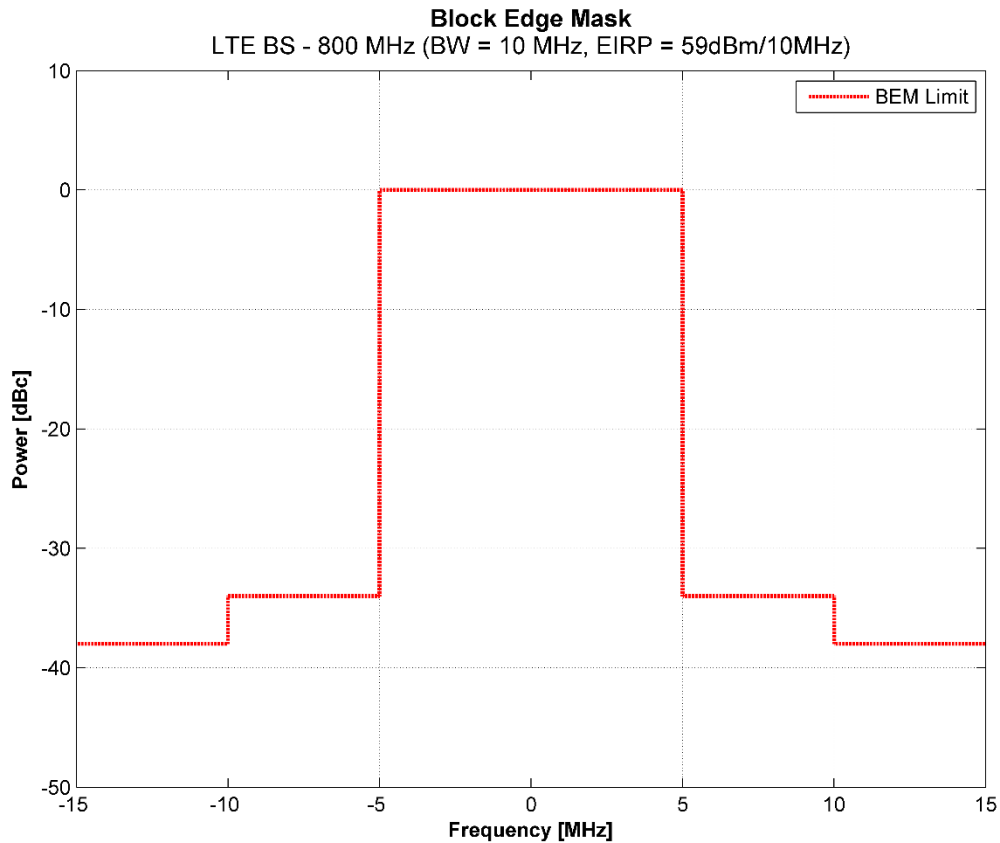


Fig. 3.3. BEM for a LTE BS emission with BW: 10 MHz and In-Block EIRP: 59 dBm/10MHz.

As mentioned above, this core BEM is only dependent on the BS in-block EIRP level. Fig. 3.4 clearly shows such a dependence, by keeping the previous assumptions, but changing now the in-block EIRP levels.

The central segment of the BEM has been defined, for a giving set of assumptions. However, in order to proceed with the design of the full BEM, additional conditions and assumptions have to be introduced bellow.

Table 3.4 establishes the out-of-block limits to be met over the uplink frequencies, and Table 3.5 sets the constraints to be observed over guard bands.

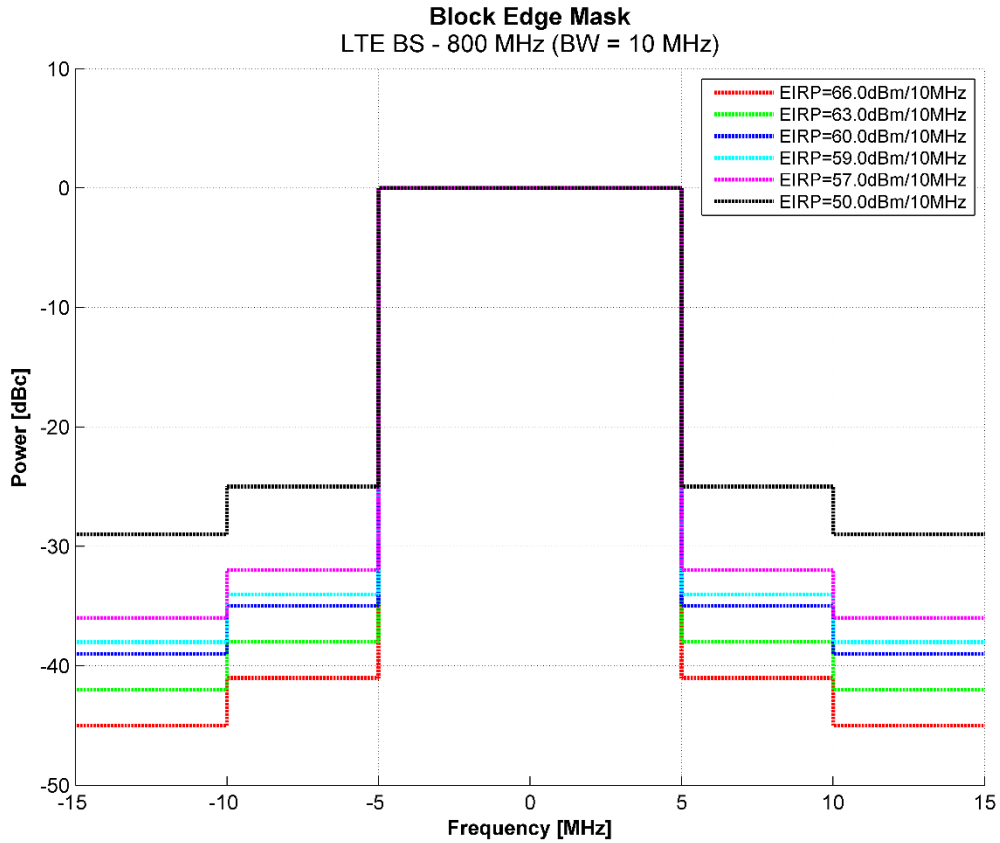


Fig. 3.4. BEMs for LTE BS emissions with BW: 10 MHz, for different In-Block EIRP's.

Out-of-Block Emissions	Maximum Mean Out-of-Block EIRP [dBm/5MHz]
<b>FDD Uplink Frequencies</b> (i.e., above 832 MHz)	-49.5
<b>TDD Frequencies</b>	-49.5

Table 3.4. Baseline requirements BS BEM Out-of-Block EIRP limits (over frequencies of FDD uplink and TDD).

Sources: [16], [42], [67], [69], [107]

It is commonly necessary to separate different types of spectrum uses, through the so-called “guard bands”, which may be used as restricted blocks. The objective of these “idle” bands is to



minimize the risk of interference and accommodate expected imperfections of the radio systems, such as, unideal filtering, low sensitivity, possible nonlinear distortion, etc.; making practical deployments feasible, under normal conditions. However, even considering guard bands, there is no guarantee that interference will not occur. Sometimes, in severer scenarios, additional counter-measures have to be taken (e.g., to reduce base station EIRP limits). [65]

The spectrum layout presented in Fig. 3.1 includes two different guard bands. The first one is to separate the DTT channels from the LTE blocks. For this purpose, a guard band of 1 MHz was reserved, between 790 and 791 MHz. The latter is the LTE duplex gap, used to keep the FDD uplink blocks away from the downlink. In this case, a more generous amount of spectrum (11 MHz guard band) was left apart, between 821 and 832 MHz.

Guard-Band Out-of-Block Emissions Frequency Range	Maximum Mean Out-of-Block EIRP [dBm/MHz]
Guard-band between broadcasting band edge and FDD downlink band edge: [790 , 791] MHz	17.4
Guard-band between broadcasting band edge and TDD downlink band edge: [790 , 797] MHz	15
Guard-band between FDD downlink band edge and FDD uplink band edge (duplex gap): [821 , 832] MHz	15

Table 3.5. Transition requirements BS BEM Out-of-Block EIRP limits (over Guard Bands).  
*Sources: [16], [42], [67], [69], [107]*

As we are expanding the BEM design towards the sides, depending on the operator's block position, the three operator's BEMs do not exactly match between themselves; i.e., they have a slightly different shape, depending on the proximity to the services to be protected, and the specific needs of protection. Though, they are perfectly equivalent regarding the constraints to be observed.

As an illustrative example, we will be still using the same set of assumptions, but now we will consider the particular assigned block: FDD2 DL, in the middle.

Table 3.6 gathers the multiple conditions from the different tables, and presents the calculations that led to the full BEM derivation, which is depicted in Fig. 3.5 (absolute power level mask, centered at 806 MHz) and in Fig. 3.6 (normalized power levels and relative frequencies, although assuming the center frequency of 806 MHz for derivation purposes).

BEM region	Frequency Band [MHz]	Relative Frequency Band [MHz]	EIRP BEM [dBm]	EIRP BEM Ref. BW [MHz]	EIRP BEM PSD [dBm/MHz]	Normalized BEM [dBc]	Notes
	< 790	< -16	22	8	13	-36	From Table 3.1, column 2, case C
Out-of-Block	[ 790 , 791 [	[ -16 , -15 [	17.4	1	17.4	-31.6	From Table 3.5
	[ 791 , 796 [	[ -15 , -10 [	18	5	11	-38	From Table 3.2
	[ 796 , 801 [	[ -10 , -5 [	22	5	15	-34	
In-Block	[ 801 , 811 ]	[ -5 , 5 ]	59	10	49	0	From Table 3.1, column 1, case C
	] 811 , 816 ]	] 5 , 10 ]	22	5	15	-34	From Table 3.2
Out-of-Block	] 816 , 821 ]	] 10 , 15 ]	18	5	11	-38	
	] 821 , 832 ]	] 15 , 26 ]	15	1	15	-34	From Table 3.5
	] 832 , 862 ]	] 26 , 56 ]	-49.5	5	-56.5	-105.5	From Table 3.4

Table 3.6. Full BEM derivation for a LTE BS emission (center frequency: 806 MHz, BW: 10 MHz, In-Block EIRP: 59 dBm/10MHz).

After representing the block edge mask, it is opportune to compare it with the aforementioned spectral emission mask. Fig. 3.7 shows an illustrative LTE FDD DL spectrum, which was generated by the SystemVue Electronic System Level Design software tool from Agilent Technologies™ [66], before any final amplification and filtering process. As observed, the BEM<sup>45</sup> compliance is clearly validated, and the SEM<sup>46</sup> compliance is tangentially achieved.

<sup>45</sup> Assuming an EIRP of 59 dBm/10MHz, in the 800 MHz band.

<sup>46</sup> As presented in [65].

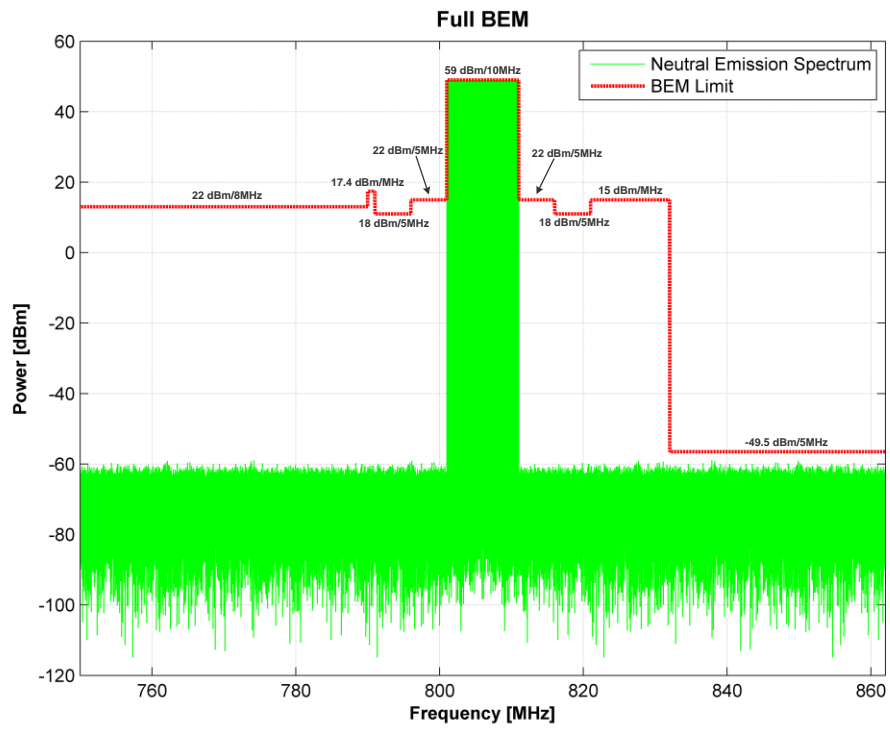


Fig. 3.5. Full BEM for a LTE BS emission (center frequency: 806 MHz, BW: 10 MHz, In-Block EIRP: 59 dBm/10MHz).

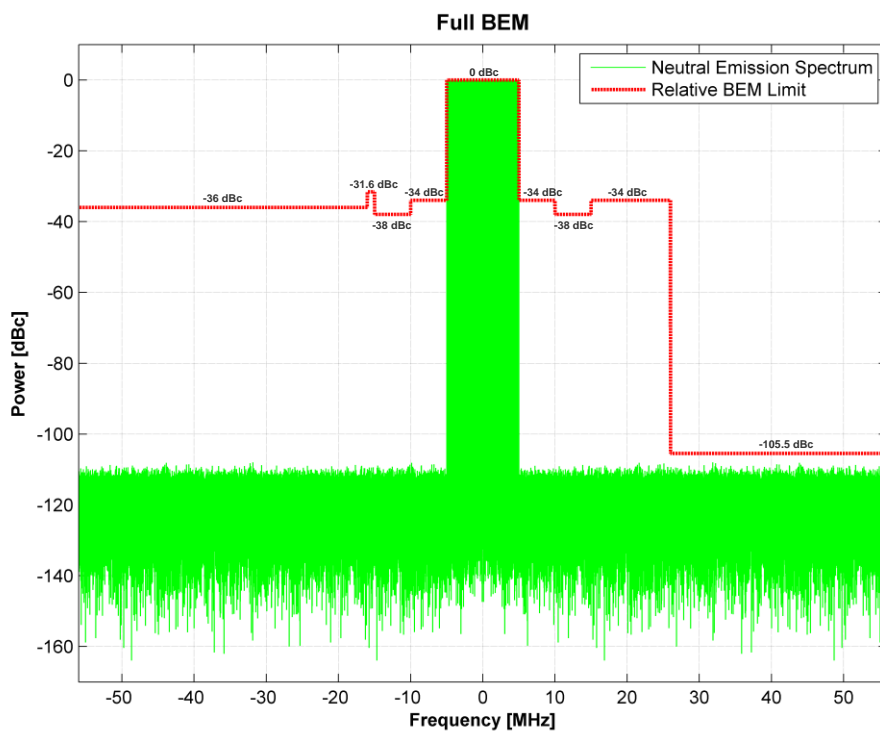


Fig. 3.6. Full Relative BEM for a LTE BS emission (BW: 10 MHz, In-Block EIRP: 59 dBm/10MHz).

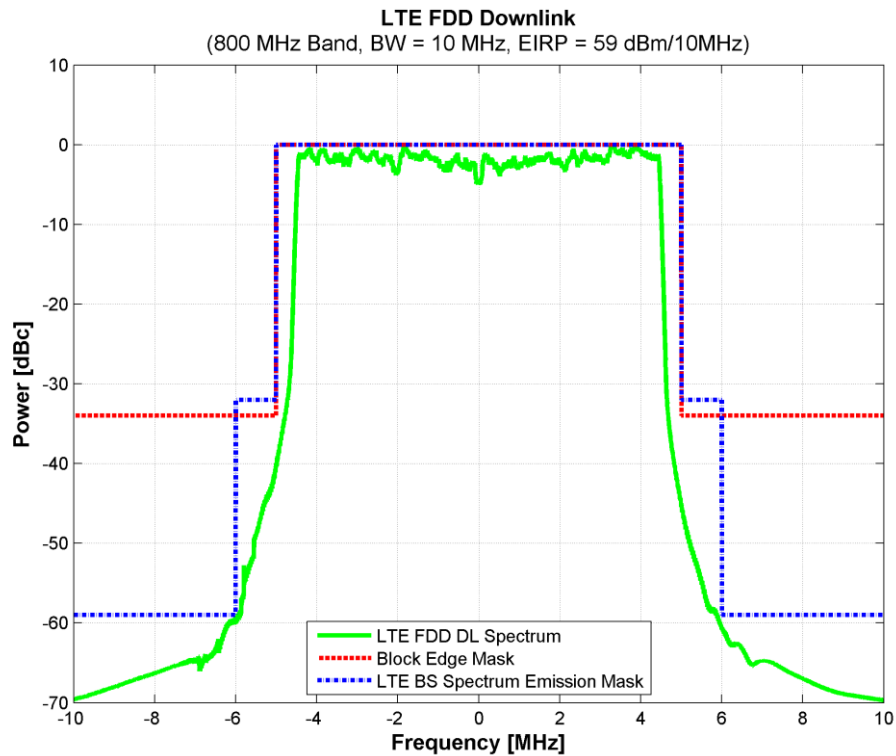


Fig. 3.7. Block Edge Mask and Spectrum Emission Mask for LTE FDD downlink.

### 3.2 Drawbacks of the Block Edge Mask Approach

A BEM is a desirably generic model. However, it may not be universally effective in all situations, and thus, it may not prevent all types of interference. In such cases, supplementary mitigation techniques may have to be adopted or additional conditions may need to be set, on a case-by-case basis, at a national or regional level. [16] Exceptional situations may require bilateral or multilateral cross-border coordination agreements.

Nevertheless, as stressed by [42], a BEM defines “upper limits on the mean EIRP or Total Radiated Power<sup>47</sup> (TRP) **over an averaging time interval**, and over a measurement frequency bandwidth. In the time domain, the EIRP or TRP **is averaged over the active portions of signal bursts** and corresponds to a single power control setting. In the frequency domain, the EIRP or TRP is determined over the [specified] measurement bandwidth”.

<sup>47</sup> According to [42], “TRP is a measure of how much power the antenna actually radiates, [and it is] defined as the integral of the power transmitted in different directions over the entire radiation sphere”.

As can be inferred by the previous statement, possible instantaneous transient effects or signal's dynamics are averaged and easily softened, which may be hiding non-neglected evidences of relevant patterns of behavior revealed by the signals under investigation.

As a matter of fact, time-frequency effects have been detected in wireless communication systems. However, **most of them have been ignored for long time**. [7], [68], [108], [109], [110], [111], [112] This is mainly because steady-state conditions have, almost always, been roughly assumed to evaluate RF signals, even when this is not the case. Actually, the steady-state analysis is suitable to determine the system's behavior, whenever the rate-of-change of the signals – that are being propagated throughout a system – is much slower than the response times of all components of the system. If so, transient effects may be ignored. [7]

Ultimately, this topic of discussion has drawn increasingly attention, due to the emergence of new radio technologies, such as LTE, cognitive radio or fast frequency hopping systems, with which, the use of time-switched or transient RF signals is strongly expected. In fact, the most recent radio systems provide bit rates increasingly higher, which demand faster response times. Furthermore, the band pass (frequency response) of the signals is delimited by even sharper edges, in order to optimize the spectrum efficiency. All these tight specifications will impose transition periods, between steady-state regimes, which are of the same order of magnitude of the times within the “steady state”. In such a case, steady state analysis cannot be used to capture these behaviors, and such properties must be analyzed in the time domain. [7]

The particular mode of operation of opportunistic radios may suggest an intense and mutable behavior like this, since they are continuously searching for available slots to transmit (white spaces). Obviously, this will cause sudden changes of frequency and, consequently, micro-interruptions on the transmission. However, this appears to be transparent to the user, who has the perception of having a seamless connection. During such transition periods, within which the frequency is instantaneously switched, **time-frequency effects are clearly observed** in Fig. 3.8.

A downfall 2D **spectrogram**, is used to show the energy distribution of the signal, which is coded in a color scale, in the time-frequency plane. This is a very intuitive solution to visualize the time-spectral characteristics of the signal. There are several possible techniques to generate this joint time-frequency representation, being the spectrogram the most common one.

The depicted illustrative example considers an opportunistic radio operation, in the 800 MHz band, within the middle block (FDD2 DL), under the assumption that such a band could

be accessed by any system (i.e., on a technology-neutral basis), even by cognitive radio<sup>48</sup>. The system uses a QPSK baseband signal to modulate a RF carrier, which is regularly jumping over different frequencies, as it gets permission to transmit.

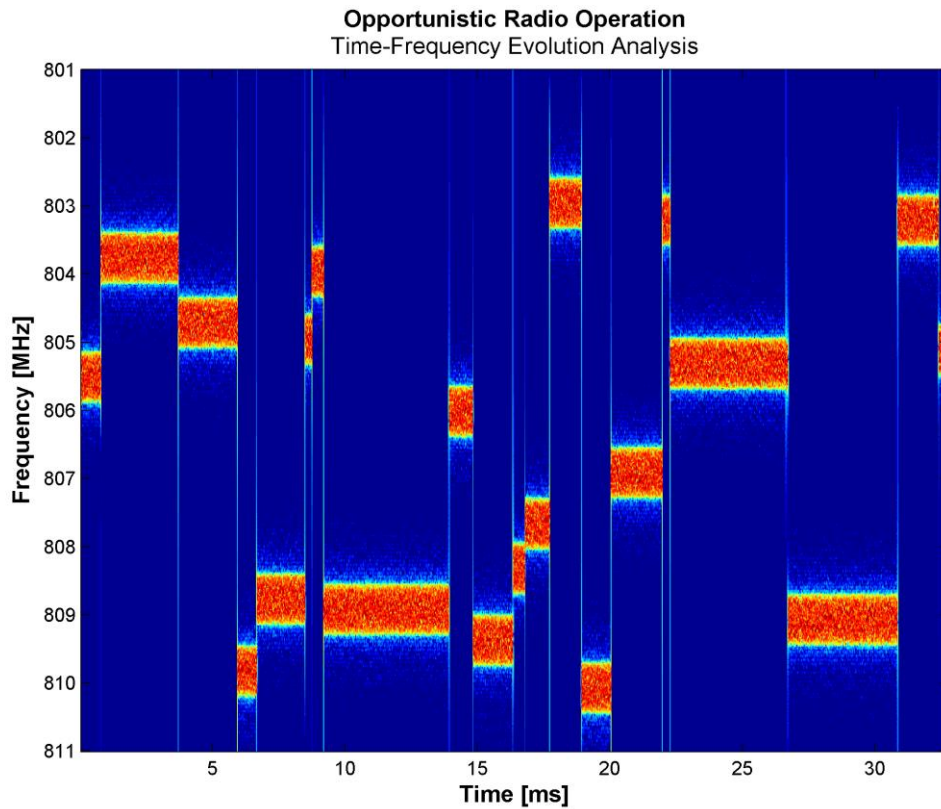


Fig. 3.8. Time-Frequency Analysis of a Cognitive Radio Operation.

If the same scenario under analysis is monitored by using **traditional measurement techniques**, typically **spectrum analysis**, as shown in Fig. 3.9, **the transient effects, previously identified, are averaged and go unnoticed**; whether instantaneous clear-write, or accumulated ‘max hold’, modes of spectrum visualization are employed.

Given the above observation, **the introduction of least restrictive conditions based on spectrum approaches**, through the definition of BEMs, **is indeed questionable**, especially if signals, with a transient behavior, have to be controlled/assessed. All the more so because many systems, which are going to operate according to technological neutrality

---

<sup>48</sup> This is a purely hypothetical scenario, since no compatibility studies were taken into account for such systems in this band.

principles, will exploit Orthogonal Frequency Division Multiplexing (OFDM) techniques. In this context, LTE and WiMax technologies will play a primary role.

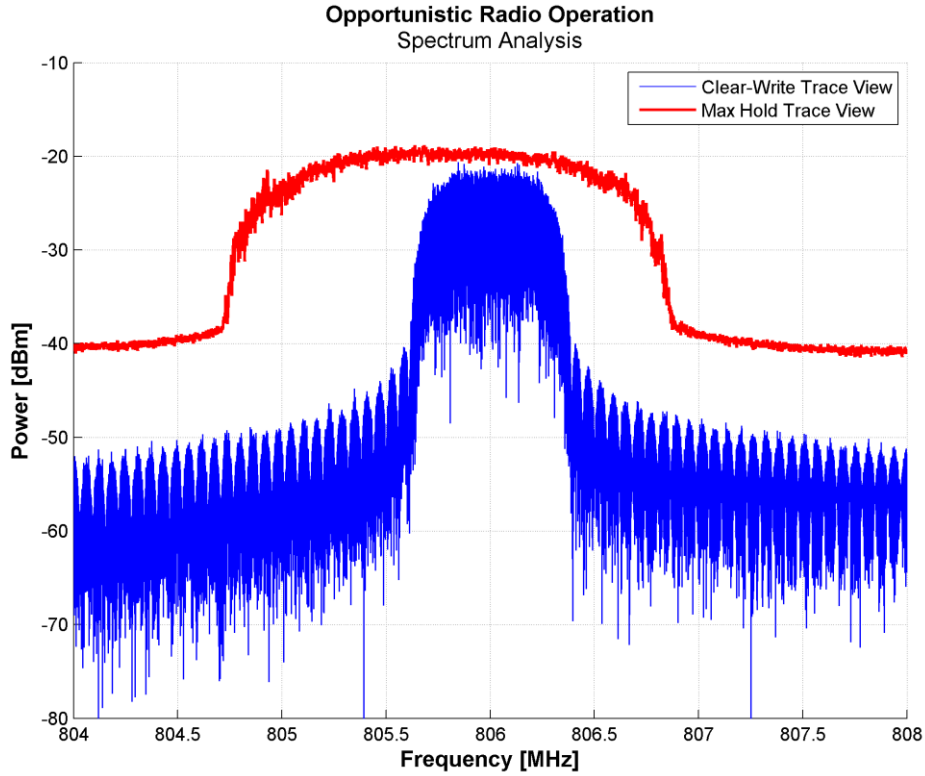


Fig. 3.9. Traditional Spectrum Analysis of the same Cognitive Radio Operation.

Notwithstanding, OFDM exhibits some problems related to high **Crest Factor (CF)**, or **Peak-to-Average Power Ratio (PAPR)**, which could make the amplifiers to work with low power efficiency and high distortion levels by putting them into nonlinear operation region.

The Crest Factor is, by definition (Eq. 3.2), the ratio between the maximum amplitude of a given signal  $x(t)$  and its time-averaged amplitude value.

$$CF = \frac{\max\{x(t)\}}{E\{x(t)\}} \quad \text{Eq. 3.2}$$

The time-averaged value of the signal is calculated according to Eq. 3.3.

$$E\{x(t)\} = \frac{1}{N} \sum_{k=0}^{N-1} x_k(t) \quad \text{Eq. 3.3}$$

The CF is quite often expressed in logarithmic units (dB), as presented in Eq. 3.4.

$$CF_{[dB]} = 20 \log_{10} \left[ \frac{\max\{x(t)\}}{E\{x(t)\}} \right] \quad \text{Eq. 3.4}$$

The Peak-to-Average Power Ratio is defined (Eq. 3.5) as the ratio between the maximum power of the signal (peak value) and its time-averaged power value. By definition, the **power of a signal  $x(t)$**  is given by the product of its amplitude:  $x(t)$ , and its complex conjugate:  $x^*(t)$ .

$$PAPR = \frac{\max\{x(t) \cdot x^*(t)\}}{E\{x(t) \cdot x^*(t)\}} = \frac{\max\{|x(t)|^2\}}{E\{|x(t)|^2\}} \quad \text{Eq. 3.5}$$

Similarly, the time-averaged power value of a signal is computed as follows (Eq. 3.6).

$$E\{|x(t)|^2\} = \frac{1}{N} \sum_{k=0}^{N-1} |x_k(t)|^2 \quad \text{Eq. 3.6}$$

The PAPR is also usually expressed in dB units, according to Eq. 3.7.

$$PAPR_{[dB]} = 10 \log_{10} \left[ \frac{\max\{|x(t)|^2\}}{E\{|x(t)|^2\}} \right] \quad \text{Eq. 3.7}$$

A high PAPR could lead, consequently, to high error data rates in the whole system [70]. Indeed, note that the multi-carrier OFDM signal results from the cumulative effect of all the signals transmitted on each narrow-band sub-carrier. Thus, as stated by the central limit theorem, the entire OFDM transmitted signal follows a Gaussian distribution, showing high peak power values when compared to the average power level. For this reason, the design of OFDM systems should involve the consideration of suitable techniques to minimize these clipping rates, so that no distortion effects and/or transmission of erroneous bits occur due to signal components exceeding the saturation limit of a nonlinear device (e.g., amplifier or analog-to-digital converter (ADC)).

The impact of different LTE BS traffic loads on the BEM compliance is studied in [113]. The bottom line is that, actually, **there is no significant contribution, due to variation of traffic, to the validation of BEM requirements.** The measurement scenario, under assessment, considers three traffic load situations: **idle**, **medium** and **heavy**, but irrespectively of the traffic that is generated, **a comfortable safety margin**, between any of the three LTE spectra and the particular BEM to be applied, **is clearly found.** However, the idle mode exhibits



the most prominent spectrum “side skirts”, when compared with the remaining situations. The heaviest traffic condition has the lowest “side skirts”. At a first glance, this could be seen as unexpected or contradictory. Since this is a peculiar and very interesting effect, we decided to investigate a similar situation.

The field measurement setup, depicted in Fig. 3.9, which includes a Real Time Spectrum Analyzer (RTSA) connected to a Yagi-Uda receiving antenna, was mounted close by a LTE base station. Two distinct sample time-waveforms were acquired, using the RTSA. One of them corresponds to the idle mode of operation of that LTE BS, and the other to a heavy traffic situation.

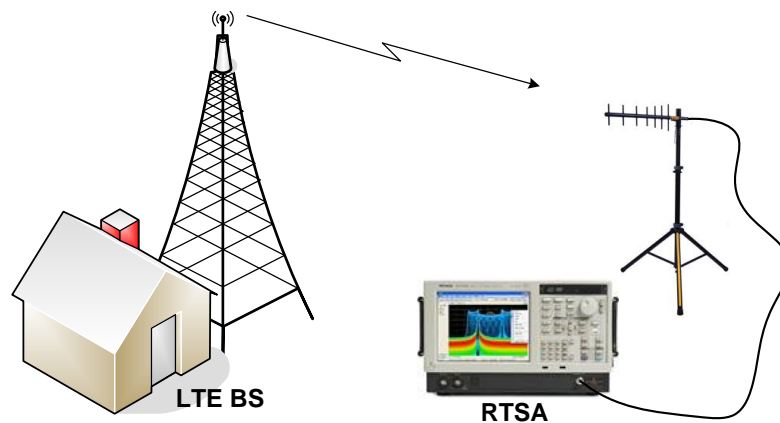


Fig. 3.10. Field Measurement Setup to Acquire LTE Waveforms.  
(RTSA image: credits to Tektronix™)

The spectrum was computed for both signals and jointly compared with a BEM, assuming an EIRP of 59 dBm/10MHz, as shown in Fig. 3.11. The same results were successfully reproduced, in particular, a relaxed BEM compliance, independently of the traffic load which was considered. But to better understand the reason why the idle mode has a bigger impact on the performance of the system, the complementary cumulative distribution function (CCDF) of the PAPR of both waveforms was calculated (see Fig. 3.12). Actually, the average power of the LTE BS in idle mode is lower than when it is under heavy traffic conditions. On the other hand, the peak power is almost the same in both situations. Thus, the PAPR is higher under idle conditions<sup>49</sup>.

<sup>49</sup> Considering this particular example, the idle mode PAPR reaches, in the worst-case, although with a small probability, about 5 dB more.

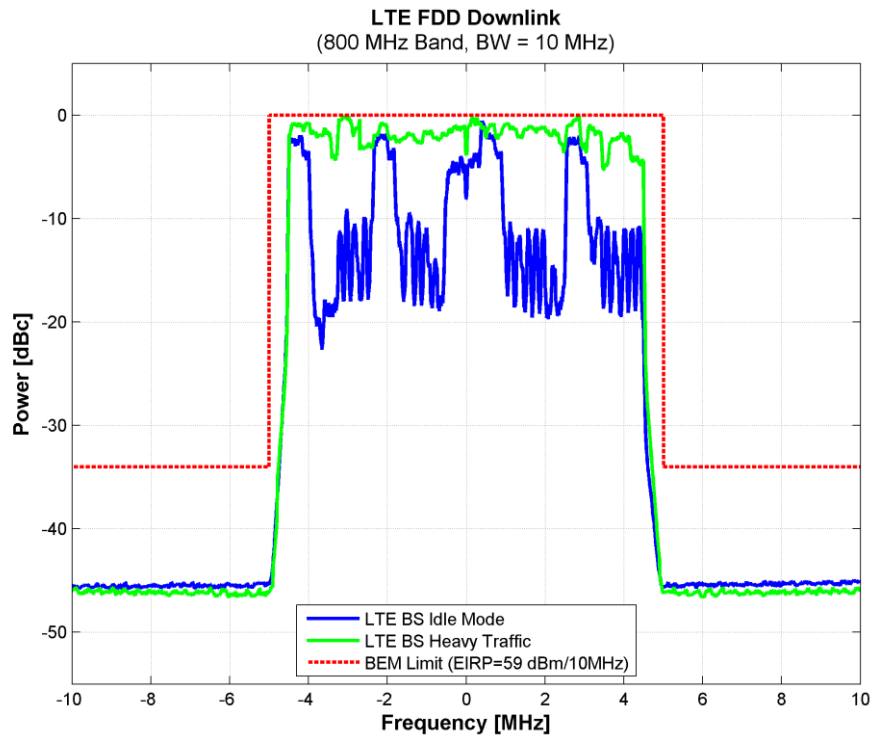


Fig. 3.11. BEM Compliance of LTE BS Idle and Heavy Traffic Modes Emission Spectra.

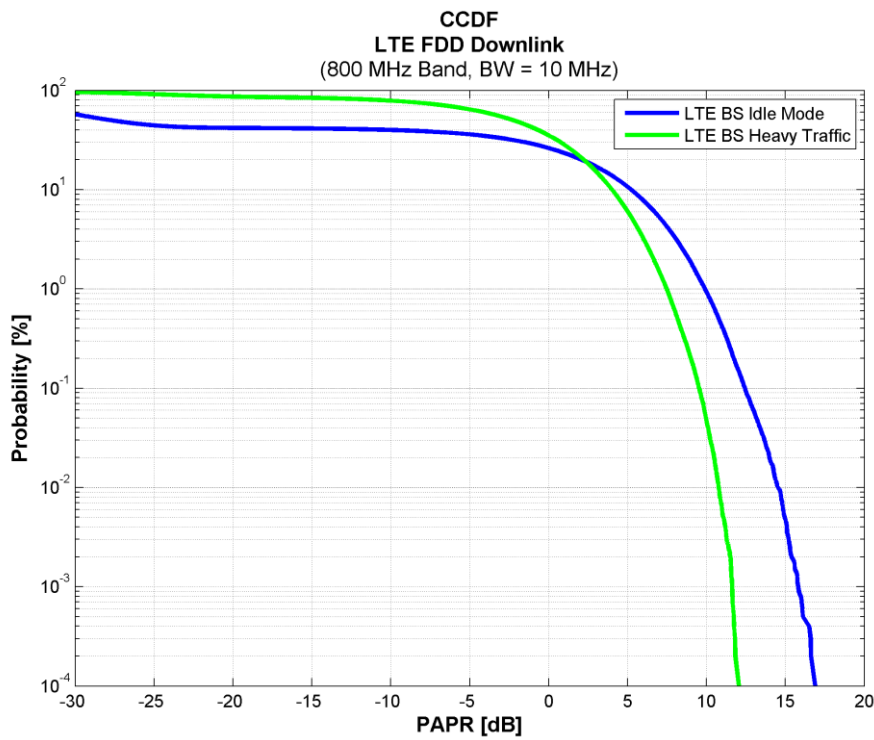


Fig. 3.12. CCDF of LTE BS Idle and Heavy Traffic Modes Emissions.

The above results are corroborated by [114], which justifies the identified behavior with the discontinuous or “bursty” nature of the idle mode emissions<sup>50</sup>. This report [114], commissioned by the Office of Communications (OFCOM<sup>51</sup>), investigated the performance of a set of DVB-T and DVB-T2 receivers (victims), in the presence of LTE BS BEM compliant emissions (interferers), under different LTE traffic conditions. The major conclusions revealed a significant influence of the LTE traffic loading on the DVB receiver’s protection ratio results, since **they are highly susceptible<sup>52</sup> to time-varying (discontinuous) emissions**, which happens mainly under idle circumstances. However, DVB-T receivers showed to be more vulnerable to the idle BS mode than the DVB-T2 ones. In fact, these latter seemed to be more affected by heavy load conditions. The study also points out that the DVB receivers are even more prone to interference if the desired signal level is higher, due to blocking, since the front-end becomes overloaded (desensitized) with strong signal levels. Under such conditions, the interferer does not need to have too much power to degrade the DVB quality parameters, and thus the broadcasting emission to be demodulated.

A practical interference case-study involving the DVB-T reception (victim) and a LTE BS emission (interferer) is carefully analyzed in Chapter 4.

In reality, it is of paramount importance **to, firstly, question if relevant effects**, such as the previously identified, which showed significant impact on radio system’s performance and high potential of interference, **are not being carelessly ignored or disguised** by adopting the BEM approach. The next natural concerns are then how to accurately measure these signals and how to properly validate such BEMs.

### 3.3 Practical Issues: How to Validate a Block Edge Mask

The ECC/CEPT approved a harmonized procedure for evaluating the Block Edge Mask compliance for LTE base stations, which is detailed in [69]. Some of the most relevant methodological issues are reviewed in the following subsections.

---

<sup>50</sup> Some bursts are somehow observable in Fig. 3.11, but they are more evident if the spectrum is captured with a faster sweep time.

<sup>51</sup> In the United Kingdom.

<sup>52</sup> This behavior is likely ascribable to the Automatic Gain Control (AGC) function, which is implemented in DVB receivers.

### 3.3.1 ECC/CEPT Block Edge Mask Measurement Methodology

This ECC/CEPT recommendation [69] establishes three measurement approaches for the BEM compliance verification, which will be described in section 3.3.1.3, namely:

- i. **Method 1:** radiated measurement under normal operating conditions;
- ii. **Method 2:** conducted measurement under normal operating conditions;
- iii. **Method 3:** conducted measurement according to ETSI EN 301 908-14 [115].

The most appropriate measurement method to be used on the BEM validation depend, not only on basic technical prerequisites, but also on the local conditions provided by the network operator, for conducted tests, or on the external environment found nearby the LTE BS, when radiated methods are only possible.

The flowchart in Fig. 3.13 guides us through the steps/criteria to be followed in the decision making process of choosing the measurement method.

Basically, there are 3 major levels of decision:

1. **Access to the BS** (network operator's facilities) is granted and **direct measurement** is feasible. If any of the above conditions are not satisfied, radiated measurements, as prescribed by **Method 1**, have to be carried out outside, close to the LTE BS. If they are jointly met, the assessment of additional conditions must be refined as follows.
2. **Interruption of the radio service** provided by the BS:
  - 2.1. **Without time constraints.** If so, the feasibility of application of **Method 3** should be explored, taking into account the ETSI test modes requirements, addressed in step 3. If there are time constraints, but interruption is still possible, the next sub-condition (2.2.) will be applied.
  - 2.2. **Instantaneously** (short term interruptions, to merely connect/insert the measurement devices and to remove them afterwards). If this is considered acceptable, then conducted measurement, under normal operation conditions, will be executed as stated by **Method 2**. Otherwise, radiated measurements, have to be performed outside, close to the LTE BS, according to **Method 1**.

3. **Configuration of ETSI Test Modes** on the BS. If the BS supports the necessary hardware and software functionalities to enable the test modes, as foreseen in ETSI EN 301 908-14 [115], and the network operator staff is skilled to reliably configure them, the conducted measurement **Method 3** is applicable. Otherwise, conducted measurement under normal operation conditions **Method 2** will be used.

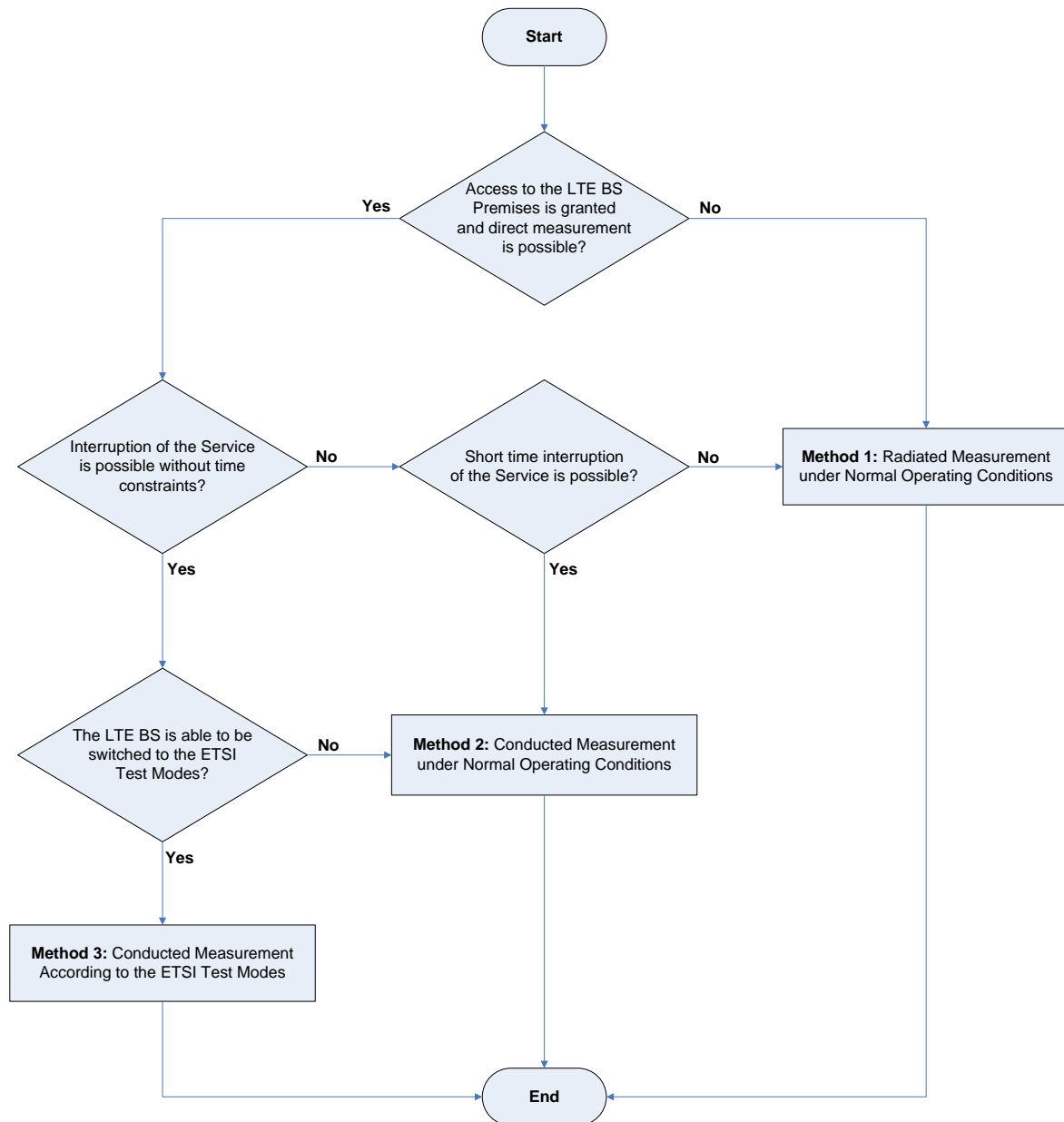


Fig. 3.13. Flowchart for the selection of an appropriate BEM measurement approach.

Source: [69]

### 3.3.1.1 EIRP Calculation for the Determination of the Applicable BEM

Regardless of the measurement method to be employed, it is essential to know the particular BEM which is applicable to the system under evaluation. The determination of the EIRP of the BS is thus crucial to properly derive such a BEM. For the identified purpose, the following two EIRP calculation approaches are recommended by [69], depending on whether the measurement is **radiated** (3.3.1.1.1) or **conducted** (3.3.1.1.2).

#### 3.3.1.1.1 Radiated Measurement (Method 1)

If a test probe or an output power connector is not provided by the BS equipment, or if the access to the BS facilities is not possible, as is the case of radiated measurement, the output power ( $P_{\text{Output}}$ ) of the LTE emission has to be estimated, under the assumptions made in [69].

Since the basic assignable unit of the LTE downlink signal is the Resource Block (RB), a LTE BS frame structure is naturally organized in RS's. A single RB, represented in Fig. 3.14, has 12 OFDM subcarriers (in the frequency domain), and lasts up to 0.5 ms, i.e., 6 or 7 OFDM symbols (in the time domain). Some RB's are filled with traffic that is generated by users, but other ones correspond to logical and control channels, which are also used for synchronizing purposes, between terminal and base stations, such as the Physical Broadcast Channel (PBCH). [69], [118], [119]

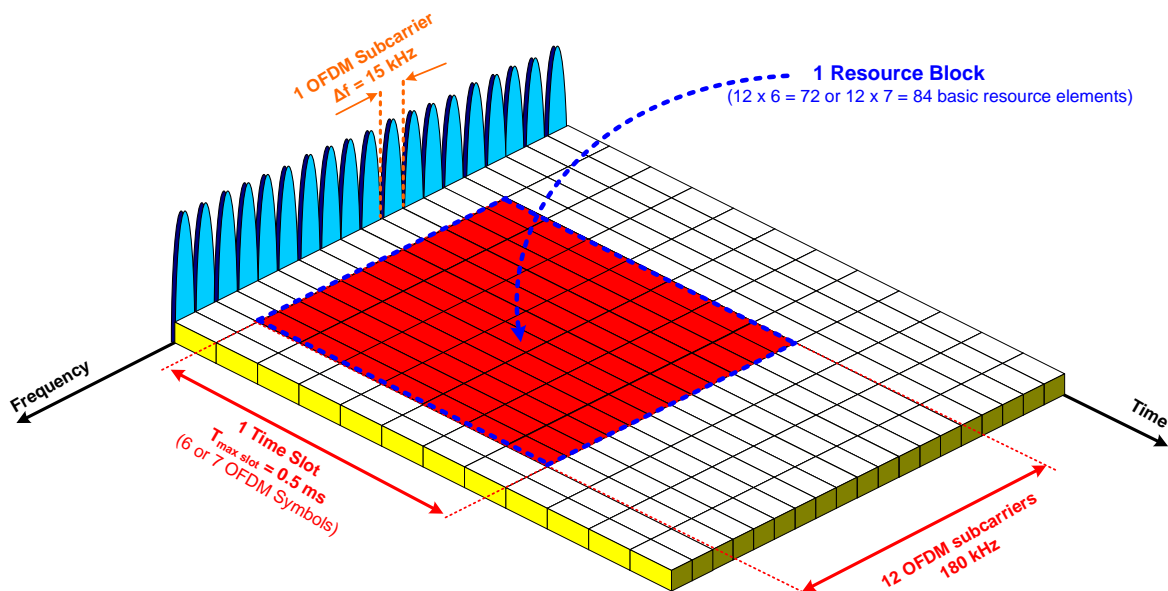


Fig. 3.14. Resource Block structure in a LTE downlink signal.  
Source: [119]

A generic LTE downlink frame structure normally produces a characteristic spectrum (e.g., see Fig. 3.7), but it is not taken for granted that the BS is operating under fully loaded traffic conditions, i.e., the worst-case output power scenario.

In principle, the PBCH is usually transmitted at the same power, keeping a constant level. The PBCH occupies 6 RB, specifically, the **72 inner OFDM subcarriers**<sup>53</sup>, of the total of 600, which form the BS OFDM signal (assuming a LTE emission with 10 MHz of bandwidth).

If the worst-case scenario is considered, i.e., the BS is transmitting at its maximum power, then, all the 600 subcarriers have, simultaneously, the same power level as the 72 inner ones (PBCH). By measuring the PBCH power level ( $\mathbf{P}_{PBCH}$ ), it is possible to extrapolate the maximum BS power level ( $\mathbf{P}_{max}$ ), using the Eq. 3.8.

$$P_{max [dBm]} = P_{PBCH [dBm]} + 10 \log_{10} \left( \frac{600}{72} \right) = P_{PBCH [dBm]} + 9.21 \text{ dB} \quad \text{Eq. 3.8}$$

The maximum EIRP of the LTE BS can be estimated, from the  $\mathbf{P}_{max}$  value, by using the free-space propagation formula [117], also known as Friis Equation (Eq. 3.9).

$$L_{fs [dB]} = 32.4 + 20 \log_{10}(f_{[MHz]}) + 20 \log_{10}(d_{[km]}) \quad \text{Eq. 3.9}$$

Fig. 3.15 introduces a possible scenario of application of the EIRP estimation calculation. As an illustrative example, let it be considered that a radiated measurement is being performed at a distance ( $\mathbf{d}$ ) of 0.5 km from the LTE BS, using a Yagi-Uda receiving antenna with an isotropic gain ( $\mathbf{G}_{Rx}$ ) of 14 dBi, connected to a spectrum analyzer, through a coaxial cable and respective connectors with a total loss ( $\mathbf{L}_{cable+connectors}$ ) of 1 dB. If the received PBCH power level ( $\mathbf{P}_{PBCH in}$ ), measured by the spectrum analyzer, is -21.7 dBm, the maximum LTE BS power at the receiver input ( $\mathbf{P}_{max in}$ ) is given by the Eq. 3.8, as follows (Eq. 3.10).

$$P_{max in} = P_{PBCH in} + 9.21 \text{ dB} = -21.7 + 9.21 = -12.5 \text{ dBm} \quad \text{Eq. 3.10}$$

---

<sup>53</sup> These 72 PBCH OFDM carriers are QPSK modulated and jointly occupy a central bandwidth of 1.080 MHz ( $72 \times 15$  kHz).

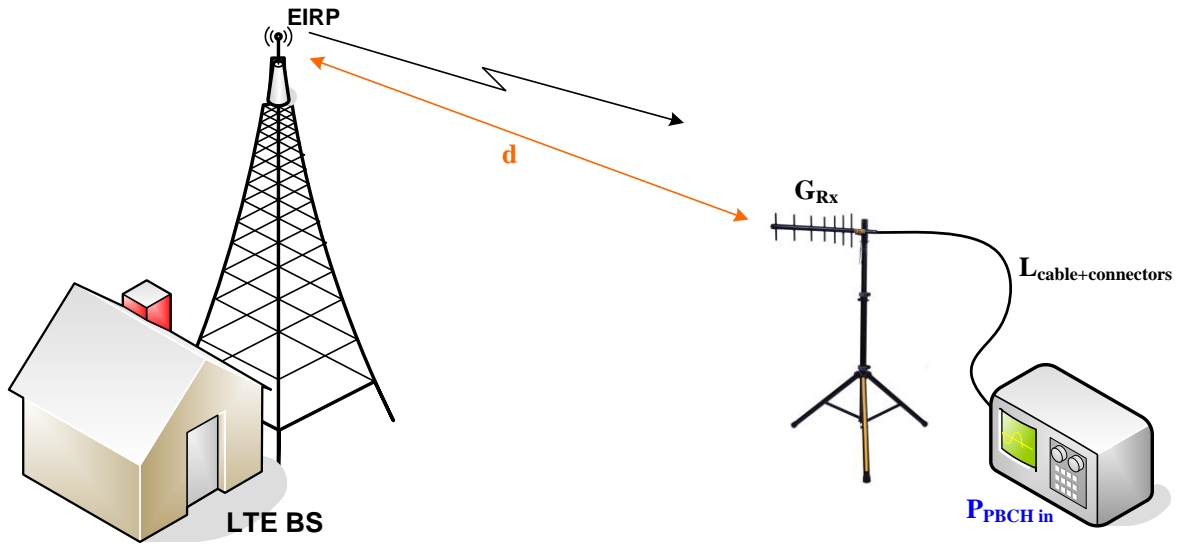


Fig. 3.15. EIRP estimation (possible radiated measurement scenario).

Assuming that the LTE BS is operating at the center frequency: 806 MHz, the free-space attenuation ( $L_{fs}$ ) can be computed using the Eq. 3.9.

$$L_{fs} = 32.4 + 20\log_{10}(806) + 20\log_{10}(0.5) = 84.5 \text{ dB} \quad \text{Eq. 3.11}$$

The maximum EIRP of the LTE BS is thus calculated back through the Eq. 3.12.

$$EIRP_{\max [dBm]} = P_{\max in [dBm]} + L_{\text{cable+connectors} [dB]} - G_{Rx [dBi]} + L_{fs [dB]} \quad \text{Eq. 3.12}$$

Substituting both results provided by the Eq. 3.10 and Eq. 3.11, and the remaining inputs into the Eq. 3.12, the maximum EIRP of 59 dBm is finally obtained (Eq. 3.13).

$$EIRP_{\max} = -12.5 + 1 - 14 + 84.5 = 59.0 \text{ dBm} \quad \text{Eq. 3.13}$$

This EIRP value would be then used to derive the BEM as exemplified in section 3.1.1.



### 3.3.1.1.2 Conducted Measurements (Methods 2 and 3)

Usually, under these circumstances (conducted measurement), the EIRP is indirectly obtained, by measuring the channel output power ( $P_{\text{Output}}$ ) of the BS and considering the antenna gain ( $G_{\text{Antenna}}$ ) and all system losses ( $L_{\text{cable+connectors}}$ ), according to the reference diagram illustrated in Fig. 3.16.

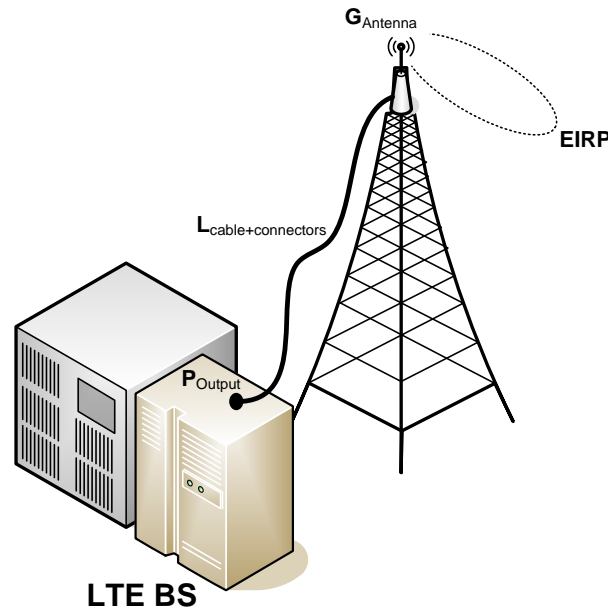


Fig. 3.16. LTE BS diagram.

The EIRP<sup>54</sup> is calculated as follows (Eq. 3.14).

$$EIRP_{[dBm]} = P_{\text{Output}} [dBm] + G_{\text{Antenna}} [dBi] - L_{\text{cable+connectors}} [dB] \quad \text{Eq. 3.14}$$

Based on this EIRP figure, the BEM is derived as exemplified in section 3.1.1. Obviously, the precision of the EIRP thus obtained is highly dependent on how accurate each system element (antenna, cable and connectors) was characterized.

<sup>54</sup> This EIRP value corresponds to the integrated power, in dBm units, within the LTE channel bandwidth. If the LTE BS is using a 10 MHz channel, the EIRP is naturally expressed in dBm/10MHz units.

### 3.3.1.2 Measurement Prerequisites

The recommendation [69] sets out some prerequisites that must be taken into consideration before starting a measurement. In short, these concerns are primarily related to the **dynamic range** – which should, as much as possible, be necessarily maximized –, and the adequate **removal/suppression of third party emissions** so as not to influence the BEM validation.

As a matter of fact, the dynamic range issue is of paramount importance, since it can dramatically limit a measurement, or even make it impracticable, particularly if a radiated method is being employed. Actually, the tight constraints imposed to the baseline limits to be observed in the FDD uplink frequencies, i.e., above 832 MHz (see Table 3.4), to meet the required out-of-block suppression, are so high that in most cases the full BEM validation is impracticable through radiated measurement approaches. This is because the BEM limits, to be assessed in such a band, are “submerged” by a higher level noise floor. Under these circumstances, a dynamic range better than 105.5 dB (see Fig. 3.6, assuming a derived BEM for an EIRP of 59 dBm/10MHz) would be necessary. This is, in fact, unrealistic, unachievable and impracticable, from the measurement perspective, in a vast majority of real scenarios, using a radiated method. Moreover, a possible emission of a mobile terminal station could not be removed and its effect would not be easily detached, then a false positive BEM violation could wrongly be diagnosed. For all the above reasons, **this method is, in practice, usually, only suitable to evaluate the core section of a BEM.**

But there are other important limitations when the radiated method is used. If other LTE BS coexist on the same site, **a potential violation cannot be directly attributable to the BS** under assessment, **without firstly understanding the actual contribution of the remaining transmitters.** This may require additional and detailed measurements.

Furthermore, the sideband levels of the other LTE emissions should be, at least, 10 dB below the sideband level of the emission under investigation, in each frequency range.

In order to provide adequate conditions for the BEM compliance evaluation, the levels of the signals of third party transmitters should be, at least, 6 dB below the BEM limits. If this suppression is not fulfilled, the measurement result is not reliable.

In any segment of a BEM, the levels or limits of the LTE sideband emissions should be above the receiver sensitivity.

However, the dynamic range can be improved in radiated measurement, by using directive antennas, on the receiving side, wisely located and positioned, in the far field region of the

transmitting antenna. A receiving antenna with a directive diagram pattern could be useful to better discriminate the desired signal and to reject the effect of unwanted emissions.

### 3.3.1.3 Measurement Methods for the Assessment of BEM compliance

The three above mentioned measurement methods, for the verification of BEM compliance, will be briefly described and inter-compared in the next subsections.

#### 3.3.1.3.1 Method 1: Radiated Measurement under Normal Operating Conditions

Despite the flaws pointed out to this measurement method, in practical monitoring applications, this can be the only method available in many cases, particularly when the access to a LTE BS is not possible.

If all measurement prerequisites are met, including the right position of the receiving antenna, the setup presented in Fig. 3.17 will be used.

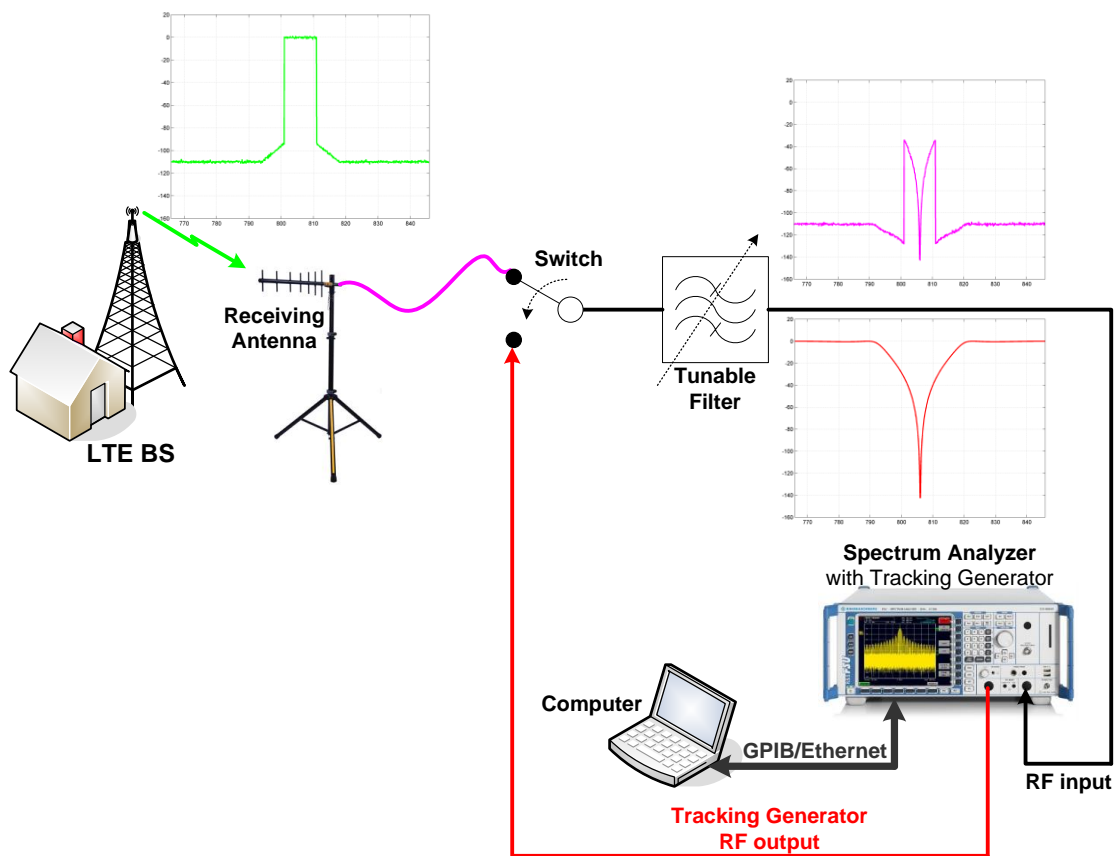


Fig. 3.17. Setup for Radiated Measurement under Normal Operating Conditions.  
Source: [69] (Spectrum analyzer image: credits to Rohde & Schwarz<sup>TM</sup>)

The setup is basically constituted by a high-gain **directional antenna** for signal reception, a purely conceptual **switch**, a **filter** (band-pass or band-stop), a **receiver** (typically, a *spectrum analyzer*), a **signal generator** (desirably, a *tracking generator*) and a **computer** to control all instruments, in order to implement a sequential measurement procedure, record the collected data and process the final results.

A spectrum analyzer with an integrated tracking generator is usually a good solution to put together a setup like this. Particularly, because it simplifies the control interfaces and connections, reducing them to a single General Purpose Interface Bus (GPIB) or Ethernet connection, between the computer and the spectrum analyzer.

In order to ensure that a measurement result is not influenced by the overloading of the receiver's front-end, a filter is used to reject strong undesired external emissions and, additionally, the control system should dynamically provide an automatic way of adjusting the receiver's input attenuation.

Therefore, a band-stop filter, typically a **notch filter**, may be used, **whenever no strong external emissions are detected**. In that case, it will be tuned to the central frequency of the LTE channel to be assessed. This solution makes the measurement process more expeditious because, once tuned the notch filter, with a single parametrization, there will be no need of further adjustments, when different sections of the BEM are being evaluated.

However, **if strong third party emissions may harm the measurement**, by overloading the receiver, a **band-pass filter** (BPF) has to be employed. In such a situation, the BPF requires multiple adjustments during the measurement, and has to be permanently tuned to the BEM section under assessment. Tunable filters of 3 or 5 cavities (poles) are recommended for the above purposes. [69]

The tracking generator is used to characterize the frequency response of the filter. Thus, the signal from the antenna is replaced by the tracking generator and the transmission characteristic of the filter is measured by the receiver. The information gathered, during this process, will be used to correct the LTE BS spectrum that is obtained at the output of the tunable filter, and then to reconstruct the original and desired LTE BS spectrum. This may have to be repeated for every individual tuning operation. The corresponding attenuation parameters will be selectively used according to the respective BEM section to which they belong.

If a spectrum analyzer is used, it has to be configured according to the settings<sup>55</sup> below (Table 3.7).

<b>Spectrum Analyzer</b>
<b>Span:</b> Zero
<b>RBW [kHz]:</b> 100
<b>VBW [kHz]:</b> $\geq 300$
<b>Detector:</b> RMS
<b>Sweep Time [μs]:</b> $71.3 \times \text{Horizontal Display Points}$
<b>Trace Mode:</b> Max Hold over 10 sweeps or more

Table 3.7. Spectrum Analyzer Configuration for BEM validation.

If, alternatively, a radiocommunications monitoring receiver is used instead, the following configuration applies (Table 3.8).

<b>Radiocommunications Monitoring Receiver</b>
<b>IF BW [kHz]:</b> 100
<b>Detector:</b> RMS
<b>Measurement Time [ms]:</b> 400
The maximum measured RMS level will be recorded

Table 3.8. Radio Monitoring Receiver Configuration for BEM validation.

The measurement is **sequentially** carried out **in steps of 50 kHz**, which is half of the RBW or IF bandwidth. Thereby, this is an **exhaustive** and **very time-consuming** measurement procedure, even when only the core segment of a BEM is evaluated. If a LTE BS signal has got a changeable and dynamic behavior, due to these time constraints, all those characteristics of the signal are completely lost.

Furthermore, the recommendation [69] also lays down precise guidelines to linearly integrate the corrected samples, within a BEM section, over the respective bandwidth, and that result is thus a series of **average power density values**, which will be compared to the relative BEM limits.

<sup>55</sup> This sweep time is defined in order to ensure that each horizontal display pixel corresponds to the RMS value of a single LTE symbol. The Max Hold trace mode is enabled over 10 sweeps in order to acquire, at least, 30 LTE radio frames and to hold the symbol with the highest RMS level. [69]

The following example aims to illustrate the use of the filter on the BEM measurement and the necessary corrections to be taken into account. For that purpose, a situation involving no strong third party emission is considered, and thus a notch filter is used.

A spectrum like a LTE downlink was generated using MATLAB™ (green line in Fig. 3.18), which represents the emission radiated by the BS<sup>56</sup>.

An infinite impulse response (IIR) digital filter was also designed in MATLAB, to emulate the notch band-stop. Concretely, a 3<sup>rd</sup> order Chebyshev filter, of type I, was implemented with a peak-to-peak ripple in the band-pass of 0.5 dB, and edge frequencies: 791 and 821 MHz, i.e. centered at 806 MHz, the central frequency of the channel under assessment. Its frequency response (transmission) is depicted, in red, in Fig. 3.18.

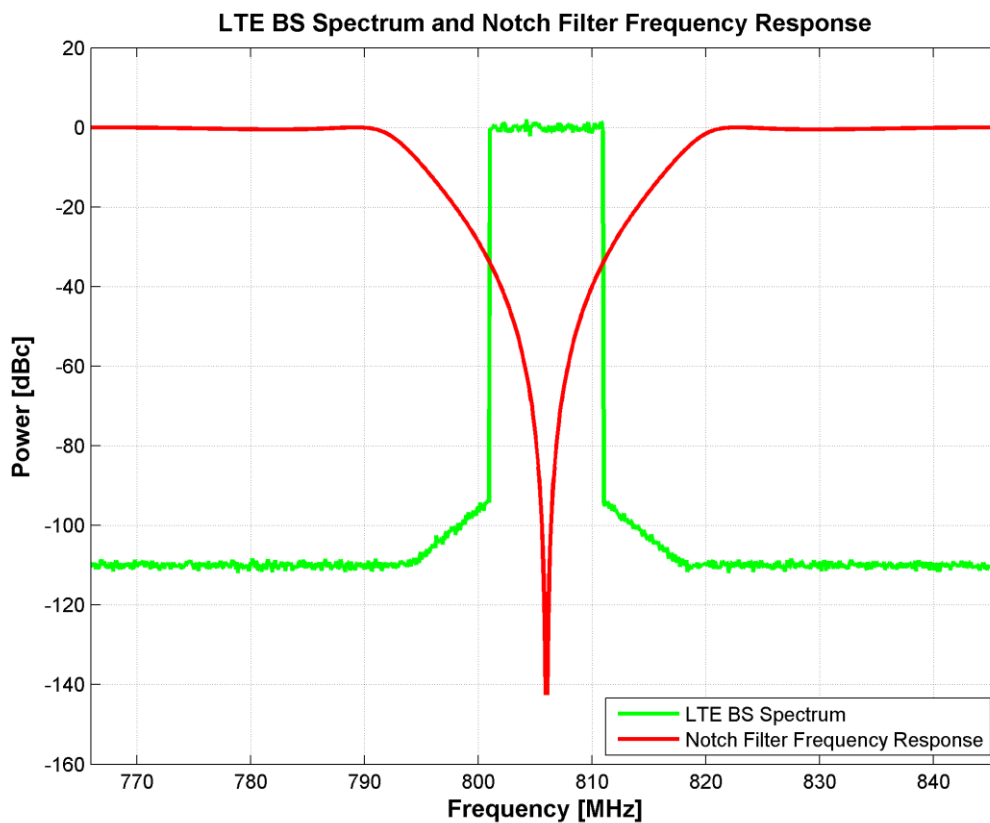


Fig. 3.18. LTE BS Spectrum to be measured and the Notch Filter frequency response (transmission).

<sup>56</sup> The spectrum colors match the corresponding spectra, as presented in Fig. 3.17, to make easy the identification of the signal, according to the stage of the measurement chain, in which it was obtained.

Considering the switch routed to the signal received by the antenna (see Fig. 3.17), after the filter, the original LTE BS spectrum is affected by its response as shown in Fig. 3.19.

The same figure also intends to highlight the heavy time-consuming characteristic of this measurement process, which iteratively progresses in step widths of 50 kHz, sweeping the entire extension of the BEM.

To give an order of magnitude, if the settings of Table 3.7 are applied, and considering 1024 horizontal display points, a sweep time of 73 ms is achieved. For the sake of simplicity, it will be rounded to 100 ms. Since 10 sweeps are, at least, needed per each measurement iteration, which corresponds to a spectrum slice of 50 kHz, then a single iteration lasts, at least, 1 second.

In order to cover the whole span ([760, 850] MHz, with a total bandwidth of 90 MHz), shown in the figure below, 1800 iterations have to be completed. Thus, the entire measurement process lasts, at least, 1800 seconds, i.e., **30 minutes!**

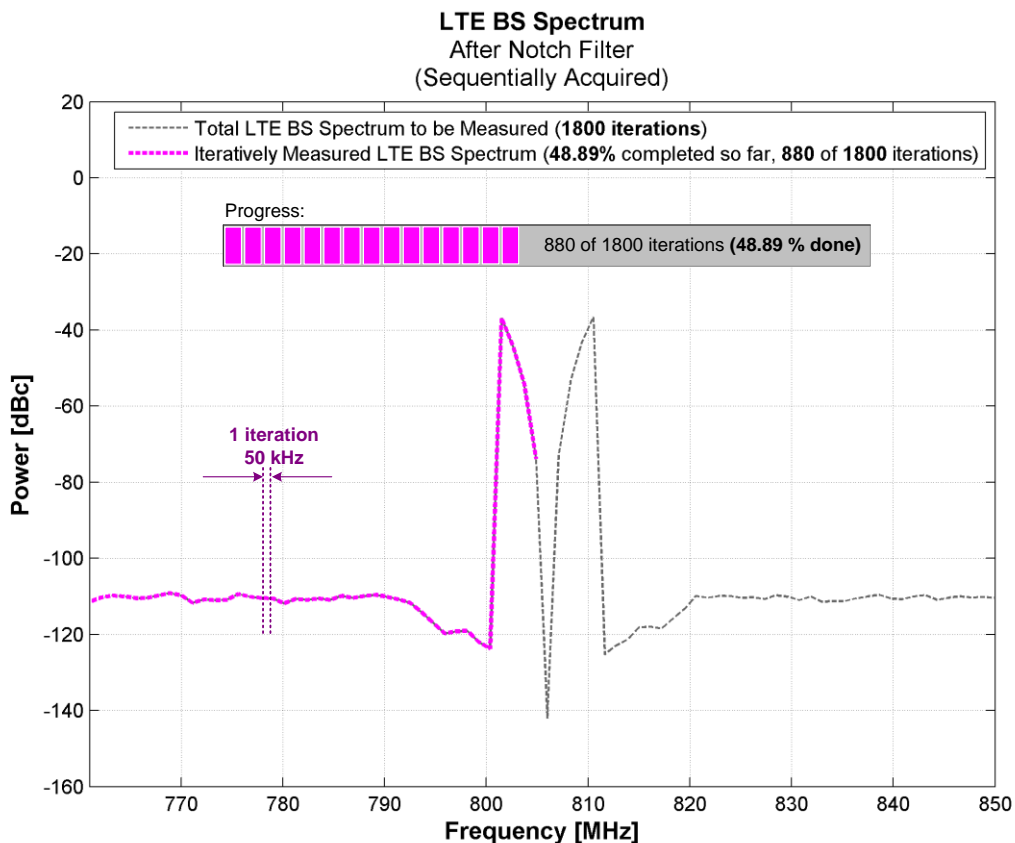


Fig. 3.19. LTE BS Spectrum iteratively measured after the Notch Filter.

After getting the complete filtered LTE BS spectrum (see magenta line, in Fig. 3.20), the desired LTE BS spectrum, to be compared to the respective BEM limits, is reconstructed from the filtered one, by compensating the frequency response, using the inverse transfer function of the notch filter (see blue line).

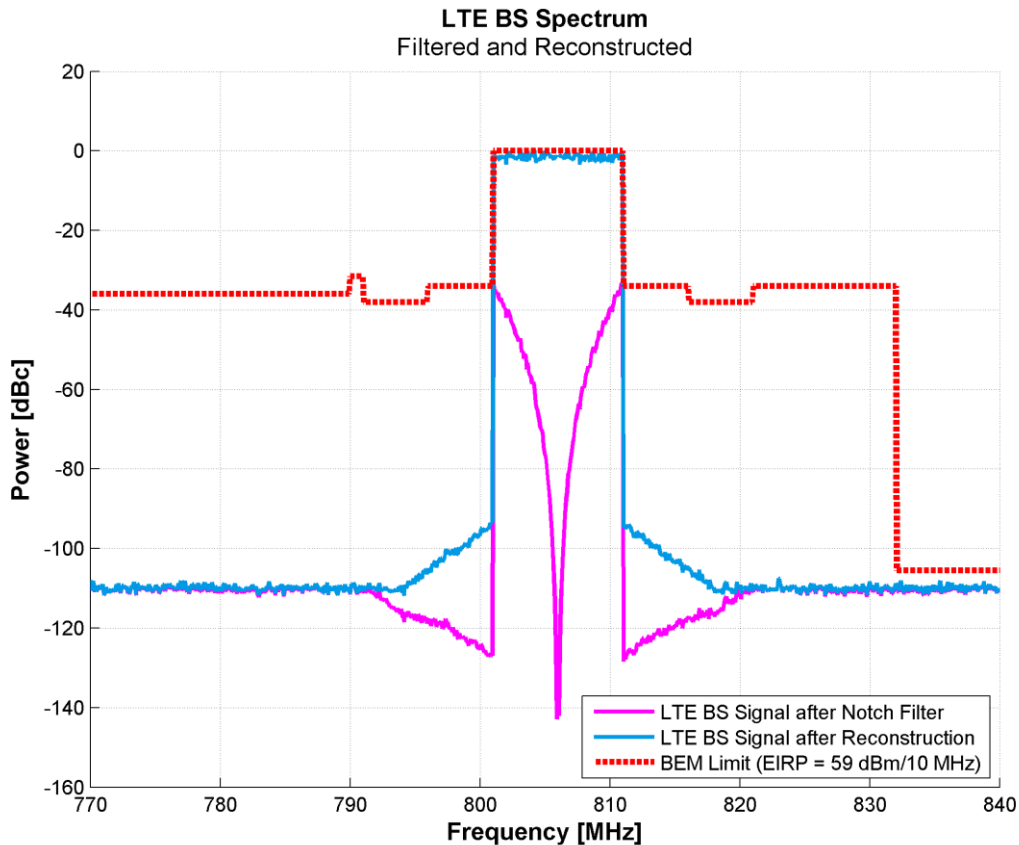


Fig. 3.20. LTE BS Spectrum: measured after the Notch Filter and reconstructed compared to the BEM limits (EIRP: 59 dBm/10MHz).

### 3.3.1.3.2 Method 2: Conducted Measurement under Normal Operating Conditions

The conducted measurement method, under normal operating conditions, is quite similar to the previously presented. The main difference is that the antenna is replaced by the power output, or test probe, taken out after the final stage of the LTE transmitter's amplifier.

Although it may degrade the global noise figure of the measurement chain, reference [113] includes an additional variable attenuator, before the tunable filter, to deal with expected higher



power levels and to protect the receiver's input. Fig. 3.21 shows the adapted setup for the present case.

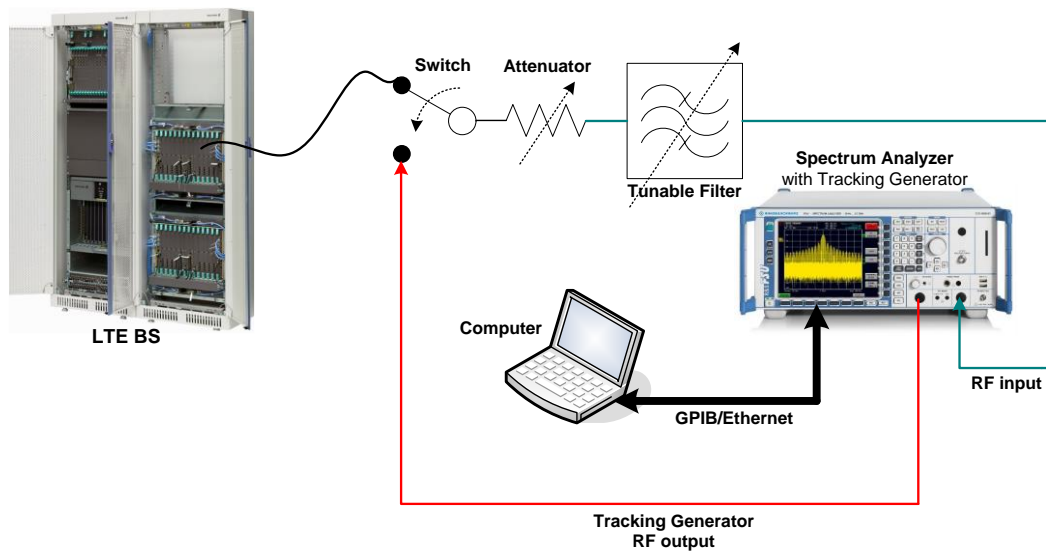


Fig. 3.21. Setup for Conducted Measurement under Normal Operating Conditions.

Sources: [69], [113]

(Spectrum analyzer image: credits to Rohde & Schwarz<sup>TM</sup>, LTE BS image: credits to Ericsson<sup>TM</sup>)

### 3.3.1.3.3 Method 3: Conducted Measurement according to the ETSI Test Modes

Among the three methods prescribed by the recommendation [69], this is perhaps the most comprehensive and accurate, since it allows to reproduce, in a controlled environment, extreme operating conditions and, that way, to carry out stress tests, which would not be possible with the previous approaches. However, it may prove to be of **little practical application** for radio monitoring, not only when the network operator is unable to interrupt the service for testing, for the required period of time; but also because it requires specific hardware and software options, which have to be provided by the BS equipment, in order to generate a predefined battery of tests, as specified by ETSI EN 301 908-14 [115]. Additionally, the measurement has to be properly supervised by a skilled technical staff, provided by the network operator.

Given the **tremendous constraints and limitations** presented by this measurement method, which **strongly humpers its practical application**, no special attention will be devoted to it, throughout this thesis. Nevertheless, further details may be obtained from [115].

### 3.3.1.3.4 The Pros and Cons of the Above Methods

Since the measurement methods have already been introduced, Table 3.9 puts in perspective their main differences, emphasizing intrinsic virtues and flaws.

Method	Pros	Cons
<b>1. Radiated Measurement under Normal Operating Conditions</b>	<ul style="list-style-type: none"> <li>• No need to involve the network operator</li> <li>• The BEM compliance can be assessed at any time</li> <li>• No interruption of the service is necessary</li> <li>• The operator cannot adjust the BS in order to pass the compliance tests</li> </ul>	<ul style="list-style-type: none"> <li>• Prerequisites may not be fully met</li> <li>• Sideband spectral components of the LTE emission under evaluation may be hidden by the noise floor</li> <li>• Adjacent emissions may make the full BEM evaluation impracticable</li> <li>• Uncertainty may be higher than that of conducted methods</li> </ul>
<b>2. Conducted Measurement under Normal Operating Conditions</b>	<ul style="list-style-type: none"> <li>• The full BEM evaluation is always possible</li> <li>• External emissions cannot influence the measurement results</li> <li>• Lower uncertainty than of the radiated method, if all gains and losses are accurately characterized</li> </ul>	<ul style="list-style-type: none"> <li>• The measurement appointment depends on the operator network availability</li> <li>• Access to the BS's premises has to be granted</li> <li>• Maximum sideband spectral components may not be evident, if the normal operation conditions do not trigger the desired behavior</li> <li>• If no test probe is available, the service will shortly be interrupted to insert a directional coupler at the transmission line</li> </ul>
<b>3. Conducted Measurement according to the ETSI Test Modes</b>	<ul style="list-style-type: none"> <li>• The full BEM evaluation is always possible</li> <li>• The test mode will force the maximum possible out-of-block LTE emissions (this is not always possible under normal operation conditions)</li> <li>• The highest reproducibility is assured by this method, because a predefined comprehensive battery of tests is used (test mode)</li> <li>• Lower uncertainty than of the radiated method, if all gains and losses are accurately characterized</li> </ul>	<ul style="list-style-type: none"> <li>• LTE service will be disrupted during the whole time of the measurement</li> <li>• The measurement appointment depends on the operator network availability</li> <li>• Access to the BS's premises has to be granted</li> <li>• Technical and skilled staff of the network operator is required to configure the BS into the necessary test modes</li> </ul>

Table 3.9. Advantages and Disadvantages of the BEM Compliance Measurement Methods.

Source: [69]

#### 3.3.1.4 Major Impairments of the ECC/CEPT Methodology

In conclusion, it is opportune to reflect on the appropriateness of the technical options adopted by the recommendation [69].

1. The core element of the measurement setup is the conventional/traditional **spectrum analyzer**. This metrological instrument has been used for years for spectrum analysis with reliable and fair results. However, they are only taken for granted if signals, under investigation, are **time invariant**, i.e., if steady-state regimes are actually reached. **That is not the case of LTE**. Thus, *the traditional spectrum analyzer is no longer suitable for the required purposes*.
2. Although, truth be told, in this context, the spectrum analyzer is not truly used as such. In fact, the **zero span** mode is configured, which provides time-domain measurement results, making a spectrum analyzer somehow “equivalent” to a frequency selective (or tuned) “oscilloscope”.
3. All in all, this greatly reduces the bandwidth of analysis. In the present case, “slender” spectrum slices of 50 kHz are sequentially analyzed, one at a time, which makes the measurement process indeed intricate, “tedious” and **very time-consuming**, even when only the core section analysis of a BEM is wished, i.e., within a central bandwidth of few 20 MHz.
4. If the assumptions made in section 3.3.1.3.1 are used, a time frame of about 7 minutes is necessary to scroll through the entire central segment, in steps of 50 kHz, from one end to the other.
5. As such, the **coincidence in time** of different spectrum slices of 50 kHz, which are being subsequently acquired, is not assured, at all, nor provided. Therefore, changeable and dynamic behaviors of LTE signals **may not be captured**, and they will be easily **ignored** or **neglected**. Particularly if, for instance, a specific group of OFDM subcarriers show a distinct behavior, within and outside the time windows, in which they were analyzed. As a consequence, the actual impact of such a behavior is not properly analyzed, and this is not innocuous in some interference scenarios, as has been demonstrated so far, and as it will be afterwards.

All these drawbacks are the right motto for developing alternative measurement approaches, in order to overcome common radio monitoring issues. This work aims to propose a new methodology **to be used on the validation of the central section of a BEM**, based on **joint time-frequency techniques**, which will be explored below.



---

# 4 Interference Scenarios in the Presence of Neutral Systems

This chapter aims to substantiate the concerns, expressed so far, on the application of resilient mechanisms to enforce suitable technical conditions to neutral systems – in order to effectively avoid interference – which are not purely conceptual issues. Indeed, they are of the utmost importance since they have very real effects in practical scenarios of coexistence of different radio technologies, as will be discussed and illustrated in the next two case-studies.

The first case-study reports an interference situation, in which a DVB-T receiver is harmed by a LTE BS emission in a close proximity. All fundamental aspects of the involved systems – victim and interferer – are carefully analyzed and a **mitigation solution** (innovative micro-strip filter) is proposed and tested, both in laboratory and in the field, in a real environment, in a small town of Alentejo, Portugal. As a matter of fact, it has proven very good performance and adequateness to tackle the identified problem.

The latter case alludes to a digitally modulated signal harmed by an unexpected narrowband spurious emission caused by a damaged TV amplifier, which was generating a peculiar behavior on the victim's received constellation, usually known as "*doughnut*" effect, an

impairment that affects in-phase and quadrature (IQ) modulators and demodulators. Such interference is mathematically addressed and reproduced, both by means of simulation and by laboratorial tests.

## 4.1 Case-Study 1: DVB-T reception harmed by a LTE BS emission

The deployment of LTE mobile communications systems has taken advantage from frequency bands of the “digital dividend”. As a consequence of this frequency-allocation planning for LTE services, some compatibility issues with DVB-T systems coexisting in adjacent bands have been encountered. This is a paradigmatic case of study, which addresses the coexistence of recent DTT (DVB-T) with mobile 4G LTE, becoming crucial to defend the TV reception [71], [72], [73], [74].

There are numerous factors that can influence the performance of radio systems; for example, modulation schemes, medium access techniques, transmitted waveform – continuous or pulsed type –, power levels, sensitivity of the receivers, transient effects, nonlinear impairments, etc. In order to properly address the coexistence problem of LTE communications systems and DVB-T, as interferer and victim, respectively, a rigorous and complete analysis has to be conducted. This includes a careful characterization of the interferer and the victim by means of suitable parameters to evaluate this radio compatibility scenario.

### 4.1.1 Scenario of Analysis

This study explores the impact of the European deployment of the LTE technology in the 800 MHz band to deliver mobile broadband services of next generation 4G, as potential technological neutral interferer to the DVB-T reception (victim).

The typical spectrum and spectrogram of a LTE downlink emission (800 MHz band) as possible DVB-T reception interferer, acquired with a RTSA, are jointly shown in Fig. 4.1. The DPX<sup>57</sup> mode of visualization of that signal is presented in Fig. 4.2. They were obtained by using a SMBV100A vector signal generator from R&S<sup>TM</sup>.

---

<sup>57</sup> DPX stands for Digital Phosphor Technology, and it is a Tektronix’s patented technology.

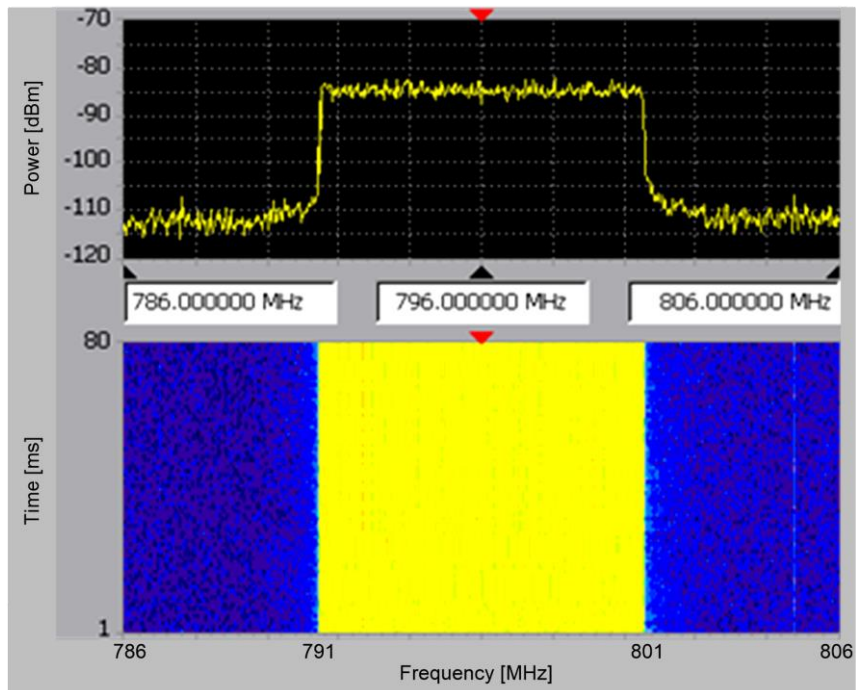


Fig. 4.1. Spectrum and spectrogram of a LTE FDD downlink (800 MHz band) signal as potential interferer to the DVB-T reception.

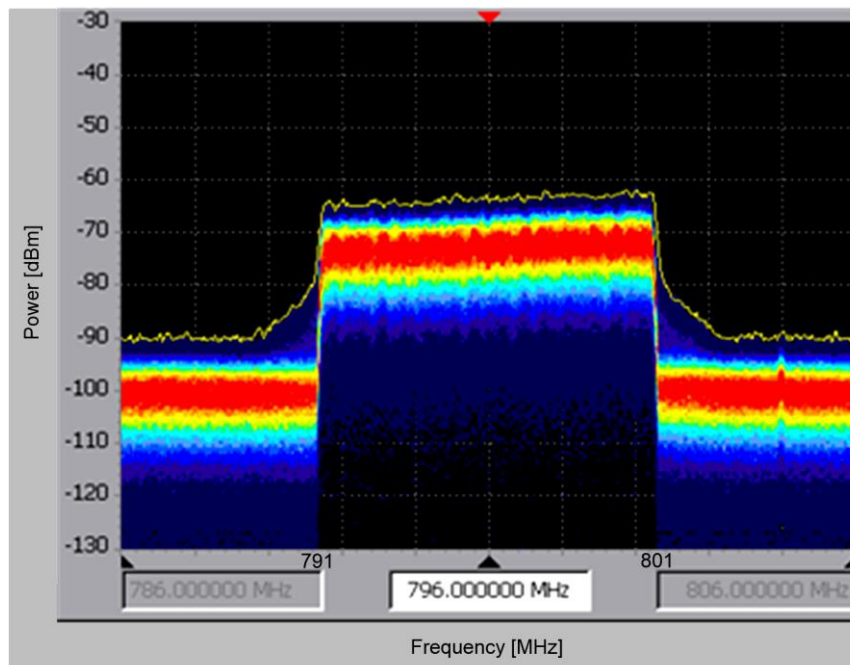


Fig. 4.2. DPX Spectrum of a LTE FDD downlink (800 MHz band) signal.

#### 4.1.1.1 DVB-T Systems: Victim

Most of DTT broadcasting networks in Europe are still based on the DVB-T standard [77]. Nevertheless, some European countries have gradually introduced the respective DVB-T2 evolution. Since the radio channels assigned to DTT are adjacent to the IMT 800 MHz band (see Fig. 2.3), the first ones become more vulnerable to suffer from interference effects caused by the latter. This could make the digital TV reception difficult, particularly if a LTE base station (BS) is in the vicinity.

##### 4.1.1.1.1 DVB-T Receiver

The block diagram depicted in Fig. 4.3 shows the architecture of a DVB-T receiver [78], [79], [80], [81].

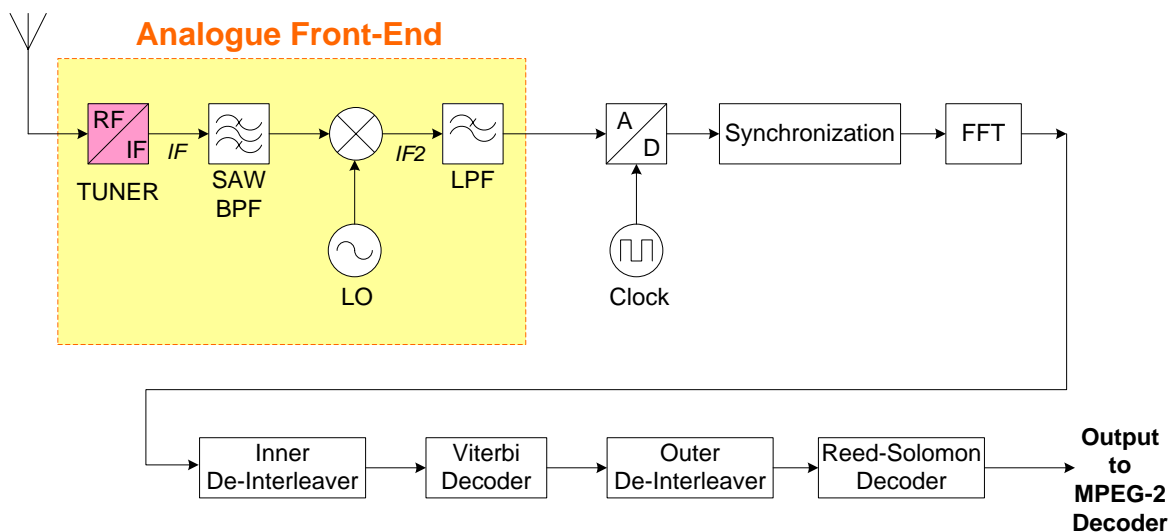


Fig. 4.3. Simplified block diagram of a DVB-T receiver.

The first main block of the DVB-T receiver is the **analogue front-end**, which should provide very good characteristics in terms of noise to assure a minimum signal-to-noise ratio (S/N) for a correct operation. The first device found inside this block is the **tuner**, which converts the received RF signal to the first intermediate frequency (IF).

Afterwards, the DVB-T signal is filtered at the IF level by means of a **surface-acoustic-wave (SAW) filter**. Such a high-selectivity band-pass filter (BPF) component enables to finely select the desired channel by efficiently rejecting the adjacent channels. Later, a **new down-**



**conversion** process takes place as a result of the beat between the previous filtered signal and a **second local oscillator**. Its task is to translate the DVB-T signal frequency range to the second IF (IF2), which is now subjected to a **low-pass filtering (LPF) process**. This anti-aliasing filter is used to remove those spectral components of the signal above the Nyquist frequency ( $f_s/2$ ) for its subsequent domain conversion through the **ADC** [82].

The autocorrelation techniques implemented in the synchronization block after the ADC are used to collect and recover synchronism information, which becomes crucial to position the fast Fourier transform (FFT) sampling window and the definition of the OFDM guard interval (GI). The echoes, which are processed within the GI, do not cause inter-symbol interference (ISI) and contribute constructively to the demodulation of the DVB-T signal. [83] The synchronism information is essential for the FFT processing stage.

Henceforth, the blocks dedicated to the channel-coding and error correction functions are found [77]. They include an inner de-interleaving module that prepares the bits and symbols to the Viterbi decoder (soft decision), which provides a preliminary error correction. The outer de-interleaving (convolution) block rearranges the information that is coming from the output of the Viterbi decoder, thus making easier and more efficient the error correction task in the Reed-Solomon decoder.

Finally, the output of the Reed-Solomon decoder feeds the input of the MPEG-2 decoder.

From the perspective of analysis of potential interferences and possible vulnerabilities, it is particularly important to address and assess the robustness of the nonlinear devices which integrate the analogue front-end. This mainly refers to the tuner, which comprises a mixer to implement the first down-conversion, and the subsequent mixer, which is used to perform the second down-conversion. Indeed, these are extremely sensitive parts when attacked by high-power signal levels.

Among them, the **tuner** is probably the most critical block, not only for being the most exposed one to the external signals received by the antenna but also because it includes a pre-amplifier (nonlinear device) preceded by a low-selectivity pre-selector filter. Moreover, the down-converter is also inherently nonlinear, even though it is preceded by an additional band-pass filter [80]. A more detailed view of the tuner block<sup>58</sup> is provided by Fig. 4.4.

---

<sup>58</sup> LNA denotes low-noise amplifier.

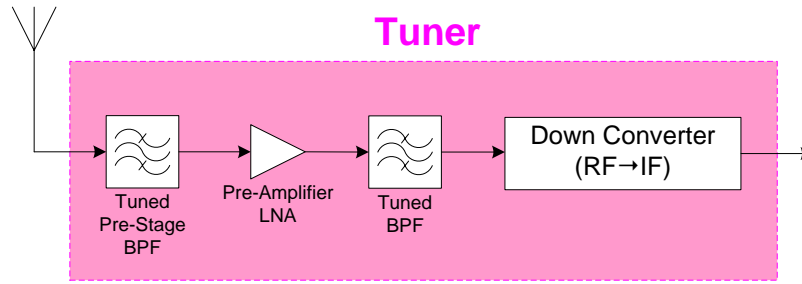


Fig. 4.4. Simplified block diagram of the tuner of a DVB-T receiver.

But the potential of interference can actually be exacerbated in more complex, but widespread installations for DVB-T reception. Specifically, external signal amplifiers (i.e., excluding the receiver amplifier) must also be considered for a more rigorous evaluation of overall system performance. These amplifiers, which typically show significant power gains and broadband operation to enable transmission of all the DVB-T channels, are very prone to nonlinear phenomena due to saturation. Distorted conditions of operation, like these, easily degenerate into a plurality of undesired effects, such as intermodulation, blocking (de-sensitivity), cross-talk, etc.

Fig. 4.5 illustrates a typical scenario of DVB-T reception, where the respective installation integrates a Yagi antenna and a low-noise mast pre-amplifier followed by a line amplifier. The latter compensates the losses of the coaxial cables, power splitters and taps, which are basic part of the entire installation employed to distribute the DVB-T signal across the building.

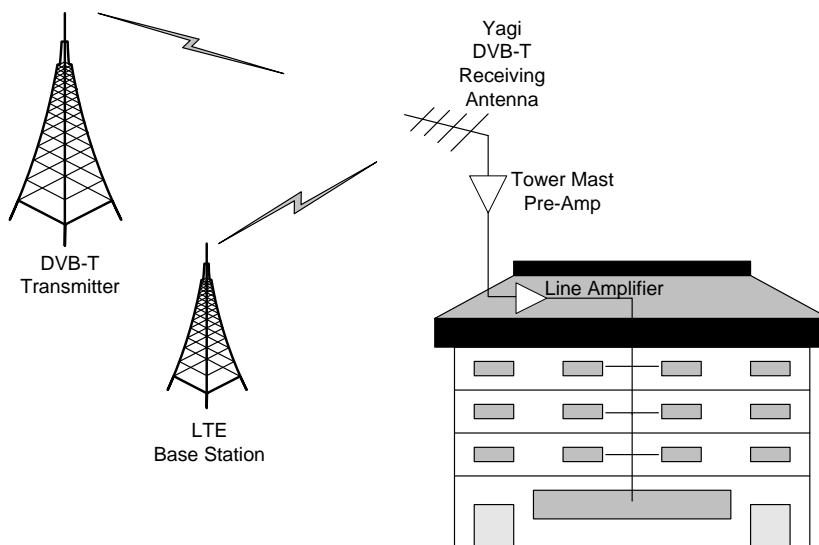


Fig. 4.5. Typical scenario of DVB-T reception affected by the proximity of a LTE BS.

#### 4.1.1.1.2 Performance Indicators for DVB-T Reception

Digital systems make use of error correction techniques to guarantee greater robustness and reliability for the information to be transmitted, thus ensuring as much as possible the whole integrity of its content. Nevertheless, in the presence of interference, they tend to react more disruptively than their analogue system counterparts. The particular case of the TV system is paradigmatic in this sense, because, even when interfered and/or presenting some degradation, the analogue reception was not interrupted most of the times. This contrasts with the typical and well known “**cliff-edge**” effect of the digital TV reception in the presence of an interferer, which prevents very often the service reception, depending on the energy of the perturbation [14].

It is therefore of paramount importance to adopt appropriate and consistent criteria to evaluate the quality and performance of DTT systems [84], [85], [86]. For the specific case of DVB-T, it is crucial to analyze the following performance key indicators and figures of merit:

- a) Received Field Strength<sup>59</sup> – or, alternatively, Signal Level<sup>60</sup>.
- b) OFDM Spectrum Shape.
- c) Carrier-to-Noise Ratio (C/N).
- d) Modulation Error Rate (MER).
- e) Bit Error Rate (BER):
  - i. Before Viterbi decoding (BER1).
  - ii. After Viterbi decoding/Before Reed-Solomon decoding (BER2).
  - iii. After Reed-Solomon decoding (BER3).
- f) Impulse Response<sup>61</sup> (Echoes Diagram).
- g) Constellation Diagram.

---

<sup>59</sup> Typically expressed in dB $\mu$ V/m units.

<sup>60</sup> Commonly presented in dB $\mu$ V units.

<sup>61</sup> Relevant in Single Frequency Networks (SFN). [87]

Without underestimating the importance of the other indicators, but purely for practical reasons, since they are quite popular in the analysis of the quality of the DVB-T reception, the attention here will focus on the **MER** and **BER** parameters.

The MER is perhaps the figure of merit that is most extensively used to evaluate the quality of a DVB-T signal, because it is very complete, rich and comprehensive. This parameter aggregates the cumulative effect of possible impairments and individual errors which directly affect digital modulated signals, hence providing a faithful and accurate description of the whole system performance [78]. The MER is mathematically described in depth in [81].

In the presence of noise (e.g., additive white Gaussian noise (AWGN)) or interference, the constellation diagram of a signal appears typically distorted and its points (symbols) tend to scatter around the centers of decision forming a cloud shape. One of the most remarkable characteristics of the MER is its ability to quantify, in a very concise way, this degree of dispersion around the theoretical or ideal position of each symbol of the constellation. Whenever significant deviations of these points are detected, the MER is automatically degraded; indeed, it signalizes the existence of problems on the signal, which is sympathetically followed by the increase of the BER as a consequence of the erroneous bits produced in the meantime.

The impairments of the transmitter chain are reflected on the signal constellation as error vectors, and the MER is also an alternative way of characterizing the Error Vector Magnitude (EVM). Both parameters are closely connected, being the relationship between the MER and EVM well defined in [81].

As the MER can be directly compared to a C/N or S/N, its interpretation is easier and more intuitive than that of the EVM. Thus, it has become a more popular and complementary method of evaluating the S/N or the capability of demodulation of a certain receiver.

If the most significant impairment which affects a signal is of AWGN type, then the MER and the S/N become equivalent. However, the MER is a more complete and richer figure of merit, since it considers not only the effect of the Gaussian noise but also all other impairments which affect the demodulated constellation (interferers, nonlinear effects: intermodulation, cross-talk, blocking, etc.). In the receiver chain, the MER is taken immediately before the Viterbi decoder in accordance with the characteristics of the reception channel (Fig. 4.6).

Another key indicator is the BER, which reflects the amount of erroneous bits among the total of the transmitted bits during a given period of time.

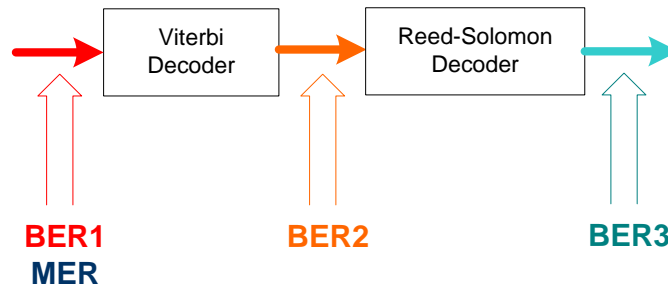


Fig. 4.6. Points of the DVB-T reception chain, where the MER and the BER are taken out.

Actually, in the DVB-T context, three fundamental kinds of BER are defined, depending on the point at which that BER is taken out:

- i. **BER1:** *BER before Viterbi decoding (or Channel BER: cBER).*
- ii. **BER2:** *BER after Viterbi decoding (or vBER), or Before Reed-Solomon decoding.*
- iii. **BER3:** *After Reed-Solomon decoding (or BER RS).*

The *Post Viterbi BER* (BER2) is a fundamental indicator to assess the quality of the reception or the degree of interference of a DVB-T system. The reference value of the BER2 is  $2 \times 10^{-4}$ , which is defined as the “**quasi-error free**” (**QEF**) condition [77]. The QEF condition states “*less than one uncorrected error event per hour*”, which corresponds to a BER3 =  $10^{-11}$  at the input of the MPEG-2 de-multiplexer. It should be emphasized that, depending on the code rate, the BER1 value to meet the QEF requisite changes [86]. For example, for a code rate equal to 2/3, then BER1 =  $4 \times 10^{-2}$ ; on the other hand, for a code rate of 3/4, then BER1 =  $2 \times 10^{-2}$ .

#### 4.1.2 Nonlinear Impairments

Commercial DVB-T receivers have been prepared so far to receive wanted digital broadcasting TV signals, up to and including the channel 69. However, after the release of the first digital dividend in Europe, the channels in-between 61 and 69 became to be exclusively allocated to electronic communications systems in accordance with a technological neutrality basis. The operation of LTE systems was not harmonized in these channels. As the launch of DVB-T was prior to that of the LTE, there are several millions of DVB-T receivers in operation which have been introduced in the market. These modules are therefore highly vulnerable to

the coexistence of LTE systems in the 800 MHz band. Indeed, they even lack of the most basic mechanisms of protection against interference, such as a suitable pre-selection filtering in the RF front-end input to reject these unwanted emissions from other co-located radio systems<sup>62</sup>.

No specifications had been provided for such filtering by manufacturers, at the time. As such, some parts of “older” DVB-T receivers are very susceptible to nonlinear phenomena. In the nearby of LTE BSs, the blocking effect has been identified as the most common cause of interference in practical situations, preventing the proper DTT reception if the LTE signal levels are significantly higher than the wanted DVB-T signal levels.

Moreover, the reception facilities of the users did not take into account additional preventive measures against interferences caused by LTE operation. It is therefore common to find wideband signal amplifiers (mast pre-amplifiers and line amplifiers) which easily saturate in the presence of strong unwanted signals, thus contributing to severely degrade the DTT received signals due to nonlinear phenomena.

As one of the key contributions of this work, an innovative and optimized **band-stop filter** device to be inserted at the RF amplifier input of the DVB-T receiver is developed and characterized.

Its capability to mitigate the DTT reception problems due to LTE coexistence will be also corroborated through its careful testing in a real scenario of interference.

#### 4.1.3 Innovative Band-stop Filter<sup>63</sup> for LTE interference Mitigation on the DVB-T Reception

One solution to the LTE interference problem in the DVB-T reception scenario is the use of a low-pass or band-stop RF filter. Such a device must be capable of sufficiently suppressing the LTE spectral range while enabling good transmission characteristics for the full operative band of DVB-T channels. Nevertheless, although simple in theory, the development of this filter can be extremely challenging due to the very stringent selectivity specifications imposed by this application and some additional practical limitations. Indeed, since the upper DVB-T channels and the lower region of the LTE band are spectrally adjacent, a very sharp cut-off slope between

---

<sup>62</sup> Currently, some manufacturers are already providing DVB-T receivers with chipsets which include in-built digital adaptive band-pass filters to reject such undesired adjacent emissions.

<sup>63</sup> The micro-strip band-stop filter device was developed in association with **Roberto Gómez-García** and **Miguel-Ángel Sánchez-Soriano**, who supervised its design, production and implementation.

transmitted and suppressed bands must be assured. The latter inevitably leads to the necessity of electrical networks with a huge number of capacitive and inductive elements, with associated problems related to insertion losses. Furthermore, the following shortcomings arise depending on the specific topology and/or technology adopted for this filter:

- In a lumped-element realization, the tolerances of commercial discrete components can make useless a practical low-pass filter design for LTE mitigation in relation to the theoretically predicted transfer function. Besides, repeatability for its mass-production can be seriously compromised due to this limitation.
- Classic stepped impedance distributed element planar low-pass filter implementations require a high number of sections to achieve such very demanding selectivity. It results in excessive circuit-size dimensions [88].
- Band-stop coupled resonator distributed element planar band-stop filter developments share the same problem regarding occupied area. Moreover, the narrow coupled-line separations that could be necessary here could make their design very critical to manufacturing tolerances.

This section reports an original and efficient alternative for the realization of LTE-suppressed band-stop planar filters for DVB-T reception. It exploits signal-interaction mechanisms along with rejection stubs to achieve very high levels of selectivity for such design simplicity [89], [90]. Also, since lumped elements and coupled-line sections are avoided, most of previously mentioned disadvantages are circumvented. For validation, a proof-of-concept micro-strip filter prototype is synthesized, manufactured, and characterized.

#### 4.1.3.1 Theoretical Principles of the Proposed Band-stop Filter

The circuit detail of the proposed band-stop filter is shown in Fig. 4.7. As can be seen, it consists of the matched mirrored cascade of two identical band-stop filtering cells, which take benefit of two different principles to attain a sharp-rejection band-stop frequency-selective function. These are as follows:

- The transversal signal-interaction phenomenon taking place between the two electrical paths of this building parallel-type transmission-line band-stop filtering cell, which generates a wide-band band-stop range around the design frequency  $f_d$ . These electrical paths are formed by connecting non-uniform impedance transmission line segments. As will be demonstrated here, it permits to maximize

as possible the sharpness between the low-pass type transmission band and the stopband region. This is a key requisite in the current application, owing to the very close spectral proximity between the intended DVB-T channels and the LTE interference.

- The open-ended rejection stubs connected at the input and output nodes of the two-path band-stop filtering cells, which further enhance the overall filter selectivity by two ways: 1) increase of the attenuation levels in the stopband range and 2) improvement of the cut-off slope sharpness when synthesized as in-band resonating poles within the low-pass type transmission band.

Note also that, through the optimized cascade of the two band-stop filtering cells, out-of-band power rejections levels higher than twice those offered by the single filtering cell are feasible in the whole filter device. Moreover, two similar transmission-line segments are inserted at the input/output nodes of the overall filter to optimize the in-band power matching levels for the low-pass type transmission range. Thus, the desired UHF DVB-T channels can be properly processed without significant amplitude-distortion effects.

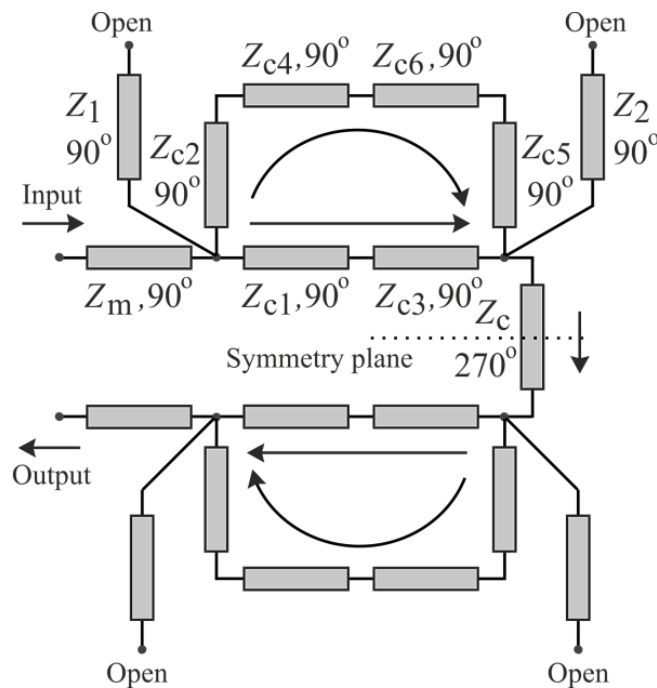


Fig. 4.7. Detail of the proposed band-stop transversal signal-interaction filter<sup>64</sup>.

<sup>64</sup> Characteristic-impedance variables and electrical lengths at the design frequency  $f_d$ , in degrees, are indicated.



To conclude, it is important to emphasize that owing to the extremely sharp rejection characteristics of the engineered band-stop filter solution of Fig. 4.7, the first transmission zero frequency  $f_{z1}$  of its stopband becomes a very reasonable approximation to the 3 dB cut-off frequency  $f_c^{3dB}$  of its low-pass type transmission band. Such frequency can be analytically derived for the simplified case  $Z_{c4} = Z_{c5} = Z_{c6} \equiv Z_c$ , giving rise to the following expression (Eq. 4.1):

$$f_c^{3dB} \cong f_{z1} = \frac{2f_d}{\pi} \cos^{-1} \left( \sqrt{\frac{-Z_{c1} + 3Z_{c2} - Z_{c3} + Z_c}{4(Z_{c2} + Z_c)}} \right) \quad \text{Eq. 4.1}$$

The above mathematical relationship can be then utilized as a first approximation in the ideal synthesis of the band-stop filter.

#### 4.1.3.2 Experimental Results

Based on the devised two-stage transversal signal interaction band-stop filter topology of Fig. 4.7, an ultra-sharp rejection band-stop filter prototype aimed at the mitigation of the LTE interference in the DVB-T reception scenario has been designed, fabricated in micro-strip technology, and measured. It was assumed that this circuit must permit the transmission of a DVB-T signal centered at 754 MHz – upper part of the transmission band region – while efficiently rejecting a generic interferer allocated at the first LTE channel, thus having a center frequency of 796 MHz and a bandwidth no higher than 10 MHz – lower part of the stopband –.

The values for the design variables of the ideal synthesized band-stop filter, in accordance with the notation adopted in Fig. 4.7, are indicated below ( $f_d = 1.295$  GHz and a  $50 \Omega$  impedance value is assumed for ease of fabrication, although the concept is also suitable for a  $75 \Omega$  one). They were obtained after an optimization process of the whole filter directed at maximizing the cut-off slope between the low-pass type transmission band and stopband regions, as needed by the very demanding specifications imposed by this application.

- Band-stop transversal filtering section:  $Z_{c1} = 118 \Omega$ ,  $Z_{c2} = 111 \Omega$ ,  $Z_{c3} = 120 \Omega$ ,  $Z_{c4} = 103 \Omega$ ,  $Z_{c5} = 109 \Omega$ , and  $Z_{c6} = 110 \Omega$ .
- Input/output open-circuit-ended stubs:  $Z_1 = 72 \Omega$  and  $Z_2 = 75 \Omega$ .

- Input/output matching transmission lines:  $Z_m = 64 \Omega$ .
- Cascading transmission line:  $Z_c = 49.5 \Omega$ .

The power transmission and reflection parameters of the ideal synthesized band-stop filter are represented in Fig. 4.8 for a broadband spectral range and the detail of the low-pass-type-transmission-band-to-stopband transition (inset).

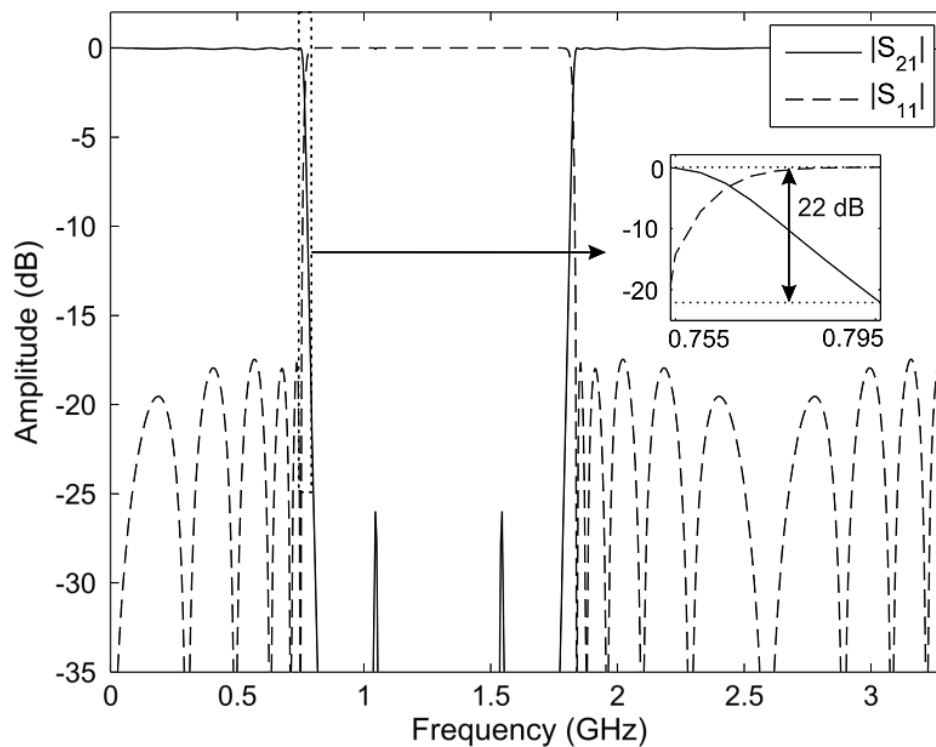


Fig. 4.8. Power transmission ( $|S_{21}|$ ) and reflection ( $|S_{11}|$ ) responses of the ideal synthesized band-stop filter for a broadband spectral range and the detail (inset) of the transition between the low-pass type transmission band and the stopband

As can be seen, a transfer function with extremely high selectivity is attained. In particular, power attenuation levels of 0.1 dB and 22.1 dB for the frequencies 754 MHz and 796 MHz, respectively, are obtained. This leads to a cut-off attenuation slope of 430 dB/GHz; to our best knowledge, it could be the highest one reported up to date for this type of planar filter for such a 25 dB attenuation level referred ultra-broad stopband bandwidth, which goes from 800 MHz to 1.789 GHz. This contributes to suppress additional interference effects that could appear from other co-located systems, such as Terrestrial Trunked Radio (TETRA) operating at the 800 MHz

band for South America and Asia Pacific. Furthermore, if necessary, greater rejection capability can be derived through this approach by cascading more transversal filtering sections, but at the expense of increased circuit size.

The layout and a photo of the constructed band-stop filter prototype are shown in Fig. 4.10 and in Fig. 4.10. For circuit fabrication, a low-loss organic ceramic micro-strip substrate TLC-30 from Taconic™ was selected. Its parameters are: relative dielectric permittivity  $\epsilon_r = 3$ , dielectric thickness  $h = 1.52$  mm, metal thickness  $t = 35$   $\mu\text{m}$ , and dielectric loss tangent  $\tan(\delta_D) = 0.0027$ .

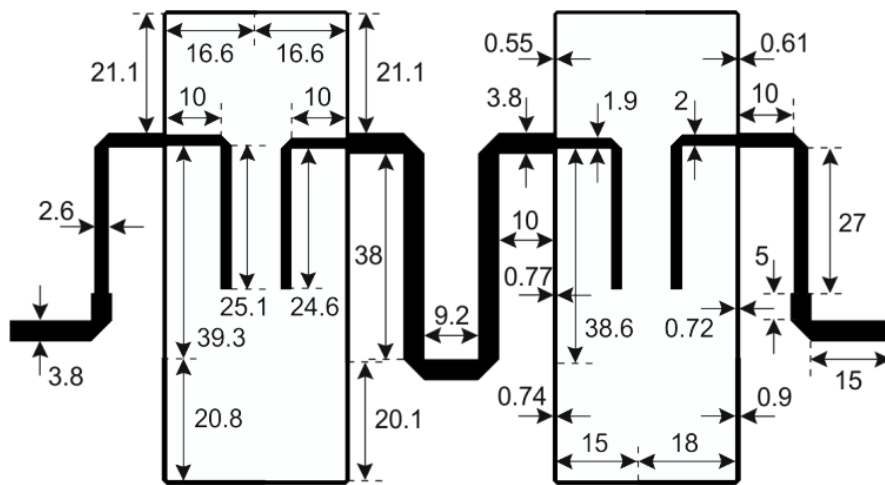


Fig. 4.9. Layout of the manufactured micro-strip band-stop filter prototype (non-redundant dimensions, in mm, are indicated)

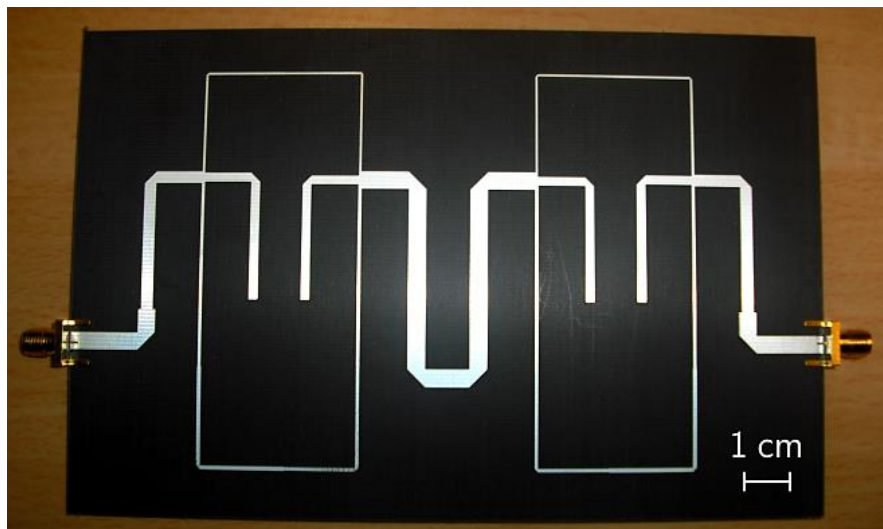


Fig. 4.10. Photo of the manufactured micro-strip band-stop filter prototype.

The simulated and measured power transmission and reflection responses of the built band-stop filter prototype are depicted in Fig. 4.11.

As a basic figure of merit to quantify the phase distortion introduced by the circuit over the DVB-T channels, the in-band group-delay results are also provided in Fig. 4.12. Simulations were performed by means of the 2.5-D electromagnetic-field software tool SONNET™ [91], whereas measurements were taken through a network analyzer HP-8713B from Agilent Technologies™ and include the effects of the SMA-type input/output connectors.

As observed, a fairly close agreement between predicted and experimental results is obtained. The measured power attenuation levels for the frequencies 754 MHz and 796 MHz are 1.1 dB and 13.6 dB, respectively. The very small upper spectral displacement observed in the measured cut-off slope between the low-pass type transmission band and the stopband (of about 10 MHz) can be due to manufacturing tolerances and deviations in the relative dielectric permittivity of the real micro-strip substrate. The maximum in-band group-delay variation in the low-pass type transmission range (it was measured between 50 MHz and the 3 dB cut-off frequency) is 9 ns.

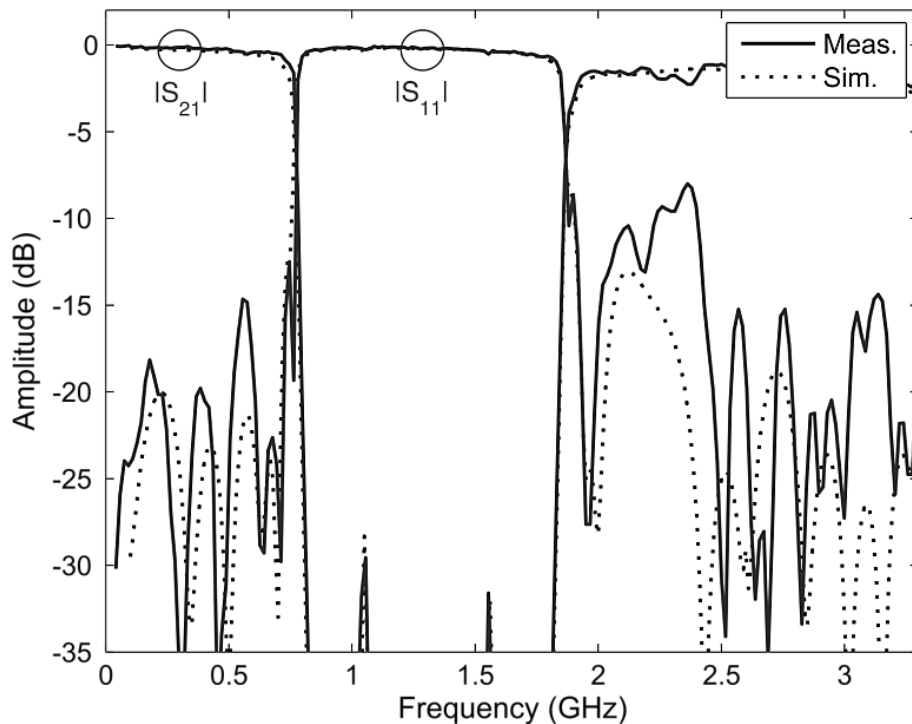


Fig. 4.11. Simulated and measured power transmission ( $|S_{21}|$ ), reflection ( $|S_{11}|$ ) responses of the manufactured micro-strip band-stop filter prototype.

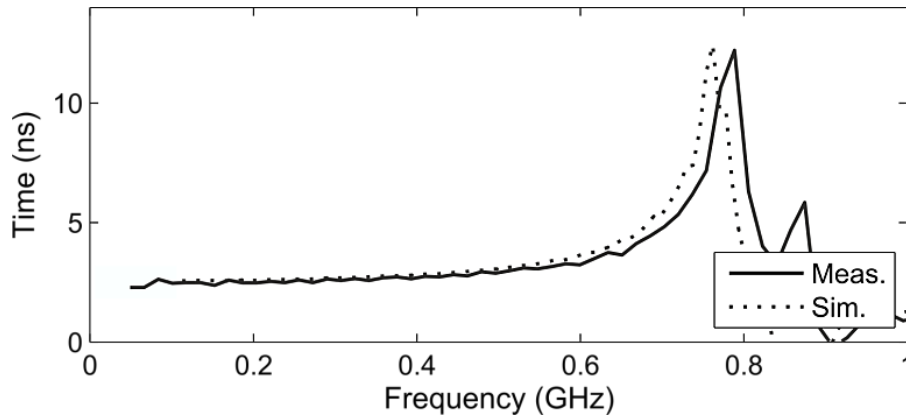


Fig. 4.12. Simulated and measured group-delay responses of the manufactured micro-strip band-stop filter prototype.

#### 4.1.3.3 Comparative Analysis of Performance

The performances of the built RF band-stop filter prototype of Fig. 4.10 have been compared with those of some LTE-suppression low-pass filters available in the market. Specifically, two samples of the same commercial low-pass filter configuration have been selected and evaluated.

Fig. 4.13 shows the power transmission and Fig. 4.14 the reflection responses of the three circuits within the 700-950 MHz range. As can be seen, despite providing less power attenuation for the LTE interference, the band-stop filter prototype of Fig. 4.10 exhibits better characteristics in terms of in-band power matching (which is very important to have a good system interconnection performance) and amplitude flatness for the DVB-T channels. This consequently implies lower amplitude and phase distortion levels for in-band DVB-T processed signals.

To complete the study, the DVB-T reception scenario in the presence of LTE interference has been emulated in the laboratory for the DVB-T channel 56. The same conditions (signals and levels) were used for the evaluation of each filter device under test (DUT).

Fig. 4.15 shows the block diagram and Fig. 4.16 a photograph of the experimental setup, when testing the RF band-stop filter, although the three circuits were evaluated.

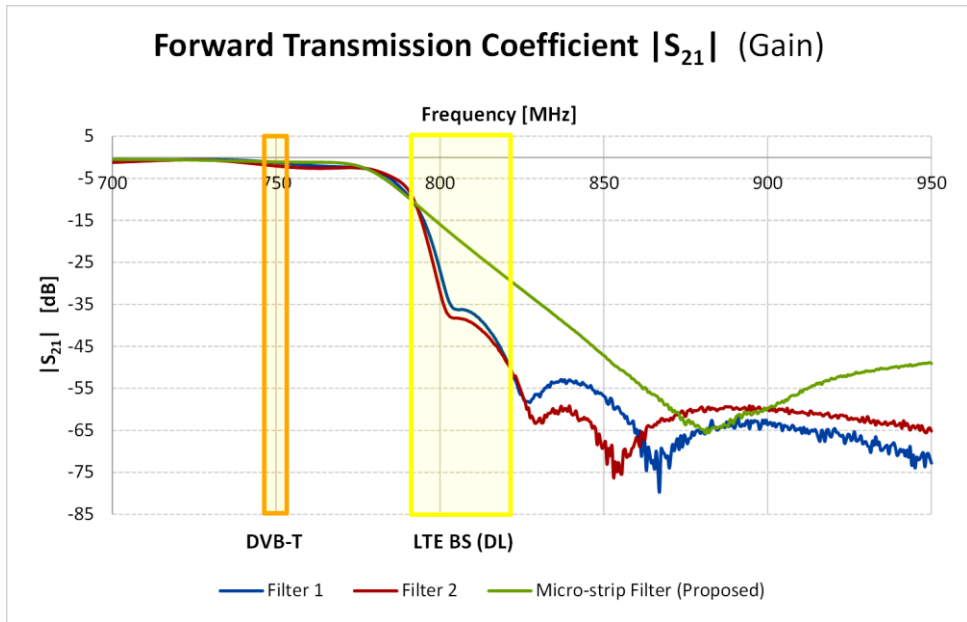


Fig. 4.13. Comparison of the measured power transmission ( $|S_{21}|$ ) responses of the manufactured micro-strip band-stop filter prototype and two commercial filter samples (filters 1 and 2).

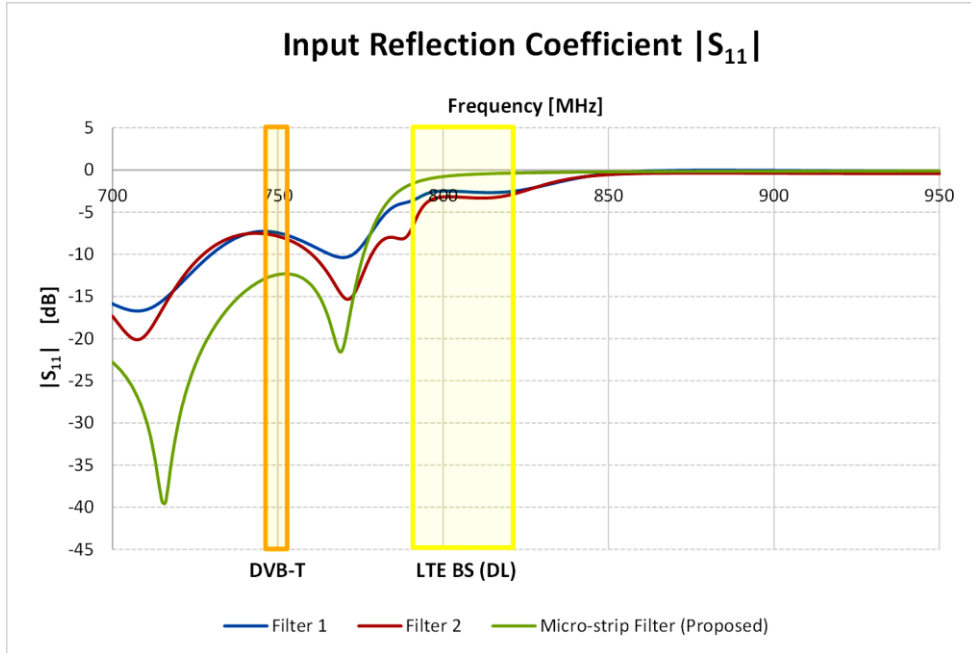


Fig. 4.14. Comparison of the measured reflection ( $|S_{11}|$ ) responses of the manufactured micro-strip band-stop filter prototype and two commercial filter samples (filters 1 and 2).

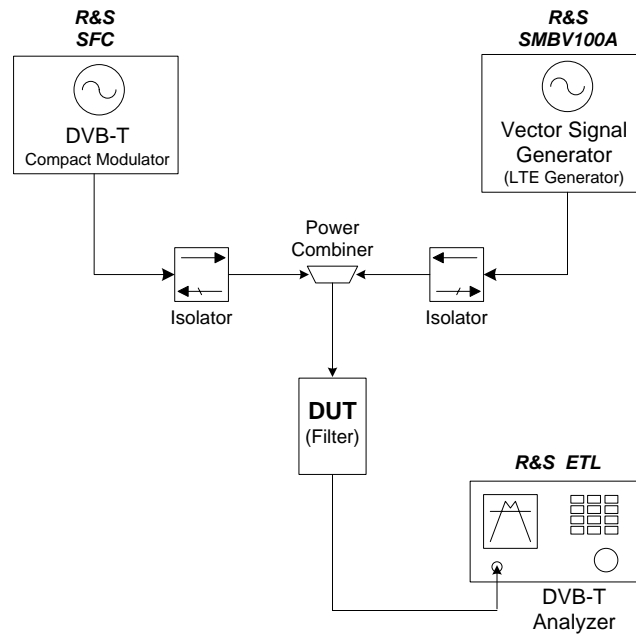


Fig. 4.15. Block Diagram: Setup to emulate the DVB-T (channel 56) reception scenario with LTE interference for filter evaluation.

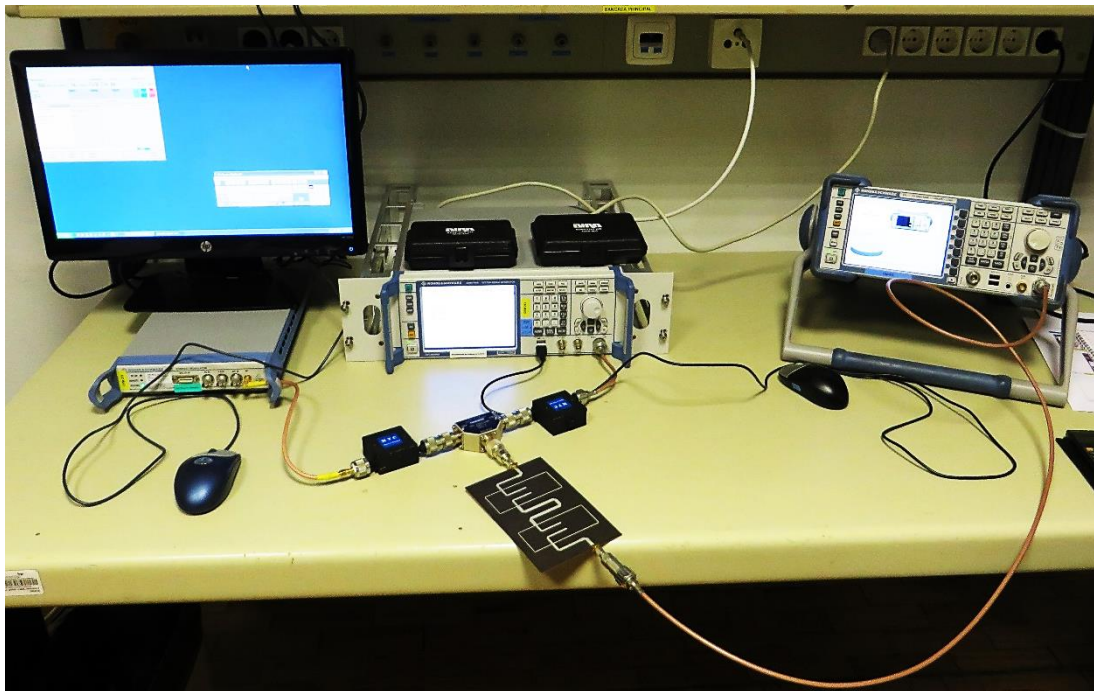


Fig. 4.16. Photo: Setup to emulate the DVB-T (channel 56) reception scenario with LTE interference for filter evaluation.

A summary of the values for main figures of merit and indicators obtained for this experiment is provided in Table 4.1. As demonstrated, the proposed RF band-stop filter slightly outperforms the commercial ones, hence corroborating its effectiveness.

Furthermore, other advantages regarding circuit simplicity, no need of post-tuning and subsequent repeatability for its mass production, and low cost must be also highlighted.

DTT Performance Indicator	Without any Filter	With Filter 1	With Filter 2	With Micro-strip Filter
Signal Level (dB $\mu$ V)	41.2	40.0	39.5	41.2
MER (dB)	17.4	23.5	23.4	23.8
BER1, cBER	$6.8 \times 10^{-2}$	$3.4 \times 10^{-4}$	$3.9 \times 10^{-4}$	$2.4 \times 10^{-4}$
BER2, vBER	$6.7 \times 10^{-3}$	0	0	0
BER3, BER RS	$1.7 \times 10^{-5}$	0	0	0
C/N (dB)	18.1	24.6	24.4	24.9
MPEG SYNC	No	Yes	Yes	Yes

Table 4.1. Comparative Analysis of Filter Performance (Channel 56)

#### 4.1.4 Mitigation of the Interference on DVB-T Reception due to LTE in Portugal

The planar RF band-stop filter circuit previously developed was also evaluated in a real interference scenario to mitigate the effect of a LTE emission on the DTT reception. The obtained results for this experiment are presented below.

The test was conducted after the installation of a LTE (800 MHz band) BS (see Fig. 4.17) in a building located at the center of a small town in the region of Alentejo, Portugal.

The coexistence of LTE and DTT technologies showed compatibility issues that did not exist before, which needed to be tackled due to its significant impact on the DVB-T reception. The interference was mainly detected in a close neighborhood from the LTE BS, preventing the access to the broadcasting service. The LTE channel assigned to the operator has 10 MHz of bandwidth in the band 791-801 MHz.



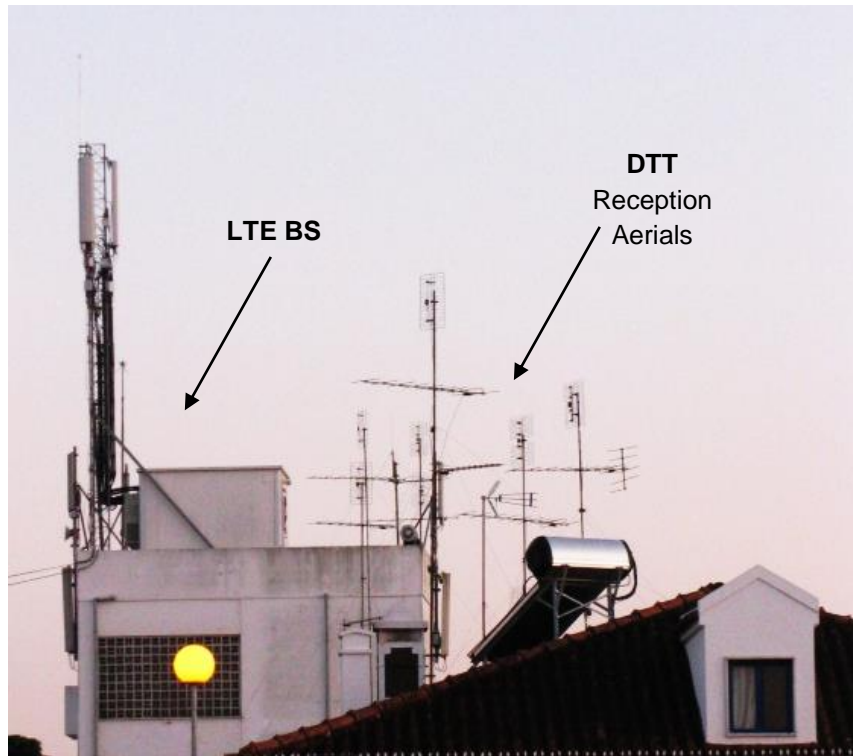


Fig. 4.17. LTE BS and surrounding environment (very close to DTT aerials).

The DVB-T coverage was provided by a SFN operating on the channel 56 (i.e., 750-758 MHz). As shown in Fig. 4.18, the correspondent best-server transmitter was situated about 4.5 km away from the building with direct line-of-sight between the transmitter and the receiver.

Under normal conditions, taking into account the technical settings of the DTT transmitter and the geo-morphological characteristics of this location, no difficulties on the DTT reception were to be expected. However, the presence of such close LTE BS contributes with additional high-power interference signals at the input of the broadband TV amplifiers, which can put them to work into nonlinear region; thus, the undesired phenomena associated to these nonlinear effects can become prohibitive for DVB-T reception.

In order to properly assess the interference problem on this particular DTT reception scenario, a worst-case point of analysis was chosen at about 100 m from the LTE station (Fig. 4.19). This worst-case location corresponds to the situation in which the DTT reception aerial is almost in the same direction of both best-server DTT transmitter and LTE BS.



Fig. 4.18. Relative positions of the receiver, the LTE BS and the DTT best-server transmitter.



Fig. 4.19. Relative positions of the DVB-T receiver (point of analysis) and the LTE BS.

The spectrum presented in Fig. 4.20 shows the difference between the levels of the DVB-T and LTE emissions when no filter is used. As observed, a considerably higher power for LTE component was measured when compared to that of the DVB-T signal of channel 56.

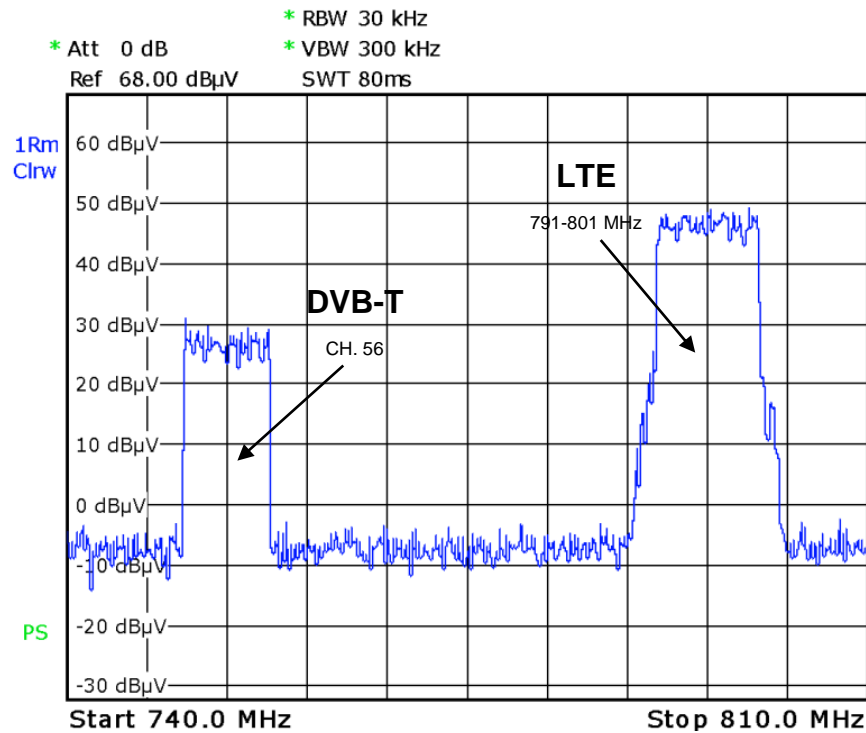


Fig. 4.20. Spectra of the DVB-T and LTE signals before filtering.

The “blocking” effect (emulated by using the pre-amp of the DVB-T analyzer) was thus identified. It prevented the demodulation of the DTT signal nearby the LTE BS, as confirmed by the constellation diagram of Fig. 4.21. This is also corroborated by the poor quality indicators listed in Table 4.2, which are not compatible with the required minimum QoS levels.

Subsequently, the micro-strip RF band-stop filter prototype, presented in section 4.1.3, was inserted before the pre-amp input in order to attenuate the contribution of the LTE signal (Fig. 4.22). As demonstrated through the constellation diagram represented in Fig. 4.23, the DTT reception was now possible with moderately fair/good conditions, as indicated in Table 4.2. Specifically, a remarkable gain of 10.7 dB was successfully achieved for the MER figure of merit, whereas a considerable improvement of the BER indicators was attained. This sufficiently confirms the practical usefulness of the developed RF band-stop filtering device for the addressed problem, even in the most adverse real scenarios of coexistence/compatibility of DTT and LTE radio systems.



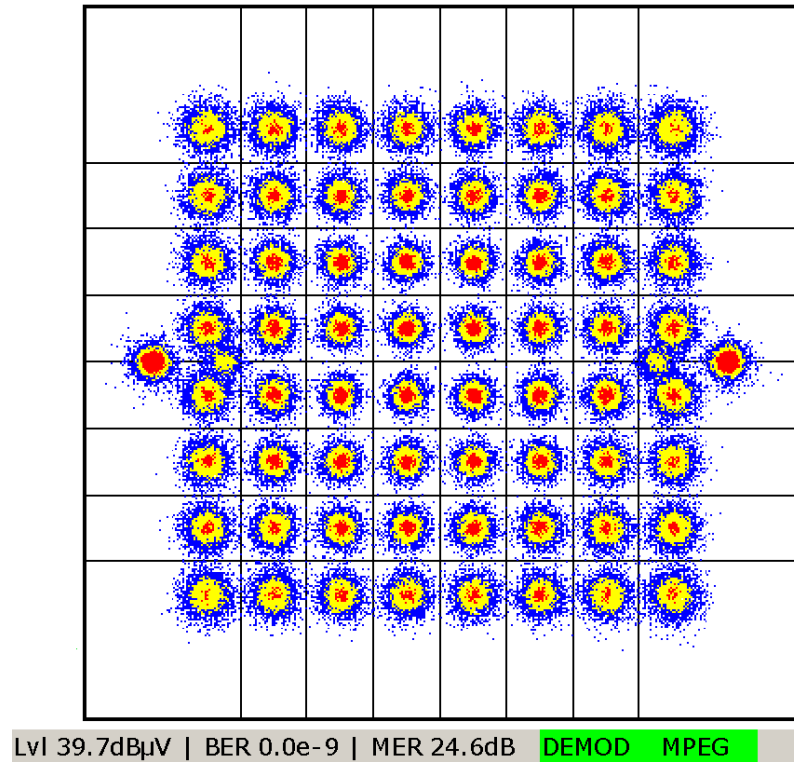


Fig. 4.23. DVB-T constellation diagram after inserting the band-stop filter before the RF front-end of the test receiver to reject the LTE signal.

DTT Performance Indicator	Without Filter	With Micro-strip Filter
Signal Level (dB $\mu$ V)	39.7	39.7
MER (dB)	13.9	24.6
BER1, cBER	$8.8 \times 10^{-2}$	$7.0 \times 10^{-5}$
BER2, vBER	$8.0 \times 10^{-3}$	0
BER3, BER RS	$6.0 \times 10^{-3}$	0
C/N (dB)	14.1	26.3
MPEG SYNC	No	Yes

Table 4.2. Summary of DVB-T Indicators: Comparative Analysis

#### 4.1.5 Summary

This case-study has addressed the important problem of DVB-T reception when affected by a neighbor LTE interferer in current wireless communications environments. This coexistence scenario has recently acquired a paramount relevance, due to the allocation of LTE services in some frequency bands of former analogue TV systems in the vicinity of DVB-T emissions.

Main aspects of the interferer (LTE) and the victim (DVB-T reception) have been expounded and key figures of merit and quality indicators to evaluate this coexistence situation have been described. Also, undesired nonlinear impairment issues that may arise as a result of inappropriate radio compatibility have been detailed. As one of the major contributions of this work, an innovative RF band-stop filter device aimed at enabling the DVB-T reception in the presence of a LTE interferer has been devised. A proof-of-concept micro-strip prototype has been built and measured, being competitive with other LTE-mitigation filter solutions available in the market. Its practical effectiveness has been successfully verified in a real case study in a small town of the region of Alentejo, Portugal.

## 4.2 Case-Study 2: The “Doughnut” Effect

This case-study describes and analyzes a peculiar effect detected by spectrum management teams in a real situation of electromagnetic interference. It consists of a practical scenario in which a digital modulated radio signal was being harmed by a spectrally adjacent narrowband spurious emission generated by a television reception amplifier, which was part of a MATV (Master Antenna TV) distribution system, used to deliver DTT broadcasting signals inside a residential building. This amplifier was oscillating in frequency due to malfunctioning. Under such abnormal conditions of operation, a “doughnut” shape was observed on each symbol of the constellation diagram of the received digital signal.

This is a particular case of IQ imbalance impairment that will be addressed here using a straightforward but consistent mathematical formulation. To complement the theoretical approach and experimentally corroborate the developed study, the “doughnut” phenomenon will be replicated by means of both simulation techniques and laboratory tests.

### 4.2.1 Scenario of Analysis

A complaint was filed to the spectrum control services, reporting a radio interference which was harming the reception of a digital quadrature amplitude modulated (QAM) emission: victim. In the field, nearby the premises of the affected receiver, the engineers observed a “doughnut” effect on the constellation diagram of the wanted signal.

The spectral analysis showed an adjacent narrowband perturbation, exhibiting a significant power level, sweeping the captured signal spectrum up and downwards. Using direction finding techniques, the perturbation source was successfully identified and localized. It resulted to be caused by a malfunctioning television (TV) reception amplifier (Fig. 4.24), in which the Barkhausen stability criterion was inadvertently being met, thus working as an oscillator and consequently producing an unwanted spurious radio emission. Moreover, as the damaged amplifying device was directly connected to the external Yagi-Uda TV receiving aerial (Fig. 4.25), the latter turned out to be transformed into a transmitting antenna with a given gain.

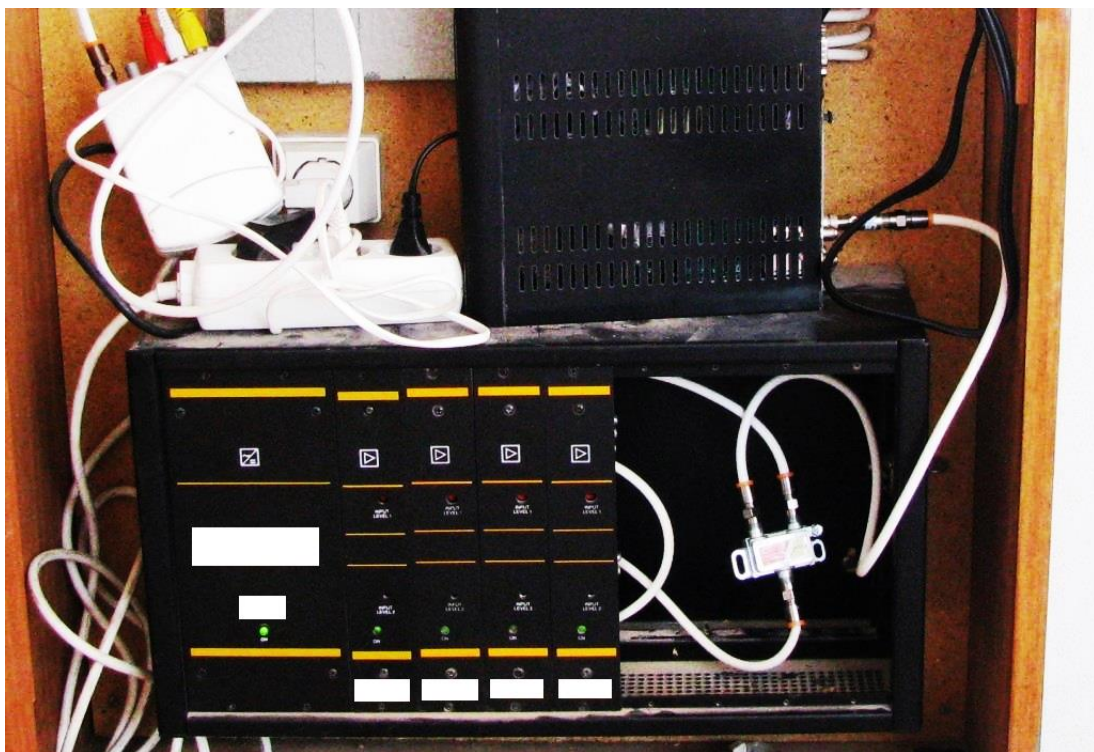


Fig. 4.24. The interferer: a damaged TV amplifier.

This contributed to further amplify the spurious energy in the direction of its maximum of radiation, leading to the worst-case reception scenario for the victim. The aforementioned spurious radiation effect was made even more critical after being magnified by the victim receiver antenna and front-end amplifier (Fig. 4.26).



Fig. 4.25. The interferer tri-axial Yagi-Uda aerial.

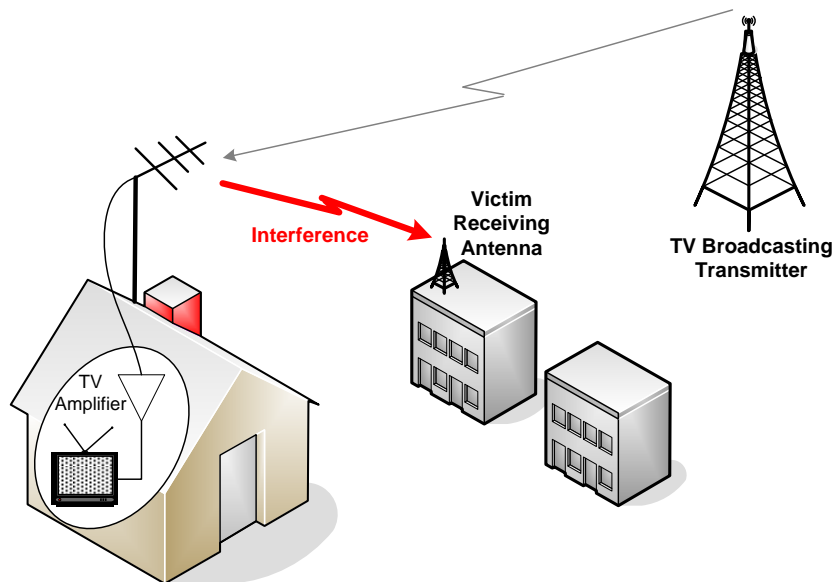


Fig. 4.26. Undesired interference-affected operation scenario.



The power level of the spurious signal, measured at the output of the TV amplifier, was of -65 dBm. Thus, considering that the cable and the connector losses were about 5 dB, and the antenna gain was 15 dBi, it turned out that this spurious narrowband signal was being radiated with a non-negligible EIRP level of -55 dBm. After identifying and localizing the perturbation source, the amplification equipment was effectively neutralized and the “doughnut” effect was cancelled, disappearing on the victim side.

It is important to mention that the “doughnut” effect has also been identified and reported in other practical scenarios of electromagnetic interference involving digital systems (e.g., DVB and, more particularly, DVB-C/T; and DOCSIS: Data over Cable Service Interface Specification) and a coherent or a narrowband interferer. The accurate modelling of this effect, as well as other kinds of interference phenomena in telecommunication applications, becomes essential for their subsequent mitigation through signal processing and/or hardware procedures, aimed at assuring a minimum QoS. [92], [93], [94], [95], [96], [97], [98], [99], [100]

Despite IQ imbalance problems are well documented in the technical literature (cf., e.g., [101], [102]), much less attention has been devoted to the particular case of the “doughnut” effect. Some complex studies can be found in [81], [103], [104], [105], [106], which describe this type of interference problem from an empirical/qualitative perspective to provide conclusions based on statistical analysis of the cloud distributions of the resulting constellation diagrams.

The analysis developed below complements the aforementioned approaches by presenting a rigorous and easy-to-follow mathematical explanation of this peculiar effect. Furthermore, the provided analytical framework is also confirmed by means of experimental results obtained from both simulation and laboratorial tests.

## 4.2.2 Interference Analysis

This section introduces a mathematical framework for the explanation of the “doughnut” effect in the addressed radio interference scenario. In relation to it, it should be noticed that the IQ demodulator embodied in the victim receiver is sensitive to the presence of a narrowband spurious, modelled here by a coherent interferer. Thus, whenever the amplitude of such interferer is sufficiently high, each symbol of the constellation associated to a demodulated signal is transformed into a “doughnut” shape distribution around each ideal center (transmitted symbol).

To explain the “doughnut” effect, let it be considered an IQ modulator and a coherent interferer – a simple continuous wave (CW) carrier – which will be both combined at the input of an IQ demodulator. The conceptual block diagram of this interference scenario is illustrated in Fig. 4.27.

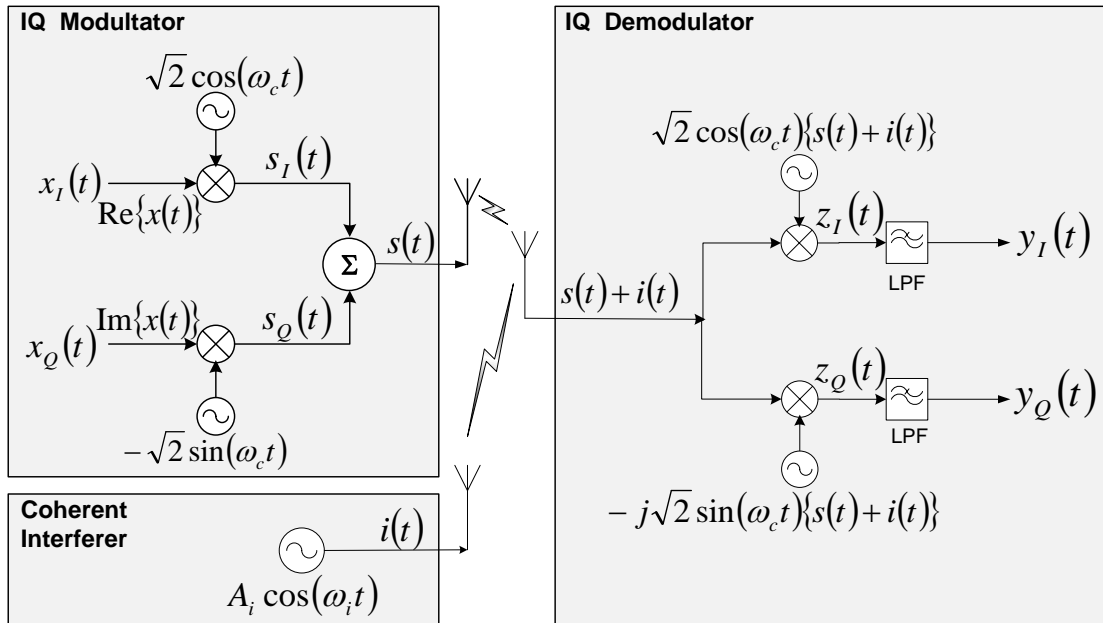


Fig. 4.27. Conceptual block diagram of the interference scenario.

Let it be assumed a complex input signal  $\tilde{x}(t)$  as follows:

$$\tilde{x}(t) = x_I(t) + jx_Q(t) \quad \text{Eq. 4.2}$$

The modulated signal  $s(t)$  obtained at the output of the IQ modulator will be then given by the following expression:

$$s(t) = \sqrt{2}x_I(t) \cos(\omega_c t) - \sqrt{2}x_Q(t) \sin(\omega_c t) \quad \text{Eq. 4.3}$$

During the transmission over the propagation channel, a coherent interferer  $i(t) = A_i \cos(\omega_i t)$  will harm the wanted signal  $s(t)$ . It affects its reception at the input of the IQ demodulator as mathematically indicated below:

$$s(t) + i(t) = \sqrt{2}x_I(t) \cos(\omega_c t) - \sqrt{2}x_Q(t) \sin(\omega_c t) + A_i \cos(\omega_i t) \quad \text{Eq. 4.4}$$

After the two down-conversion processes towards the base-band, two signals will be obtained. These signals are referred here as  $z_I(t)$  and  $z_Q(t)$  for the upper and the bottom branches, respectively (Fig. 4.27). The expression of  $z_I(t)$  is given by:

$$z_I(t) = \sqrt{2} \cos(\omega_c t) \{ \sqrt{2}x_I(t) \cos(\omega_c t) - \sqrt{2}x_Q(t) \sin(\omega_c t) + A_i \cos(\omega_i t) \} \quad \text{Eq. 4.5}$$

After developing Eq. 4.5, the following equation is derived:

$$z_I(t) = 2x_I(t) \cos^2(\omega_c t) - 2x_Q(t) \cos(\omega_c t) \sin(\omega_c t) + \sqrt{2}A_i \cos(\omega_c t) \cos(\omega_i t) \quad \text{Eq. 4.6}$$

Using adequate trigonometric identities, Eq. 4.6 can be further simplified in the following equivalent form:

$$z_I(t) = 2x_I(t) \left[ \frac{1}{2} + \frac{1}{2} \cos(2\omega_c t) \right] - x_Q(t) \sin(2\omega_c t) + \frac{\sqrt{2}}{2} A_i \{ \cos[(\omega_c + \omega_i)t] + \cos[(\omega_c - \omega_i)t] \} \quad \text{Eq. 4.7}$$

At this stage, a low-pass filtering operation denoted as  $LPF\{\blacksquare\}$  is performed over  $z_I(t)$  that gives rise to  $y_I(t)$  as follows:

$$y_I(t) = LPF\{z_I(t)\} = x_I(t) + \frac{\sqrt{2}}{2} A_i \cos[(\omega_c - \omega_i)t] \quad \text{Eq. 4.8}$$

The same approach can be applied to the remaining (bottom) branch of the IQ demodulator. Thus, it is found that:

$$z_Q(t) = -j\sqrt{2} \sin(\omega_c t) \{ \sqrt{2}x_I(t) \cos(\omega_c t) - \sqrt{2}x_Q(t) \sin(\omega_c t) + A_i \cos(\omega_i t) \} \quad \text{Eq. 4.9}$$

The development of Eq. 4.9, as before, leads to the equation below:

$$z_Q(t) = -j2 x_I(t) \sin(\omega_c t) \cos(\omega_c t) + j2x_Q(t) \sin^2(\omega_c t) - j\sqrt{2}A_i \sin(\omega_c t) \cos(\omega_i t) \quad \text{Eq. 4.10}$$

Again, using trigonometric identities, Eq. 4.11 is obtained:

$$\begin{aligned} z_Q(t) = & -j x_I(t) [\sin(2\omega_c t)] + j2x_Q(t) \left[ \frac{1}{2} - \frac{1}{2} \cos(2\omega_c t) \right] \\ & - j \frac{\sqrt{2}}{2} A_i \{ \sin[(\omega_c + \omega_i)t] + \sin[(\omega_c - \omega_i)t] \} \end{aligned} \quad \text{Eq. 4.11}$$

Repeating the low-pass filtering operation, but now over  $z_Q(t)$ , the output signal  $y_Q(t)$  is derived:

$$y_Q(t) = LPF\{z_Q(t)\} = jx_Q(t) - j \frac{\sqrt{2}}{2} A_i \sin[(\omega_c - \omega_i)t] \quad \text{Eq. 4.12}$$

Arriving to this point, the received constellation  $c(t)$  can be finally expressed as:

$$\begin{aligned} c(t) = y_I(t) + jy_Q(t) = & x_I(t) + jx_Q(t) + \frac{\sqrt{2}}{2} A_i \{ \cos[(\omega_c - \omega_i)t] - j \sin[(\omega_c - \omega_i)t] \} \\ = & x_I(t) + jx_Q(t) + \frac{\sqrt{2}}{2} A_i e^{j(\omega_i - \omega_c)t} = \tilde{x}(t) + \frac{\sqrt{2}}{2} A_i e^{j(\omega_i - \omega_c)t} \end{aligned} \quad \text{Eq. 4.13}$$

The complex expression (Eq. 4.13) can be represented over an IQ-axis system, as shown in Fig. 4.28. As can be seen, the “doughnut” shape naturally appears around the symbol of the constellation as a result of the respective phasor rotation.

According to the above calculations, the radius of the “doughnut” is given by the length of the rotating vector,  $r = \frac{\sqrt{2}}{2} A_i$  (i.e., the RMS value of the amplitude of the coherent interferer), and its phase is given by  $\theta(t) = (\omega_i - \omega_c)t$ . This means that the phasor rotates as stated by the difference between the carrier frequency of the victim signal and the frequency of the CW interferer.

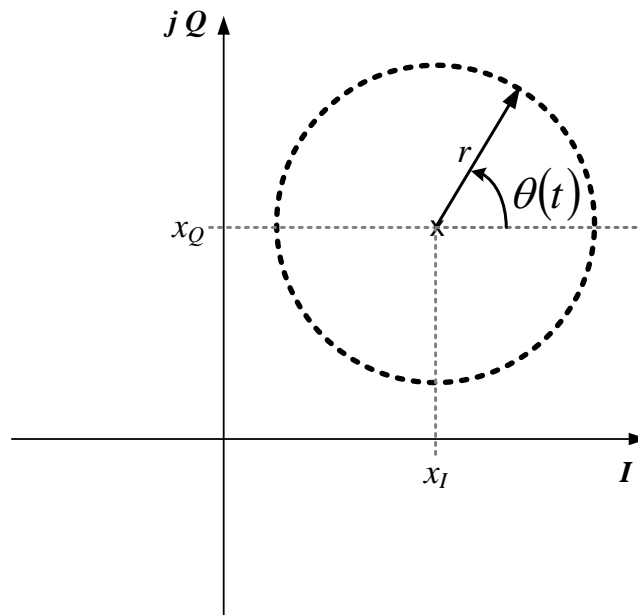


Fig. 4.28. The “doughnut” effect as a result of a rotating phasor centered at each constellation symbol.

### 4.2.3 “Doughnut” Effect Reproduction

To complement the provided mathematical analysis, the “doughnut” effect is reproduced here by using two different approaches: **simulation** and **laboratorial tests**. The obtained results in both cases are reported below.

#### 4.2.3.1 Simulation

With MATLAB™, a baseband a 16-QAM signal was generated and employed to modulate a carrier frequency of 754 MHz showing a power level of -30 dBm. A CW co-sine type signal of 749 MHz with a power level of -10 dBm was also produced.

Both signals were combined at the input of a power amplifier with a power gain of 20 dB. Subsequently, the “doughnut” effect was effectively reproduced at the output of the amplifier, as it is shown in Fig. 4.29.

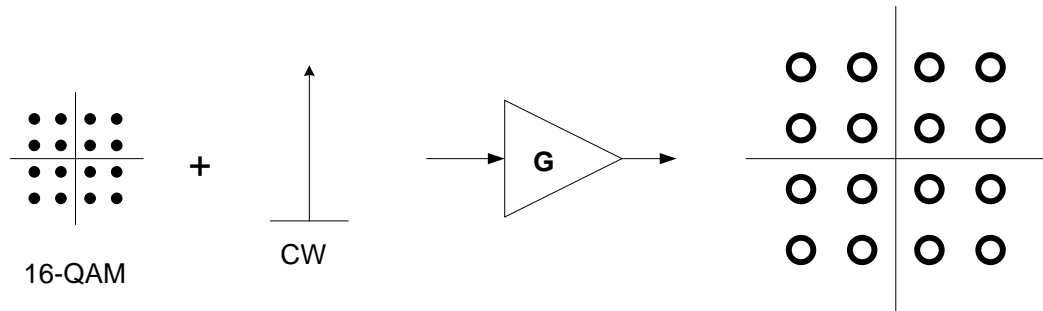


Fig. 4.29. Simplified block diagram of the simulation process.

The IQ output constellation diagram yielded by the simulation is presented in Fig. 4.30, hence confirming the “doughnut” effect appearance.

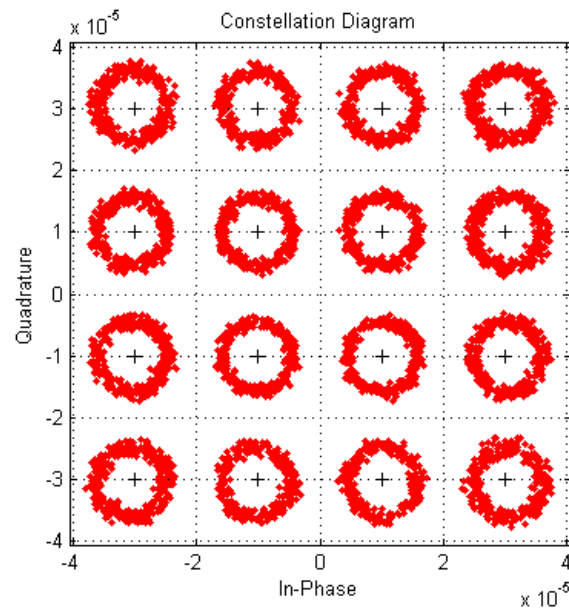


Fig. 4.30. Output of the simulation: “doughnut” effect on the constellation diagram.

#### 4.2.3.2 Laboratorial Tests

Using the measurement setup of Fig. 4.31, a QPSK signal with a -40 dBm power level and centered at 762 MHz was generated by means of a vector signal generator (model R&S SMBV100A).

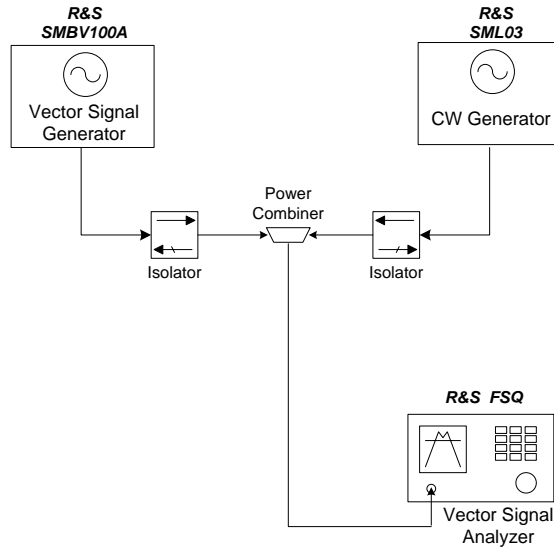


Fig. 4.31. Laboratory measurement setup used to reproduce the “doughnut” effect.

A CW signal of -11 dBm power level centered at 790 MHz was obtained from another signal generator (model R&S SML03). These signals were subsequently combined – their spectra are detailed in Fig. 4.32 – and delivered to the input of the vector signal analyzer (model R&S FSQ). Although the “doughnut” effect was successfully reproduced as corroborated by Fig. 4.33, it was found that the “doughnuts” were not exactly centered at the symbol position markers. These deviations are attributable to the pre-amplifier’s gain compression of the vector signal generator.

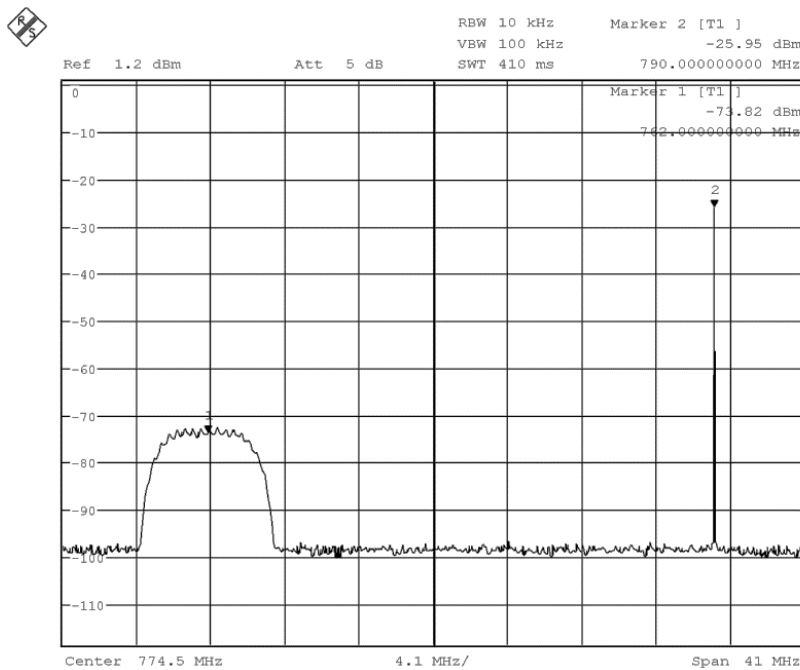


Fig. 4.32. Spectra of the QPSK and CW signals used to reproduce the “doughnut” effect.

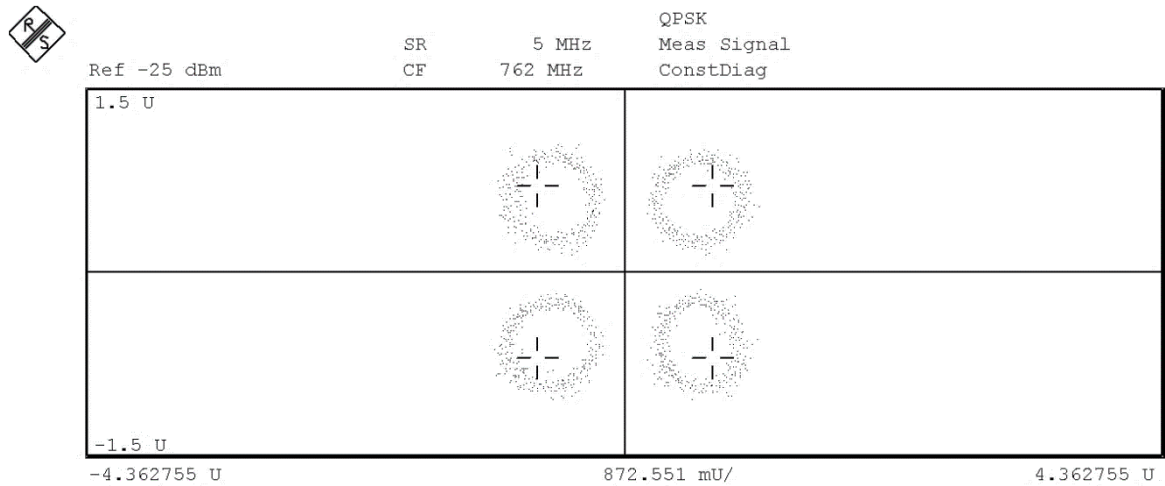


Fig. 4.33. Constellation diagram resulting from the experimental tests to demonstrate the “doughnut” effect generation.

#### 4.2.4 Summary

This case-study has provided a straightforward explanation based on a consistent mathematical formulation for the “doughnut” effect, as a particular type of IQ imbalance impairment.

This is a typical problem found in coexisting radio service scenarios, in which a narrowband interferer is affecting the reception of a digital modulated signal. The impact of the “doughnut” phenomenon on the constellation diagram of the received digital signal has been clearly analyzed. Furthermore, such an effect has been successfully reproduced by means of simulation techniques and laboratory tests, hence validating the expounded analytical framework.



# 5 Time-Frequency Mixed Domain Signal Processing Tools

Traditional tools used for years for signal analysis, in the frequency domain – typically, spectrum approaches, based on Fourier techniques – are no longer suitable in many situations, due to intrinsic characteristics of the signals used by emerging radiocommunication systems, such as LTE, as has been emphasized so far, by an extensive variety of examples.

In fact, it is fundamental to understand why the conventional techniques may be failing and how the analysis and measurement issues can be adequately addressed, mitigated and improved.

This chapter provides an overview of the classic approaches to deal with deterministic<sup>65</sup> and stochastic<sup>66</sup> signals. Then, a wide-ranging collection of simple, but intuitive, examples are

---

<sup>65</sup> A **deterministic** signal assumes values, which are completely defined with respect to its independent variable. Thus, it is exactly described in the time domain. If there is a formula or rule that establishes a correspondence between an independent variable value to a signal value, then the signal is deterministic. [122]

<sup>66</sup> A **stochastic** signal is a signal, for which, the exact future values are impossible to predicted, even when its full past history is known. [127]

presented to illustrate the inappropriateness of some frequency domain methods and to accentuate the importance of adopting alternative techniques. Finally, the most notable time-frequency mixed domain signal processing transforms (*Gabor Transform*, *Short-Time Fourier Transform*, *Spectrogram* and *Wigner-Ville Distribution*) will be gradually introduced.

## 5.1 Fourier Transform and Spectrum

In radio monitoring applications, signal analysis in the frequency domain has been, by far, the most popular. The above methods resort to diverse techniques based essentially on the **Fourier**<sup>67</sup> transformation of the signal.

The Fourier Transform (FT) exists only for deterministic signals, defined by a time function that is known for all time, and its integral must exist. Therefore, the FT of a time domain signal  $x(t)$ , exists if  $x(t)$  is finite-energy<sup>68</sup>, i.e. *absolutely integrable* (the condition of Eq. 5.1 is satisfied), or *square integrable* (the condition of Eq. 5.2 is met).

$$\|x(t)\| = \int_{-\infty}^{+\infty} |x(t)| dt < +\infty \quad \text{Eq. 5.1}$$

$$\|x(t)\|^2 = \int_{-\infty}^{+\infty} |x(t)|^2 dt < +\infty \quad \text{Eq. 5.2}$$

Then, the FT, denoted by  $X(\omega)$ , is given by the Eq. 5.3. [122]

$$X(\omega) = \mathcal{F}[x(t)](\omega) = \int_{-\infty}^{+\infty} x(t) e^{-j\omega t} dt \quad \text{Eq. 5.3}$$

In the previous expression,  $\omega$  is the angular or radial frequency<sup>69</sup>, expressed in rad/s, and  $j$  is the imaginary unit ( $j = \sqrt{-1}$ ). This equation is also known as radial Fourier transform.

---

<sup>67</sup> **Jean-Baptiste Fourier (1768 – 1830)**, French mathematician and physicist, who first developed, even though, based on an idea without a rigorous justification at the time, the concept of Fourier series to solve problems of heat transfer and vibrations. [122]

<sup>68</sup> Actually, the FT exists for all real world signals found in practical applications.

<sup>69</sup> The radial frequency is given by  $\omega = 2\pi f$ , where  $f$  is the linear frequency in Hz units.

In fact, the FT compartmentalizes  $x(t)$  into complex sinusoids. Thus, it finds the similitude between the value of  $X$ , at a given frequency  $\omega$ , and the amplitude and phase of the correspondent sinusoidal component embedded in  $x(t)$ . [7]

Eq. 5.3 can also be presented in the so-called normalized form (Eq. 5.4).

$$X(\omega) = \frac{1}{\sqrt{2\pi}} \int_{-\infty}^{+\infty} x(t) e^{-j\omega t} dt \quad \text{Eq. 5.4}$$

Assuming that a given signal  $x(t)$  has an **autocorrelation function**  $R_X(\tau)$ , as stated by the expression of Eq. 5.5, the **power spectrum**, or simply “**spectrum**”, of  $x(t)$ , denoted by  $S_X(\omega)$ , is defined by the Fourier transform of its autocorrelation function (Eq. 5.6)

$$R_X(\tau) = \lim_{T_0 \rightarrow \infty} \left( \frac{1}{T_0} \int_{-\frac{T_0}{2}}^{\frac{T_0}{2}} x(t + \tau) x(t) dt \right), \quad \text{with } -\frac{T_0}{2} \leq t \leq \frac{T_0}{2} \quad \text{Eq. 5.5}$$

$$S_X(\omega) = \mathcal{F}[R_X(\tau)](\omega) = \int_{-\infty}^{+\infty} R_X(\tau) e^{-j\omega t} dt \quad \text{Eq. 5.6}$$

The spectrum (or frequency) analysis, based on FT, provides graphical tools, which allow to identify the sinusoidal behavior of a signal. Actually, it permits the visualization of signals as the weighted sum (or integral) of sinusoidal functions. As a consequence, a time function that shows slow variations will have its noteworthy spectral content concentrated around lower frequencies. On the other hand, a time function with fast variations will show weighty spectral components at higher frequencies. [129]

Indeed, FT lays out the frequency contents of the signal, according to the preponderance as they occurred (or are occurring); and from that, the identification of spectral regions, where the signal comprises substantial energy, is thus possible.

But modern spectral analysis applications make use of digital signal processing techniques, implemented by computers, most of them based on algorithms, such as the **Fast Fourier Transform** (FFT), developed for **discrete calculation** of the FT, in particular, the **Discrete Fourier Transform** (DFT).

The DFT is defined (Eq. 5.7)<sup>70</sup> for a discrete signal  $x(n)$ , and  $N > 0$ , as  $X(k)$ :

$$X(k) = \sum_{n=0}^{N-1} x(n) e^{-j\frac{2\pi nk}{N}}, \quad k = 0, 1, 2, \dots, N-1 \quad \text{Eq. 5.7}$$

Next sections explore some basic drawbacks of the Fourier analysis.

### 5.1.1 The same Spectrum does not always represent the same Signal

This is, in fact, a trivial observation. However, it is not always clear that the same spectrum may not represent the same signal. As a matter of fact, different signals may produce the “same spectrum”, as can be seen in the following situations.

#### 5.1.1.1 Two Signals formed by two half-length “mirrored” Sinusoids of different Frequencies

Let it be considered two signals:  $r(t)$  and  $s(t)$ , defined by Eq. 5.8 and Eq. 5.9, respectively. They last together 40 ms, and are formed by two half-length co-sinusoids of different frequencies:  $f_1=100$  kHz and  $f_2=300$  kHz, which are reversely ordered in  $r(t)$  and  $s(t)$ .

$$r(t) = \begin{cases} \cos(2\pi f_1 t), & 0 \leq t \leq 20 \text{ ms} \\ \cos(2\pi f_2 t), & 20 < t \leq 40 \text{ ms} \end{cases} \quad \text{Eq. 5.8}$$

$$s(t) = \begin{cases} \cos(2\pi f_2 t), & 0 \leq t \leq 20 \text{ ms} \\ \cos(2\pi f_1 t), & 20 < t \leq 40 \text{ ms} \end{cases} \quad \text{Eq. 5.9}$$

Fig. 5.1 separately depicts the time-domain and frequency-domain (spectrum) representations of both signals.

---

<sup>70</sup> In general,  $X(k)$  is complex. Thus, its complex norm  $|X(k)|$  is termed *discrete magnitude spectrum* of  $x(n)$  and  $\angle X(k)$  is the *discrete phase spectrum* of  $x(n)$ , for  $0 \leq k < N$ . [122]

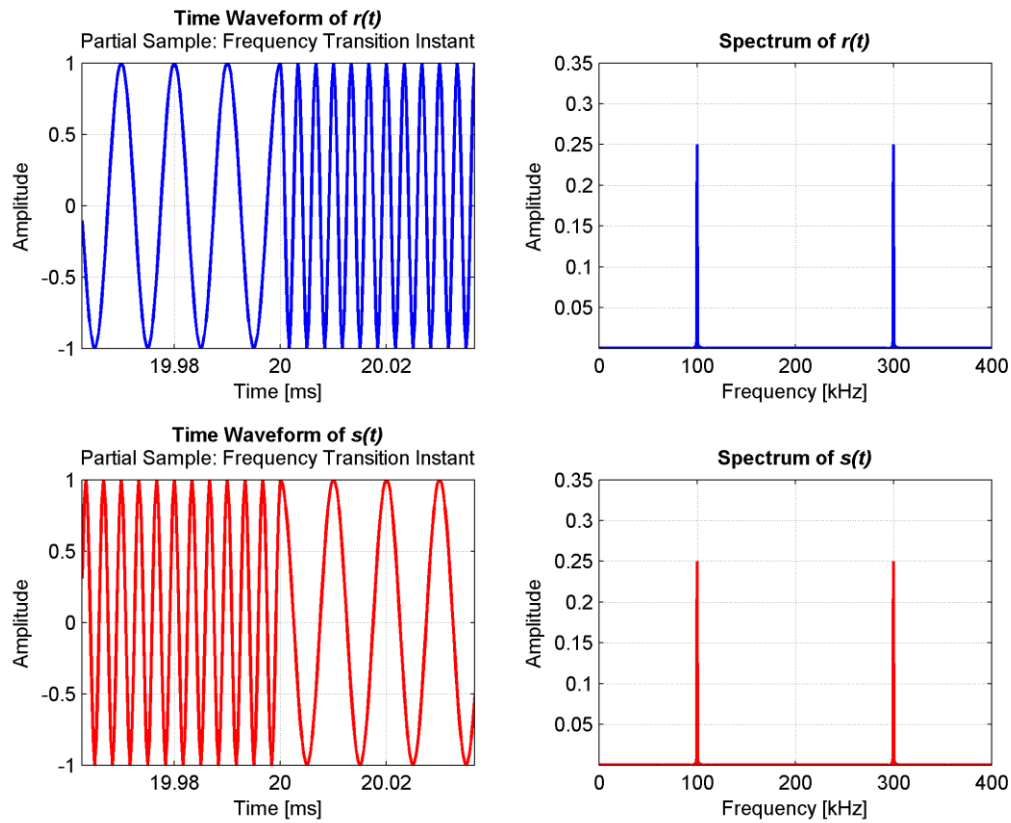


Fig. 5.1. Time-domain and frequency-domain independent representations of the signals  $r(t)$  and  $s(t)$ .

It is clearly evident the difference between  $r(t)$  and  $s(t)$ , when their time-domain representations are observed, but looking at the frequency-domain, their spectra, separately computed, are entirely coincident. Therefore, it is impossible to distinguish  $r(t)$  and  $s(t)$ , if only their spectra are analyzed. This means **that is not feasible to recover back the original signals**, i.e. time waveforms, **from the spectrum information**. Actually, **spectrum analysis based on the magnitude of the Fourier Transform loses the original time information**.

The bottom line is that these **two particular and distinct signals have the same spectrum**, which is equivalent to demonstrate that **the same spectrum does not univocally represent the same signal**.

The time-frequency mixed domain representations of  $r(t)$  and  $s(t)$ , shown in Fig. 5.2, on the other hand, provide not only a more detailed view, but also much richer information about the signal's behavior, both in the time and in the frequency domains.

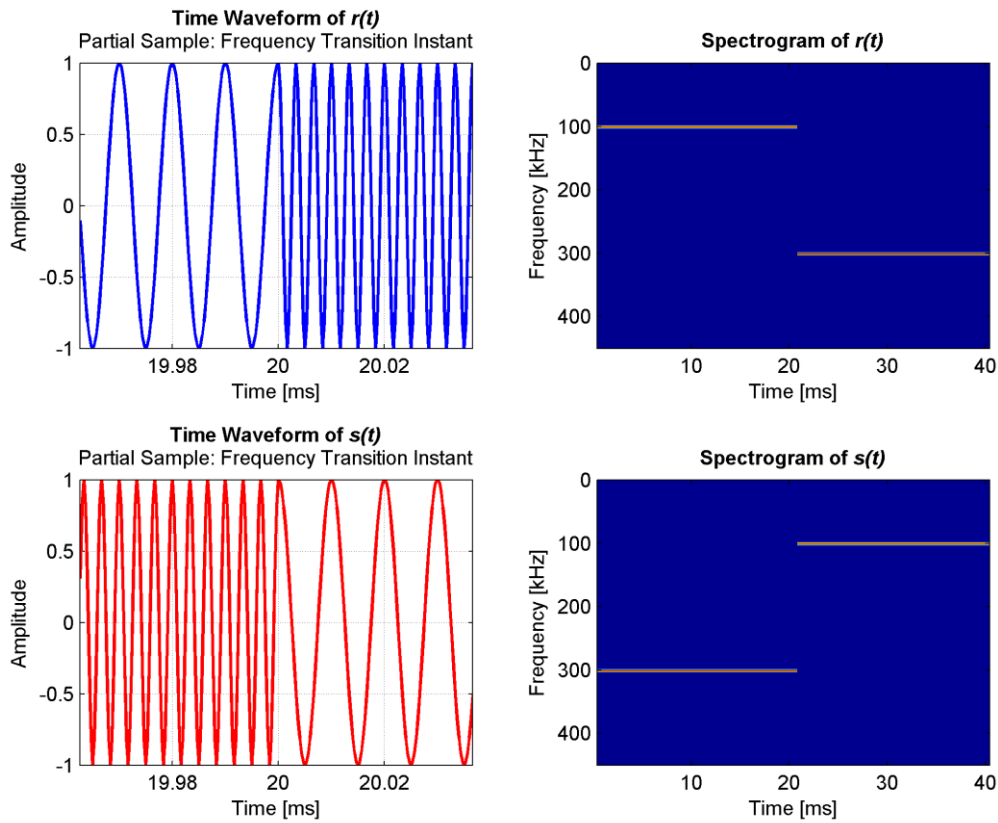


Fig. 5.2. Time-domain and time-frequency mixed domain (spectrogram) representations of the signals  $r(t)$  and  $s(t)$ .

#### 5.1.1.2 Possible Transient Effects

Some discontinuities or transient effects may occur during limited periods or very short instants of the signal, which may result from electromagnetic compatibility issues, internal or external perturbations, unexpected behavior of electrical systems, and physical characteristics of the devices, among many others. Transients may impact on the performance of radio systems. Indeed, they may have a non-neglected potential of interference, particularly in the presence of nonlinear elements. In such a situation, their effects tend to be truly exacerbated.

As a **potential source of interference**, **transients** have to be properly identified, but most of the times **they go unnoticed to the spectrum analysis**.

### 5.1.1.2.1 Sinusoid corrupted due to a Voltage Spike

Let it be considered a co-sinusoidal (original) signal:  $c_{orig}(t)$ , of frequency  $f=100$  kHz, which lasts 40 ms, as defined by Eq. 5.10. If such a signal is instantaneously corrupted, i.e. only during 1.333  $\mu$ s, exactly in the middle, by a voltage spike (a DC component of 2 “units” is added), a corrupted signal  $c_{corr}(t)$  is obtained, as mathematically expressed by Eq. 5.11.

$$c_{orig}(t) = \cos(2\pi ft), \quad 0 \leq t \leq 40 \text{ ms} \quad \text{Eq. 5.10}$$

$$c_{corr}(t) = \begin{cases} c_{orig}(t) + 2, & 19.999000 \leq t \leq 20.000333 \text{ ms} \\ c_{orig}(t), & \text{otherwise} \end{cases} \quad \text{Eq. 5.11}$$

Both time waveforms and respective spectra are depicted in Fig. 5.3.

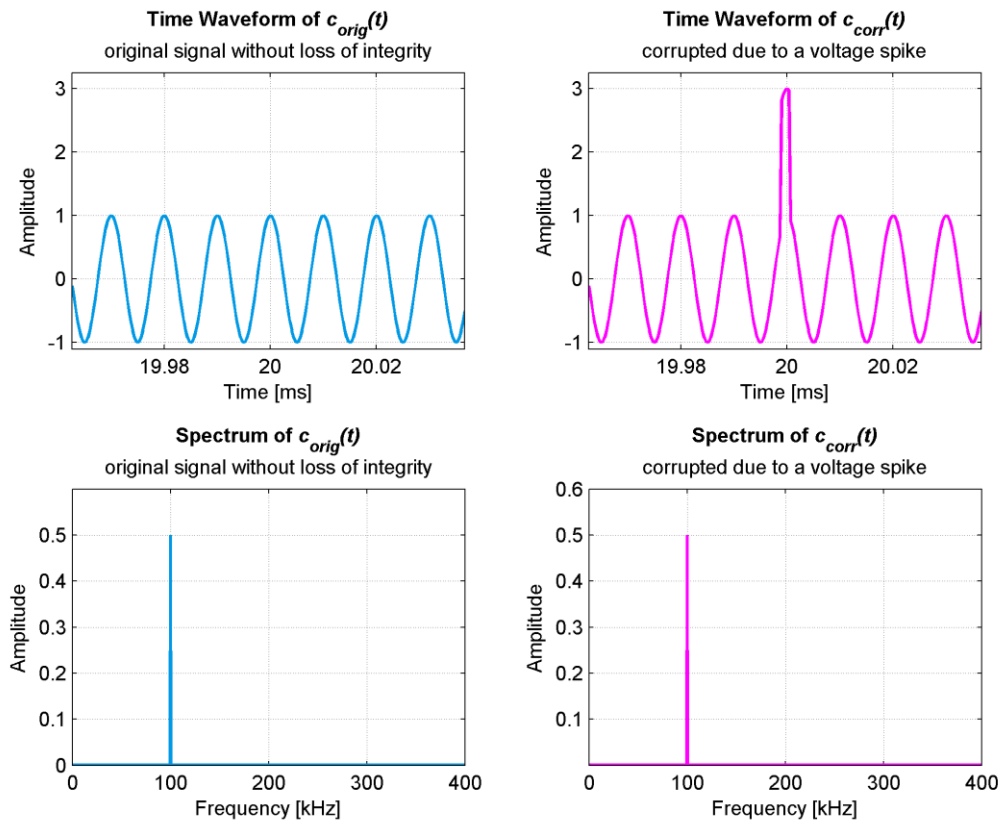


Fig. 5.3. Time-domain and frequency-domain representations of  $c_{orig}(t)$  and  $c_{corr}(t)$ .

As observed, the spectrum analysis is completely blind to the voltage spike, since the spectrum of the corrupted version of the signal is again a faithful copy of the original.

However, in the time-frequency analysis (spectrogram), presented in Fig. 5.4, the instantaneous event is captured, and the transient effect, which is spread over a wide-range of frequencies, is clearly visible.

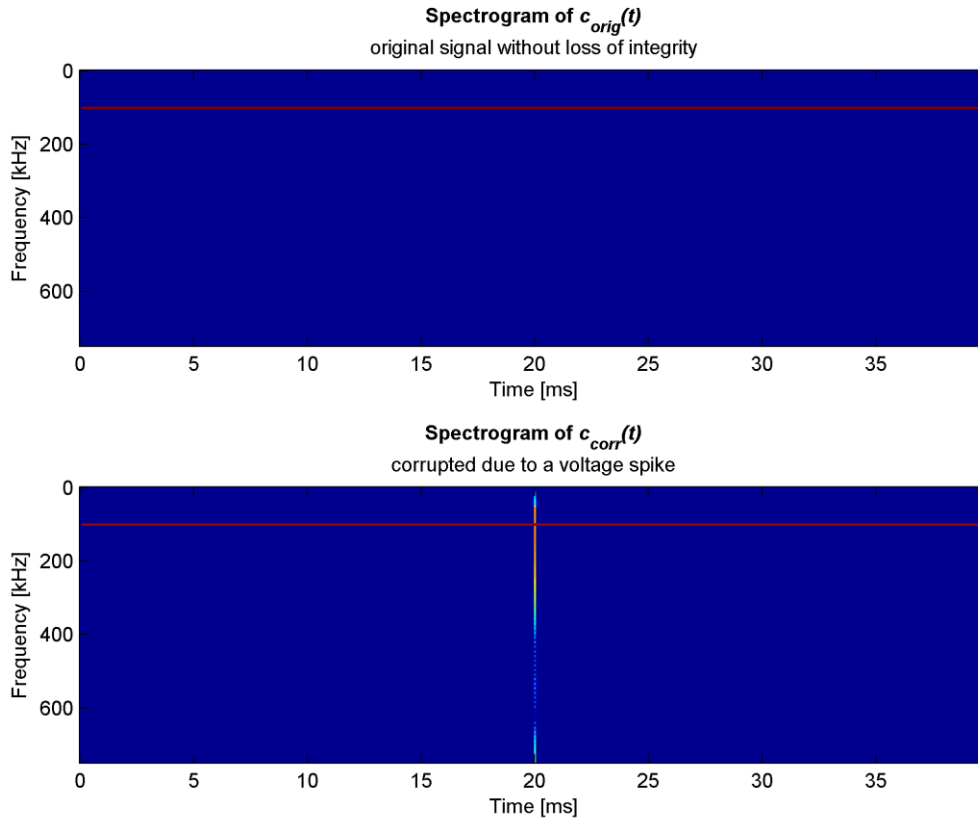


Fig. 5.4. Time-frequency mixed domain (spectrogram) representations of the signals  $c_{orig}(t)$  and  $c_{corr}(t)$ .

#### 5.1.1.2.2 QPSK signal abruptly interrupted

The previous examples have been based on simple unmodulated carriers – “pure” sine waves –, but more complex situations can be analyzed. Let it be considered a first scenario of analysis, in which, a baseband QPSK (complex) signal, generated by SystemVue™ (Agilent), is modulating a carrier frequency of 1800 MHz that is continuously transmitted, during 32.76775 ms.



A second scenario of analysis is now introduced, assuming that, exactly after 16.35875 ms, the original transmission, under the aforementioned conditions, is abruptly and instantaneously interrupted – the signal breakdown lasts only 50  $\mu\text{s}$  –, after that, the service is effectively recovered until the end of the transmission.

Both scenarios of analysis are illustrated in Fig. 5.5.

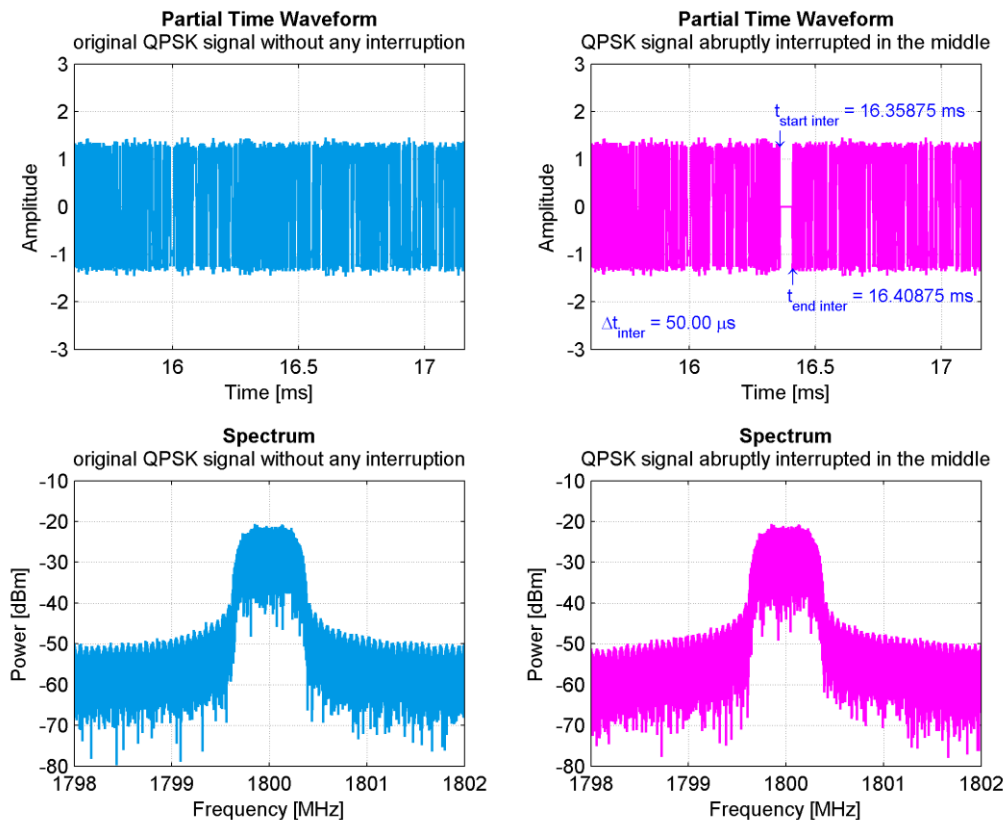


Fig. 5.5. Time-domain and frequency-domain representations of the original QPSK signal without any interruption and the same signal abruptly interrupted in the middle.

Contrary to the frequency-domain approach (spectrum), which is **completely silent upon an interruption that really occurred**; the time-frequency analysis (spectrogram), provided by Fig. 5.6, **undoubtedly marks a vertical line, right in the middle of the transmission** (bottom chart), which corresponds to the wanted event, i.e. the signal breakdown.

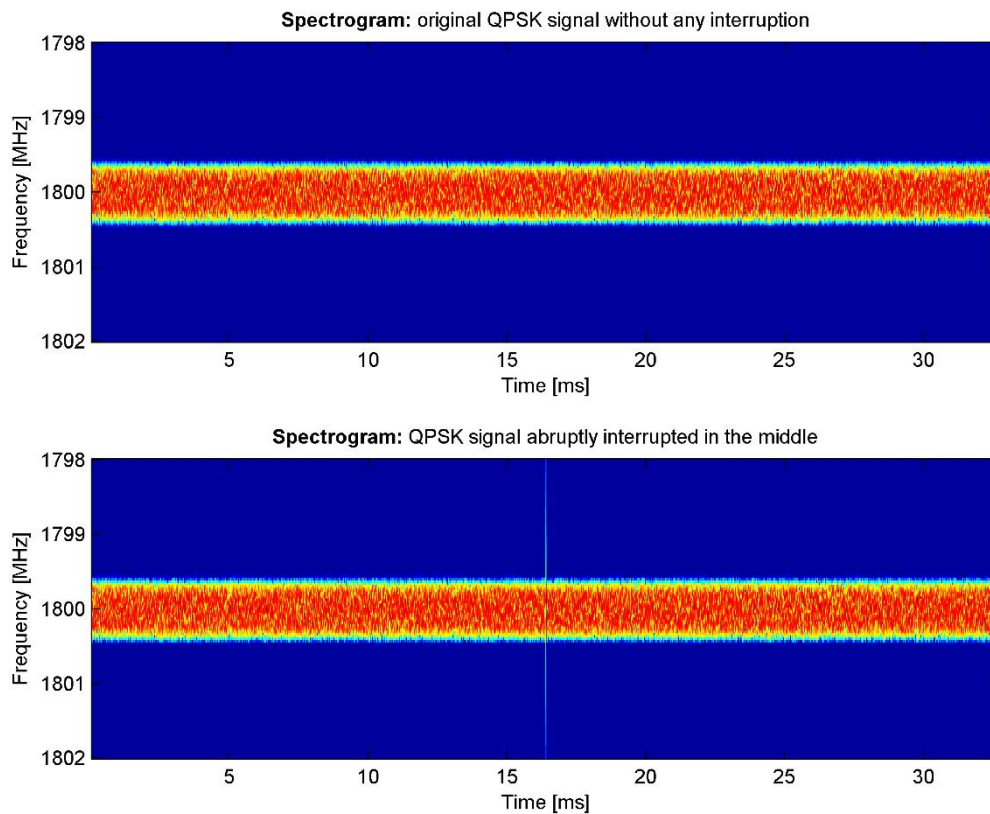


Fig. 5.6. Time-frequency mixed domain analysis (spectrogram) of the original QPSK signal without any interruption and of the same signal abruptly interrupted in the middle.

### 5.1.2 The same Spectrum does not always “produce” the same Interference

It has been demonstrated so far that different signals may originate the same spectrum, but more importantly is to realize that **different signals, with the same spectrum, may cause distinct interference situations, with very dissimilar degrees of severity.**

This is a point of the utmost importance, which must be properly scrutinized, since **constraints to be applied to technology-neutral systems** – through the **Block Edge Masks** – are, in reality, **spectrum conditions**. But if **the same spectrum requirements do not assure unique and expected working conditions**, at least from the interference perspective, it is indeed legitimate to question **if the BEM approach is truly useful and effective as a fundamental instrument** to ensure the coexistence of radio systems and to control possible harmful interference.

The interference will be analyzed by using a nonlinear element, which could be a mere amplifier, e.g., a LNA of a receiver's front-end, to understand how it actually responds to two distinctive input signals, but both with the same spectrum.

The first example considers a 256-QAM input signal that is differently transmitted: continuously and in bursts (or switched). Then, multi-sine signals will be adopted to model generic wideband emissions, in order to observe distinct patterns of interference.

#### 5.1.2.1 Continuous and Switched Transmission of a 256-QAM Signal

A baseband 256-QAM signal – generated with Simulink™ – modulates a RF carrier of frequency 2.5 GHz, which is continuously “on air”, in one situation; and discontinuously transmitted (switched), according to the need for transmitting or not, in the remaining situation.

Actually, the 256-QAM switched signal, considered in the latter case, results from the multiplication of the continuously transmitted 256-QAM signal with a square wave. In the frequency domain, this corresponds to convolve the original signal with a *sinc* shaped waveform.

Although, the two time waveforms are different, they have quite coincident spectra and the integrated power is almost the same, as can be seen in Fig. 5.7.

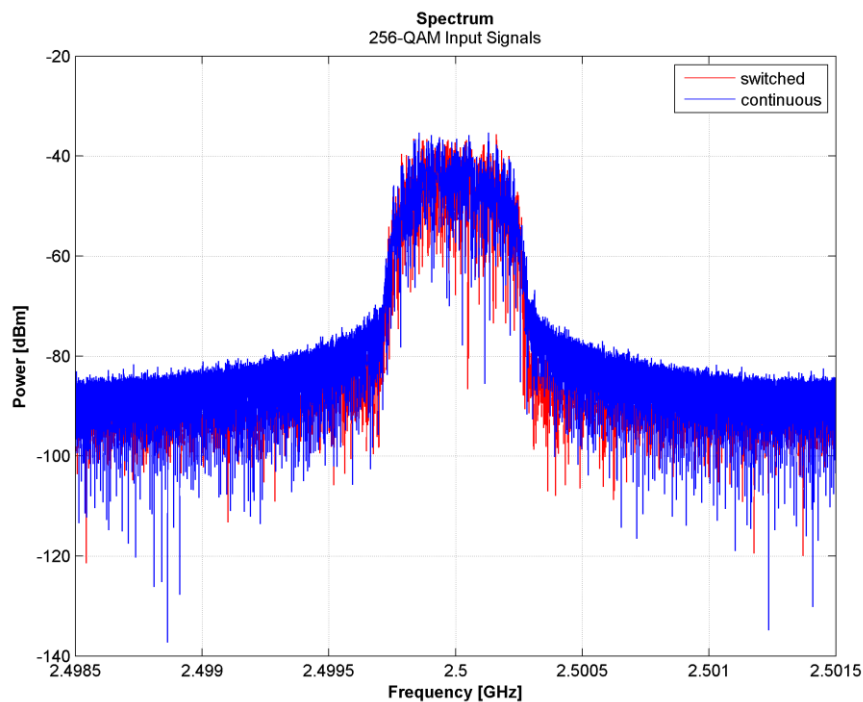


Fig. 5.7. Spectra of the Continuous and Switched 256-QAM Input Signals.

If the above signals traverse a nonlinearity, as indicated in the block diagram of Fig. 5.8, and if the respective nonlinear function is given by the Eq. 5.12 – where  $G$  is the gain of the device –; the nonlinear distortion, generated by such a device, is not the same in both situations, as observed in Fig. 5.9.

$$y(t) = f_{NL}[x(t)] = G[x(t) + 0.2x^3(t)] \quad \text{Eq. 5.12}$$

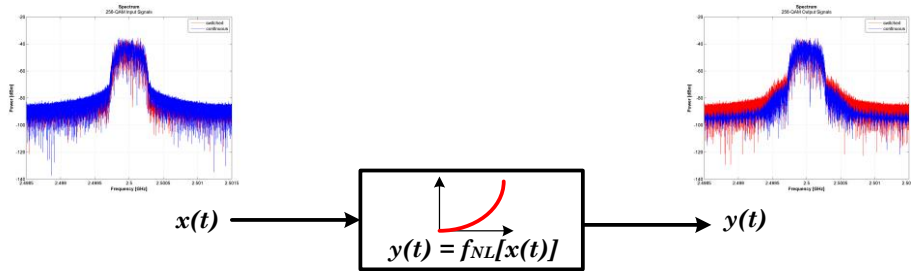


Fig. 5.8. Block diagram: nonlinearity and input and output signals' spectra.

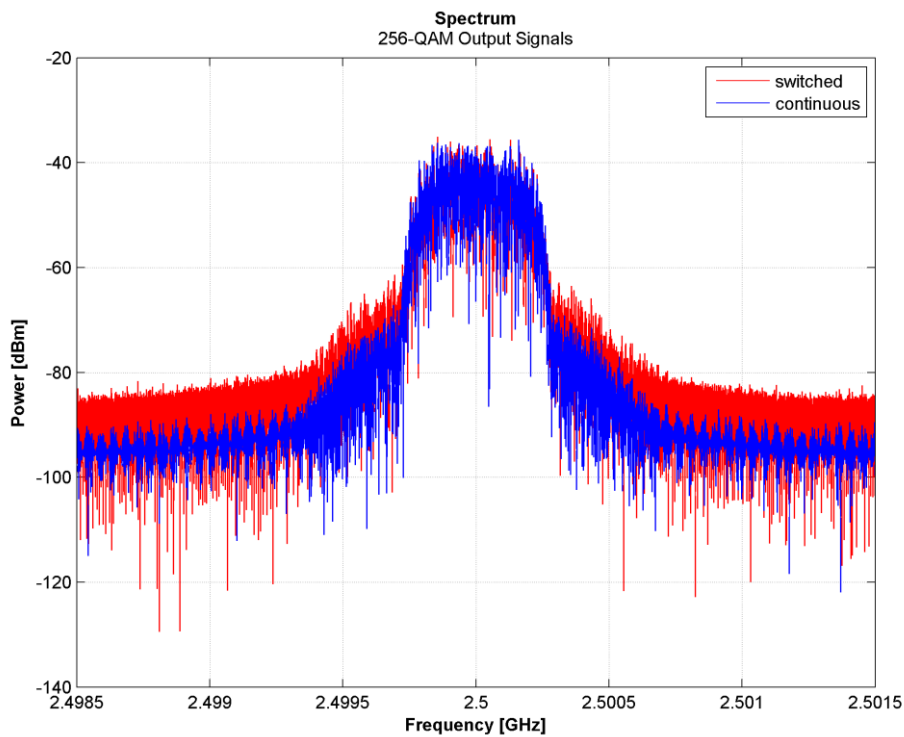


Fig. 5.9. Spectra of the Continuous and Switched 256-QAM Output Signals, after traversing the nonlinearity.

In fact, the latter figure shows that the switched signal has a **stronger value of Adjacent Channel Power Ratio (ACPR)**, i.e. as the integrated power within the channel is almost the same in both cases, the integrated power in the adjacent bands, as a consequence of the distortion generated by the nonlinear block, is higher when it is excited by the discontinuous (switched) signal. Since the adjacent channel energy is in fact perceived, by spectrally-adjacent systems, as interference, then, **signals with the same spectrum do not always originate the same interference.**

However, it is arguable that if the nonlinear block is, for instance, the final stage of a power amplifier of a LTE BS, then the BEM would be likely to be violated, as expected, without flaws. But, if the nonlinear block is the LNA of the front-end receiving circuit of a mobile terminal equipment, and the 256-QAM input signals model two BEM compliant LTE BS emissions; the impact on the performance of that TS is completely different, depending on which signal (continuous or switched) is actually present.

These two distinct time waveforms have, of course, dissimilar statistical behaviors, as illustrated by the histograms of Fig. 5.10 and by the CCDFs of Fig. 5.11.

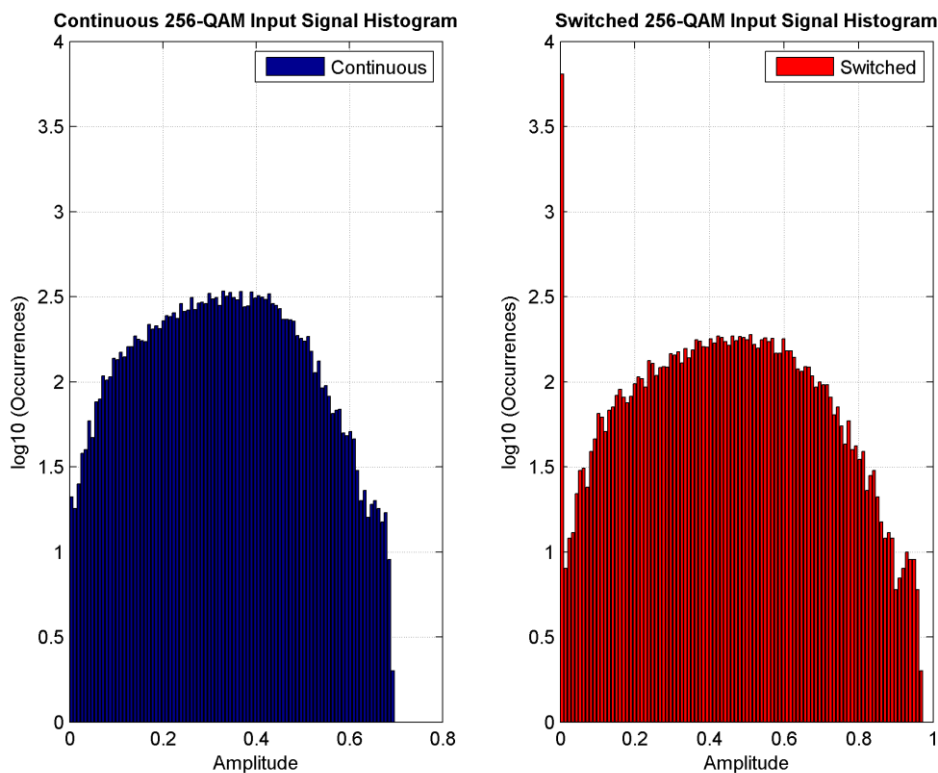


Fig. 5.10. Statistical behavior of the 256-QAM Input Signals (Continuous and Switched).

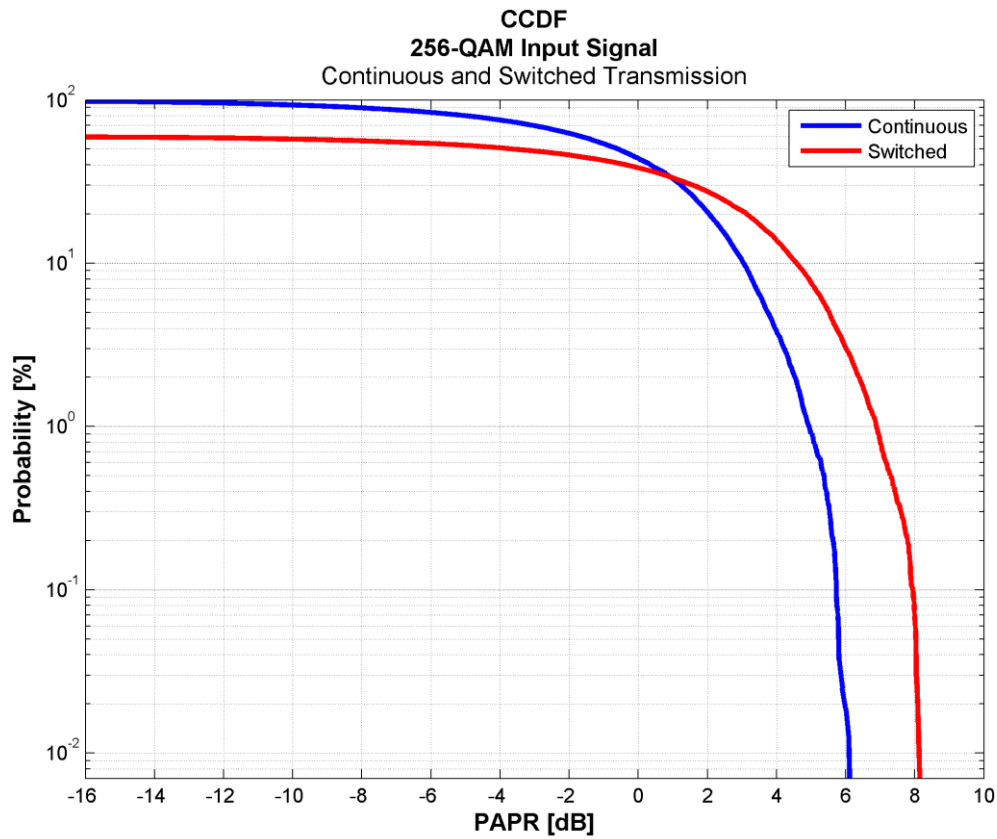


Fig. 5.11. CCDF of the 256-QAM Input Signals (Continuous and Switched).

The spectrograms (joint time-frequency analysis) of Fig. 5.12 provides much richer and much more interesting information about the above signals.

The switching behavior is perfectly identifiable whether at the input or output of the nonlinear block, and some transients are visible, precisely on the transitions between transmission and silent/inactive periods.

The adjacent channel distortion is also observable, at the output of the nonlinearity, both in the continuous and switched transmissions; although this latter shows higher interference levels, as supported by our earlier conclusions.

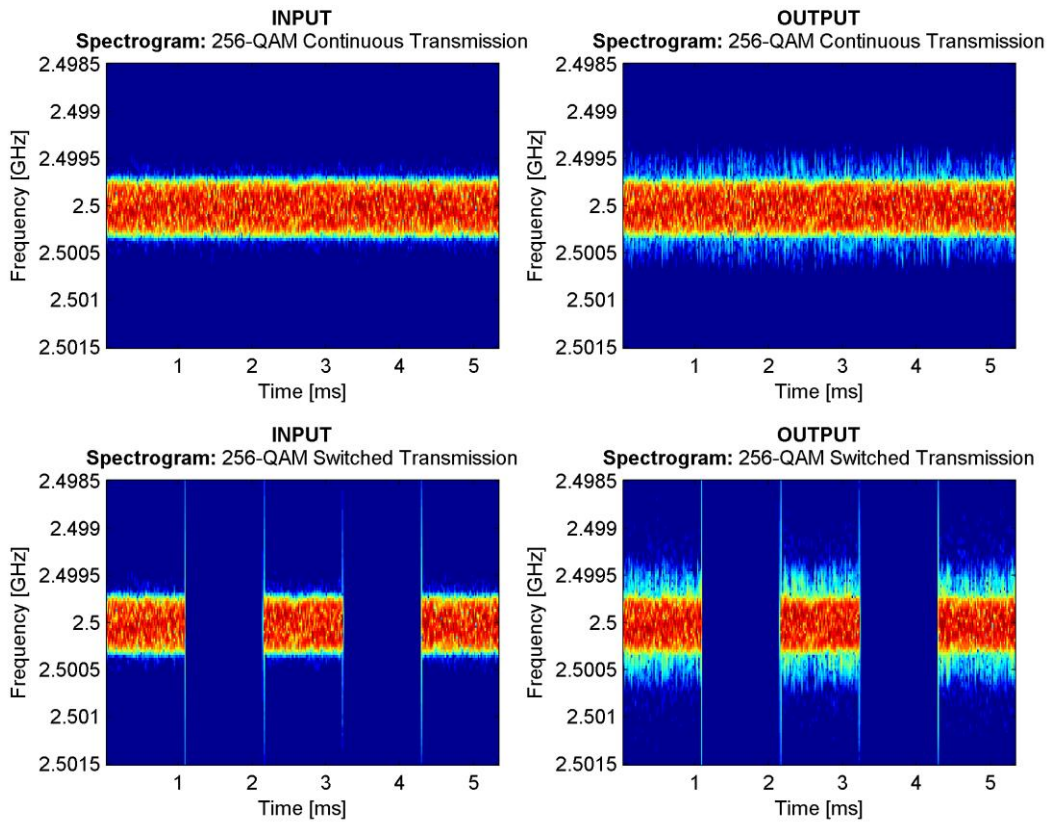


Fig. 5.12. Spectrograms of the 256-QAM Input/Output Signals (Continuous and Switched).

### 5.1.2.2 Multi-sine Signal Analysis

Multi-sine (MS) signals possess very suitable characteristics to model and simulate complex modulated radio signals. They are, in fact, very shapeable, easily configurable and straightforwardly generated and implemented. Thus, they are frequently used for system testing, mask compliance verification and mask generation, and calibration. [132]

A multi-sine is a summation of a set of simultaneous generated sinusoids or tones, mathematically described by the Eq. 5.13.

$$x(t) = \sum_{k=1}^N A_k \cos(\omega_k t + \theta_k) \quad \text{Eq. 5.13}$$

In the above expression,  $A_k$  is the amplitude of the  $k^{\text{th}}$  sinusoid,  $\theta_k$  is the phase of the  $k^{\text{th}}$  sinusoid,  $\omega_k$  is the radial frequency of the  $k^{\text{th}}$  sinusoid, given by Eq. 5.14, and  $N$  is total number of sinusoids.

$$\omega_k = \omega_0 + k(N - 1)\Delta\omega \quad \text{Eq. 5.14}$$

In the previous expression,  $\omega_0$  is the frequency of the first tone, and  $\Delta\omega$  is the constant frequency separation between adjacent tones.

Fig. 5.13 shows a partial sample of the time waveform and the positive part of the spectrum of a multi-sine signal of 20 tones, with random phases following a uniform distribution:  $\theta_k \sim \mathcal{U}(-2\pi, 2\pi)$ , separated by 50 kHz, and centered at 4 MHz, which was generated and will be used in the present analysis.

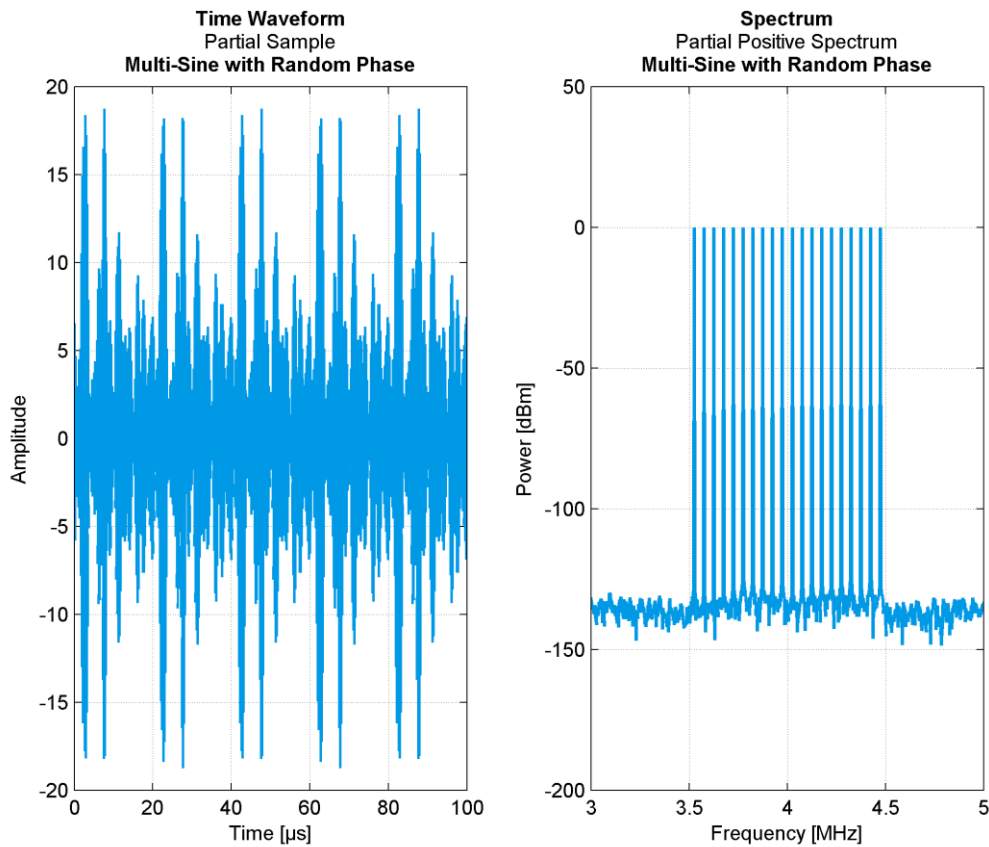


Fig. 5.13. Time waveform and Spectrum of the generated Multi-Sine Signal with Random Phases.

An additional multi-sine signal was also synthesized, keeping the basic parameters previously itemized, but now assigning a constant phase to all tones:  $\theta_k = 0$  rad.

Although the two generated multi-sine differ only in phase, they are actually quite different, as shown by the respective time waveforms, presented in Fig. 5.14.



As a matter of fact, the constant phase MS signal has much more exuberant amplitude peaks over the time. On the other hand, the random phase MS shows a smoother time progression.

Nevertheless, **they have remarkably coincident spectra**, as can be observed in the same figure.

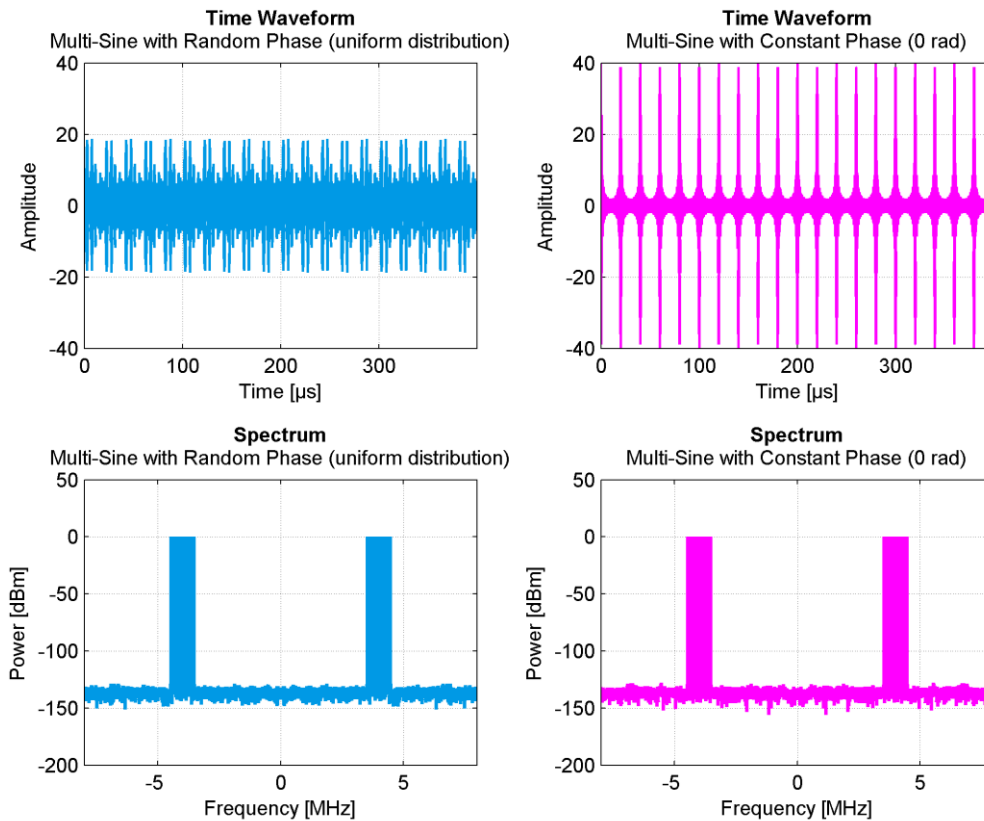


Fig. 5.14. Time waveforms and Spectra of the generated Multi-Sine Signals (Random and Constant Phases).

But the dissimilarities between both signals are, by far, evident, when their statistical behaviors are analyzed, through the respective CCDFs depicted in Fig. 5.15. Particularly, the PAPR of the constant phase MS is higher than the random phase one, which is in line with the behavior already denoted by the time representation.

Now, both multi-sine signals (random and constant phases) will pass, one at a time, through the nonlinearity defined by the function given by Eq. 5.12.

Although the spectra of the input signals match perfectly, this is no longer the case of the spectra of the output signals, which are expressively different, as shown in Fig. 5.16.

In fact, the response of the non-linear system to the **constant phase MS** reveals **higher levels of ACPR**, hence **generating severer interference**.

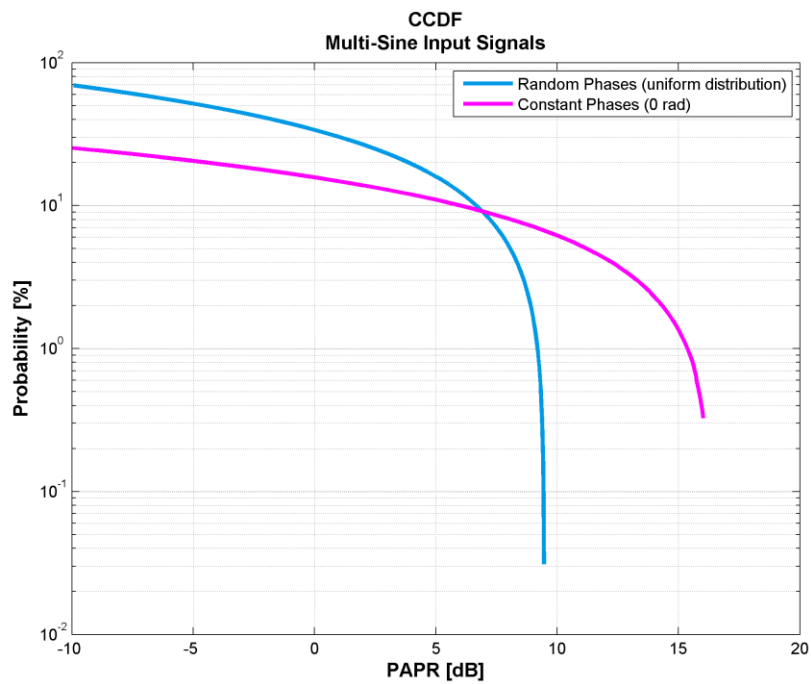


Fig. 5.15. CCDFs of the generated Multi-Sine Signals (Random and Constant Phases).

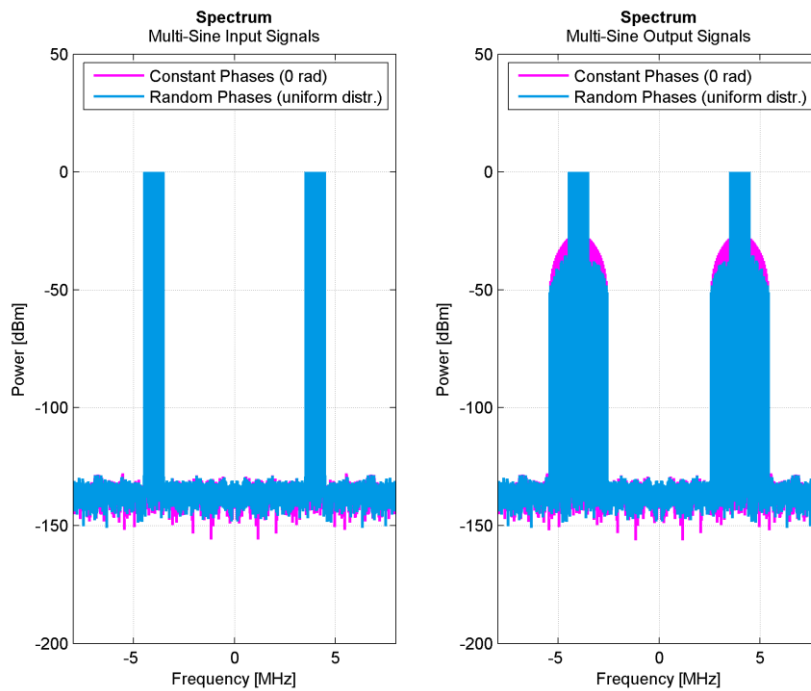


Fig. 5.16. Spectra of the Multi-Sine (Random and Constant Phases) Input and Output Signals.

Fig. 5.17 highlights the higher interference caused by the constant phase MS, which introduces, in the worst case situation, **more than 10 dB of degradation** (ACPR).

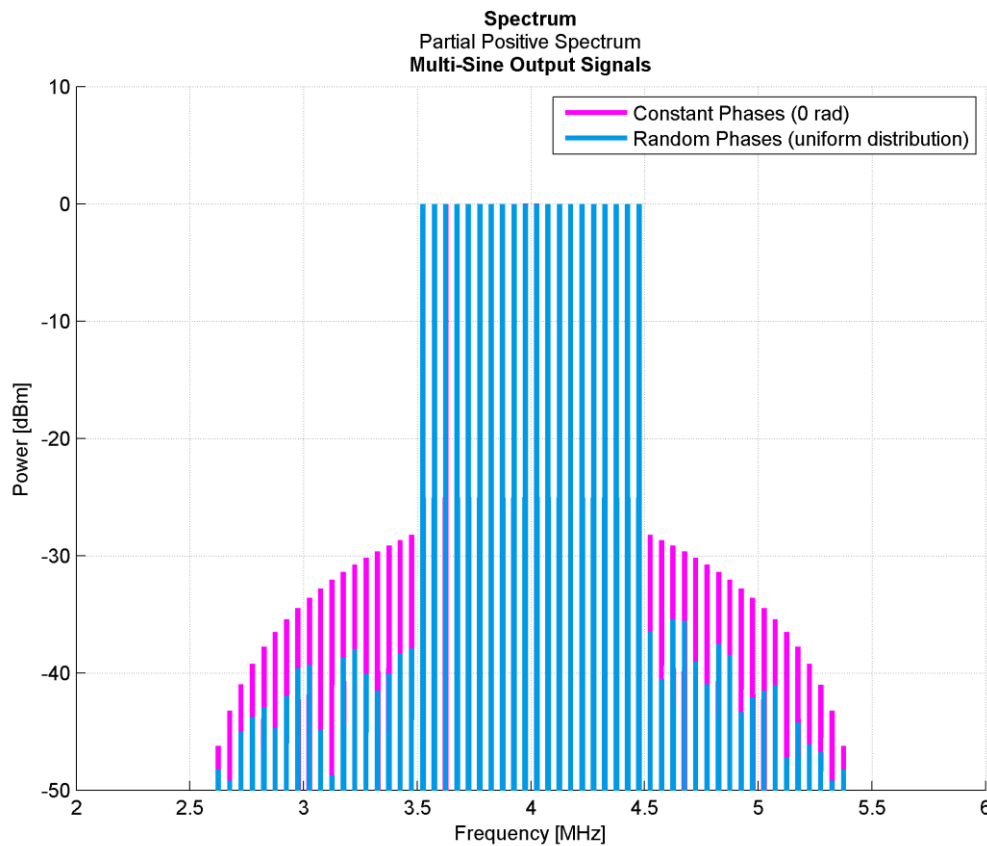


Fig. 5.17. Spectra of the Multi-Sine (Random and Constant Phases) Output Signals.

The spectrograms of Fig. 5.18 provide very interesting details about the signals that are being analyzed.

The first curiosity is the phase distribution of the MS signal information, which is given by the small yellow dots that are vertically aligned, within the channel, when the constant phase MS signal is captured. If the random phase MS signal is acquired, such yellow dots appear randomly distributed.

Another aspect that should be emphasized is the interference or the ACPR, obtained at the output of the nonlinear system, which is clearly more harmful if a constant phase MS signal is used for the excitation. The adjacent channel interference is visible through the horizontal light blue bar or border, surrounding the central channel.

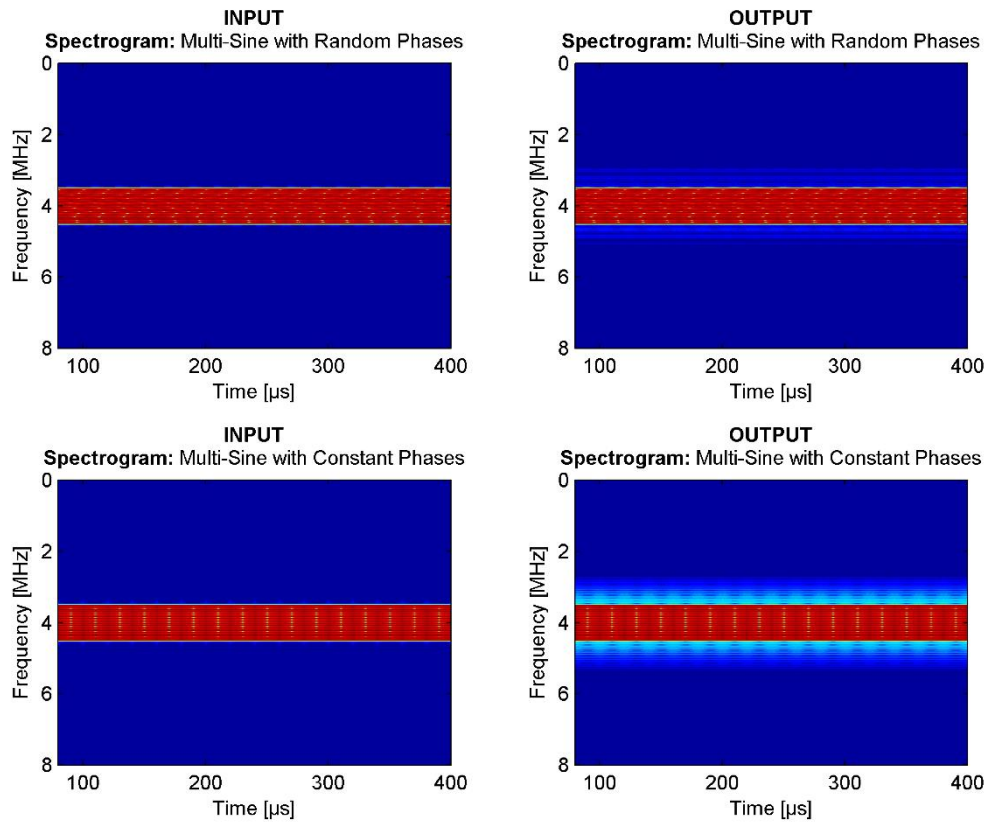


Fig. 5.18. Spectrograms of the Multi-Sine (Random and Constant Phases) Input and Output Signals.

Again, it was demonstrated that **two different signals, with perfectly matched spectra, did not produce the same interference.**

Moreover, the **time-frequency analysis has proven to be exceptionally useful to deal with time-varying or non-steady-state signals**, which are not properly addressed when spectrum techniques are separately used.

#### 5.1.2.2.1 Analysis of Interference caused by Narrowband and Wideband Signals

This simple situation explores possible limitations of the spectrum analysis, if signals significantly alternate their patterns of evolution. The opportunity will be also taken to illustrate distinctive impacts on interference, depending on if narrowband or wideband signals are used in the presence of a nonlinear element.

A multi-sine signal with 20 tones is considered, but, initially, only a single tone is active at a time, and after going through all tones individually, the entire multi-sine, i.e. the 20 tones, will be simultaneously displayed.

The separate tones subsequently evolve, in ascending order, starting with the edge tone of lowermost frequency.

Adjacent tones are separated by 50 kHz, and all of them were generated with random phases according to an uniform distribution:  $\theta_k \sim \mathcal{U}(-2\pi, 2\pi)$ . The MS is centered at 3 MHz.

If the above signal is taken as whole and the spectrum is then computed, as shown in Fig. 5.19, the individual narrowband tones might go unnoticed, which could lead to possible misinterpretations of the signal behavior.

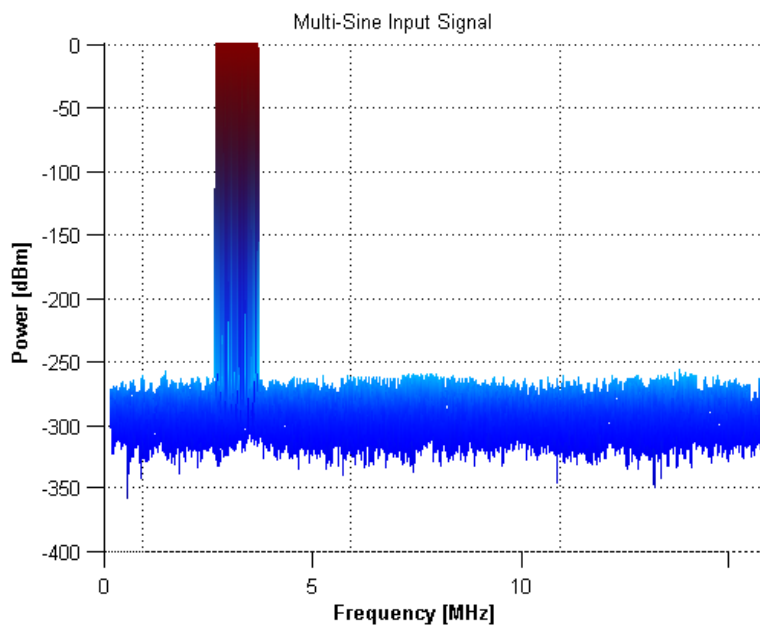


Fig. 5.19. Spectrum of the Multi-Sine and Single Tones Input Signal.

However, the 2D spectrogram of Fig. 5.20 provides part of the MS signal evolution along the time axis, showing the sequential jumps in frequency. Thus, it is possible to discriminate which carrier or carriers are part of the signal at any time.

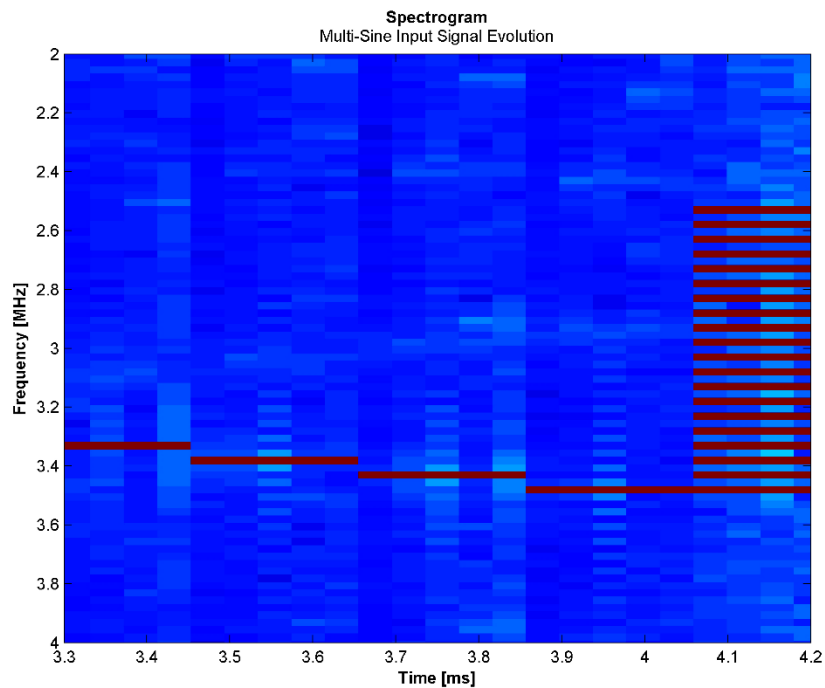


Fig. 5.20. Spectrogram of the Multi-Sine and Single Tones Input Signal Evolution.

Actually, the 2D spectrogram introduced before is, in fact, a 3D representation of the signal, since the amplitude is coded using a color scale, equivalent to the tridimensional spectrogram of Fig. 5.21.

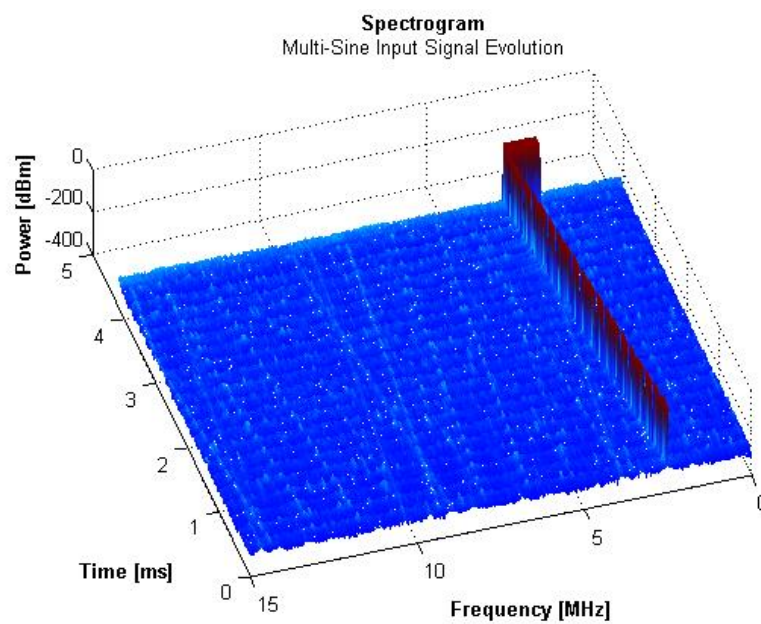


Fig. 5.21. 3D Spectrogram of the Multi-Sine and Single Tones Input Signal Evolution.

If the signal, characterized above, traverses a nonlinear block, which is described by Eq. 5.12, some **distortion (interference)** is observable, not only, around the MS signal (at the fundamental frequencies), but also, at the second-harmonics (see Fig. 5.22).

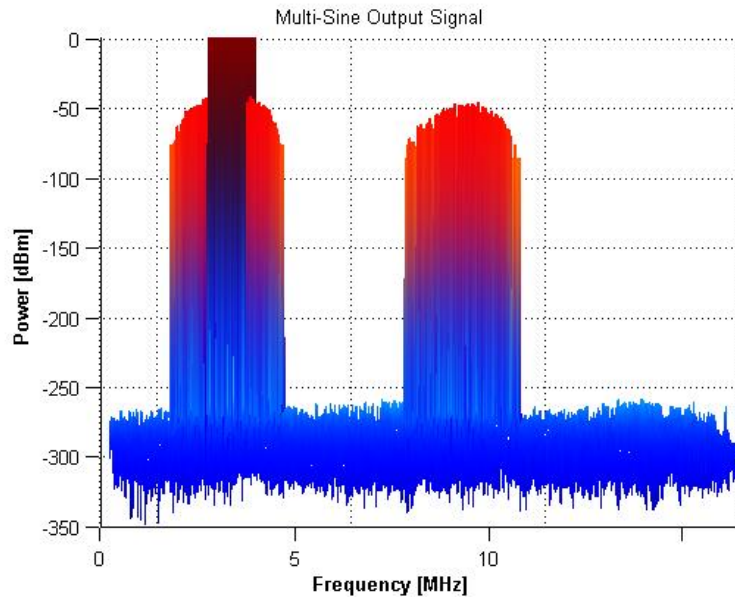


Fig. 5.22. Spectrum of the Multi-Sine and Single Tones Output Signal.

The previous analysis may be significantly improved, if a 3D spectrogram is generated (Fig. 5.23).

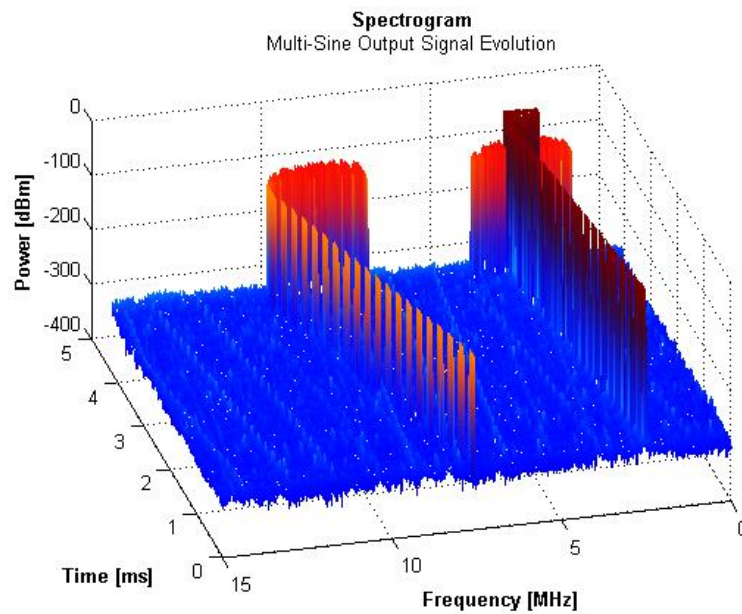


Fig. 5.23. 3D Spectrogram of the Multi-Sine and Single Tones Output Signal Evolution.

From the above chart, it is possible to distinguish a completely different nonlinear output distortion, depending on whether all tones are simultaneously active, or a single tone is being separately transmitted. In fact, under such conditions, **the whole MS (wideband signal) produces severer interference than an isolated tone (narrowband signal)**. This aspect is better perceived using the 2D spectrogram of Fig. 5.24.

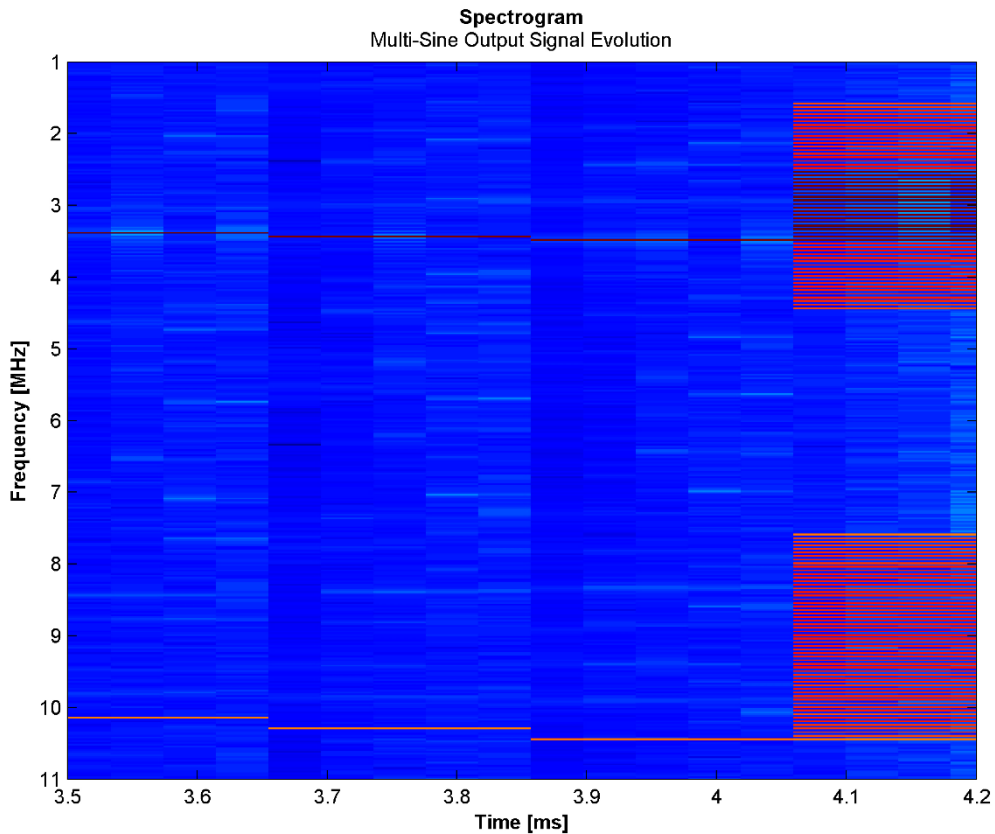


Fig. 5.24. 2D Spectrogram of the Multi-Sine and Single Tones Output Signal Evolution.

This example has reinforced the benefits of adopting more resilient joint time-frequency techniques to capture specific characteristics of the signals, which may be overlooked, if only spectrum analysis is used. Such limitations may lead to the underestimation or overestimation of important signal behaviors.

Therefore, it is essential to realize when and why time-frequency techniques should be applied. This topic is addressed in the following sections.



## 5.2 Time-Frequency Mixed Domain Analysis

Fourier analysis provides reliable results for signals that concentrate the bulk of their energy in relatively well-defined oscillatory components, i.e., if they are constant or **periodic**<sup>71</sup>, and not subject to major variations for their entire extent. If so, they are considered to be in **steady-state**. Pure tones, which assume a sinusoidal form as described by Eq. 5.15, or other narrowband signals, typically, meet this requirement. [7], [122]

$$x(t) = A\cos(\omega t + \phi) \quad \text{Eq. 5.15}$$

Under a steady-state regime, the Fourier Transform (Eq. 5.3) **assertively matches** their **amplitude** ( $|X(\omega)|$ ) and **phase** ( $\angle X(\omega)$ ) **outputs**, in the frequency domain, to the respective **sinusoidal components** of  $x(t)$ , in the time domain. For example, for the MS signal given by Eq. 5.13, the FT magnitude of the  $k^{\text{th}}$  component is  $A_k$  and the phase is  $\theta_k$ . In such a situation, a well-defined correspondence between values in the time domain, and in the frequency domain, is achieved, because **the time domain sinusoidal components exist during the whole extent of the signal and the complex exponentials, which are elementary functions of the FT, also exist for the same extent.** [7]

However, **not all signals**, used in practice in common applications, **are entirely periodic**, for their full extents. Actually, **a vast majority will not be**, in fact. In that case, the transformation between both domains (time and frequency), via FT, is not so direct, nor so well-defined, as previously described. Hence, it may not be possible to define an unambiguous frequency or set of frequencies for a non-periodic signal of the generic form of Eq. 5.16.

$$x(t) = A\cos(\omega t + \phi(t)) \quad \text{Eq. 5.16}$$

But, to overcome this “impossibility”, the concept of **instantaneous frequency** (Eq. 5.17) is introduced. [7], [133]

---

<sup>71</sup> A **periodic** signal repeats a given part of itself over intervals, being possible to identify a distinct set of values which will be successively repeated. The time interval during which this distinct set of values occurs is called **period**. The inverse of the period is the frequency of the signal.

Formally, a signal  $x(t)$  is **periodic**, if there is a constant  $T > 0$ , which satisfies the condition:  $x(t+T) = x(t)$ , for all  $t$ . Then, a signal with period  $T$  will repeat on intervals of length  $T$ , and such intervals are designated as periods. [122]

$$\omega_i(t) = \frac{d}{dt}\{\phi(t)\} \quad \text{Eq. 5.17}$$

The *instantaneous frequency* definition, given by the derivative of the phase function  $\phi(t)$  with respect to the time, somehow suggests that there is a sinusoid that best represents  $x(t)$ , at a given instant  $t$ . That is to say, the frequency of a signal, at each time instant, is univocally expressed by the instantaneous rate of change of its phase function.

The instantaneous frequency may be used for **disambiguating** whether a non-periodic signal is in steady-state, or in a transient regime.

Whereas the instantaneous frequency characterizes a *local frequency behavior as a function of time*, a dual figure of merit, which characterizes a *local time behavior as a function of frequency*, is defined, by the **group delay** (Eq. 5.18), for a given signal represented in the frequency domain by a phase function:  $\varphi(\omega)$ . [7], [133]

$$\tau(\omega) = -\frac{d}{d\omega}\{\varphi(\omega)\} \quad \text{Eq. 5.18}$$

The *group delay* measures the average time arrival of the frequency  $\omega$ .

A **chirp**<sup>72</sup> is a transient waveform that is commonly used to model **deterministic non-stationary**<sup>73</sup> signals. Eq. 5.19 represents a linear (rising) chirp that produces a linear frequency modulation.

$$x(t) = A \cos\left(\phi_0 + 2\pi\left(f_0 t + \frac{k}{2} t^2\right)\right) \quad \text{Eq. 5.19}$$

---

<sup>72</sup> Chirps may be found both in nature (e.g., bird songs or “chirps”, frogs, whales and other animal vocalizations; bats ultrasounds for echolocation) and in man-made systems (e.g., radar and sonar). [135]

<sup>73</sup> A deterministic signal is considered **stationary** if it can be expressed as a summation of sinusoids, with constant instantaneous amplitude ( $A_k = \text{const}$ ) and constant instantaneous frequency ( $\frac{d}{dt}\{\phi_k\} = \text{const}$ ), of the form:  $x(t) = \sum_{k=1}^N A_k \cos(\omega_k t + \phi_k)$ . A signal is **non-stationary** if any of the previous conditions are no longer satisfied. A **Transient** signal, for which the length is much shorter than the whole extent under analysis, is non-stationary. [133]

The above expression was utilized to generate the linear chirp signal, illustrated in Fig. 5.25, from different perspectives, using some possible representations.

For such a purpose, the following particular parameters were implemented: (a) constant unitary amplitude:  $A = 1$ ; (b) initial phase constant (at  $t = 0$ ):  $\phi_0 = 0$  rad; (c) initial frequency (at  $t = 0$ ):  $f_0 = 100$  MHz; (d) chirp rate<sup>74</sup>:  $k = 10^{17}$  s<sup>-2</sup>; (e) total length of the signal: 50 ns; (f) final frequency (at  $t = 50$  ns): 5.1 GHz.

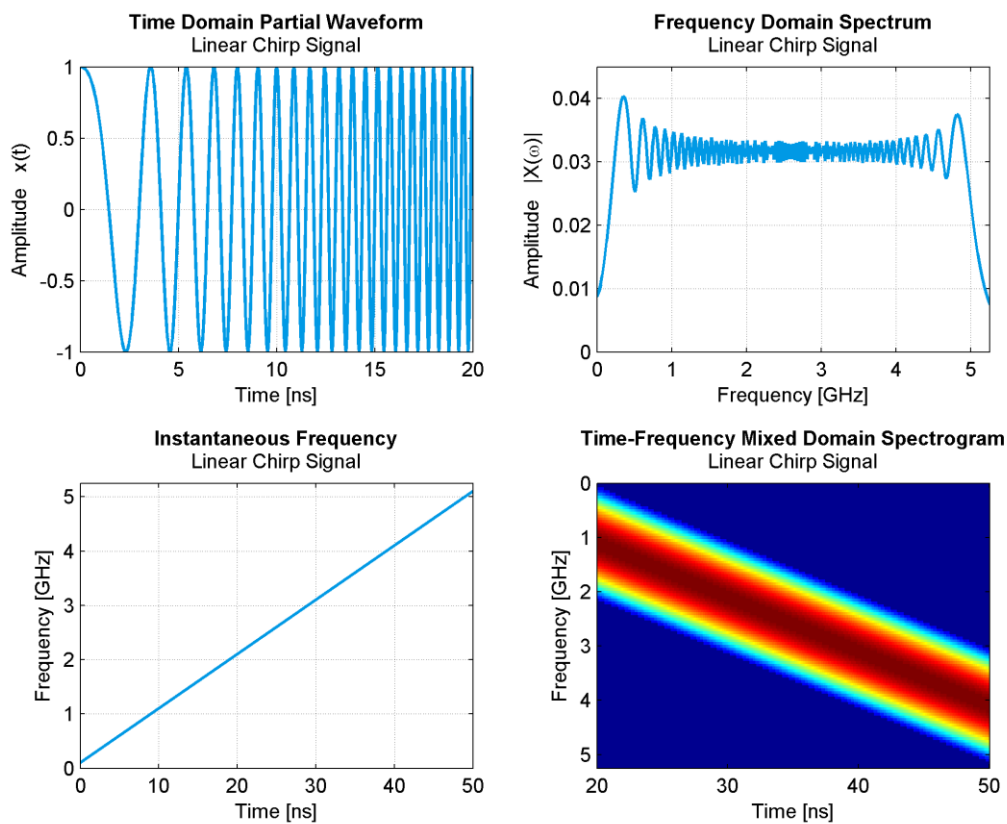


Fig. 5.25. Linear Chirp Signal representations: Time Domain Waveform, Frequency Domain Spectrum, Instantaneous Frequency and Time-Frequency Mixed Domain Spectrogram.

<sup>74</sup> The **chirp rate** ( $k$ ) expresses the rate as the frequency of the chirp signal is increased, from an initial frequency  $f_0$ , at time  $t=0$ , to a final frequency  $f_f$ , at time  $t_f$ , and is given by:  $k = \frac{f_f - f_0}{t_f}$  (this meaning is a direct consequence of Eq. 5.22, when solved with respect to  $k$ ).

An alternative definition of chirp rate is given by the second derivative of the phase function:  $k = \frac{d^2}{dt^2} \{\phi(t)\}$ . [136]

From the **time domain waveform** – which is partially reproduced (up to 20 ns) for clarity reasons – it is observable that the signal frequency is increasing with time, but how does it increase? In fact, it is not straightforward to realize, just by looking at the time representation, if such a variation follows a linear, a square, or any other law of evolution.

The **spectrum**, computed with the FFT algorithm, which is depicted in Fig. 5.25 from DC to 5.25 GHz, displays a wideband signal, with spectral content, more or less “evenly” distributed, between 100 MHz and 5.1 MHz, looking like a “top hat” shape. That spectrum shows sharp edges, as a consequence of a variable ripple, around an average amplitude of  $3.3 \times 10^{-4}$ , which is more pronounced close the ends, but smoother as it reaches the center. The frequency domain information of the signal suggests that it exhibits spectral content across a wide spectral range, but says nothing about how and when the spectral components actually appear during the course of the signal. Did they continuously manifest themselves with a moderate amplitude? Or, did they occasionally appear, but with higher amplitudes (e.g. instantaneous peaks), which in average produce a spectrum like that?

As a matter of fact, spectrum does not provide useful information that could be used to describe the time evolution of the frequency content of the signal<sup>75</sup>.

The **instantaneous frequency** representation may be calculated, by using Eq. 5.17. The linear chirp signal, defined by Eq. 5.19, has a phase function which is described by Eq. 5.20.

$$\phi(t) = \phi_0 + 2\pi \left( f_0 t + \frac{k}{2} t^2 \right), \quad \text{with } \phi_0 = 0 \quad \text{Eq. 5.20}$$

Its instantaneous frequency is then given by the following expression (Eq. 5.21).

$$\omega_i(t) = \frac{d}{dt} \left\{ 2\pi \left( f_0 t + \frac{k}{2} t^2 \right) \right\} = 2\pi(f_0 + kt) \quad \text{Eq. 5.21}$$

---

<sup>75</sup> Reference [133] justifies this omission with the fact that FT is a decomposition on complex exponentials of infinite duration, which are entirely displaced in time. Besides, time information is coded in phase of the FT – which is basically obliterated by the spectrum representation –; however, it is not direct, nor intuitive, to extract such time information from that. “Phase unwrapping” is pointed out as a major issue.

The previous equation may be rewritten in the linear instantaneous frequency form (Eq. 5.22), which is also plotted in Fig. 5.25.

$$f_i(t) = f_0 + kt \quad \text{Eq. 5.22}$$

Despite it adds suggestive information about the time evolution of the signal, in particular, the accurate linear progression of the frequency as a function of time – which is the true essence of a chirp – **the amplitude information is not provided**, at all.

The three approaches scrutinized before – *time waveform*, *spectrum* and *instantaneous frequency* – are not flawless.

An **optimal solution to analyze transients or time-varying signals**, such as chirps, **should simultaneously combine**: *time*, *frequency* and *amplitude* information.

Such an approach is presented in Fig. 5.25, through the time-frequency spectrogram (see bottom-right chart). At first glance, it could seem a 2D time-frequency plot. However, the amplitude information is coded in a color scale. In practice, it is a tridimensional equivalent graph, and a very intuitive way of analyzing the time-spectral content of the signal.

The major time-frequency mixed domain transforms – in which the spectrogram is included – are introduced below.

### 5.2.1 Windowed Fourier Transforms

To overcome some of the aforementioned issues, which prevent the correct signal analysis – i.e., when oscillations of interest only occur within particular regions, or prominent periodic characteristics are only active for limited lapses of time –, time-limiting (windowing) techniques will be explored, in order to, wisely and accurately, capture those occurrences, before calculating the spectrum.

Accordingly, the Gabor Transform (GT) and the Short-Time Fourier Transform (STFT) will be presented.

### 5.2.1.1 Gabor Transform

Among the signals commonly used to model everyday phenomena of real life, the most trivial are sinusoids and exponentials. However, there is another one of great interest, in a broad range of eclectic areas (e.g., engineering, physics, medicine, mathematics and statistics), that is the **Gaussian signal** (Eq. 5.23).

$$g_{\mu,\sigma}(t) = \frac{1}{\sigma\sqrt{2\pi}} e^{-\frac{(t-\mu)^2}{2\sigma^2}} \quad \text{Eq. 5.23}$$

The parameters of the Gaussian signal  $g_{\mu,\sigma}(t)$  are its mean  $\mu$  and standard deviation  $\sigma$ .

Fig. 5.26 illustrates some Gaussian signals, by considering different pairs  $(\mu, \sigma)$ .

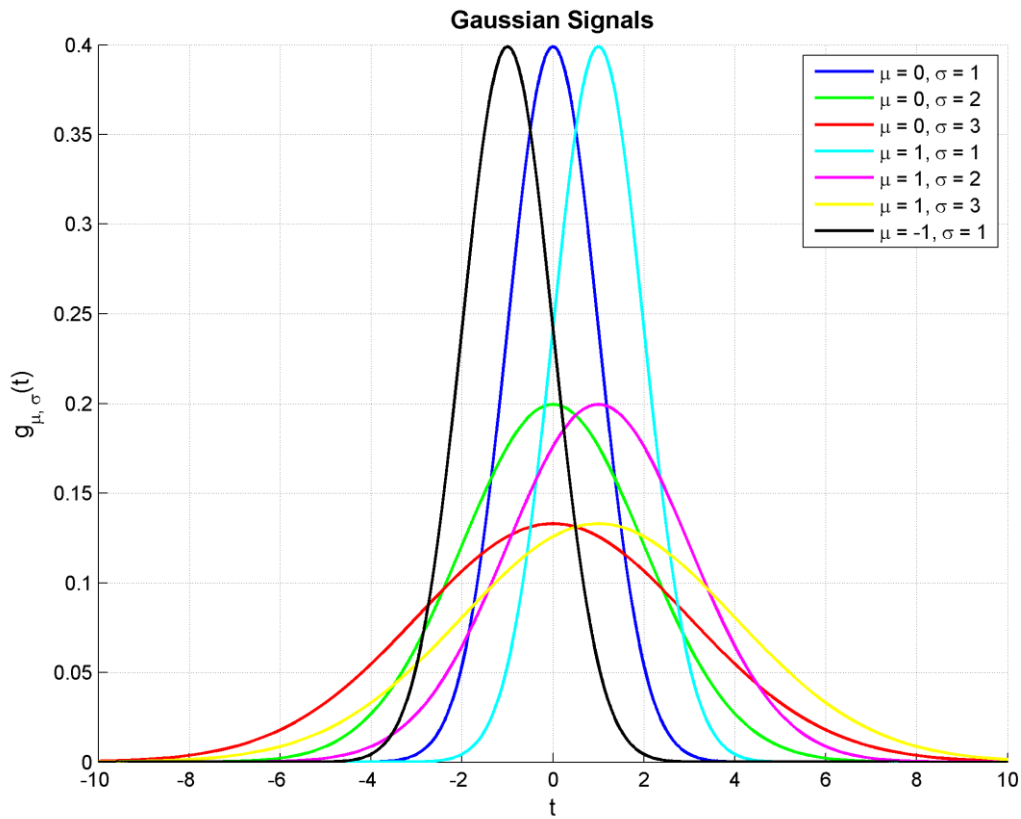


Fig. 5.26. Gaussian Signals with several means and standard deviations.

The Gaussian signal is a “bell-shaped” curve that is symmetric about its mean ( $t = \mu$ ), at which, it reaches its maximum. Thus, if  $\mu$  is changed, the whole signal is, accordingly, shifted along the  $t$ -axis (independent variable).

On the other hand, the standard deviation  $\sigma$  adjusts the width of the curve (“bell shape”), i.e., its spread or dilatation.

In addition, this signal has an important property: **the total area under the curve is 1**, which is preserved by the normalization factor:  $\frac{1}{\sigma\sqrt{2\pi}}$ . Therefore, the height of the curve will also be accordingly adjusted.

It should also be noted that **the side tails** of a Gaussian signal **decay very quickly toward zero** (*asymptote*). As a matter of fact, this signal is not time limited. As such, it decays forever ( $|t| \rightarrow \infty$ ). However, a Gaussian signal drops much faster<sup>76</sup> than other ordinary functions, concentrating the bulk of its energy within a few  $\sigma$ 's around its  $\mu$ . [122], [128]

Another remarkable property of a Gaussian signal is that its Fourier transform is also a Gaussian. Moreover, it is the most concentrated signal, in terms of energy, simultaneously, in time and frequency.

In essence, the **Gabor<sup>77</sup> Transform** (GT) makes use of a *Gaussian window* to implement a *time window*, which will partially delimit the content of the signal. This **windowing** operation, that precedes the spectrum computation, is based on particular values of the signal, which are selectively localized. Then, the most relevant oscillatory occurrences are thus confined. Hence, the GT is able to provide enhanced estimates of the spectrum of a signal.

The concept behind this transform is based on a grid, which is defined over a time-frequency ( $t$ - $\omega$ ) plane, as shown in Fig. 5.27. Each of these elementary grid cells was originally designated, by Gabor, as a “*logon*”. All logons should have the same size.

The logons are, actually, **time-frequency windows**, which will retain local frequency information of the signal. As the windowing process is evenly replicated to all logons included in the  $t$ - $\omega$  plane – i.e., it is applied to the entire extent of the signal –, a structural interpretation

---

<sup>76</sup> After  $2\sigma$ , it drops to  $\approx 1/19$ ; after  $4\sigma$ , to  $\approx 1/7563$ ; and after  $6\sigma$ , to  $\approx 1/(166 \times 10^6)$ . [128]

<sup>77</sup> **Dennis Gabor (1900 - 1979)**, Hungarian-British physicist and electrical engineer. Although he had studied optimal time-frequency signal representations for pulse-like signals, he gained more notoriety in the field of Physics, when he was awarded with the Nobel Prize, in 1971, by inventing holography. [122]

is then possible, and thus, frequency components will be captured and referenced, by the transform, with respect to their locations in time.

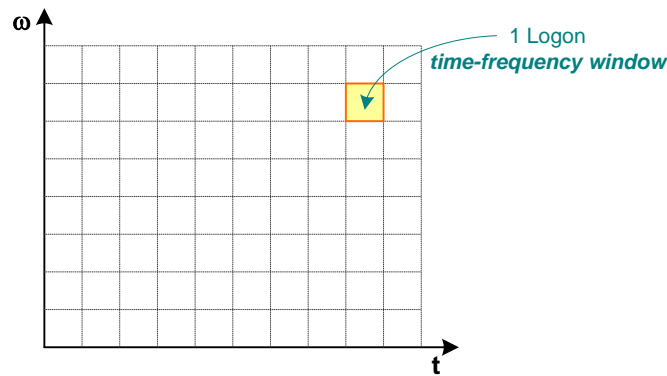


Fig. 5.27. Conceptual diagram of logons over a time-frequency plane, underlying the Gabor Transform.

The  $t$ - and  $\omega$ -dimensions, of a time-frequency window, impact on the resolution that is obtained, both in the time and frequency domains, as explained in Fig. 5.28. This is also known as the Heisenberg Uncertainty Principle, which is detailed in section 5.2.1.2.2.

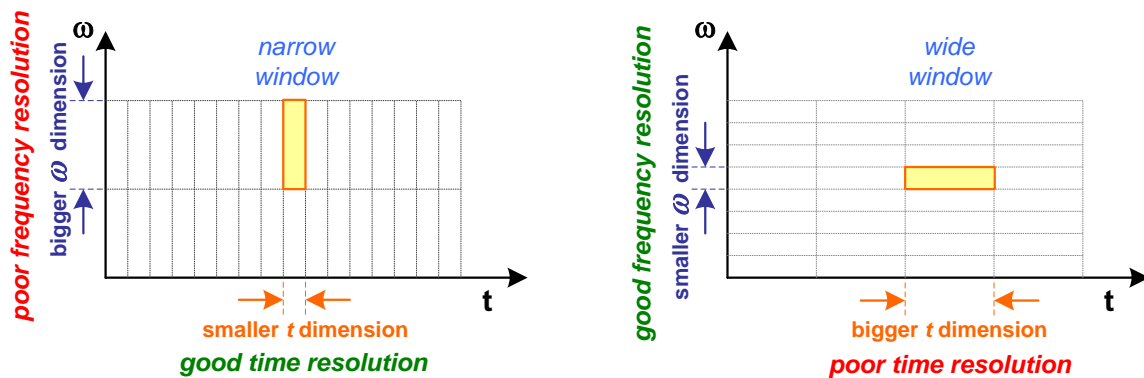


Fig. 5.28. Time-Frequency resolution as a consequence of the windows dimensions ( $t$ - $\omega$ ).



The Gabor Transform is formally defined by Eq. 5.24, assuming a normalized Gaussian window.

$$X_g(\mu, \omega) = \mathcal{G}_g[x(t)](\mu, \omega) = \frac{1}{\sigma\sqrt{2\pi}} \int_{-\infty}^{+\infty} x(t) e^{-\frac{(t-\mu)^2}{2\sigma^2}} e^{-j\omega t} dt \quad \text{Eq. 5.24}$$

The GT is a function of two variables:  $\mu$  – time domain variable which represents the center or mean of the window function; and  $\omega$  – frequency domain variable.

The above expression may be rewritten (Eq. 5.25), for clarity reasons, using the definition of Eq. 5.23, to show that the GT is, in fact, the Fourier transform of (windowed) segments of the signal, which are being captured by a sliding Gaussian window  $g_{\mu,\sigma}(t)$ .

$$X_g(\mu, \omega) = \int_{-\infty}^{+\infty} x(t) g_{\mu,\sigma}(t) e^{-j\omega t} dt \quad \text{Eq. 5.25}$$

As noticed before, the Gaussian window is not truly finite in its full extent, but its abrupt decay ensures that, in practical applications, it is more than sufficient to satisfy the goal of localizing incidences of the signal. Fig. 5.29 shows both time and frequency domains representations of a truncated Gaussian window. The “*wvtool*” provided by the Signal Processing Toolbox of MATLAB™ was used to generate such outputs.

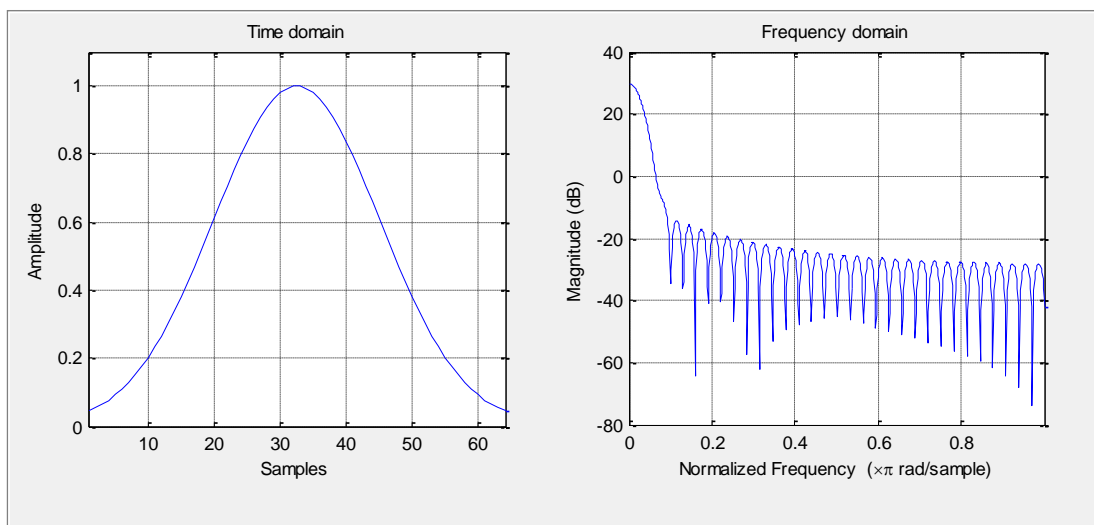


Fig. 5.29. Time and Frequency domains Representations of a Gaussian Window.

It should be remarked that the **width** of the **Gaussian window** used by the GT, which is adjusted through the standard deviation  $\sigma$  parameter, is **constant**<sup>78</sup> **during a transformation**, i.e. *from the beginning to the end*. [122]

Fig. 5.30 illustrates the application of the Gabor transform, when used to iteratively compute the short-time spectrum of a given signal  $x(t)$ .

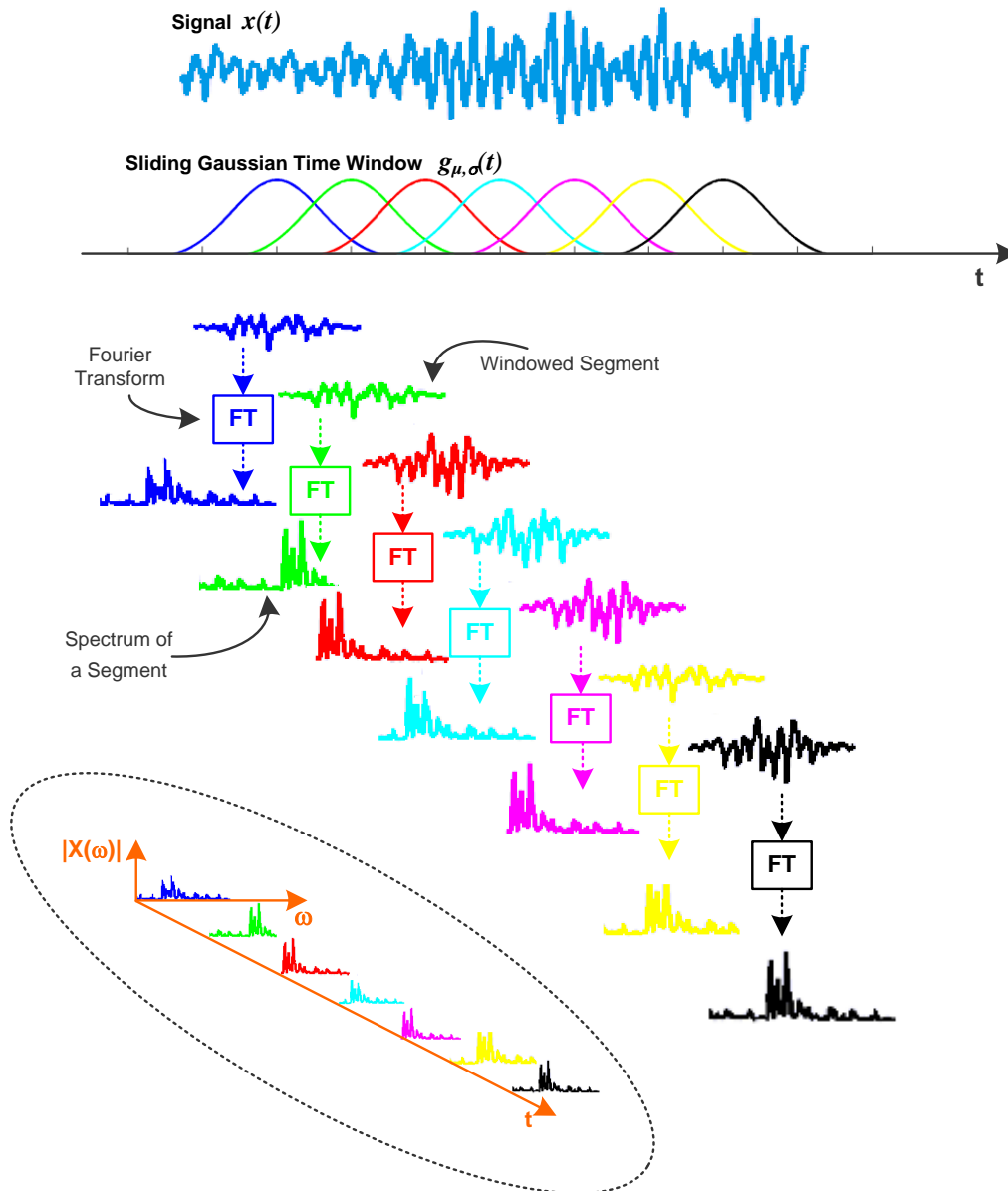


Fig. 5.30. Conceptual illustration of the Gabor Transform.

<sup>78</sup> Although the width of the window can be changed during a transformation, – and despite this may be advantageous in specific scenarios –; if such is allowed, the essence of the transform is somehow compromised as a time-frequency tool.

The GT is itself a **filtering operation**, since the windowing suppresses the effect of oscillatory components of the signal  $x(t)$  which are far away from  $t = \mu$ .

On the other hand, it enhances the values of  $x(t)$  which are in a close vicinity of  $t = \mu$ . Therefore, it captures the spectral content of  $x(t)$  confined to a Gaussian circumscription.

### 5.2.1.2 Short-Time Fourier Transform

The Gaussian is the basic window function of the Gabor transform. However, it is opportune to realize if such a window is comprehensively appropriate to analyze all kinds of signals. Since the performance of the transform depends on the match between the shapes of both – the *window* and *signal* –, in the regions where this latter is being analyzed; other window functions may effectively provide better results, depending on the intended application or signal under scrutiny.

The Short-Time Fourier Transform (STFT), defined by Eq. 5.26, generalizes the GT by allowing a generic sliding window function  $w(t)$ . [122] The STFT is also known as *windowed Fourier Transform*.

$$X_{\mathcal{W}}(\mu, \omega) = STFT[x(t)](\mu, \omega) = \int_{-\infty}^{+\infty} x(t)w(t - \mu)e^{-j\omega t} dt \quad \text{Eq. 5.26}$$

Similarly to what was stated above for the GT, the STFT also uses a fixed windowing function  $w(t)$  throughout the transformation.

It should be noted that, if  $w(t)$  is a Gaussian window, the STFT of a given signal  $x(t)$ , obtained through  $w(t)$ , is, in fact, the GT of  $x(t)$ , i.e.,  $X_{\mathcal{W}}(\mu, \omega) = X_g(\mu, \omega)$ , if  $w(t) = g_{\mu, \sigma}(t)$ .

There is a multitude of standard windowing functions, which can be properly accommodated in the STFT, in accordance with the expected types of signals to be analyzed. Some of the most common windows<sup>79</sup> are summarized in Table 5.1, which also includes the respective definitions. Then, Table 5.2 separately presents the corresponding time and frequency responses, and Table 5.3 provides a brief insight into possible scenarios of application of the above windows.

Nevertheless, the GT is, among the diverse STFT techniques, that which has the smallest time-frequency window. As a matter of fact, the Gaussian window is the one that offers the best joint time-frequency resolution and, in that sense, it outperforms any other window. That is the

---

<sup>79</sup> **Rectangle** or ‘*boxcar*’, **Blackman**, **Bartlett** or ‘*triangle*’, **Hamming**, and **Hanning**

reason why the **GT is considered the optimal STFT**. [122], [137] Such an aspect will be addressed in the next subsection (5.2.1.2.1).

Window	Definition	
<b>Rectangle</b>	$w(t) = \begin{cases} b, &  t  \leq a \\ 0, & \text{otherwise} \end{cases}$	Eq. 5.27
<b>Blackman</b>	$w(t) = \begin{cases} 0.42b + 0.5b \cos\left(\frac{\pi t}{a}\right) + 0.08b \cos\left(\frac{2\pi t}{a}\right), &  t  \leq a \\ 0, & \text{otherwise} \end{cases}$	Eq. 5.28
<b>Bartlett (Triangle)</b>	$w(t) = \begin{cases} \frac{b}{a}t + b, & -a \leq t < 0 \\ -\frac{b}{a}t + b, & 0 \leq t < a \\ 0, & \text{otherwise} \end{cases}$	Eq. 5.29
<b>Hamming</b>	$w(t) = \begin{cases} 0.54b + 0.46b \cos\left(\frac{\pi t}{a}\right), &  t  \leq a \\ 0, & \text{otherwise} \end{cases}$	Eq. 5.30
<b>Hanning (von Hann)</b>	$w(t) = \begin{cases} b \cos^2\left(\frac{\pi t}{a}\right), &  t  \leq a \\ 0, & \text{otherwise} \end{cases}$	Eq. 5.31

**Note:**  $a > 0$  is a parameter to adjust the window width to capture the desired incidences of interest of a signal;  
 $b > 0$  is used to normalize the window function.

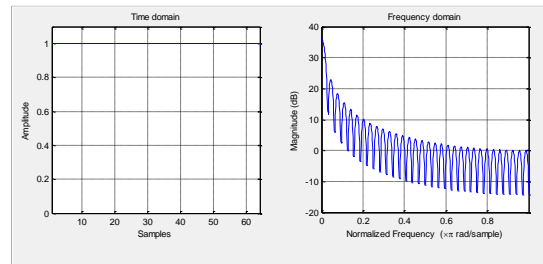
Table 5.1. The most common Short-Time Fourier Transform Window Functions.  
 Source: [122]

## Window

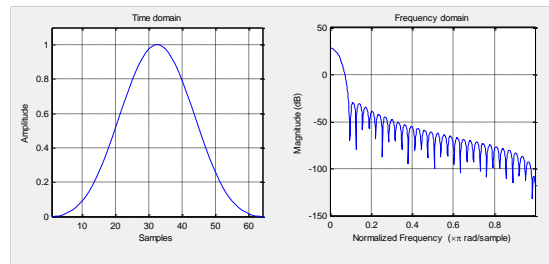
## Time and Frequency Representations

**Rectangle**

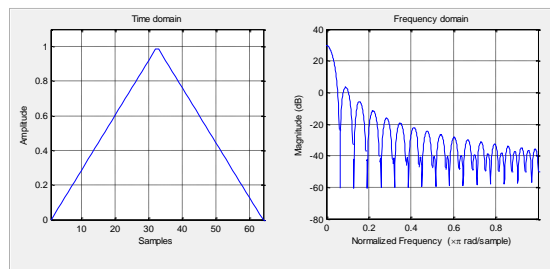
(Eq. 5.27)

**Blackman**

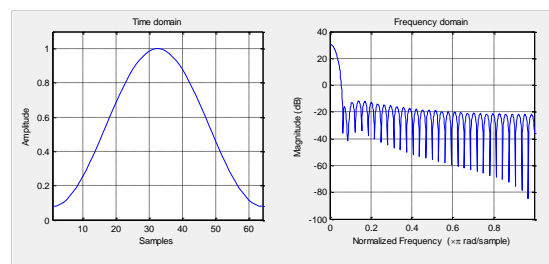
(Eq. 5.28)

**Bartlett**  
*(Triangle)*

(Eq. 5.29)

**Hamming**

(Eq. 5.30)

**Hanning**  
*(von Hann)*

(Eq. 5.31)

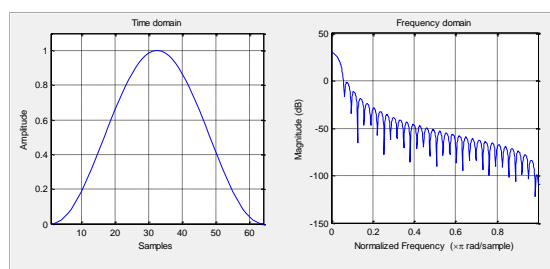


Table 5.2. Time and Frequency Responses of the most common STFT Window Functions.

Window	Type of Signal
<b>Rectangle</b>	<ul style="list-style-type: none"> <li>- Transients whose duration is shorter than the length of the window</li> <li>- Spectral analysis (frequency-response measurements), for pseudo-random excitation</li> <li>- Separation of two tones with frequencies very close to each other, but with almost equal amplitudes</li> <li>- Broadband random (white noise)</li> </ul>
<b>Blackman</b>	<ul style="list-style-type: none"> <li>- Single tone measurement, due to its low maximum side lobe level and a high side lobe roll-off rate</li> </ul>
<b>Hamming</b>	<ul style="list-style-type: none"> <li>- Closely spaced sine waves</li> </ul>
<b>Hanning</b>	<ul style="list-style-type: none"> <li>- Transients whose duration is longer than the length of the window</li> <li>- General-purpose applications</li> <li>- Spectral analysis (frequency-response measurements), for random excitation</li> <li>- Sine wave or combination of sine waves</li> <li>- Narrowband random signal (vibration data)</li> <li>- Unknown content</li> </ul>
<b>Kaiser-Bessel<sup>80</sup></b>	<ul style="list-style-type: none"> <li>- Separation of two tones with frequencies very close to each other but with widely differing amplitudes</li> </ul>
<b>Flat Top<sup>81</sup></b>	<ul style="list-style-type: none"> <li>- Accurate single-tone amplitude measurements</li> <li>- Sine wave and amplitude accuracy is important</li> </ul>

Table 5.3. Windows applications according to the type of signal to be analyzed.  
Source: National Instruments [139]

#### 5.2.1.2.1 Time-Frequency Localization

A straightforward method of “mapping” a signal, simultaneously, into time and frequency, i.e., a way of localizing it in the  $t$ - $\omega$  plane, is to determine its mean localizations and dispersions, in both dimensions ( $t$ - $\omega$ ). Thus, the relationship between the (time) **duration** and the (frequency) **bandwidth** of a signal is of paramount importance for the *joint time-frequency analysis*, used to describe the signal’s behavior.

The **expected value**, or mean, and the **standard deviation** and **variance** concepts, in the sense of the probability theory, will be applied to the signal, in order to characterize its duration and bandwidth. [122], [133], [137]

<sup>80</sup> The definition of this window can be found in **Appendix A**.

<sup>81</sup> Idem (previous footnote).

Assuming that a signal  $x(t)$  is finite-energy (or *square-integrable*), with energy  $\mathcal{E}$ , and that  $|x(t)|^2$  and  $|X(\omega)|^2$  are the probability density functions of the signal, in the time and frequency domains, respectively, the expression below (Eq. 5.32) is satisfied.

$$\mathcal{E} = \int_{-\infty}^{+\infty} |x(t)|^2 dt < +\infty \quad \text{Eq. 5.32}$$

Using the Parseval's formula<sup>82</sup>, the following relationship is then established (Eq. 5.33).

$$\|x(t)\|^2 = \int_{-\infty}^{+\infty} |x(t)|^2 dt = \frac{1}{2\pi} \int_{-\infty}^{+\infty} |X(\omega)|^2 d\omega = \mathcal{E} \quad \text{Eq. 5.33}$$

Let it be considered the normalized energy density functions:  $\frac{|x(t)|^2}{\mathcal{E}}$  and  $\frac{|X(\omega)|^2}{\mathcal{E}}$ , to calculate the *average time*:  $\bar{t}$  (Eq. 5.34) and *average frequency*:  $\bar{\omega}$  (Eq. 5.35), by applying the expression<sup>83</sup> of the  $n^{\text{th}}$  moment of a random variable. In this particular case, both means are given by the first moment.

$$\bar{t} = \frac{1}{\mathcal{E}} \int_{-\infty}^{+\infty} t |x(t)|^2 dt \quad \text{Eq. 5.34}$$

$$\bar{\omega} = \frac{1}{2\pi\mathcal{E}} \int_{-\infty}^{+\infty} \omega |X(\omega)|^2 d\omega \quad \text{Eq. 5.35}$$

The concepts of standard deviation and variance will be adopted to characterize the spread of the signal, both in time and frequency. Let it be assumed that  $\sigma_t$  and  $\sigma_\omega$  are the standard deviations of the signal in the time and frequency domains, respectively. Therefore, its time duration (width) is  $2\sigma_t$ , and its frequency bandwidth is  $2\sigma_\omega$ .

---

<sup>82</sup> From the Parseval's Formula:  $\int_{-\infty}^{+\infty} |x(t)|^2 dt = \frac{1}{2\pi} \int_{-\infty}^{+\infty} |X(\omega)|^2 d\omega$  results that the FT is compliant with the principle of energy conservation. In fact, the FT preserves the energy of the signal, i.e., the total energy of  $x(t)$ , evaluated over all time instants  $t$ , is equal to the total energy contained in all frequency components. [137]

<sup>83</sup> The  $n^{\text{th}}$  moment of a variable Y is given by:  $E[Y^n] = \int_{-\infty}^{+\infty} t^n f_Y(t) dt$ , where  $n$  is the order of the moment, and  $f_Y(t)$  is the probability density function of the variable Y. [129]

As the variance is the standard deviation squared ( $\sigma^2$ ), the signal dispersions in terms of variances  $\sigma_t^2$  (Eq. 5.36) and  $\sigma_\omega^2$  (Eq. 5.37) are related<sup>84</sup> to the corresponding mean values (Eq. 5.34 and Eq. 5.35, respectively).

$$\sigma_t^2 = \frac{1}{\mathcal{E}} \int_{-\infty}^{+\infty} t^2 |x(t)|^2 dt - \bar{t}^2 \quad \text{Eq. 5.36}$$

$$\sigma_\omega^2 = \frac{1}{2\pi\mathcal{E}} \int_{-\infty}^{+\infty} \omega^2 |X(\omega)|^2 d\omega - \bar{\omega}^2 \quad \text{Eq. 5.37}$$

Then, a signal can be characterized in the  $t$ - $\omega$  plane, by its mean position, defined by a generic point  $C(t, \omega) \sim (\bar{t}, \bar{\omega})$ , and by its dispersion  $2\sigma_t$  and  $2\sigma_\omega$  around  $C$ . Therefore, it is possible to define a region  $[\bar{t} - \sigma_t, \bar{t} + \sigma_t] \times [\bar{\omega} - \sigma_\omega, \bar{\omega} + \sigma_\omega]$ , centered at  $C$ , within which, the signal concentrates the bulk of its energy as illustrated in Fig. 5.31 (the yellow ellipse area corresponds to a Gaussian signal).

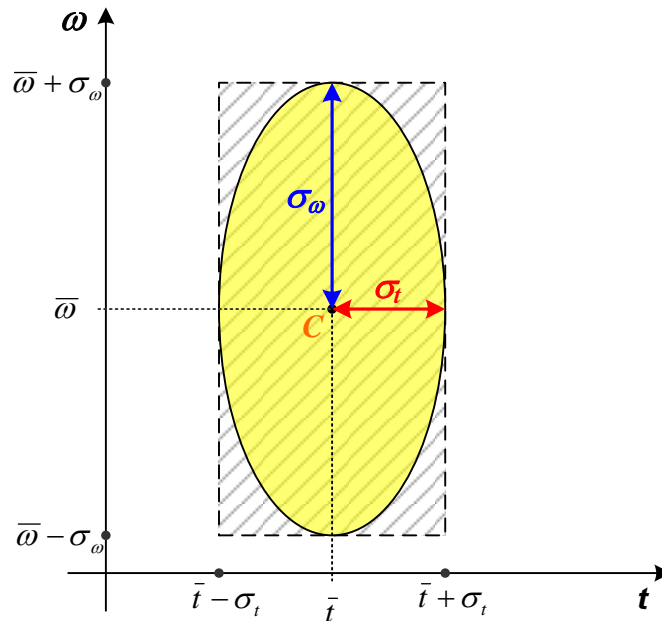


Fig. 5.31. Signal localization in the  $t$ - $\omega$  plane.

<sup>84</sup> The variance of a variable  $Y$  is given by:  $\sigma^2 = \text{VAR}[Y] = E[(Y - E[Y])^2]$ . This expression can be simplified as follows:  $\text{VAR}[Y] = E[Y^2 - 2E[Y]Y + E[Y]^2] = E[Y^2] - 2E[Y]E[Y] + E[Y]^2 = E[Y^2] - E[Y]^2$ . [129]



As a consequence, in practice, if a given generic windowing function  $w(t)$  is, for instance, positioned at  $C$ , and if  $w(t)$  has a time duration  $2\sigma_t$  and bandwidth  $2\sigma_\omega$ , then the STFT (Eq. 5.26), with such a window function, will capture the content and the behavior of the signal somewhere within or in a close vicinity of the rectangle depicted in Fig. 5.31.

#### 5.2.1.2.2 Resolution Issues: The Heisenberg Uncertainty Principle

As has already been touched upon, when introducing Fig. 5.28, there is an important trade-off between both time and frequency resolutions. If a given window  $w(t)$  is configured to have good time resolution (a smaller  $t$  dimension, i.e. a smaller  $\sigma_t$ ), the frequency resolution will be unfortunately sacrificed, since a bigger  $\sigma_\omega$  is sympathetically imposed. If, on the other hand,  $w(t)$  is chosen to have good frequency resolution (smaller  $\sigma_\omega$ ), the time resolution is naturally degraded (bigger  $\sigma_t$ ).

This is, however, a classic problem, transversal to different areas, which is ruled by the so-called **Heisenberg<sup>85</sup> Uncertainty Principle<sup>86</sup>**.

The **uncertainty principle theorem** states that [137]:

If

$$\lim_{t \rightarrow \infty} \left( \sqrt{|t|} |w(t)| \right) = 0 \quad \text{Eq. 5.38}$$

Then,

$$\sigma_t \cdot \sigma_\omega \geq \frac{1}{2} \quad \text{Eq. 5.39}$$

It is being assumed that  $w(t)$  is a limited window function, otherwise  $\sigma_t = \infty$ ; and that  $X(\omega)$  is also a window function, otherwise  $\sigma_\omega = \infty$ . The proof of the above theorem can be found in [122], [137].

---

<sup>85</sup> **Werner Heisenberg (1901 – 1976)**, German theoretical physicist, who was awarded with the Nobel Prize in Physics, in 1932, by creating *quantum mechanics*. He discovered that there is a trade-off between the probable location of a particle and its probable momentum, showing that:  $\Delta p \cdot \Delta x \geq 2\hbar$ , where  $\Delta p$  is the width of a particle's momentum distribution,  $\Delta x$  is the width of its position distribution, and  $\hbar$  is the Planck's constant. This is the classic formulation of the Heisenberg Uncertainty Principle. [122]

<sup>86</sup> This is also known as Heisenberg-Gabor Uncertainty Principle.

The inequality, given by Eq. 5.39, becomes an **equality**, i.e.,  $\sigma_t \cdot \sigma_\omega = \frac{1}{2}$ , **only if**  $w(t) = g_{\mu,\sigma}(t)$ . In other words, **only the Gaussian window, and thus, the Gabor transform provides an optimal time and frequency locality**, as a consequence of the Heisenberg Uncertainty Principle.

### 5.2.1.2.3 Window Effects

The windowed transforms are, in essence, dependent on a windowing function. Then, the choice of the most appropriate window  $w(t)$  is crucial to obtain satisfactory results, taking into account the properties of the signal under investigation. In fact, the behavior and performance of the transform can be undesirably, or inadvertently, influenced by the adopted window.

The spectral effects due to the intrinsic properties of the analyzed signal are indiscriminately merged with those of the  $w(t)$ . This is a major impairment, since it may be very difficult, or even impossible, to distinguish the spectral effects of the signal from those ones introduced by the window.

However, the window effects and the window dependence may be overcome if particular quadratic transforms (e.g., *Wigner-Ville*) are used.

## 5.2.2 Quadratic Time-Frequency Transforms

The distinctive feature of the quadratic time-frequency transforms is that they are based on the evaluation of the signal  $x(t)$  as a **quadratic** term, instead of a linear term, as is the case of the windowed Fourier transforms. [122]

### 5.2.2.1 Spectrogram

The **spectrogram**, which has been heavily used throughout this thesis, although based on the calculation of the STFT, can be envisaged as a quadratic time-frequency transform.

By definition, the *spectrogram*  $X_{S,W}(\mu, \omega)$  of a signal  $x(t)$  is the squared magnitude of the STFT of  $x(t)$ , using a windowing function  $w(t)$  (Eq. 5.40).

$$X_{S,W}(\mu, \omega) = |X_W(\mu, \omega)|^2 = \left| \int_{-\infty}^{+\infty} x(t)w(t - \mu)e^{-j\omega t} dt \right|^2 \quad \text{Eq. 5.40}$$

The spectrogram basically displays the energy distribution of the signal in the time-frequency mixed domain. Its interpretation is simple and intuitive, which explains the huge popularity that it has achieved.

Whereas the output values of the original STFT are, in general, complex, the spectrogram always takes non-negative real values.

Nonetheless, it inherits the same vulnerabilities of the STFT, *inter alia*, resolution issues, dependence on the window, and possible detrimental window effects.

Such susceptibilities will be illustrated below, using spectrograms.

Let us return to the signal  $s(t)$ , previously defined by Eq. 5.8, which is basically a sequence of two co-sinusoids of distinct frequencies (100 kHz and 300 kHz). Since,  $s(t)$  is formed by single tones, according to Table 5.3, the Blackman window should be used to compute the STFT of  $s(t)$  and, then, four different spectrograms as a result of the application of diverse window widths (lengths): 12.5  $\mu\text{s}$ , 62.5  $\mu\text{s}$ , 125.0  $\mu\text{s}$  and 500.0  $\mu\text{s}$ , but keeping the window step<sup>87</sup> fixed (1.25  $\mu\text{s}$ ).

The impact of the use of different widths on time-frequency resolution is clearly illustrated in Fig. 5.32, corroborating, in practice, the aforementioned and expected behavior described in Fig. 5.28, which is a consequence of the uncertainty principle.

Fig. 5.33 emphasizes this aspect, by zooming the transition instant between different frequencies, and by choosing the extreme width values (the smallest: 12.5  $\mu\text{s}$ , and the biggest: 500.0  $\mu\text{s}$ ), which had been previously used. In fact, if the window width is narrow, a very well discriminated “vertical separation line” is identifiable in the precise moment of the transition between tones, but the exact frequency representation of each tone is significantly fuzzy (poor frequency resolution). On the other hand, a wide window expressively improves the frequency resolution, but the identification of the transition instant (which occurs at  $t = 20$  ms) is quite uncertain (poor time resolution).

---

<sup>87</sup> The **window step** defines the time step of the sliding window function  $w(t)$  between two consecutive positions.

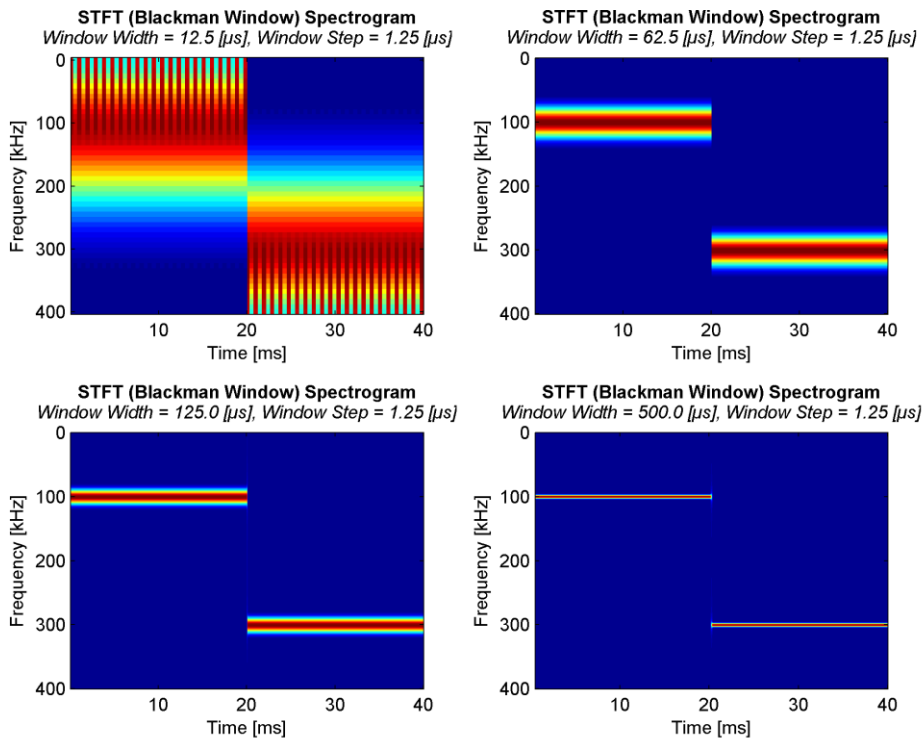


Fig. 5.32. Resolution Issues: the Uncertainty Principle. Spectrograms with distinct Window Widths.

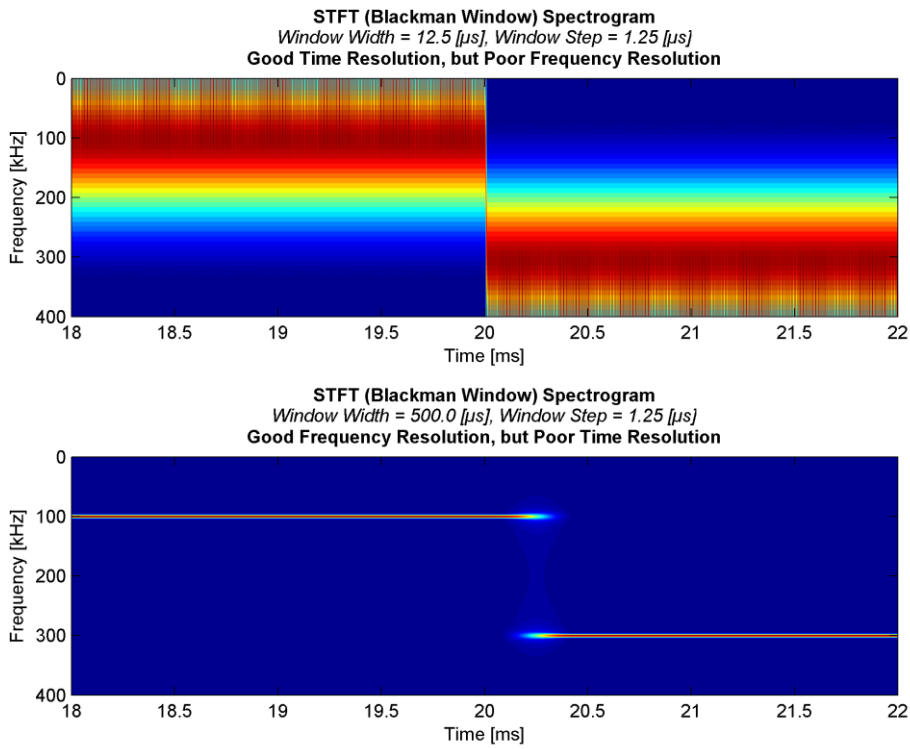


Fig. 5.33. Resolution Issues: the Uncertainty Problem. Trade-off between Time and Frequency Resolutions.

Resuming the example of the linear chirp signal, which was introduced before in Eq. 5.19, six distinct spectrograms were obtained (Fig. 5.34) by changing the window type, i.e. the windowing function  $w(t)$  of the STFT, namely, *Gaussian*, *Rectangle*, *Blackman*, *Bartlett*, *Hamming* and *Hanning*. Both *window width* and *window step* parameters were kept fixed, with the values 20 ns and 50 ps, respectively.

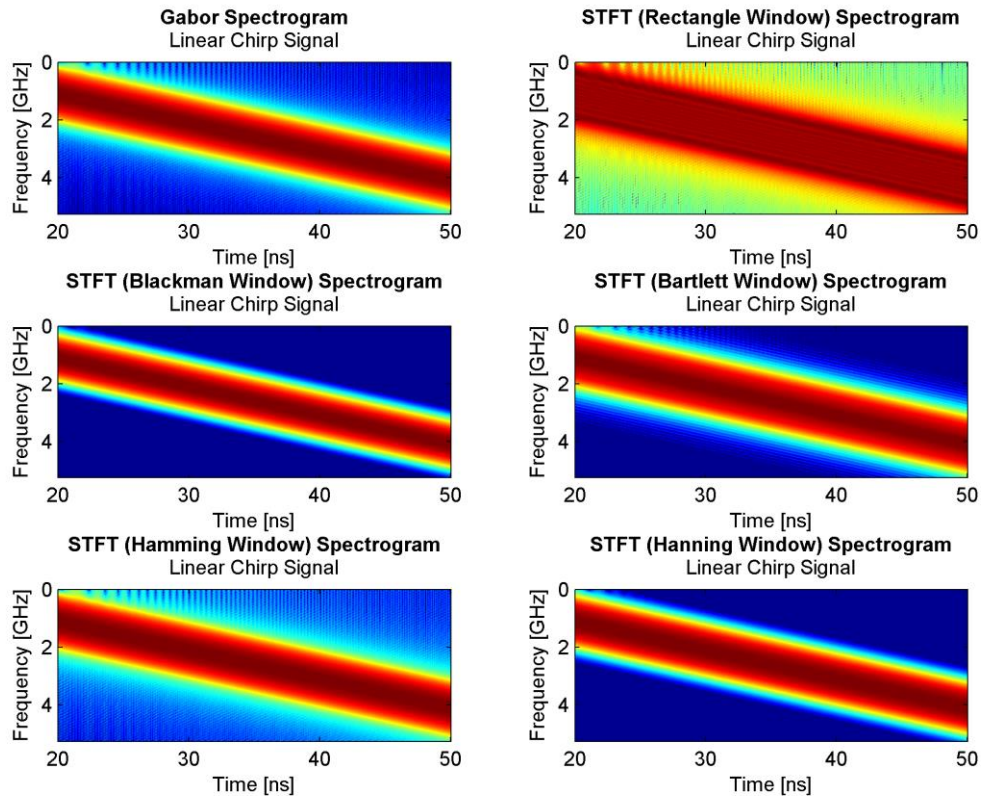


Fig. 5.34. Impact of the Type of Window on the Final Spectrogram of the Chirp Signal.

As can be observed, the final results are somehow influenced by the adopted window. However, in this particular case, that has no noteworthy relevance, since all of them show a common and aligned “interpretation” about the chirp behavior. Although the spectrogram conveys a clear idea on the time progress of the chirp, it suggests a possible overestimated instantaneous signal bandwidth of about 2 GHz.

Notwithstanding, the STFT and spectrogram have overcome and mitigated important drawbacks of the Fourier transform, but they are not flawless. As a matter of fact, the spectrogram may underperform, if the signal has sharply varying frequencies (*e.g.*, *chirps*,

*transients, and unconstrained frequency modulation*), as is the case. [122] Moreover, it is sensitive to the window selection, to be used in the transformation.

The Wigner-Ville Transform outperforms the spectrogram in many key aspects. The most remarkable one is to be **independent** of a **window function**.

### 5.2.2.2 Wigner-Ville Transform

The **Wigner<sup>88</sup>-Ville<sup>89</sup> Distribution (WVD)**, or transform, is the oldest time-frequency transform, dating to the beginning of the 1930 decade, and according to [122], it is “*the preeminent quadratic signal representation*”.

The WVD of a signal  $x(t)$ , designated as  $X_{WV}(\mu, \omega)$ , is defined as the Fourier transform of the product of the signal with its complex conjugate (Eq. 5.41) and, in that sense, it can be envisaged as a sort of “*power spectral density*” calculation, and interpreted as a kind of *probability density function*.

$$X_{WV}(\mu, \omega) = \int_{-\infty}^{+\infty} x\left(\mu + \frac{t}{2}\right) x^*\left(\mu - \frac{t}{2}\right) e^{-j\omega t} dt \quad \text{Eq. 5.41}$$

It is clear from the definition above that **there is no windowing function**, and therefore, the WVD only depends on the properties of the analyzed signal, which eliminates the *window effect* and a possible *erroneous window selection*, both with impact on the performance of the transform.

The WVD effectively overcomes, with superior performance, some problems of the STFT to deal with some abruptly time-varying signals, providing, in general, better resolutions. Fig. 5.35 depicts the Wigner-Ville time-frequency representation of the linear chirp signal (Eq. 5.19), in which, is possible to perceive a better resolution offered by the WVD, when compared to the spectrogram approach.

---

<sup>88</sup> **Eugene Wigner (1902 – 1995)**, Hungarian-American chemical engineer, theoretical physicist and mathematician. He was awarded with the Nobel Prize of Physics in 1963, for his contributions to the theory of the atomic nucleus and the elementary particles, through the discovery and application of fundamental symmetry principles. Wigner developed this transform applied to quantum mechanics. [140], [122]

<sup>89</sup> **Jean-André Ville (1910 – 1989)**, French mathematician and researcher in the field of probability and statistics, and also signal and communication theory. He developed the same transform as Wigner, applied to instantaneous frequency. [122]

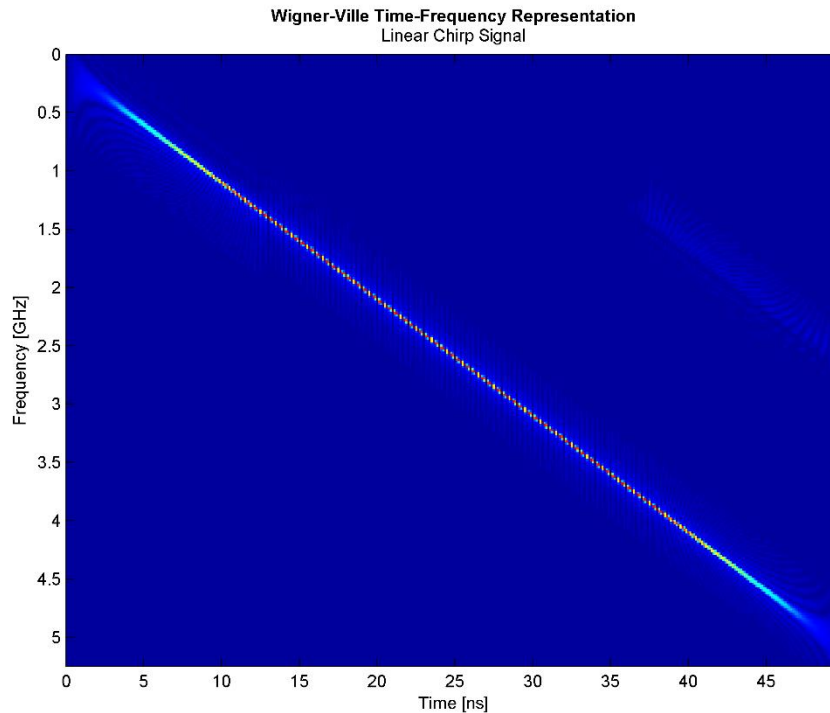


Fig. 5.35. Wigner-Ville Time-Frequency Representations of the Chirp Signal.

Contrary to the spectrogram (squared norm), which always takes non-negative values, the **WVD is real (positive and negative) valued**.

However, the WVD is not perfect. Indeed, the superposition principle fails for this transform, since the linearity conditions are not met. This is, actually, its major flaw. As a consequence, undesired “*false positive*” components may arise – the so-called **cross-terms** or *interference terms* – which will be indistinctly displayed, jointly with the “genuine” coefficients of the transform.

The cross-terms are interpreted as energy, in the time-frequency mixed domain that, in fact, do not truly exist in the original signal. In that sense, they represent an **interference**. Such terms have an oscillatory nature, then, their unwanted effects can be mitigated, if removed through filtering operations, but some degradation may be introduced (e.g., resolution loss). Even so, the scientific community has devoted, over the last few years, significant attention to the development of improved techniques, to remove the cross-term effects.

Getting back to the signal  $s(t)$ , defined by Eq. 5.8, which is a sequence of two co-sinusoids of distinct frequencies (100 kHz and 300 kHz), and applying now the WVD, the time-frequency representation of such a signal (Fig. 5.36), indeed, provides a good frequency resolution. Nonetheless, an undesired cross-term is added, when the frequency is switched.

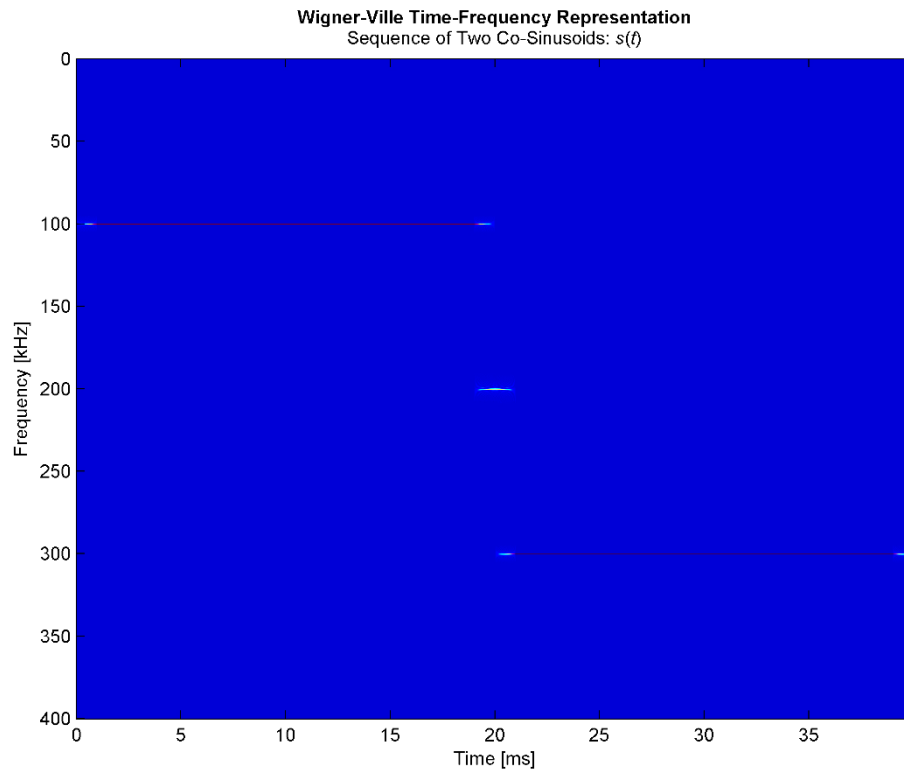


Fig. 5.36. Cross-Term Interference of WVD of the signal  $s(t)$ .

To illustrate other harmful consequences due to WVD cross-terms, the Time-Frequency Toolbox [134] for MATLAB™ was used. Fig. 5.37 shows a Gaussian amplitude modulation signal that was generated, which is represented in terms of *energy spectral density*, *time waveform*, and *WVD*. [133]

In reality, only four signal terms (within green ellipses) would be expected, but other six additional cross-terms (delimited by red ellipses) are also included (actually, the central ellipse accumulates the combined interference effect of two cross-terms).

After introducing fundamental techniques to deal with time-varying signals, the next chapter will explore their practical implementation. Therefore, a software tool, to be used on the validation of specific technical parameters of transient waveforms, will be developed.



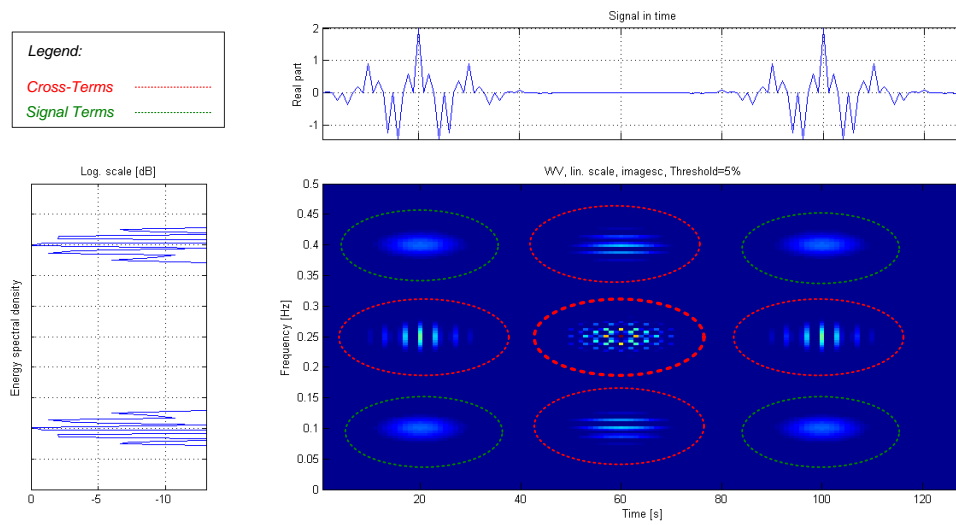


Fig. 5.37. Cross-Terms Interference of WVD of a Gaussian Amplitude Modulation Signal.



---

# 6 Test and Validation of Transient Waveforms

The previous chapters have opportunely introduced legitimate concerns, not only on the suitability of the BEM approach to enforce technical conditions of operation of technology-neutral systems, but also on the methodology that is used in its practical validation. Hence, some of the main vulnerabilities were identified through particular illustrative examples, and supported with theoretical background.

In the present chapter, efforts will be directed to propose a more efficient and expeditious alternative methodology, to be used on the validation of the central segment of a BEM. This approach permits to capture well the dynamic/transient behavior of a LTE BS signal, preserving the genuine integrity of such a type of signal, even if just for a limited or partial section of a BEM.

Then, a general setup, for acquiring the signal to be validated, will be proposed, and a software tool for data processing and validation will be prototyped, developed and implemented. The chapter will be concluded with a comparative analysis, using some reference LTE BS signals, in order to figure out how such a validation is sensitive to different time-frequency techniques, parameter configuration, and types of signals.

## 6.1 Overview of the Proposed Approach

The methodology developed, by the ECC/CEPT, to validate a BEM, presented in Chapter 3, section 3.3, apart from being very time-consuming, it does not provide the necessary simultaneity for the entire measurement process. Thus, it is based on assumptions that may not be verified for transient waveforms, as in the case of LTE signals.

The alternative methodology, which is being proposed in the context of this thesis, tackles the BEM validation problem by separately addressing two fundamental phases:

1. **Signal acquisition** (methodology and setup);

A Real-Time Spectrum Analyzer (RTSA) is used, in order to overcome major impairments revealed by spectrum analyzers, and to capture transients and dynamic characteristics of LTE BS signals. Indeed, the utilization of this instrument is also crucial to speed up the measurement process.

2. **Data processing and waveform validation**, using a software tool, developed in Labview<sup>90</sup>.

The software tool is then fed with the data acquired by the RTSA, and uses the GT, STFT (with different windowing functions) and WVD to analyze and validate a given transient waveform.

## 6.2 Signal Acquisition

The RTSA is, as mentioned before, a fundamental equipment to acquire the LTE BS waveforms. Therefore, two different setups will be presented, in order to address both radiated and conducted measurement scenarios. Afterwards, the RTSA working principle and main blocks will be presented, including the way as the data will be collected for the intended purposes.

---

<sup>90</sup> *Labview* is a trademark of *National Instruments*. [146]

### 6.2.1 General Setup

The radiated measurements should be carried out close to the BS, but at a distance, at which, the far-field conditions are met. Then, a directive receiving antenna (e.g. Yagi-Uda or log-periodic), mounted on a mast, is connected to the RF input of the RTSA, as depicted in the setup of Fig. 6.1.

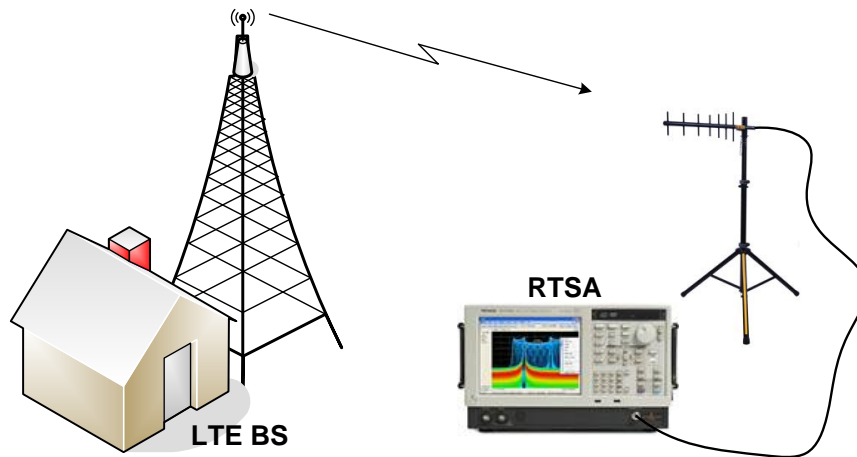


Fig. 6.1. Radiated Measurement Setup to Acquire LTE Waveforms.  
(RTSA image: credits to Tektronix™)

However, special attention has to be devoted to some key aspects, namely, to find a suitable measurement spot and the best orientation for the receiving antenna, in order to privilege the discrimination of the main-lobe of radiation of the transmitting LTE BS antenna, and also to avoid undesired reflections or other possible perturbations.

The conducted measurement setup, shown in Fig. 6.2, assumes that the access to the BS facilities is granted and direct measurements are allowed. Under such circumstances, the RTSA is connected to the BS equipment power output or test probe (directional coupler). If the power levels are too high, a RF attenuator has to be inserted between the transmission line and the RTSA to protect its RF input.

Moreover, for both setups, the dynamic range of the measurement should be properly maximized and potential situations of saturation – of the RTSA RF front-end – must be promptly detected, and eliminated by taking adequate countermeasures.

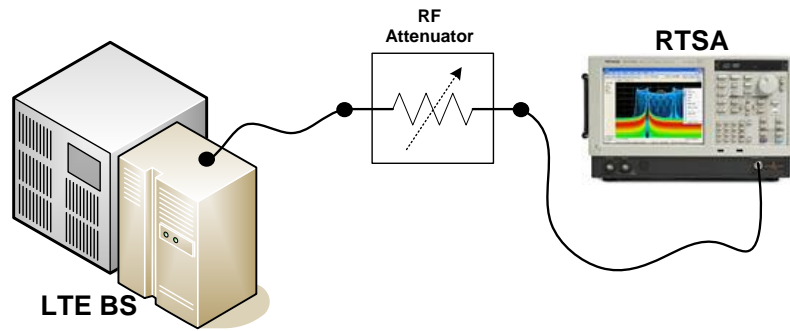


Fig. 6.2. Conducted Measurement Setup to Acquire LTE Waveforms.  
(RTSA image: credits to Tektronix™)

There are substantial reasons for adopting the RTSA equipment, but to realize them better, its working principle should be firstly introduced.

#### 6.2.1.1 The Real Time Spectrum Analyzer

The spectrum measurement implemented by conventional spectrum analyzers is typically a result of the beat of the input signal, to be analyzed, with a fixed intermediate frequency (IF), through a swept local oscillator. The input signal is then subjected to successive down-conversion operations, through different mixing stages, until being delivered to the analogue resolution filter, which defines the resolution bandwidth (RBW) of such a measurement. However, on the one hand, the RBW filter has an intrinsic settling time and, on the other hand, the local oscillator takes some time to get back from the highest frequency of a sweep to its initial frequency, which is usually known as “*retrace time*”. During this “inactive” measurement period, no acquisition data is effectively provided by the instrument. Thus, if a noteworthy event occurs in the meantime, it will simply be ignored. Therefore, this defective period, during which, supplementary background processing operations take place, is termed “*blind time*”. The above mentioned behavior is illustrated in Fig. 6.3, in which, several sequential sweeps are shown, alternated with unavoidable blind spots. As a matter of fact, a non-neglected peak (event) is overlooked within the second blind window.

The blind time has been considerably mitigated with the latest generations of spectrum analyzers, which make use of FFT methods, with multiple narrowband FFT filters. Such improvements, indeed, optimize processing times, providing much quicker sweep cycles and shorter inactive periods. Nevertheless, the blind time, even reduced, is not totally eliminated. Consequently, there is still a potential risk of losing information, if spectrum analyzers – even the brand-new ones – are used to evaluate an actual spectrum activity. [142]

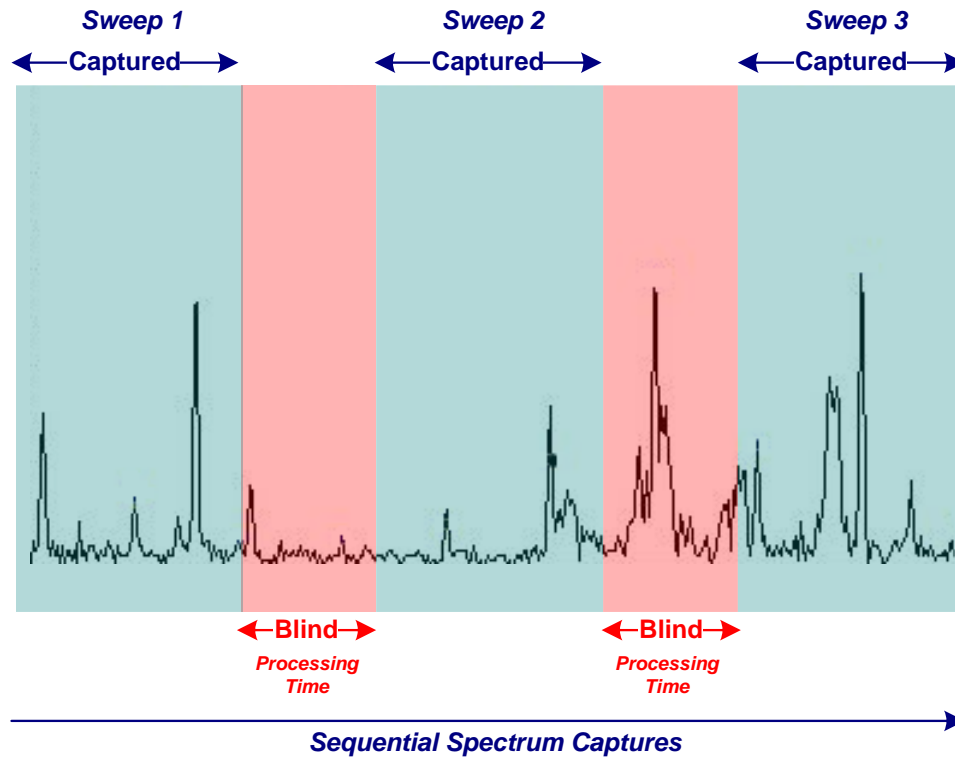


Fig. 6.3. Sequential Spectrum Captures and Analysis implemented by Traditional Spectrum Analyzers.

Providentially, the RTSA has introduced a major qualitative leap forward in spectrum analysis, by avoiding the waste of potentially useful spectrum information. Such a purpose is positively achieved since, both memory and high speed processors are employed to uninterruptedly acquire data (sampling) and also to calculate, in parallel, multiple FFTs. In practice, the sampler keeps working while FFTs are being computed through different processing units, normally, Field-Programmable Gate Arrays (FPGA). As a result, before capturing a new window, the FFT has already been recorded in memory. [141]

Typically, such multiple FFTs are, in fact, the Short-Time Fourier Transform (STFT) introduced in the previous chapter (Eq. 5.26), which RTSA implements in its discrete form. The discrete STFT is thus defined, for a given discrete signal  $x(n)$  and for a generic discrete windowing function  $w(n)$ , with period  $N > 0$ , by the Eq. 6.1.

$$X_w(m, k) = \sum_{n=0}^{N-1} x(n)w(n-m)e^{-j\frac{2\pi nk}{N}} \quad \text{Eq. 6.1}$$

In the above expression,  $m = 0, 1, 2, \dots, N-1$ , and  $k = 0, 1, 2, \dots, N-1$ . Some common discrete windowing functions are detailed in **Appendix A**.

It should be noted that there is an overlap of a few consecutive FFTs meanwhile computed, as shown in Fig. 6.4. Hence, a transient event, such as the pulse that is represented, will be surely detected by distinct captured windows.

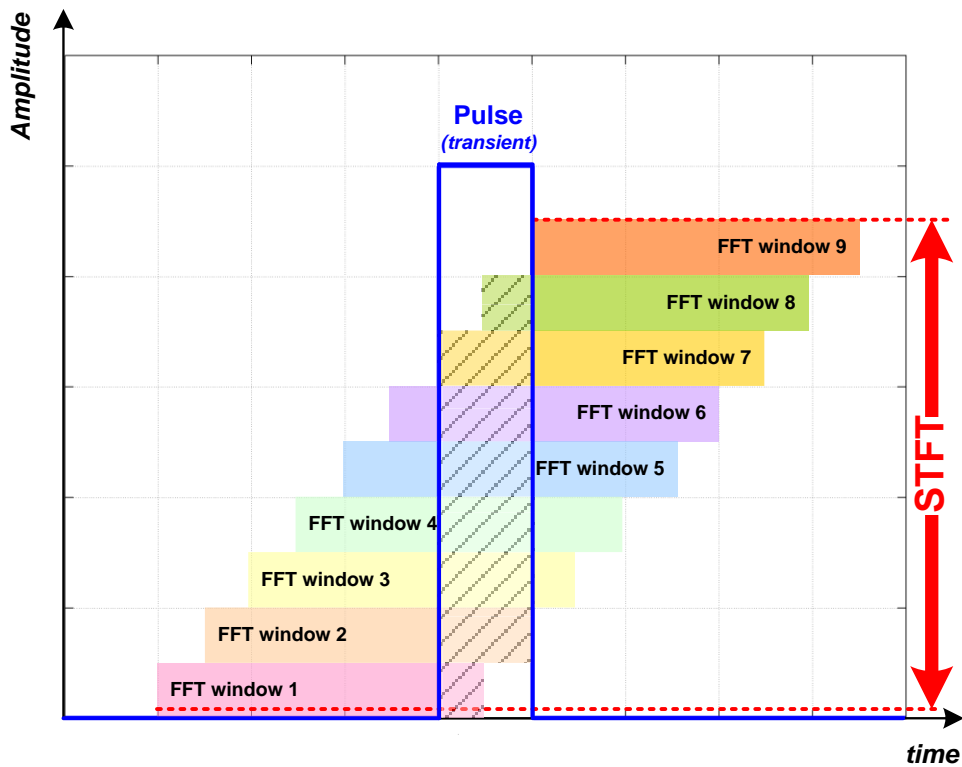


Fig. 6.4. Signal Capture using multiple consecutive and overlapped FFT windows.

Nonetheless, the real-time spectrum analysis may be affected by some errors, due to possible window effects, such as the ones identified in Chapter 5.

A simplified block diagram of a RTSA is presented in Fig. 6.5, in which, an analogue front-end precedes the digital processing blocks. Inside the input stage, the signal, to be analyzed, is firstly down-converted to an IF and filtered out before being delivered to the ADC, to be digitized.



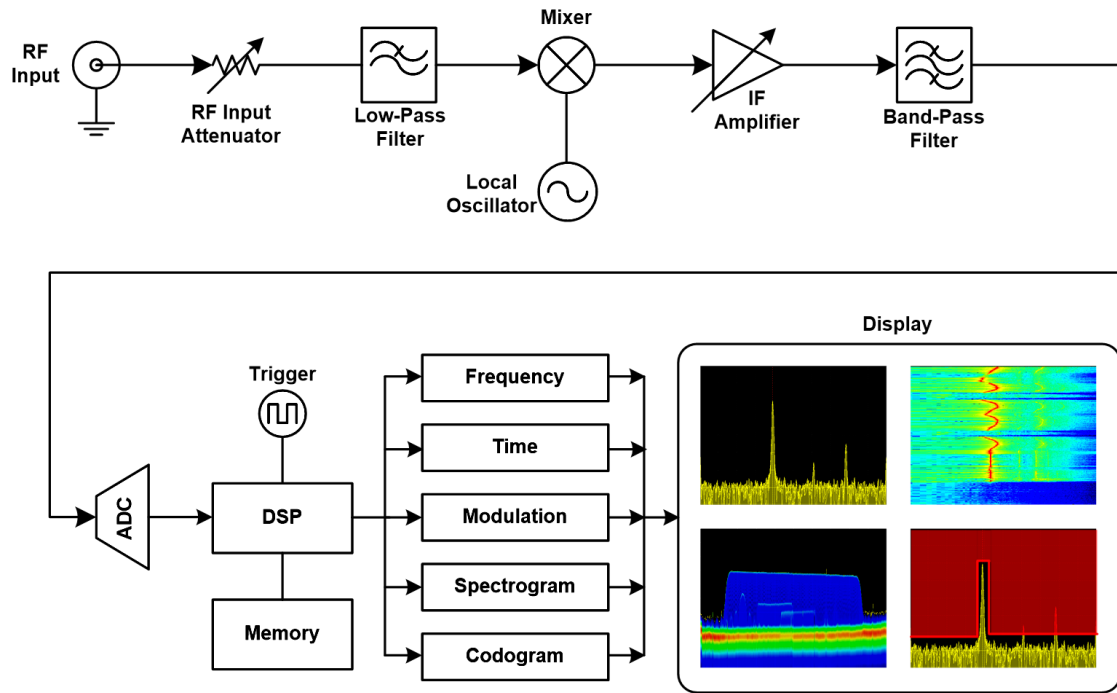


Fig. 6.5. RTSA Block Diagram.

Afterwards, the signal is subjected to joint time-frequency techniques (STFT), using powerful Digital Signal Processors (DSP) and memory, to generate some novel, intuitive and suggestive representations of the input signal: *real-time spectrum*, *spectrogram*, *persistence spectrum* and *mask triggering and validation*, which are displayed by the monitor of the device. Some RTSAs also implement automatic signal classification. These innovative concepts are indeed revolutionary to the spectral analysis and also fundamental to deal with the utmost demanding interference scenarios. One of the most popular and useful time-frequency representation provided by a RTSA is the spectrogram (Fig. 6.6 and Fig. 6.7).

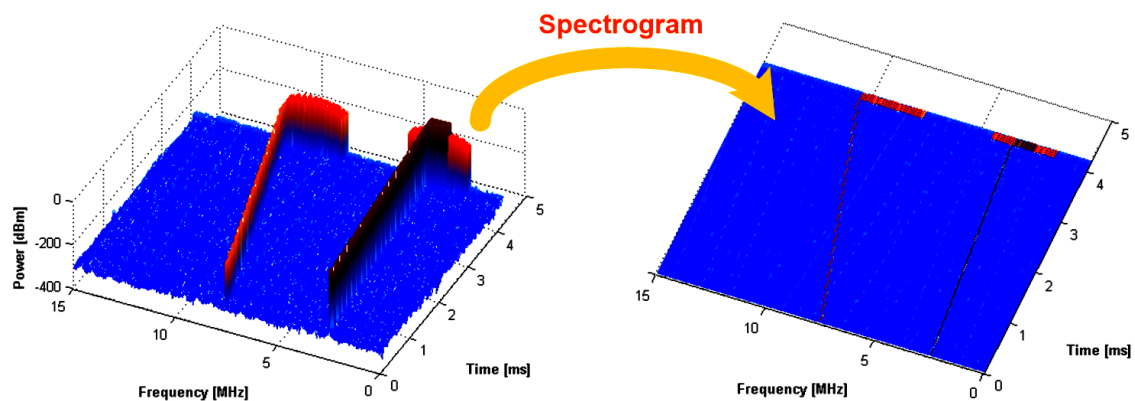


Fig. 6.6. Illustrated concept of the Spectrogram generated by a RTSA.

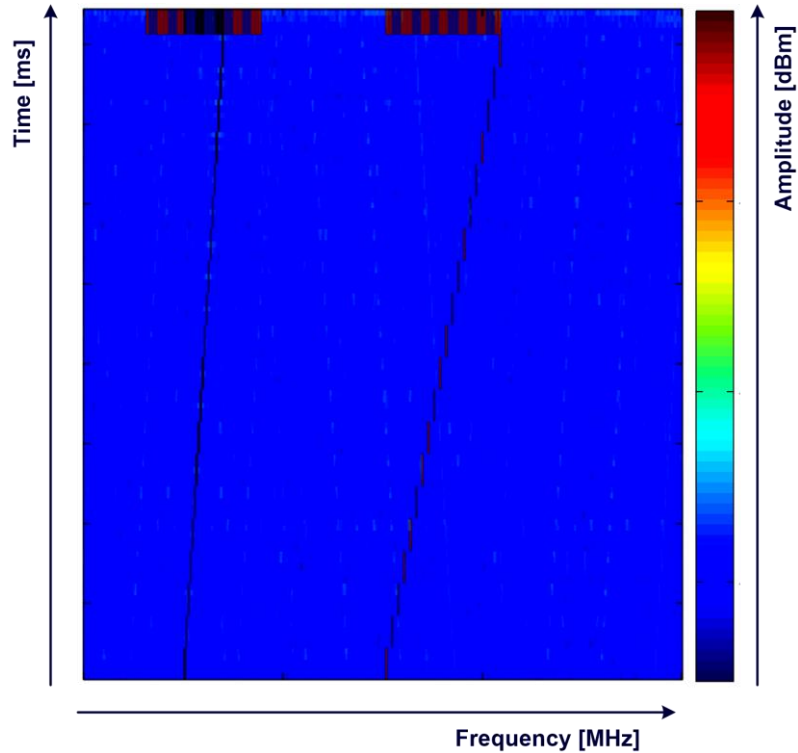


Fig. 6.7. Spectrogram as commonly displayed by a RTSA.

The digital processing block diagram of a RTSA is depicted in Fig. 6.8.

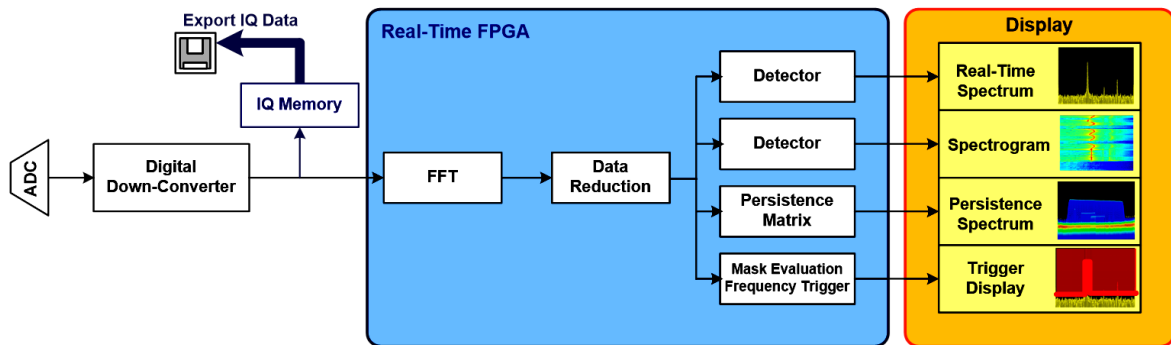


Fig. 6.8. RTSA Digital Processing Block Diagram.

Once in the digital domain (i.e., after the ADC), the signal is digitally down-converted to the IQ (complex) baseband format and stored in a memory. These data are then delivered to the following real-time FPGA block to be processed, but some instruments also allow the exportation of the acquired IQ waveform, typically in mat-file (\*.mat) MATLAB™ format, to be separately

analyzed, in non-real-time environments, with other digital signal processing tools. This latter approach will be followed in the context of the present thesis.

Indeed, the RTSA could be autonomously used to fully implement the proposed methodology, including the mask validation using the frequency triggering module. However, RTSAs make available a limited and fixed set of standard options. Usually, only the STFT is included in current commercial solutions, with few windowing functions. Kaiser and Blackman-Harris are quite common, and sometimes Hanning, but nothing else. Moreover, the configuration of trivial parameters is not often accessible to the user, whether because they are automatically adjusted, or because default values are assumed.

If the RTSA had been used, no representative analysis would be possible, due to the lack of available options. Actually, the developed test and validation tool, besides the basic transient signal evaluation, aims to compare the performance of different techniques, windows and other relevant parameters, in order to figure out the best options to deal with specific types of signals.

Despite all impressive merits introduced by RTSAs, **the validation of a complete BEM is still a considerable challenge**. In fact, there are two key aspects that, simultaneously, are unlikely satisfied: *the significant bandwidth covered by a full BEM*, of about **110 MHz** and *an extensive dynamic range*, **better than 105.5 dB** (assuming the derived BEM of Fig. 3.6, for an EIRP of 59 dBm/10MHz).

Although the most recent RTSA models provide *Real Time Bandwidths*<sup>91</sup> (RTBW) up to 165 MHz; the dynamic range, usually defined by the *Spurious Free Dynamic Range*<sup>92</sup> (SFDR) parameter, **falls short of expectations**.

Indeed, the SFDR is probably one of the most limitative features of the RTSA for specific applications, such as the validation of a full BEM. But the difficulty of providing this demanding dynamic range is also extensive to other measurement equipment, including traditional spectrum analyzers.

That is the main reason why the proposed methodology only encompasses the **validation of the core segment of a BEM** (i.e., a bandwidth of 25 MHz around the center frequency of the LTE channel).

---

<sup>91</sup> This parameter is also known as *IQ Demodulation Bandwidth*. Some typical RTBWs found in commercial versions are, for example, 20, 25, 80, 110 and 165 MHz.

<sup>92</sup> Typical SFDRs currently provided by commercial RTSA models: 70 or 75 dBc.

Even so, it significantly outperforms the ECC/CEPT methodology [69], not only by shortening the measurement time, but also by adding truthfulness introduced by improved techniques to properly analyze time-varying signals. But, and above all, it ensures the necessary **concurrency** of such a measurement.

The IQ waveforms to be used, both on validations and on benchmarking/performance tests below, were acquired with a **Tektronix**<sup>TM</sup> RTSA, model **RSA6114A**.

### 6.3 Data Processing using the Waveform Validation Tool

A prototype of a software tool was developed, in Labview, as a proof of concept, for transient waveform testing and validation purposes. This validation tool is basically organized in three major modules:

1. **General Configuration** (Definitions)
2. **Block Edge Mask Generation** (Mask)
3. **Output Results** (Graphs)

The following subsections cover and illustrate specific functionalities of each of these modules.

#### 6.3.1 General Configuration

When the tool is started, a general configuration page is displayed (Fig. 6.9).

This interface is used to select data files, to be analyzed (mat-files provided by the RTSA, with IQ waveforms), from their respective locations (folders), and also to define the destination path of the output data files (Fig. 6.10).

The joint time-frequency transforms, introduced in Chapter 5, were then implemented, from the Labview's blocks provided by its *Advanced Signal Processing Toolkit*, namely:

- **STFT** with 17 distinct windowing functions
- **Gabor Transform** (STFT with a Gaussian window)
- **Wigner-Ville Distribution**.

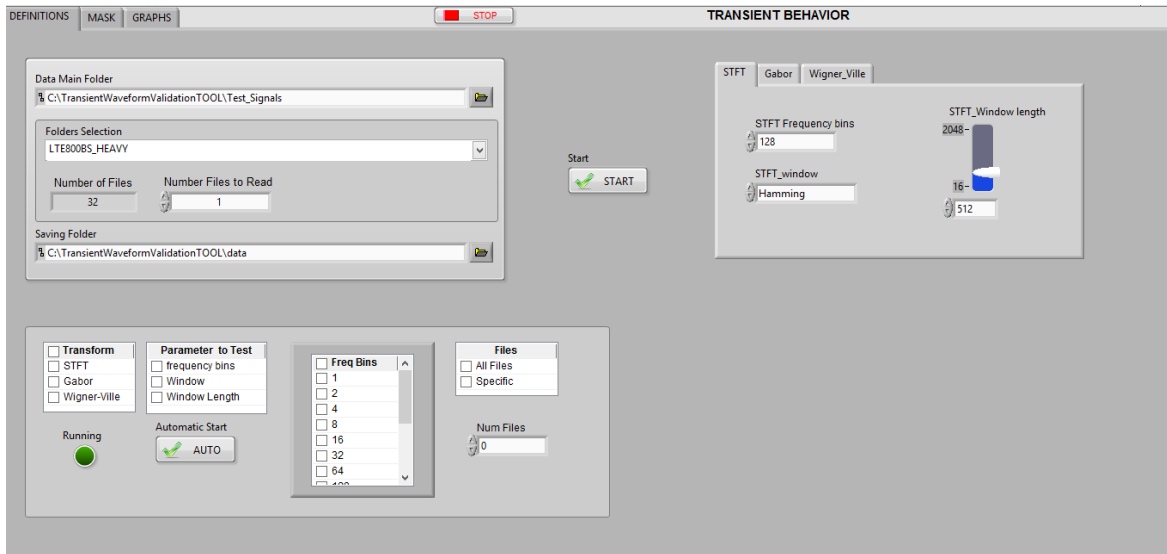


Fig. 6.9. General Configuration Page.

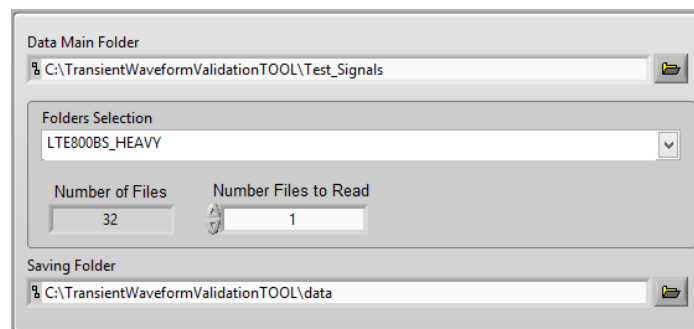


Fig. 6.10. Selection and Location of Input IQ Waveforms and Output Files.

Both STFT and Gabor Transform have a similar configuration form, since they share a common essence. The parameters to be set for the STFT (Fig. 6.11) are the number of *frequency bins*, the *window type* and the *window length*. For the Gabor Transform (Fig. 6.12), since the Gaussian windowing function is fixed, the configurable parameters are just the number of *frequency bins* and the *window length*.

The **frequency bins** parameter defines the FFT block size of the STFT, and represents the number of bins along the frequency axis to sample the signal in the joint time-frequency domain. The number of frequency bins corresponds to the  $N$  in Eq. 6.1. [147]

The **window length** specifies the length, *in samples*, of the sliding window. As mentioned in the previous chapter, it controls the relationship between the time resolution and the

frequency resolution of the joint time-frequency representation. Accordingly, a large window length provides better frequency resolution, but poorer time resolution, and *vice-versa*. [147]

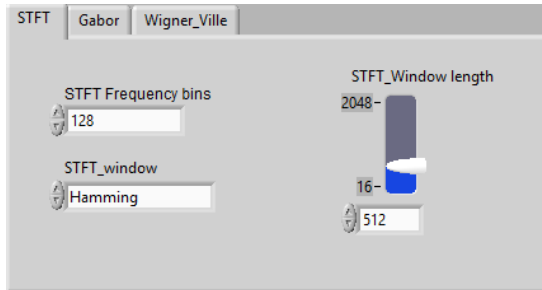


Fig. 6.11. STFT Parameters Configuration.

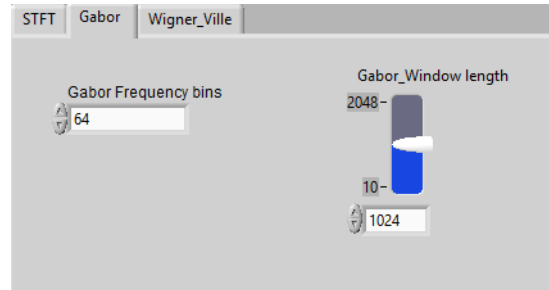


Fig. 6.12. Gabor Parameters Configuration.

The **window type** specifies the sliding window to be used in the STFT. Fig. 6.13 shows all the 17 types of windows which were implemented in the validation tool. The respective windowing functions are detailed in **Appendix A**.

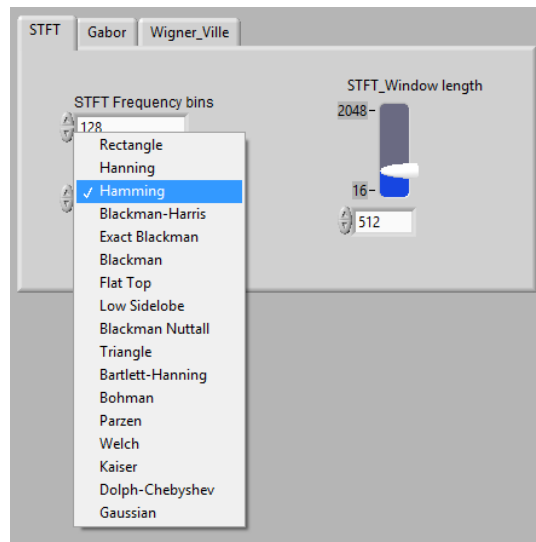


Fig. 6.13. STFT Window Selection.

The WVD only has the number of *frequency bins* to be configured (Fig. 6.14), which specifies the number of bins along the frequency axis to sample the signal in the joint time-frequency domain.



Fig. 6.14. WVD Parameter Configuration.

There is also the option of configuring automatic batch jobs of diverse time-frequency analysis, by choosing different techniques (transforms) and parameters, including all the possible combinations between them. This functionality will be used to carry out the sensitivity analysis below.

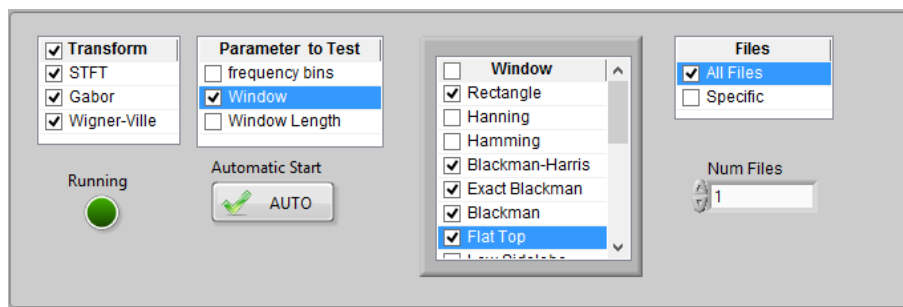


Fig. 6.15. Automatic Batch Jobs Configuration.

### 6.3.2 Block Edge Mask Generation

The Block Edge Mask, to be used on the validation process, as a maximum reference limit to be met, will be calculated, on a case-by-case basis, taking into consideration the desired EIRP.

The BEM calculation for STFT and Gabor Transform is straightforward and directly results from the methodology presented in Chapter 3.

However, if the WVD is used to analyze and validate a transient signal, the output of that transformation cannot be directly compared with a BEM “standard-shape”, as usually defined for the previous transforms. Simply, because the WVD of a BEM “standard-shape” does not have the same original shape, as it will be demonstrated below.

Although it is not clear if, in practice, the WVD validation makes some sense, it is assumed that the mere possibility of introducing a time-frequency transform, which is not dependent on a window function, is itself very useful, interesting and adds considerable value to the present study, even if only for purely academic purposes.

Thus, a “WVD-BEM-equivalent” will be generated from a BEM “standard-shape”, using the multi-sine approach already implemented.

### 6.3.2.1 STFT and Gabor Transform BEM

The BEM generation for STFT and Gabor analysis simply needs the introduction of the *EIRP* of the LTE BS, the respective *reference bandwidth* (“EIRP Ref BW”, in Hz), and the *width of the block of spectrum assigned to the operator* (“Block Width”, in Hz). Then, the desired relative BEM is derived and displayed, as shown in Fig. 6.16.

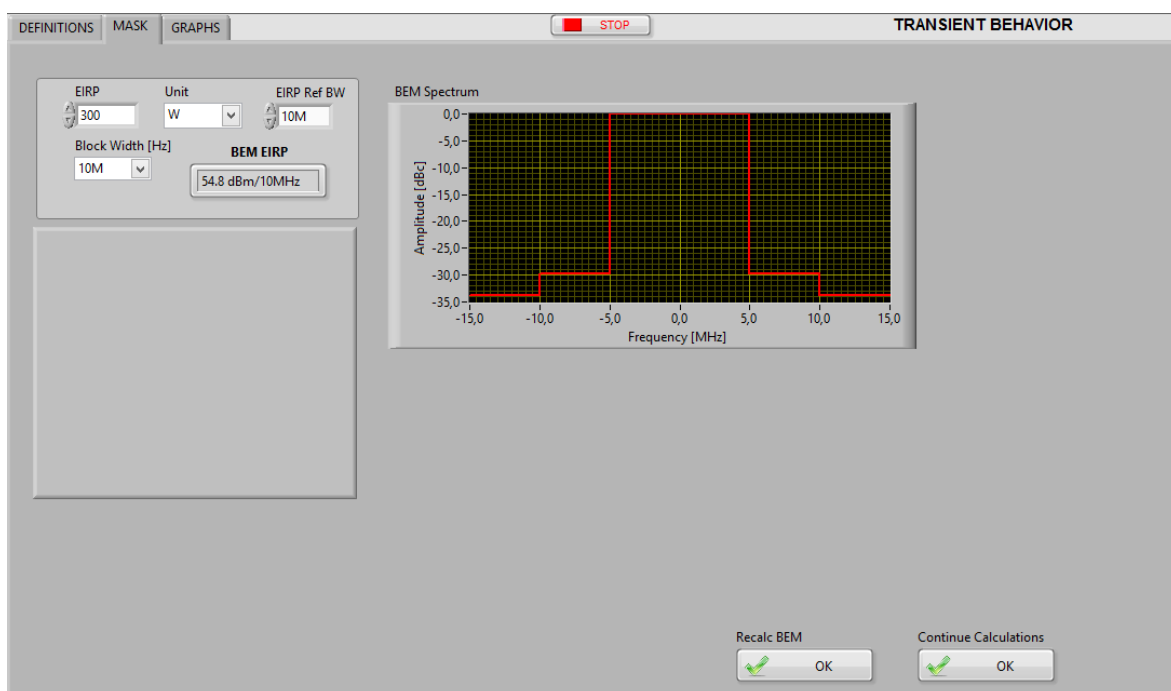


Fig. 6.16. Block Edge Mask Generation Page (Option: STFT and Gabor Analysis).

The interface gives the user the possibility of introducing the EIRP value using linear (W) or logarithmic (dBW or dBm) power units. (Fig. 6.17)



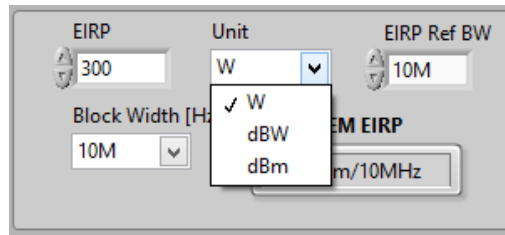


Fig. 6.17. BEM Parameters Configuration.

As an illustrative example, a BEM of a LTE BS emission with 20 dBW (100 W) of EIRP, with respect to a reference bandwidth of 10 MHz (i.e., 50 dBm/10MHz), is presented in Fig. 6.18.

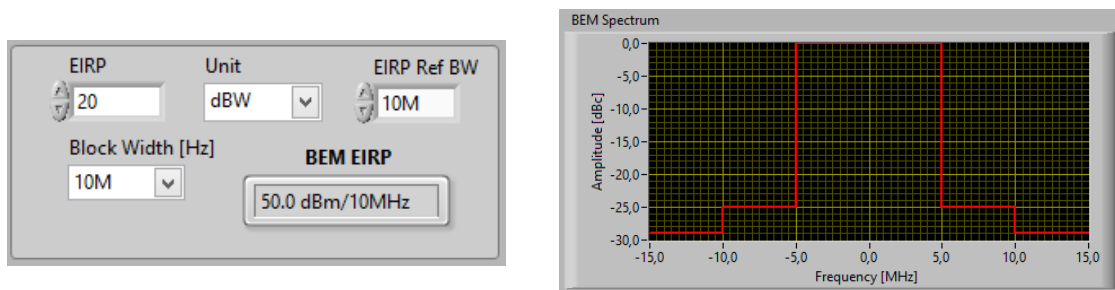


Fig. 6.18. BEM Configuration and Generation (EIRP = 50 dBm/10MHz).

### 6.3.2.2 Generation of a Wigner-Ville BEM Equivalent

As an exploratory approach, a *WVD BEM equivalent* will be generated, from a multi-sine signal, with random phases, and with a spectrum delimited by a core BEM “standard-shape”, as conceptually illustrated in Fig. 6.19, for an EIRP of 59 dBm/10MHz. Then, such a multi-sine signal is transformed through the WVD, and a proposed *WVD BEM equivalent*, which is represented in Fig. 6.20 (blue line), is thus obtained.

This modified BEM shape (WVD BEM equivalent) is used, as a maximum reference limit to validate a waveform, whenever the WVD is applied to the input transient signal under investigation.

The aforementioned conversion procedure, between a BEM “standard-shape” and a WVD BEM equivalent, is embedded in the software tool (Fig. 6.21), which is activated if the WVD is selected in the initial configuration page (Fig. 6.9). The input parameters used to generate the equivalent mask are exactly the same as those considered in the case of STFT and Gabor Transform analysis.

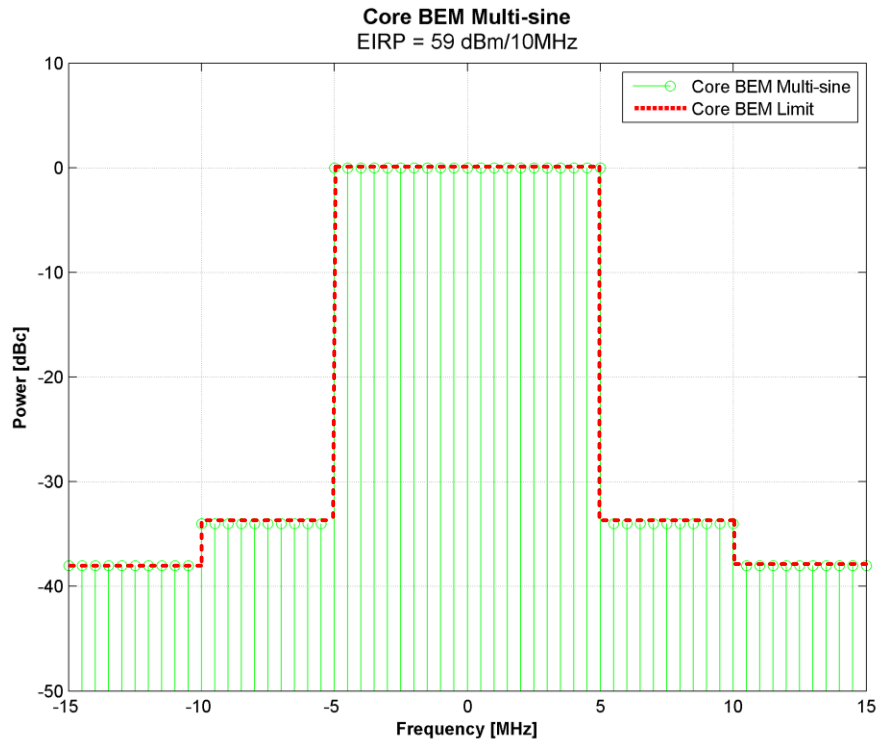


Fig. 6.19. Core BEM Multi-sine Concept (for an EIRP = 59 dBm/10MHz).

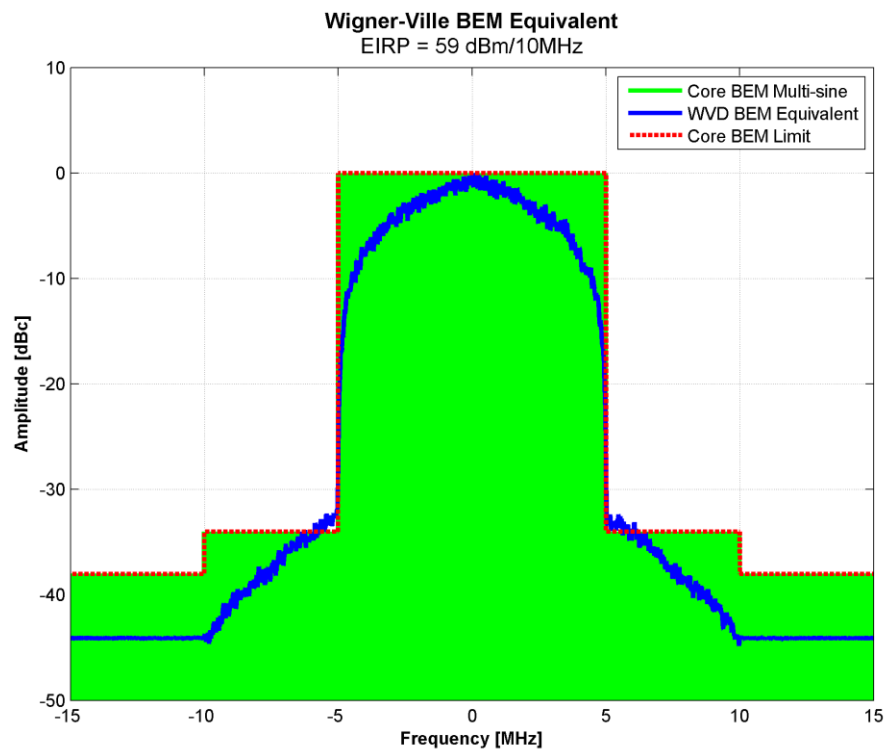


Fig. 6.20. Wigner-Ville Core BEM Equivalent (for an EIRP = 59 dBm/10MHz).

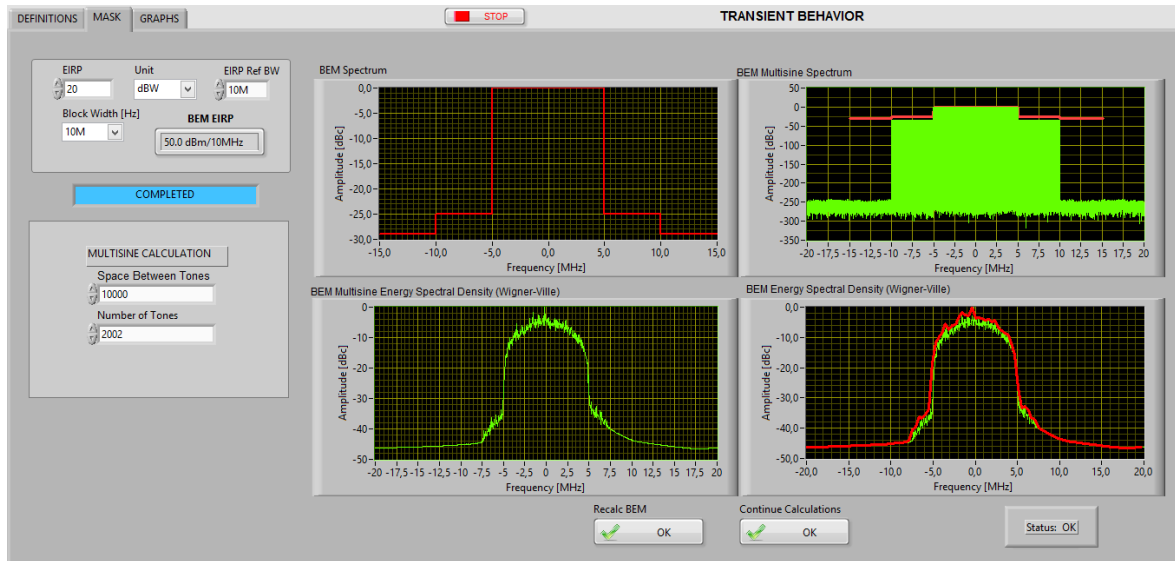


Fig. 6.21. Block Edge Mask Generation Page (Option: WVD Analysis).

The sequential steps of the BEM transformation procedure are illustrated in the preceding figure. From the initial BEM limits (“BEM spectrum” window), a multi-sine signal is generated, so that its spectrum perfectly fits within the mask defined by such limits (“BEM Multisine Spectrum” window). After that, the WVD spectral energy density corresponding to the initial BEM is displayed (“BEM Multisine Energy Spectral Density (Wigner-Ville)” window), and finally, a sort of “Max Hold” is applied to it, in order to define the WVD BEM equivalent limit (red line, in the “BEM Energy Spectral Density (Wigner-Ville)” window) to be used as a validation threshold.

### 6.3.3 Output Results

The output results page concentrates a wide variety of important indicators, which includes the *spectrogram*, *time waveform*, “instantaneous” *spectrum “slices”* produced by the multiple iterations of the selected time-frequency transform, *conventional spectrum* and relevant *statistical information* about the PAPR of the analyzed signal, namely, *histogram*, *probability distribution function (PDF)*, *cumulative distribution function (CDF)* and *complementary cumulative distribution function (CCDF)*.

In order to keep a certain consistency in viewing the output results, the user interface layout is common to all transforms.

The results depicted in Fig. 6.22 were produced by a STFT, applied to a LTE input signal, carrying heavy traffic.

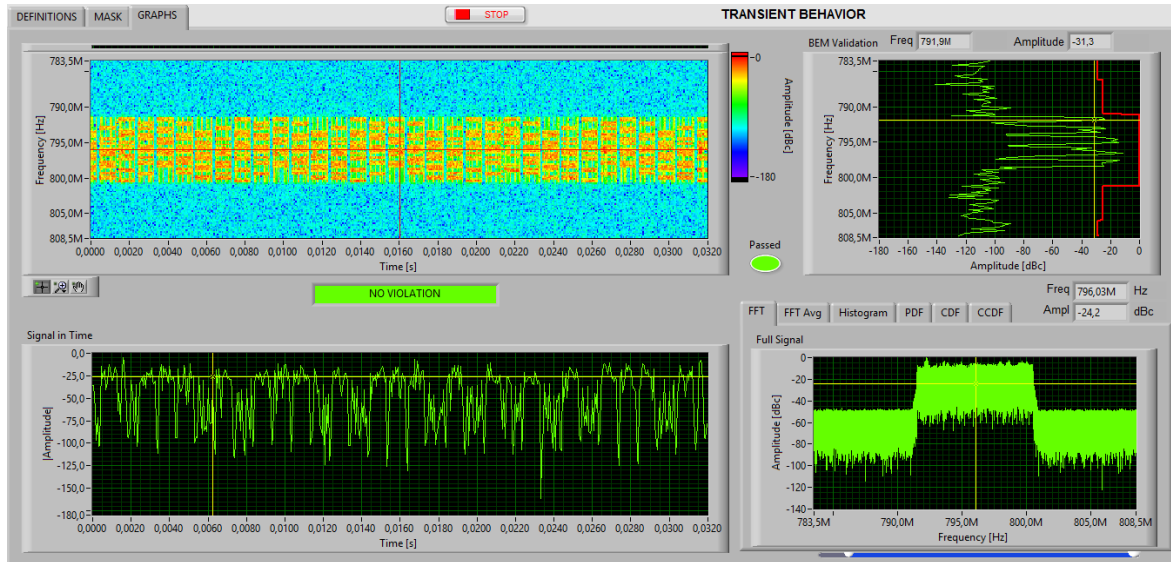


Fig. 6.22. Output Results Page (Option: STFT Analysis, with Hamming window).

From the spectrogram (Fig. 6.23) the traffic activity is visible, but no BEM violation is detected. The validation tool makes available zoom functions to inspect in detail specific sections of the spectrogram, and also a time-frequency (X-Y) cursor (marker), which is sympathetically linked to the time and frequency representations cursors (Fig. 6.24 and Fig. 6.25, respectively).

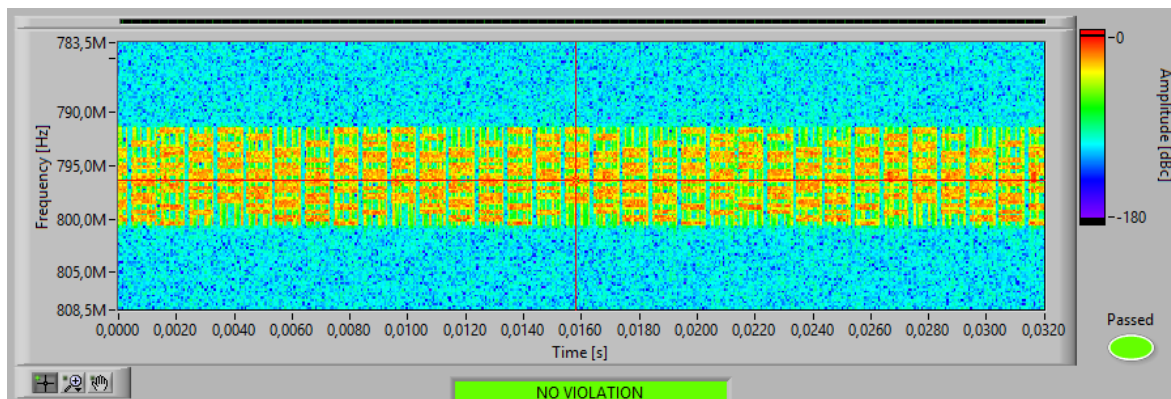


Fig. 6.23. Spectrogram of the LTE input signal (STFT, Hamming window).

The time waveform, represented in Fig. 6.24, is a result of the absolute value calculation of the IQ baseband samples of the input signal, collected by the RTSA.

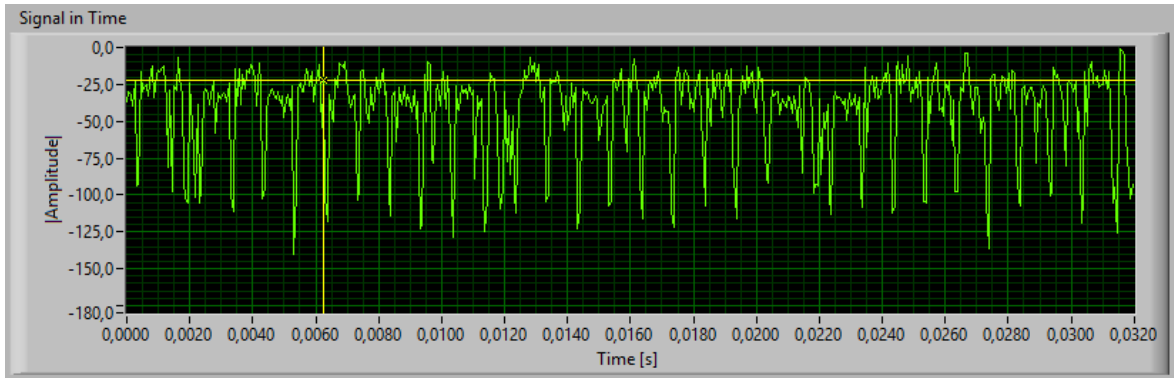


Fig. 6.24. Time Waveform of the LTE input signal (STFT, Hamming window).

The chart below (Fig. 6.25) displays successive spectrum “slices”, as the vertical cursor of the spectrogram (Fig. 6.23) is being moved. Since the BEM is shown together, the compliance may be scrutinized on step-by-step basis. If a violation is detected, it is graphically identified.

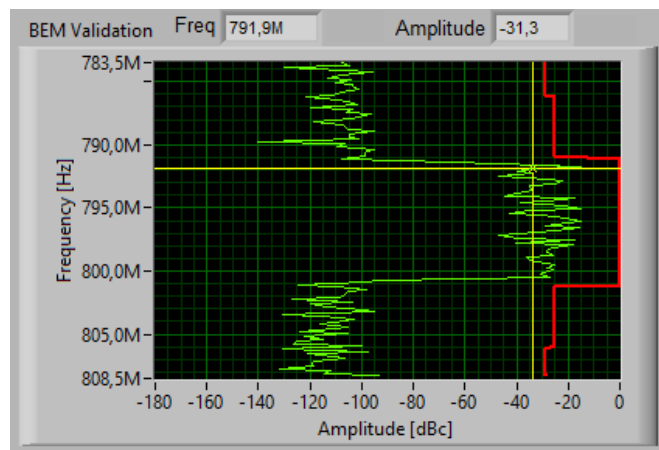


Fig. 6.25. BEM compliance Test with subsequent STFT Spectrum “Slices” (STFT, Hamming window).

The conventional spectrum (Fig. 6.26) is also provided, which is computed using the FFT algorithm, applied to the entire input signal. For all the charts contained within this window (including the remaining separators), an X-Y cursor is available, and the respective marker values, at a selected position, are shown on the upper right corner. In addition, a blue sliding

bar, at the bottom, allows the zooming of particular areas of interest, in the chart, to be visualized, according to the user's preferences.

Alternatively, the same spectrum can be displayed with a smoother trace (Fig. 6.27), which is obtained by applying a moving average to the previous representation, in order to better define the spectrum shape. This operation is quite similar to the video bandwidth (VBW) filtering, implemented by regular spectrum analyzers. The number of points, used to calculate such averages – i.e., the length of the sliding window of the moving average –, is defined by the user.

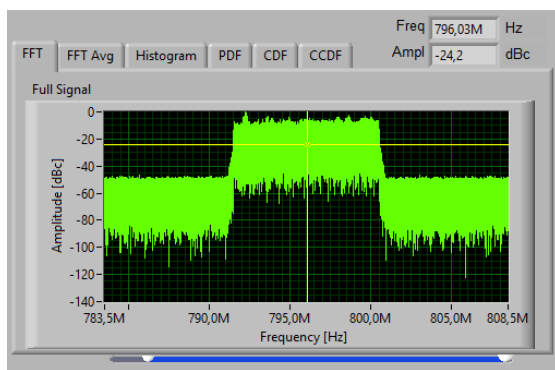


Fig. 6.26. Spectrum of the LTE input signal (FFT applied to all acquired samples).

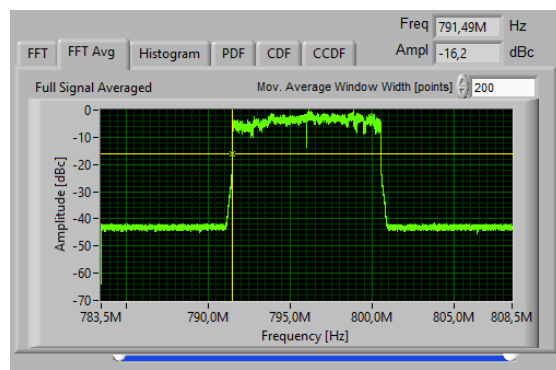


Fig. 6.27. Spectrum of the LTE input signal (Smoothed Trace with Moving Average).

Some statistical information about the signal's behavior, based on the PAPR figure of merit, are provided by the histogram (Fig. 6.28), PDF (Fig. 6.29), CDF (Fig. 6.30) and CCDF (Fig. 6.31) charts.

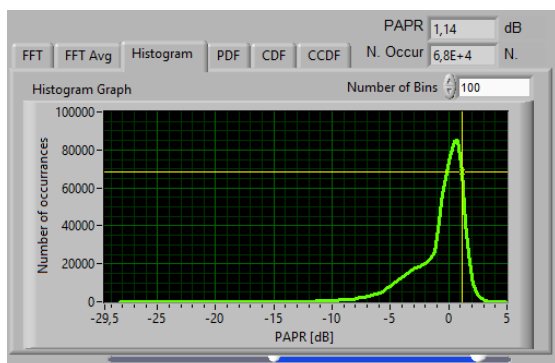


Fig. 6.28. Histogram of PAPR of the LTE input signal.

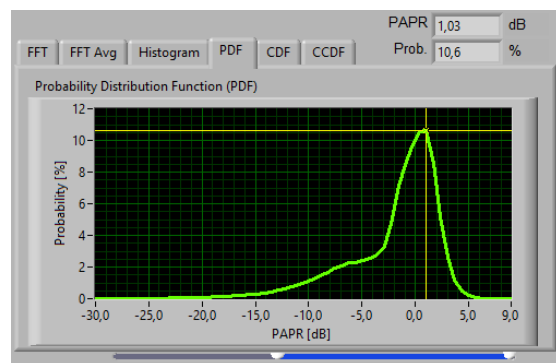


Fig. 6.29. Probability Distribution Function of PAPR of the LTE input signal.

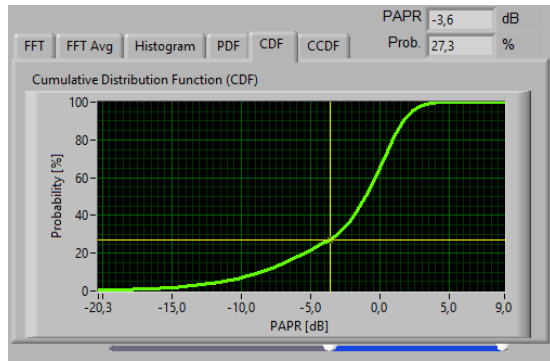


Fig. 6.30. Cumulative Distribution Function of PAPR of the LTE input signal.

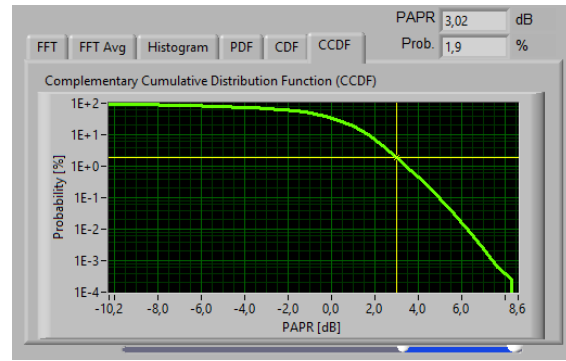


Fig. 6.31. Complementary Cumulative Distribution Function of PAPR of the LTE input signal.

The outputs of the Gabor Transform Analysis, applied to a LTE input signal with an idle traffic profile, are presented in Fig. 6.32. Once again, in this specific example, no BEM violations were detected.

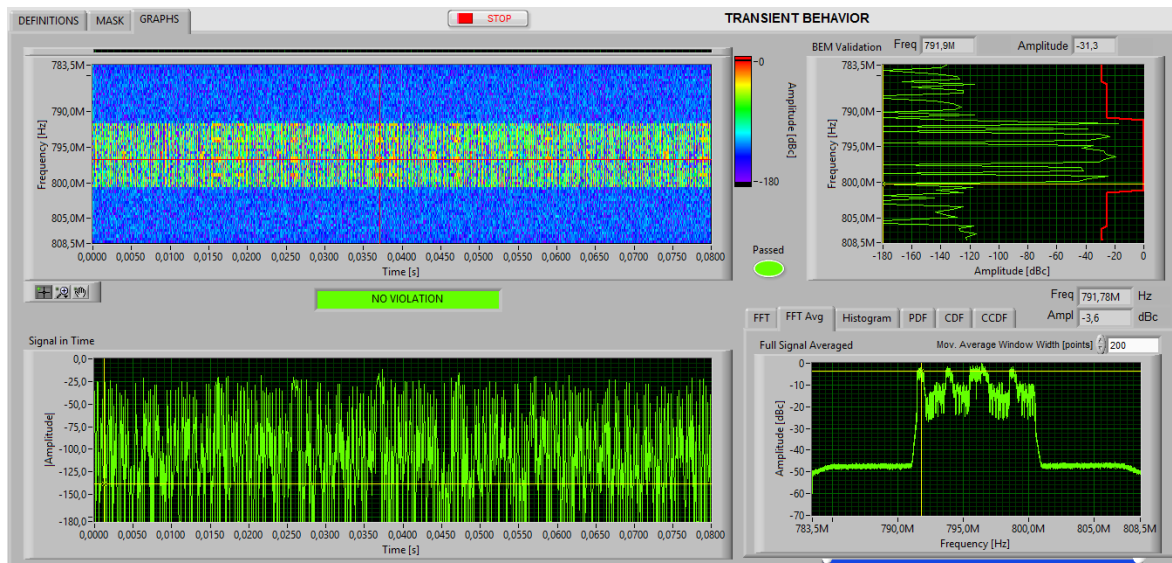


Fig. 6.32. Output Results Page (Option: Gabor Transform Analysis).

Finally, the results yielded by our exploratory approach – which introduces the WVD analysis to validate transient waveforms, taking a proposed BEM equivalent limit as a reference – are shown in Fig. 6.33. A LTE input signal, with a medium traffic profile, was used in this particular situation. Considering that such an approach is valid, **445** violations of the “*WVD BEM equivalent*” were detected.

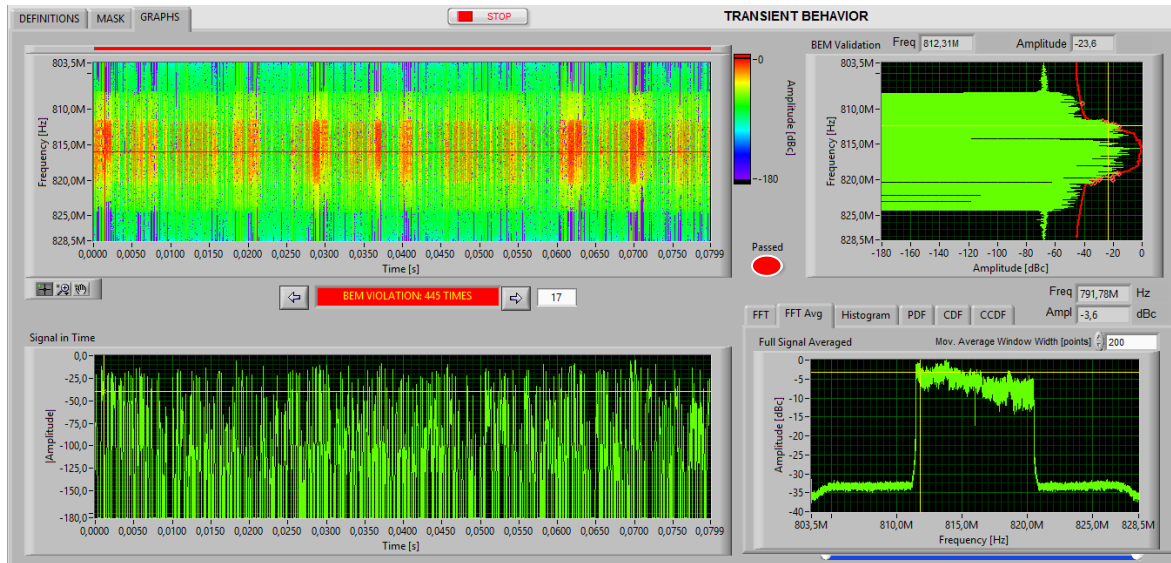


Fig. 6.33. Output Results Page (Option: Wigner-Ville Analysis).

In the next section, the waveform validation tool will be used to assess the performance achieved by the different solutions introduced thus far.

## 6.4 Sensitivity Analysis

The sensitivity analysis aims to identify optimal time-frequency techniques and parameters, taking into consideration the types of signals to be investigated and validated. Therefore, multiple combinations of possible settings will be tested, to find a benchmark or a metric on the performance of the adopted transforms, windowing functions, and remaining adjustable parameters.

Thus, a set of basic assumptions will be made, test signals will be characterized, and final results and conclusions will be drawn.

### 6.4.1 Assumptions

In order to obtain noteworthy performance variations, which could produce suggestive comparisons between distinct scenarios and options, more adverse conditions of analysis had to be created. Otherwise, no significant effects would be observable, since, under normal conditions, no substantial violations would be detected.



Consequently, a particularly demanding BEM was considered, to increase the amount of violation detections. For the above reasons, an **EIRP of 60 dBm/10 MHz** is assumed.

As a matter of fact, the “**number of BEM violations**” indicator will be used throughout this sensitivity analysis as a reference metric of performance.

However, the adopted BEM limits are more stringent than they would normally be, for the selected test signals. Therefore, it should be noted that **the number of BEM violations** – which will be presented in the outputs below –, **do not represent, in absolute terms, the reality.**

Since the basic assumptions are common and transversal to all performance tests, the comparative analysis is thus possible and valid. This permits to distinguish separate performances and identify the best options, considering all fixed conditions.

Notwithstanding, **the absolute number of BEM violations cannot be generalized to any other particular situation or considered as a real infraction.** Indeed, the output results only remain valid for the expounded purposes and under the assumptions made in the context of this study.

## 6.4.2 Test Signals

In the present sensitivity analysis, three LTE 800 MHz band downlink signals – with distinct traffic profiles: *idle*, *medium* and *heavy* – will be jointly investigated. Such signals were acquired with a RTSA (*Tektronix*, model *RSA6114A*), at a sample rate of 25 MHz, and all of them have the same length of 8 million samples, which corresponds to a duration of 320 ms.

In fact, LTE traffic activity has a direct correspondence with the amplitude of the OFDM subcarriers of the signal. This aspect is highlighted by Fig. 6.34, in which, the probability density functions of the normalized absolute value of the time waveform amplitude is depicted for the three signals (traffic profiles). Indeed, the heavy traffic signal exhibits higher amplitude values (close the maximum, i.e., around -10 dBc) with much higher probability than the remaining ones. Another interesting figure of merit that can be used to characterize the test signals is the PAPR, which is represented, in terms of CCDF, in Fig. 6.35.

The above test signals were carefully selected in order to study the impact of the LTE traffic on the BEM compliance.

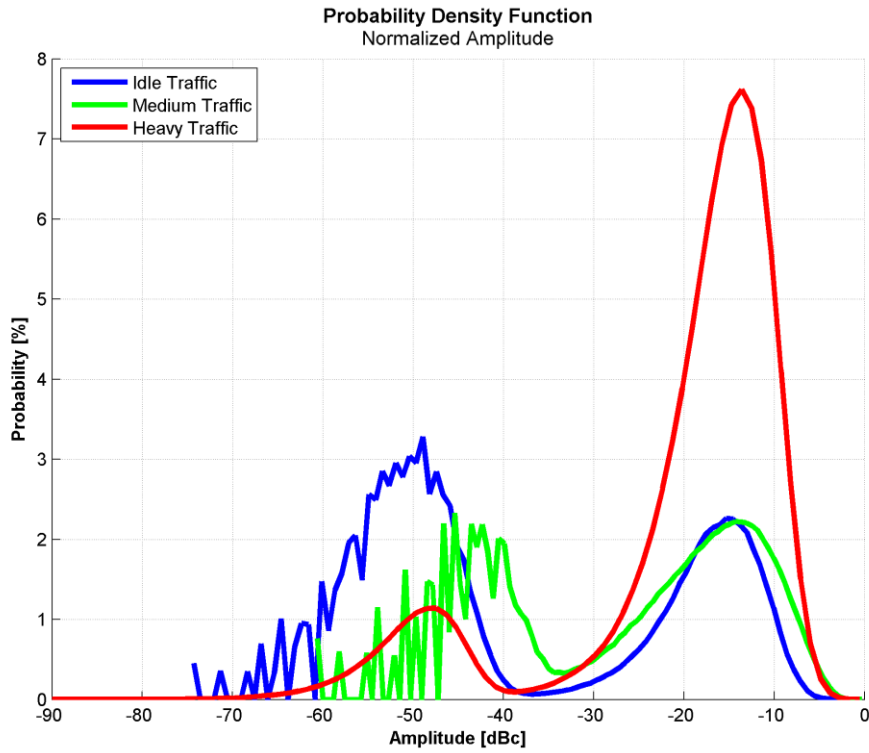


Fig. 6.34. PDF of Normalized Amplitude of the Test Signals.

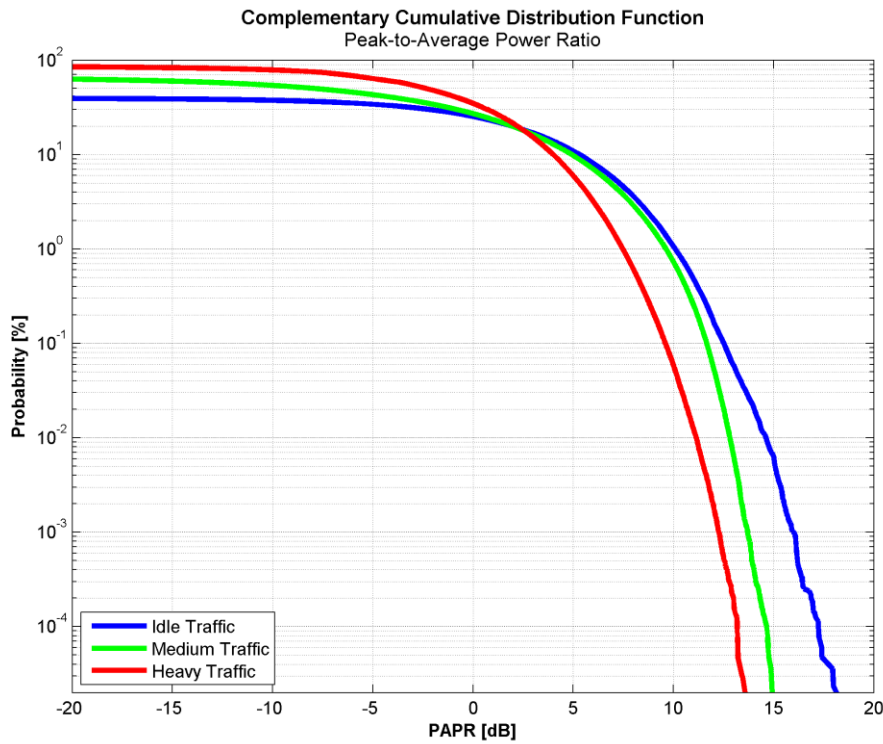


Fig. 6.35. CCDF of PAPR of the Test Signals.

### 6.4.3 Results

This study begins with a comparative analysis of the performance offered by each STFT window function, targeting the maximization of the number of BEM violation detections, taking into account, not only the impact of both *window length* and *frequency bins* parameters, but also de three aforementioned dissimilar LTE signals with particular traffic profiles.

Afterwards, optimal options, to deal with those signals, will be identified. This includes the type of transform and respective parameters to be adopted.

#### 6.4.3.1 Sensitivity to the STFT Window

This sensitivity analysis starts by considering the STFT, and 16 windowing functions: *Rectangle*, *Hanning*, *Hamming*, *Blackman-Harris*, *Blackman*, *Flat Top*, *Low Sidelobe*, *Blackman-Nutall*, *Bartlett (Triangle)*, *Bartlet-Hanning*, *Bohman*, *Parzen*, *Welch*, *Kaiser* and *Dolph-Chebyshev*.

In all cases, all the possible combinations of the elements of both sets of *frequency bins* and *window lengths* were tested.

**Frequency Bins:** {32, 64, 128, 256, 512, 1024, 2048} bins.

**Window Lengths:** {32, 64, 128, 256, 512, 1024, 2048} samples.

Therefore, an extensive collection of 49 graphics was then generated, which are available in **Appendix B**, sorted by frequency bins (window length is varying) and by window length (frequency bins are changing). The first group of charts makes easy the assessment of the impact of the window length, whereas the latter emphasizes the influence of the frequency bins.

However, to illustrate the main conclusions to be drawn from that comprehensive battery of tests, and for the sake of simplicity, only few representative graphs will be selected.

In general, and irrespective of the number of frequency bins and window length which are configured, **all windowing functions perform quite similar in terms of BEM violation detections**. Nevertheless, **Rectangle and Kaiser windows slightly outperform the other ones, and Flat Top and Low Sidelobe marginally underperform the remaining**, as can

be observed in Fig. 6.36. This a mutual tendency, which can also be generalized to the universe of tests that were conducted, in this context.

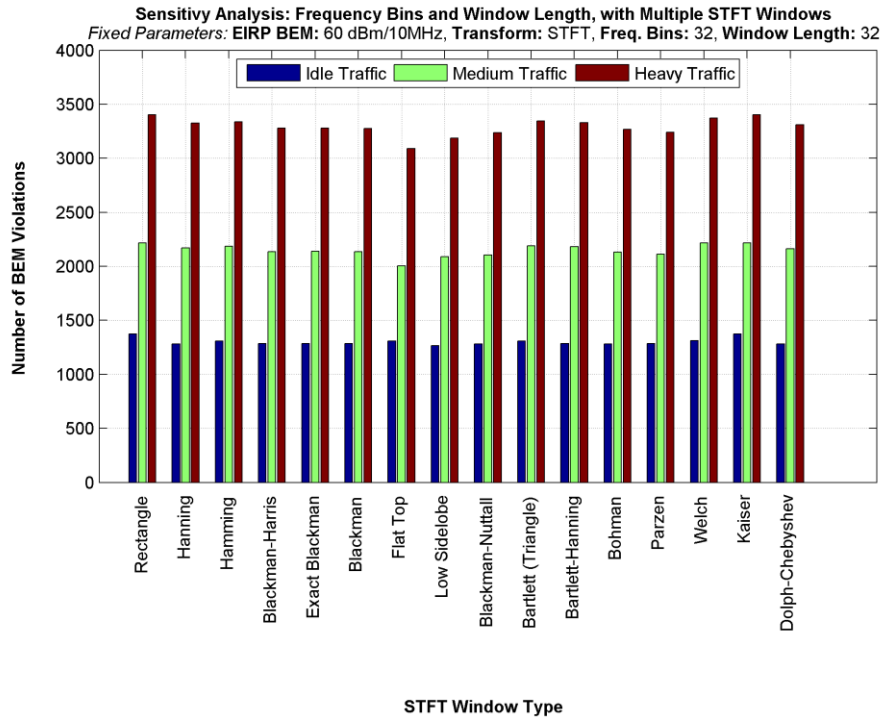


Fig. 6.36. Multiple STFT Windows, Frequency Bins: 32, Window Length: 32 samples.

#### 6.4.3.1.1 Impact of the Window Length

If the frequency bins parameter is kept fixed, regardless of the number of bins and the traffic profile signal that are considered, **the number of detections increases as the window becomes wider** (i.e., larger window lengths).

This common behavior, which is shown by all types of windows, is illustrated in the following charts (Fig. 6.37, Fig. 6.38, Fig. 6.39 and Fig. 6.40).

The number of violations caused by the idle traffic signal shows a regular performance for different window lengths, reaching about 1500 detections.

However, such a value is moderately increased, when the window has 2048 samples of length, i.e. the widest tested length in this scenario of analysis.

If the medium traffic signal is being analyzed, the amount of detections follows a similar trend, showing small increments as the window length is being increased, with a peak of detection for the widest length (2048 samples).

The heavy traffic signal leads to the largest number of BEM violations, which initially are situated a little below 3500 detections (for a window length of 32 samples), is moderately increased until the window length reaches 128 samples. Then, it remains almost stabilized around 3600 detections.

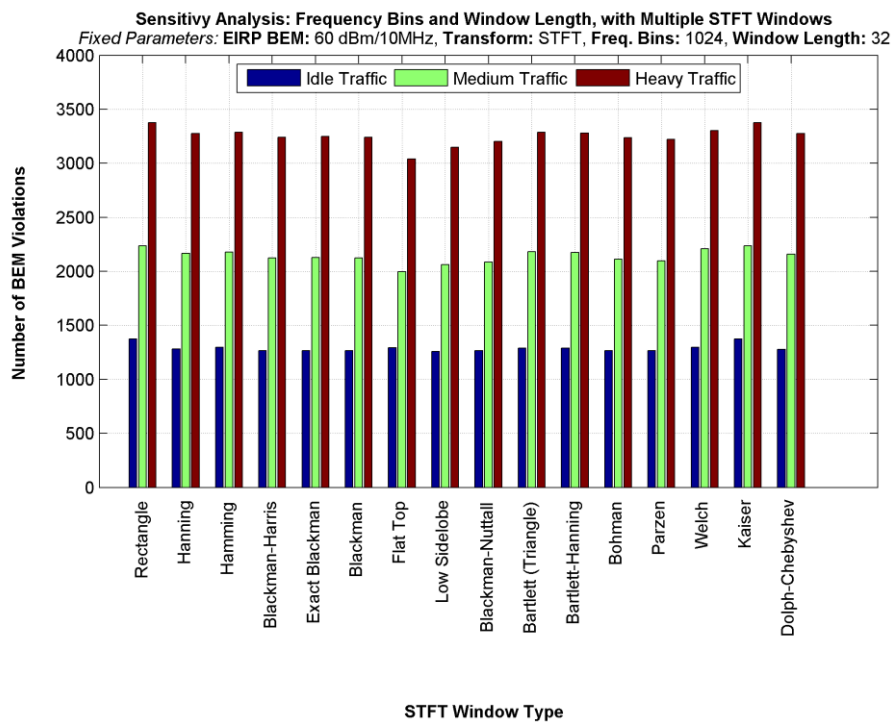


Fig. 6.37. Multiple STFT Windows, Frequency Bins: 1024, Window Length: 32 samples.

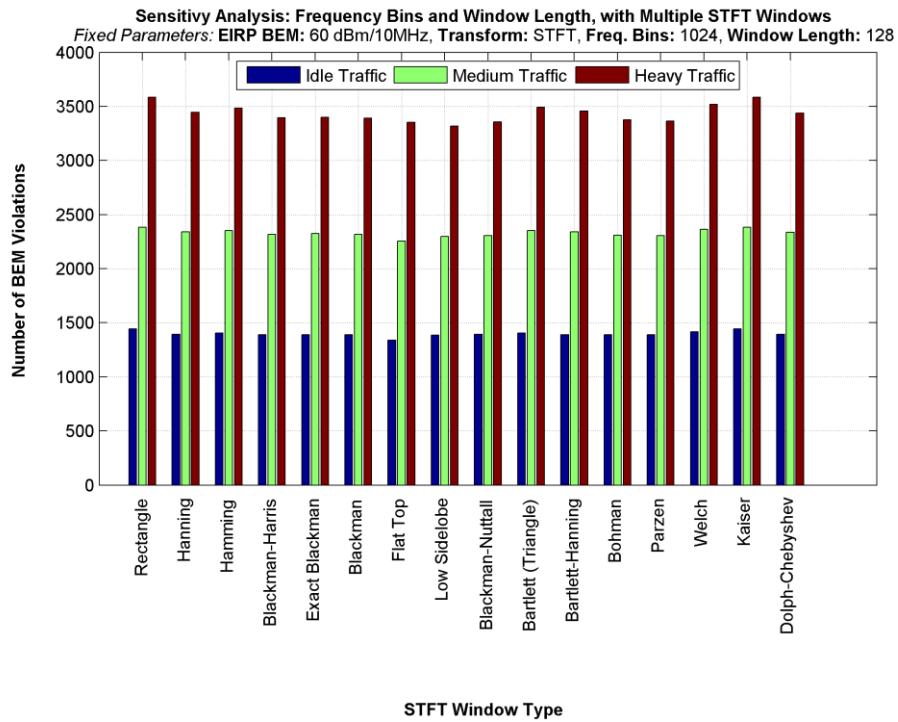


Fig. 6.38. Multiple STFT Windows, Frequency Bins: 1024, Window Length: 128 samples.

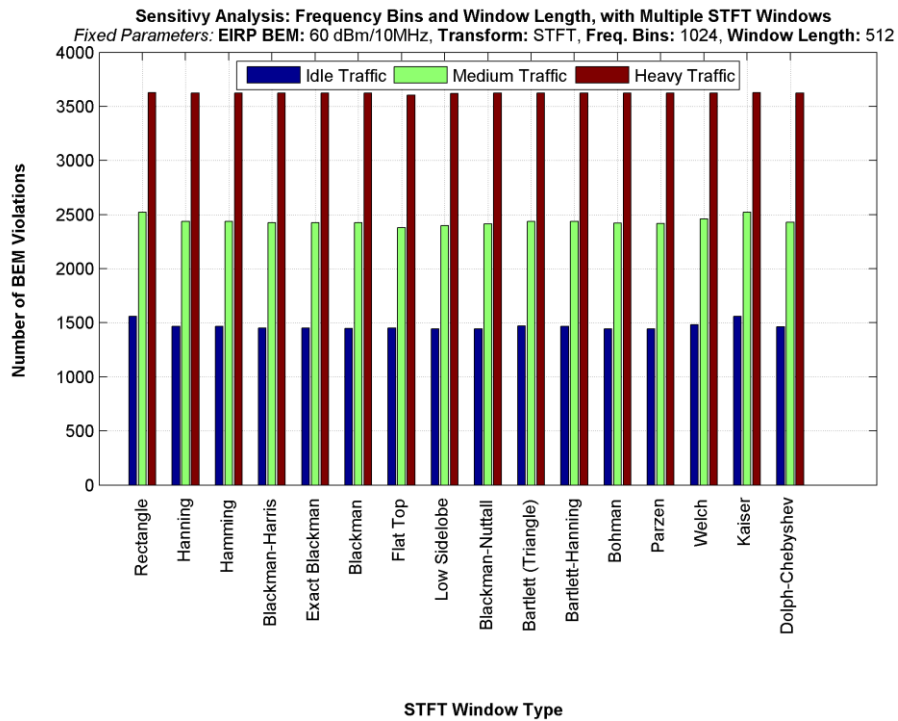


Fig. 6.39. Multiple STFT Windows, Frequency Bins: 1024, Window Length: 512 samples.

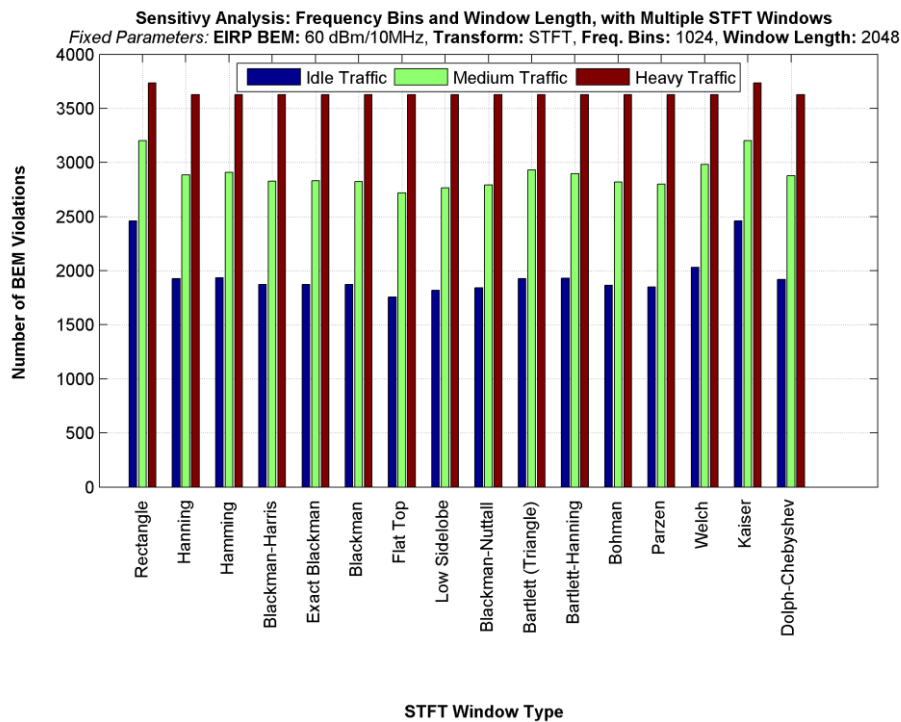


Fig. 6.40. Multiple STFT Windows, Frequency Bins: 1024, Window Length: 2048 samples.

#### 6.4.3.1.2 Impact of the Frequency Bins

**The impact of the frequency bins parameter is not as strong as the window length.** In fact, when the window length parameter remains fixed, independently of the traffic profile signal that is considered, the number of detections initially rises, at a moderate rate, as the number of bins increases, but after reaching a given threshold, the amount of detections stabilizes. For example, considering a fixed window length of 512 samples, the number of detections is being improved until 256 bins (see Fig. 6.41, Fig. 6.42 and Fig. 6.43). However, after that, **the detection pattern is quite similar for all types of signals**, as can be observed in Fig. 6.44 and Fig. 6.45.

As a matter of fact, the idle traffic signal practically leads to a constant number of detections, around 1500, for all window functions, and for all tested frequency bins. The medium traffic signal starts with, more or less, with 2200 detections (for 32 bins), for all types of windows, which are being slowly increased until 256 bins, and under such circumstances, about 2500 violations are identified. The heavy traffic signal approximately originates 3400 detections, for the smallest number of tested frequency bins, i.e. 32, and then, such detections are gradually rising until 256 bins, reaching a stabilized threshold around 3600.

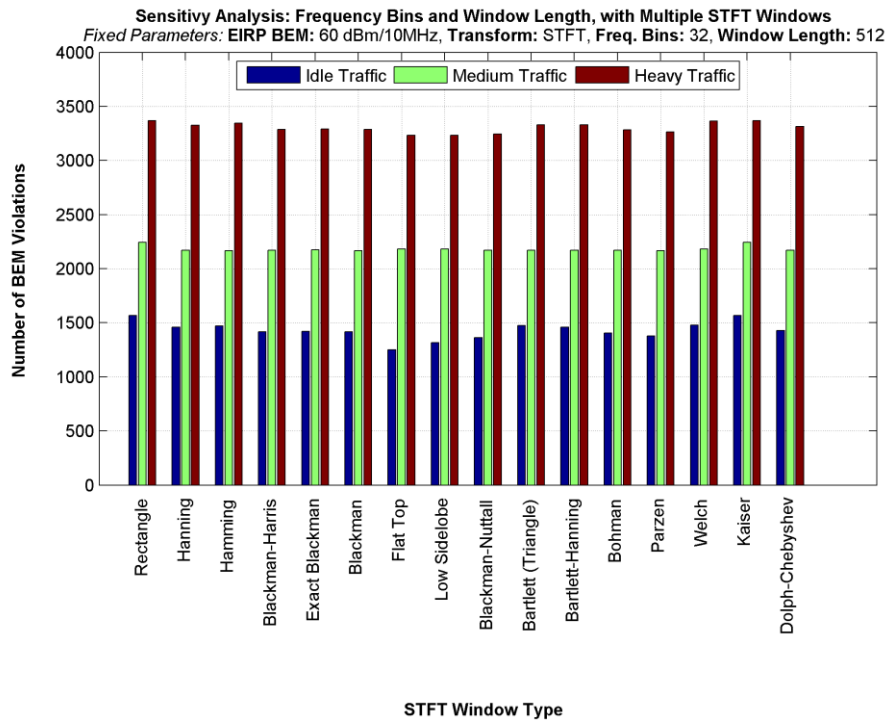


Fig. 6.41. Multiple STFT Windows, Window Length: 512 samples, Frequency Bins: 32.

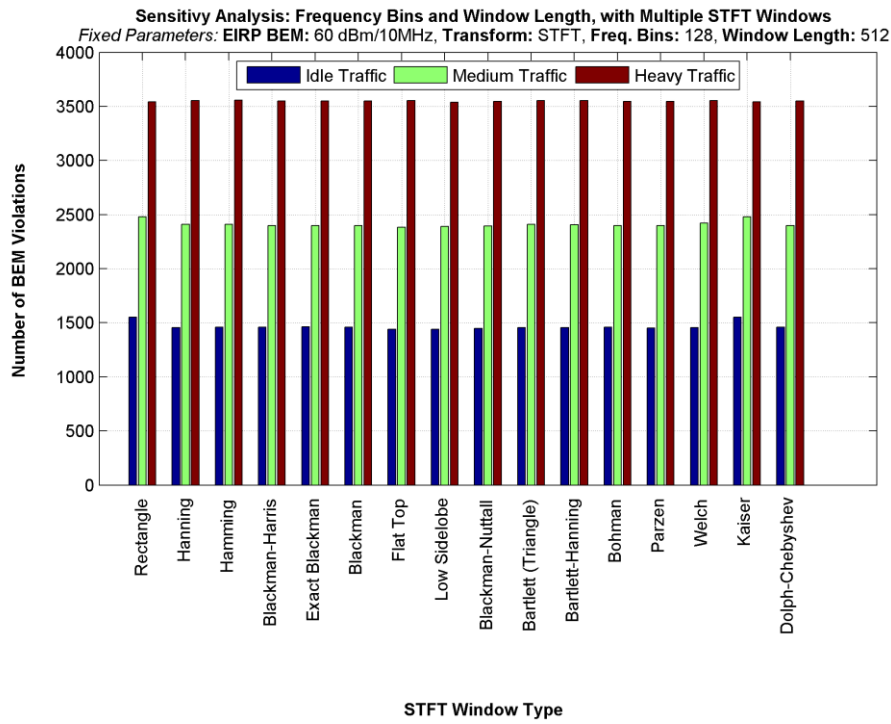


Fig. 6.42. Multiple STFT Windows, Window Length: 512 samples, Frequency Bins: 128.



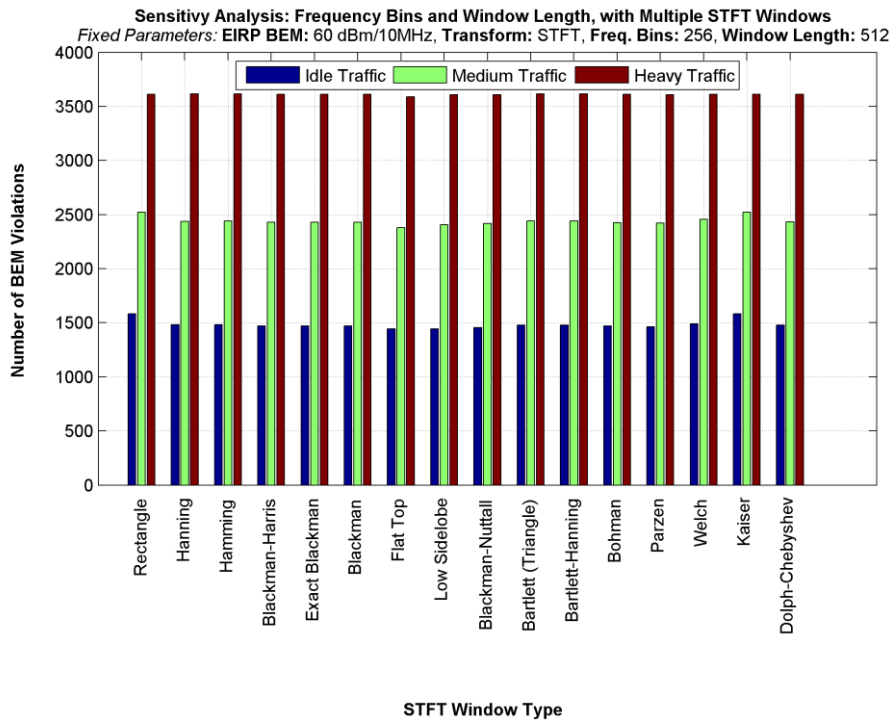


Fig. 6.43. Multiple STFT Windows, Window Length: 512 samples, Frequency Bins: 256.

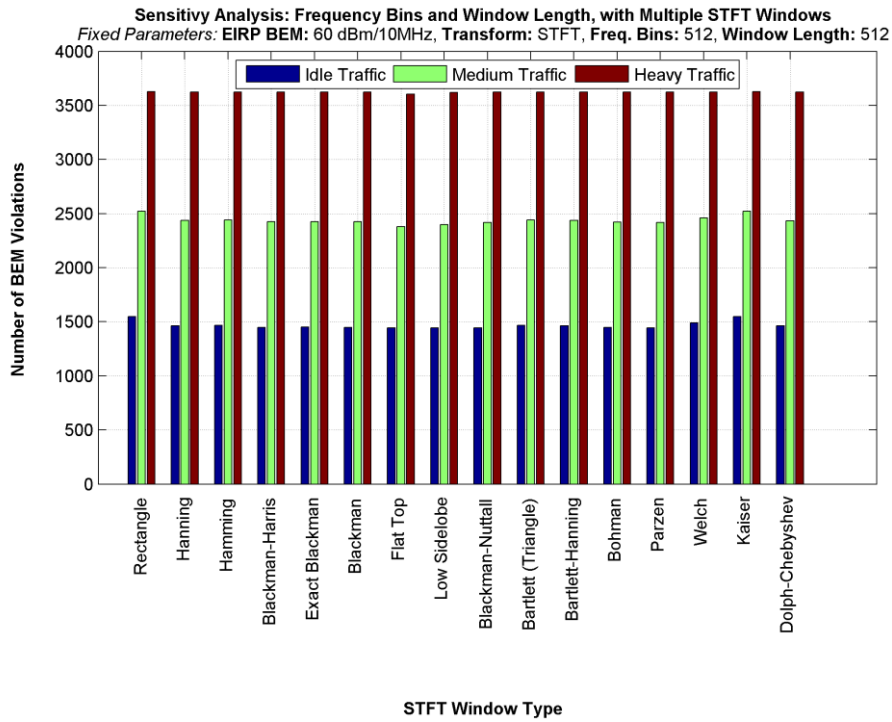


Fig. 6.44. Multiple STFT Windows, Window Length: 512 samples, Frequency Bins: 512.

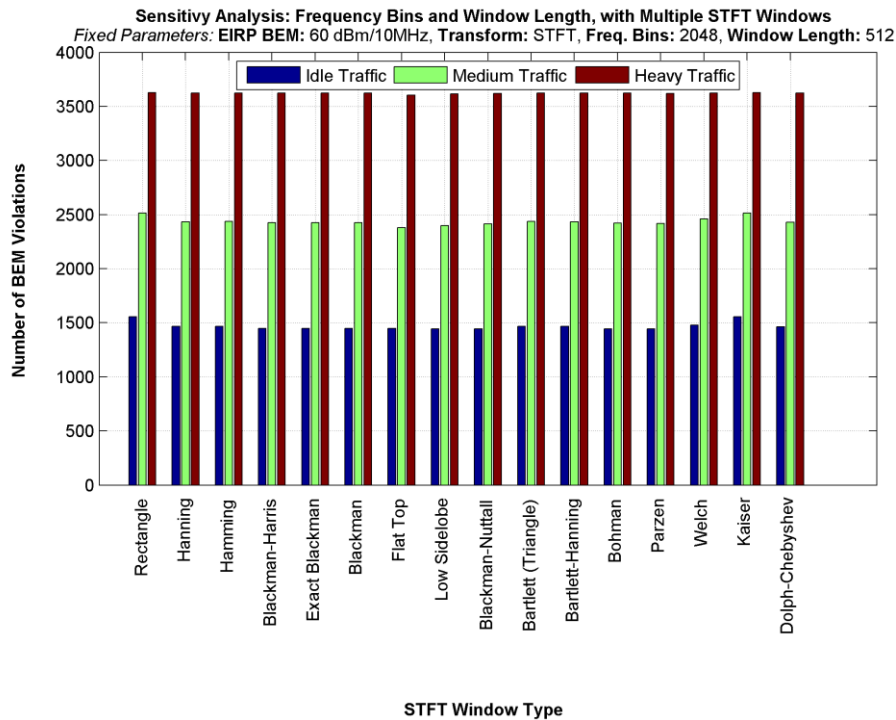


Fig. 6.45. Multiple STFT Windows, Window Length: 512 samples, Frequency Bins: 2048.

#### 6.4.3.2 Sensitivity to the Transform

Since all STFT windows generally show an identical performance, for the sake of simplicity, the sensitivity analysis to the type of transform will be carried out with four representative STFT windowing functions: *Rectangle* and *Kaiser* (which outperform) and *Flat Top* and *Low Sidelobe* (which underperform). In addition, Gabor Transform and Wigner-Ville Distribution will be jointly compared to the previous ones.

Thus, four scenarios of analysis will be studied (Table 6.1). Although WVD and STFT (including GT) have distinct natures, the same number of frequency bins will be used for them all, in order to compare the respective performances. Extreme tested values of both frequency bins and window lengths will be considered: 32 (the smallest) and 2048 (the largest).

Scenario	STFT and Gabor Transform			Figures	More Detections
	WVD	Frequency Bins	Window Length		
	Frequency Bins	Frequency Bins	Window Length		
	[bins]	[bins]	[samples]		
1	32	32	32	Fig. 6.46	STFT/Gabor
2	32	32	2048	Fig. 6.47	STFT (Rectangle)
3	2048	2048	32	Fig. 6.48	WVD
4	2048	2048	2048	Fig. 6.49	STFT (Rectangle and Kaiser)

Table 6.1. Sensitivity to the Transform – Scenarios of Analysis.

In all of the above scenarios, **the STFT and Gabor transform show the most regular performance**, and only in scenario 3, the WVD slightly outperforms the remaining.

A good trade-off solution seems to be provided by the **STFT with a rectangle window** function.

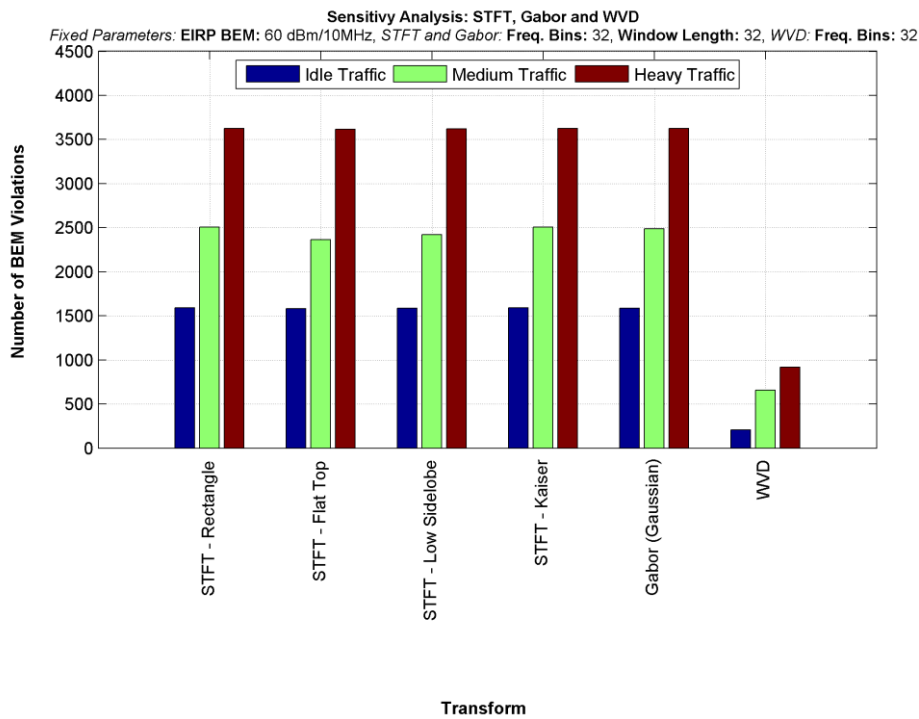


Fig. 6.46. Sensitivity Analysis: STFT, Gabor Transform and WVD (Scenario 1).

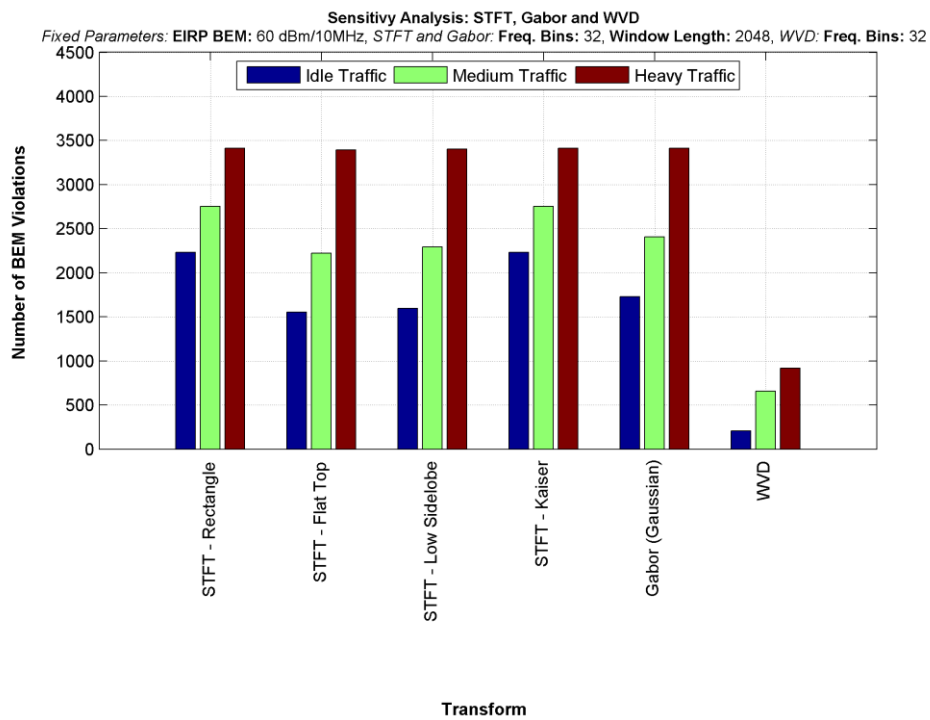


Fig. 6.47. Sensitivity Analysis: STFT, Gabor Transform and WVD (Scenario 2).

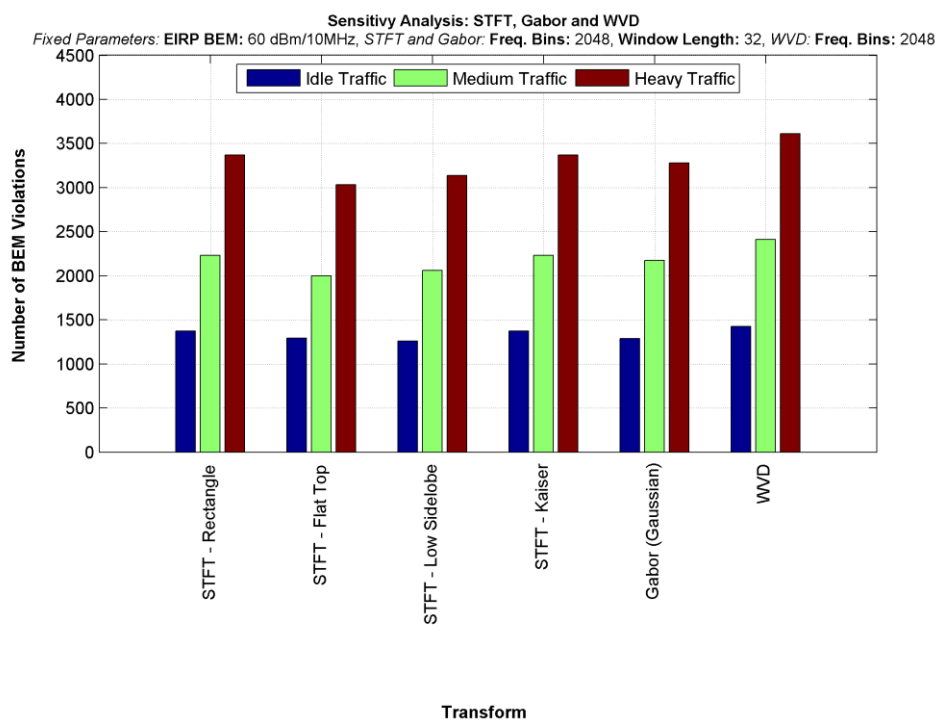


Fig. 6.48. Sensitivity Analysis: STFT, Gabor Transform and WVD (Scenario 3).

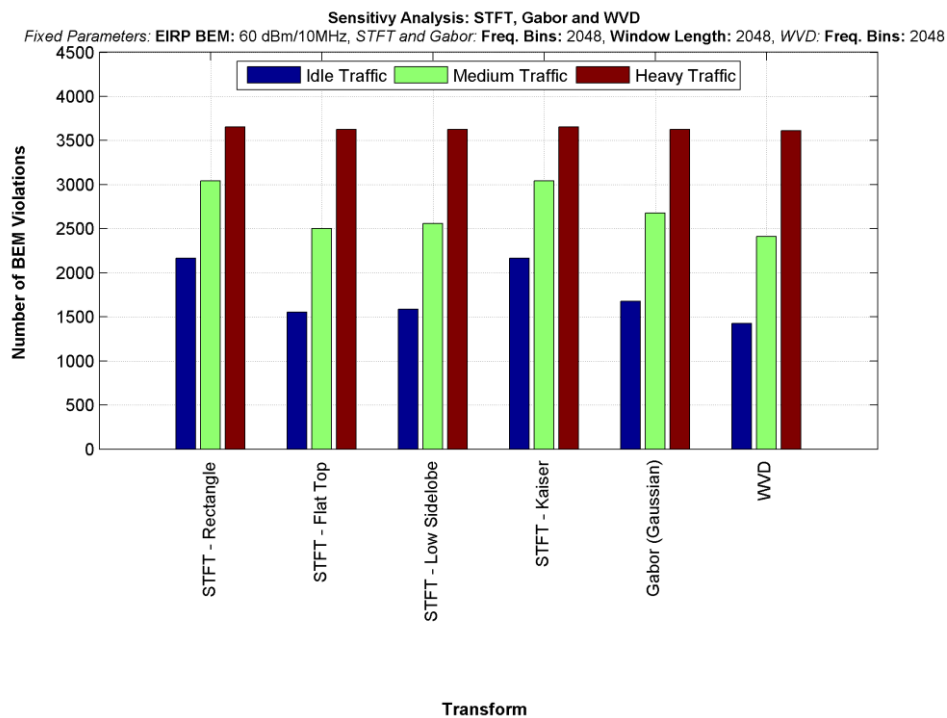


Fig. 6.49. Sensitivity Analysis: STFT, Gabor Transform and WVD (Scenario 4).

### 6.4.3.3 Sensitivity of the STFT and Gabor Transform to the Window Length

In order to make more visible the effect of the window length on the performance of a windowed transform, the Gabor Transform and the STFT, with a Rectangle (best performance) and a Flat Top (poorest performance) windows, were considered. The number of frequency bins was kept fixed in 2048 bins, since it has provided the best results.

Under the above conditions, the following distinct lengths were tested.

**Window Lengths:** {32, 64, 128, 256, 512, 1024, 2048, 4096} samples.

The results, illustrated by the charts below (Fig. 6.50, Fig. 6.51 and Fig. 6.52), show that, in all cases, i.e. **irrespective of the transform which is considered, a widest window always leads to the highest amount of BEM violation detections**. Again, this in line with previous conclusions, and **the STFT with the Rectangle window stands out among the other solutions**.

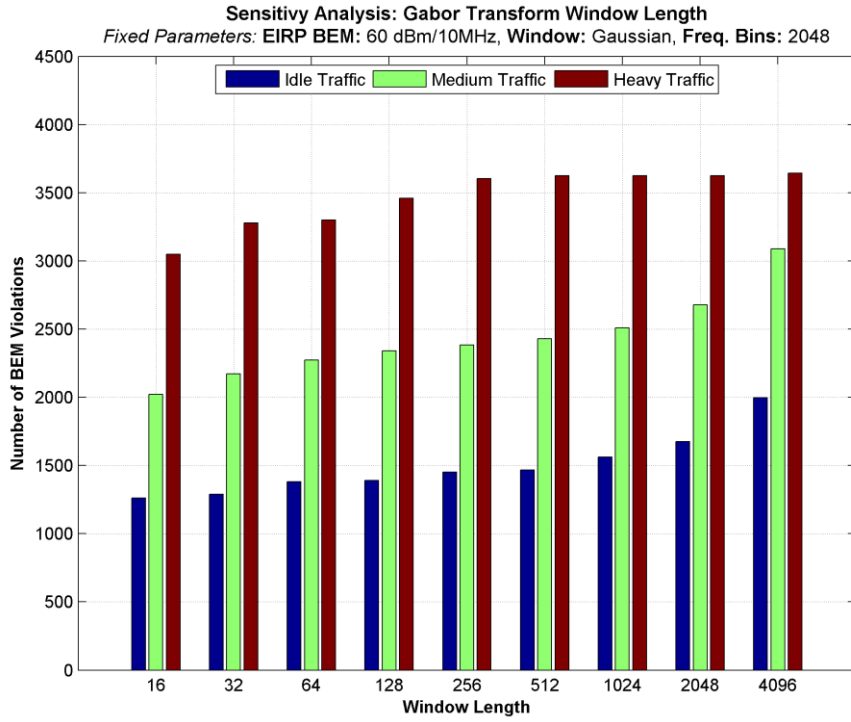


Fig. 6.50. Sensitivity Analysis of the Gabor Transform to the Window Length (Frequency Bins: 2048).

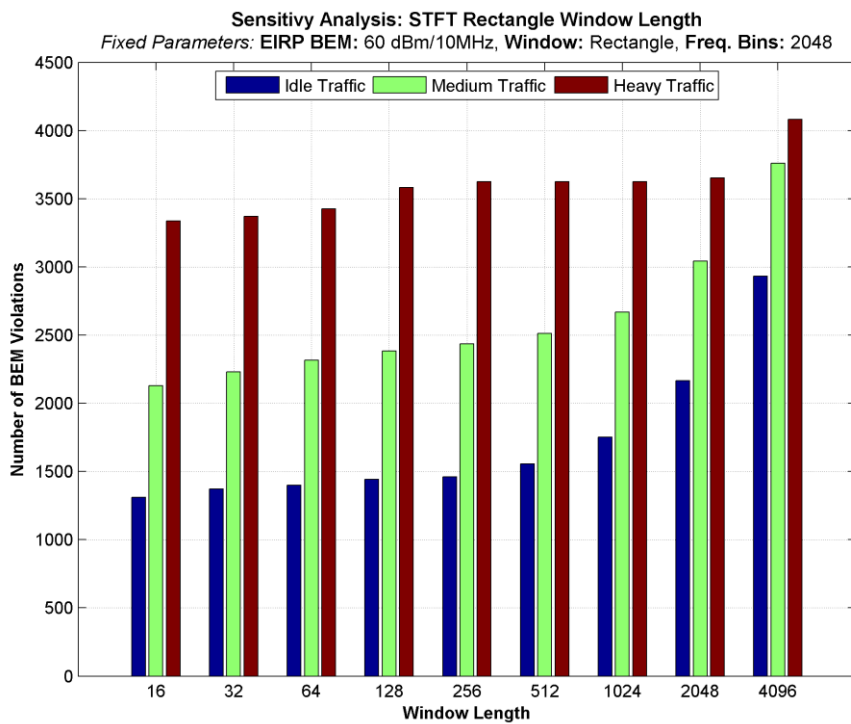


Fig. 6.51. Sensitivity Analysis of STFT (Rectangle window) to the Window Length (Frequency Bins: 2048).

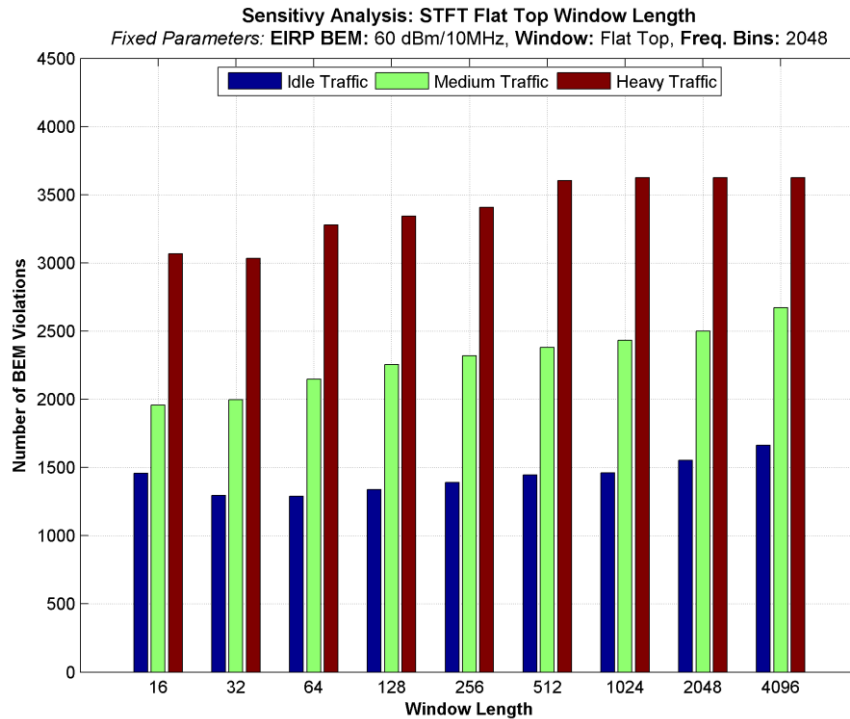


Fig. 6.52. Sensitivity Analysis of STFT (Flat Top window) to the Window Length (Frequency Bins: 2048).

#### 6.4.3.4 Sensitivity of the STFT and Gabor Transform to the Frequency Bins

The aim is now to emphasize the effect of the frequency bins. The same basic assumptions, as defined in the preceding comparative analysis (section 6.4.3.3), will be reused, but instead of fixing the number of frequency bins, in this case, it will be sequentially increased, in powers of 2, from 32 to 4096. The window length will assume a constant value of 2048 samples.

The outputs (Fig. 6.53, Fig. 6.54 and Fig. 6.55) suggest that there is an optimal number of frequency bins, which should not be greater than 2048 bins, because thenceforward (i.e. considering more bins), the number of detections show a visible reverse tendency.

In absolute terms, once again, **the STFT with the Rectangle window is superior to the other tested windows (Gaussian and Flat Top)**. Furthermore, **the number of detections is indeed maximized with 256 frequency bins**, considering a window length with 2048 samples, for all traffic profiles.

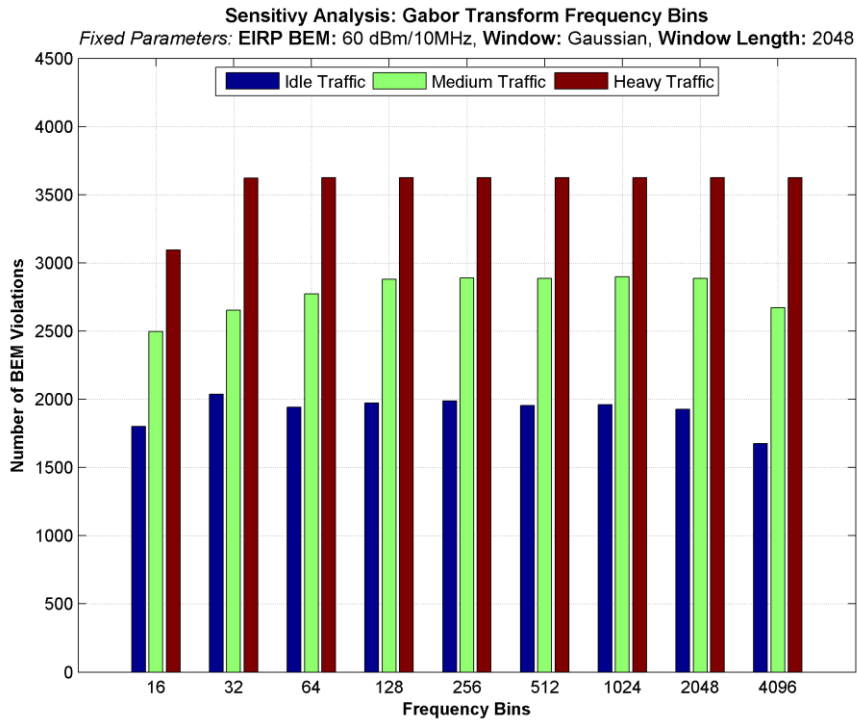


Fig. 6.53. Sensitivity Analysis of Gabor Transform to the Frequency Bins (Window Length: 2048 samples).

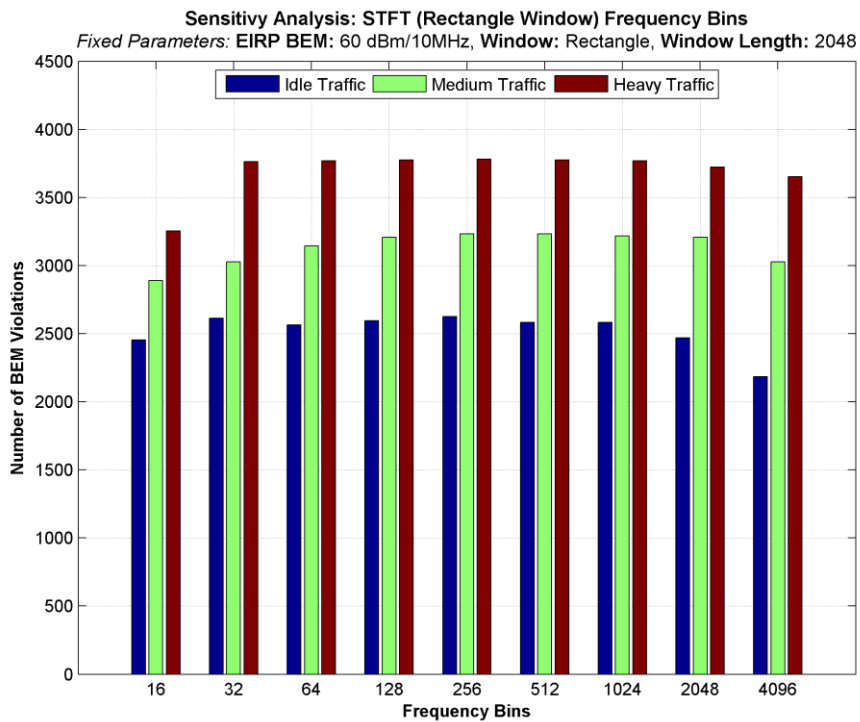


Fig. 6.54. Sensitivity Analysis of STFT (Rectangle window) to the Frequency Bins (Window Length: 2048 samples).



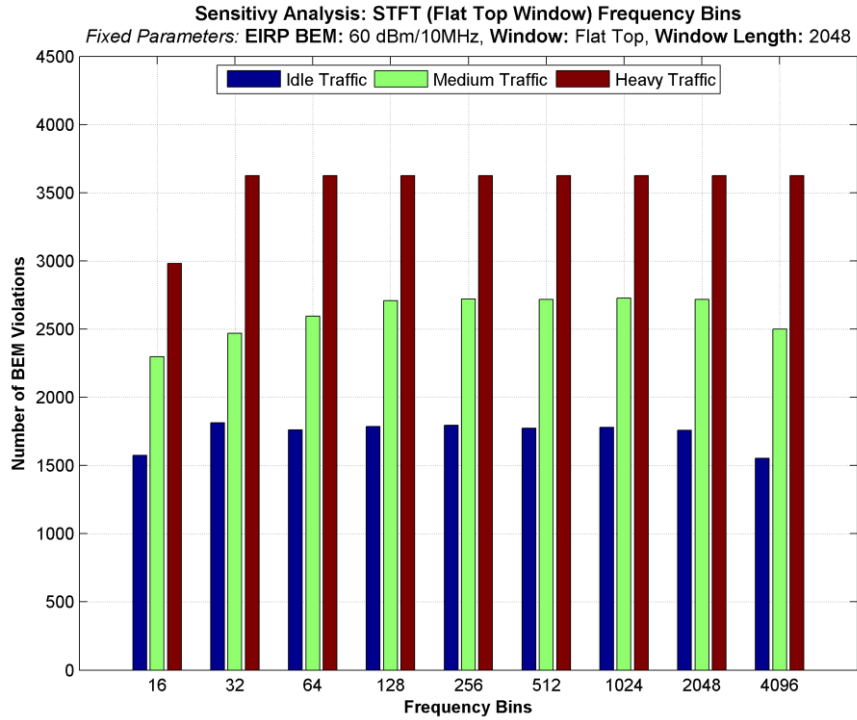


Fig. 6.55. Sensitivity Analysis of STFT (Flat Top window) to the Frequency Bins (Window Length: 2048 samples).

#### 6.4.3.5 Sensitivity of the WVD to the Frequency Bins

Since the WVD is independent of a windowing function, there is only one parameter to vary: the number of frequency bins. Hence, this test scenario intends to evaluate the sensitivity of the WVD to it, by considering the following set of values.

**Frequency Bins:** {32, 64, 128, 256, 512, 1024, 2048, 4096} bins.

From the results of this sensitivity analysis (Fig. 6.56), the general trend is that **the number of violation detections increases as the number of frequency bins is higher.**

However, the number of violations stabilizes (saturates), at around 3600, for the heavy traffic signal, when more than 256 bins are considered. The detections rise, for the medium traffic signal, as the number of bins is increased, and shows a significant peak of detections for 4096 bins. The idle traffic signal shows a significant increment of the detections from 16 to 128 bins, but after that, i.e. for more than 128 bins, it remains stable around 1400 detections.

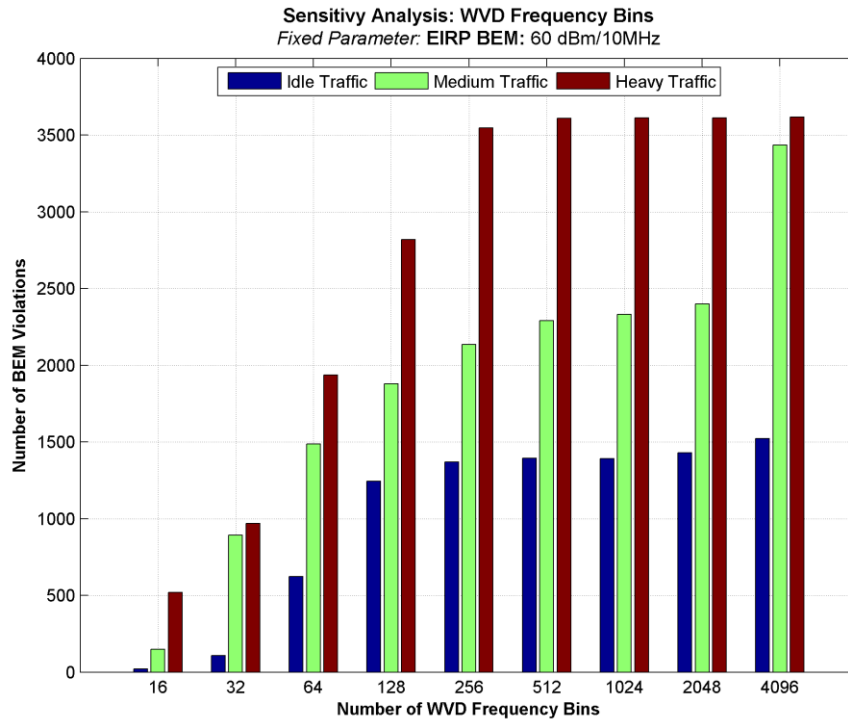


Fig. 6.56. Sensitivity Analysis of WVD to the Frequency Bins.

#### 6.4.4 Summary

The foregoing sensitivity analysis has shown that, for the LTE signals considered, a noticeable trend is common to all scenarios of analysis: **the heavy traffic signal always originates the largest amount of BEM violations** and, in contrast, **the idle traffic signal is the one that leads to fewer detections**.

At a glance, **all windowing functions perform quite similar**, in terms of BEM violation detections. Notwithstanding, **Rectangle** and **Kaiser** slightly **outperform the other ones**, and **Flat Top** and **Low Sidelobe** marginally **underperform the remaining**.

**The number of BEM violation detections always increases as the window length is becoming higher**. This seems to be a consequence of the Uncertainty Theorem. Since the BEM compliance is verified in the frequency domain, wider windows provide spectra with better resolutions, which are more likely detected.

On the other hand, the impact of the frequency bins parameter is not as strong as the window length. However, the tests, which were carried out, suggest that, in general, **the**

**maximum number of detections** is achieved when the **frequency bins** parameter is set **between 512 and 2048 bins**.

**The number of violations detected by the VWD grows as the number of frequency bins is becoming higher.**

Nevertheless, **the STFT with the Rectangle window stands out among all the other options**, including the WVD, **both in relative and in absolute terms**.

As a matter of fact, **the STFT using the Rectangle window** is also the transform which shows **the most regular behavior and performance**.

Besides the WVD is not the transform that offers the best performance, it still has the problem of defining a suitable “*WVD BEM equivalent*”. In fact, it is not clear that the followed methodology, which makes use of a multi-sine signal with random phases, is applicable or valid.

In view of the reported results, and taking into account the types of signals considered in the present study, the **STFT with a Rectangle<sup>93</sup> window** is the solution of choice. Accordingly, a **window length** of **2048** or **4096** samples, and a number of **frequency bins** between **512** and **2048**, should be used, in order to **maximize** the number of **BEM violation detections**.

---

<sup>93</sup> This result is interestingly consistent with the information provided in Table 5.3, which refers that the **Rectangle window** is suitable for “**spectral analysis (frequency response measurements)**”. In fact, this is the case, since the BEM compliance test is based on the frequency response of the analyzed signal, provided by the STFT.



# 7 Conclusions

This Thesis has expounded current, concrete and relevant issues, within the domains of spectrum engineering and spectrum management, which are a consequence of the European regulatory framework for emergent radio systems. In this context, future trends, innovative models, and new key-concepts, such as “neutrality” (technologies and services) and “flexibility”, and also emerging models of shared use of spectrum, including the “collective use of spectrum” and “licensed shared access”, were introduced. In addition, dynamic models of spectrum allocation, based on the concepts of “white-space”, “software defined radio” and “cognitive radio” were concisely explored.

In particular, the definition of technical conditions to be met by radio systems, which will operate in specific bands, selected to introduce such novel concepts of **flexibility** and **technological neutrality**, is still a challenge of paramount relevance.

In fact, the importance of defining robust technical parameters to ensure the coexistence between distinct radio systems was highlighted by two real case-studies, which demonstrated that, despite technical requirements are met, it is not taken for granted that interference does not arise.

The first situation reported the interference caused by a LTE base station emission that was inhibiting the normal operation of a DVB-T receiver. The origin of such an interference problem was carefully investigated and ascertained, using factual measurement data, collected in the field. Indeed, an undesired nonlinear impairment has arisen, as a consequence of “susceptibilities” on the DVB-T receiver. Particularly, lack of the most basic mechanisms of protection against interference, such as a suitable pre-selection filtering in the RF front-end input to reject these unwanted emissions from other co-located radio systems.

As one of the major contributions of this Thesis, an innovative RF band-stop filter device aimed at enabling the DVB-T reception in the presence of a LTE interferer has been devised. A proof-of-concept micro-strip prototype was tested and measured, being competitive with other LTE-mitigation filter solutions available in the market. Its practical effectiveness was successfully verified in a real case study in a small town of the region of Alentejo, Portugal.

The second case-study reported a peculiar effect detected by spectrum management teams in a real situation of interference. Specifically, a digital modulated radio signal was being harmed by a spectrally adjacent narrowband spurious emission generated by a television reception amplifier, which was oscillating in frequency due to malfunctioning. Under such non-expected operation conditions, a “doughnut” shape was observed on each symbol of the constellation diagram of the received digital signal. The problem was thoroughly analyzed from the analytical perspective (mathematical formulation), and by simulation and through laboratorial tests.

The previous situations have shown that, in practice, it is vital to come up with resilient ways of controlling interference, in order to provide the necessary co-existence between radio systems.

The BEM is the generic model, which was adopted to impose technical conditions of operation to neutral systems. However, it is not universally effective in all situations, and thus, it may not prevent all types of interference.

Another pertinent and practical issue is to define an appropriate methodology to be used to measure a transient or time-varying signal, in order to check the compliance with the respective BEM. As a matter of fact, some basic drawbacks were identified in the ECC/CEPT recommendation, which prescribes the BEM validation procedure, namely:

- The core element of the measurement setup is the conventional/traditional **spectrum analyzer**. This metrological instrument has been used for years for spectrum analysis with reliable and fair results. However, they are only taken for

granted if signals, under investigation, are **time invariant**, i.e., if steady-state regimes are actually reached. **That is not the case of LTE**. Thus, *the traditional spectrum analyzer is no longer suitable for the required purposes*.

- Notwithstanding, for this purpose, the spectrum analyzer is not truly used as such. In fact, the **zero span** mode is configured, which provides time-domain measurement results, making a spectrum analyzer somehow “equivalent” to a frequency selective (or tuned) “oscilloscope”.
- This greatly reduces the bandwidth of analysis. In the present case, “slender” spectrum slices of 50 kHz are sequentially analyzed, one at a time, which makes the measurement process indeed intricate, “tedious” and **very time-consuming**.
- The **coincidence in time** of different partial spectrum slices (of 50 kHz), subsequently acquired, is not assured, at all, nor provided. Therefore, changeable and dynamic behaviors of LTE signals **may not be captured**, and they will be easily **ignored** or **neglected**. Particularly if, for instance, a specific group of OFDM subcarriers show a distinct behavior, within and outside the time windows, in which they were analyzed. As a consequence, the actual impact of such behavior is not properly analyzed.

Then, some illustrative examples have presented recurrent drawbacks of the traditional Fourier methods, when used to analyze radio signals, in the frequency domain. **Indeed, it is fundamental to consider both and jointly the time-frequency domains, whenever transient or non-steady-state signals are present.**

Therefore, the most remarkable time-frequency mixed domain signal processing transforms (windowed: *Gabor Transform*, *Short-Time Fourier Transform*, quadratic: *Spectrogram* and *Wigner-Ville Distribution*) were introduced, to overcome major flaws of the conventional approaches.

An important trade-off between both time and frequency resolutions should be taken into account for the windowed transforms. The so-called **Uncertainty Principle**. As a consequence, narrower windows have good time resolution, but poorer frequency resolution. On the other hand, wider windows provide good frequency resolution, but the time resolution is naturally degraded.

The **Gabor Transform**, which corresponds to the STFT with a Gaussian window, is the one that offers the best joint time-frequency resolution, and thus, it is considered the **optimal STFT**.

The **windowed transforms** are, in essence, **dependent on a windowing function**. Then, the choice of the most appropriate window is crucial to obtain satisfactory results, taking into consideration the properties of the signal under investigation. Hence, the behavior and **performance** of the transform can be undesirably, or inadvertently, **influenced by the adopted window**. The spectral effects due to the intrinsic properties of the analyzed signal are indiscriminately merged with those of the window. This is a major impairment, since it may be very difficult, or even impossible, to distinguish the spectral effects of the signal from those ones introduced by the window.

Notwithstanding, the STFT and spectrogram have overcome and mitigated important drawbacks of the classic Fourier transform, but they are not flawless.

Alternatively, the Wigner-Ville Distribution overcomes the dependence on the window function, and only depends on the properties of the analyzed signal. This eliminates the window effect and a possible erroneous window selection, both with impact on the performance of the transform.

However, the WVD is also not perfect. Indeed, the superposition principle fails for this transform, since the linearity conditions are not met. This is, actually, its major flaw. As a consequence, undesired “false positive” components may arise – the so-called **cross-terms** or interference terms – which are indistinctly displayed, jointly with the “genuine” coefficients of the transform. The cross-terms are interpreted as energy, in the time-frequency mixed domain that, in fact, do not truly exist in the original signal. In that sense, they represent an interference.

After presenting some of the most noteworthy time-frequency transforms, a more efficient and expeditious alternative methodology, to be used on the validation of the central segment of a BEM, was then proposed.

This approach permits **to capture well the dynamic/transient behavior of a LTE signal**, preserving the genuine integrity of such a type of signal, even if just for a limited or partial section of a BEM. But, and above all, it ensures the necessary **concurrency** of the measurement procedure.



A general setup, based on a **Real Time Spectrum Analyzer**, was proposed, for acquiring the signal, to be validated. A **software tool**, for data processing and validation, was also prototyped as a proof of concept, developed and implemented.

A comparative analysis, using some reference LTE signals, was conducted, in order to figure out how such a proposed validation is sensitive to different time-frequency techniques, parameter configuration, and types of signals.

**Under the assumptions made**, the sensitivity analysis has shown that a noticeable trend is common to all scenarios of analysis: **the heavy traffic signal always originates the largest amount of BEM violations** and, in contrast, **the idle traffic signal is the one that leads to fewer detections**.

At a glance, **all windowing functions perform quite similar**, in terms of BEM violation detections. Notwithstanding, **Rectangle** and **Kaiser** slightly **outperform the other ones**, and **Flat Top** and **Low Sidelobe** marginally **underperform the remaining**.

**The number of BEM violation detections always increases as the window length is becoming higher**. This seems to be a consequence of the Uncertainty Theorem. Since the BEM compliance is verified in the frequency domain, wider windows provide spectra with better resolutions, which are more likely detected.

On the other hand, the impact of the frequency bins parameter is not as strong as the window length. However, the tests, which were carried out, suggest that, in general, **the maximum number of detections** is achieved when the **frequency bins** parameter is set **between 512 and 2048 bins**.

**The number of violations detected by the WVD grows as the number of frequency bins is becoming higher**.

Nevertheless, **the STFT with the Rectangle window stands out among all the other options**, including the WVD, **both in relative and in absolute terms**.

As a matter of fact, **the STFT using the Rectangle window** is also the transform which shows **the most regular behavior and performance**.

Besides the WVD is not the transform that offers the best performance, it still has the **problem of defining a suitable “WVD BEM equivalent”**. Actually, it is not clear that the followed generation method, which makes use of a multi-sine signal with random phases, is applicable or valid.

In view of the reported results, and taking into account the types of signals considered in the present study, the **STFT with a Rectangle window** is the solution of choice. Accordingly, a **window length** of **2048** or **4096**, and a number of **frequency bins** between **512** and **2048**, should be used, in order to **maximize** the number of **BEM violation detections**.

In light of all the above facts, and considering relevant concerns on the use of the BEM model, the main conclusion is that **the BEM conditions should be set, on a case-by-case basis, taking into account the idiosyncrasies of each “neutral” technology, in order to be really effective. In that sense, the model is not truly neutral, nor universal.** But, in fact, this is the best way of avoiding possible interference issues or coexistence problems.

On the other hand, the proposed methodology for transient waveform validation, although outperforms the ECC/CEPT methodology in some fundamental aspects, it only allows the evaluation of the core segment of a BEM, due to limits imposed by the current RTSAs, in particular, insufficient dynamic range. Thus, it does not cover the full BEM extent analysis. However, **it may be seen as a complement of the official methodology, with clear advantages**, and its use may be optimized, if the configuration options, extracted from our sensitivity analysis, are adopted.

---

## Bibliography

- [1] J. P. Borrego and N.B. Carvalho, *A Distorção Não Linear como Causa de Interferências Radioelétricas*, 1<sup>st</sup> Seminar of the URSI Portuguese Committee, Theme: “*Radiocomunicações - Novos paradigmas e impacto na saúde*”, Rectory of the Universidade Nova de Lisboa, Lisbon, Portugal, Nov. 2007.
  
- [2] J. P. Borrego and N. B. Carvalho, *Harmful Interferences to Aeronautical Radio Communications Arising from Passive Intermodulation*, XXIX URSI General Assembly, Chicago, IL, USA, Aug. 2008.
  
- [3] J. P. Borrego, *Estudo do Impacto da Distorção Não Linear na Gestão do Espectro Radioelétrico*, MSc. Dissertation (in Portuguese), Universidade de Aveiro, 2008.
  
- [4] J. P. Borrego, S. Antunes, O. Postolache, N. B. Carvalho and J.N. Vieira, *Novos Desafios à Monitorização e Controlo do Espectro, na perspectiva dos Sistemas de Medida*, 5th Congress of the Portuguese Committee of URSI, Lisbon, Portugal, Nov. 2011.
  
- [5] J. P. Borrego and N. B. Carvalho, *Transient Nonlinear Figures of Merit for Wireless Communications*, INMMiC2010 – Workshop on Integrated Nonlinear Microwave and Millimeter-wave Circuits, Chalmers University of Technology, Göteborg, Sweden, Apr. 2010.

- [6] J. P. Borrego, N. B. Carvalho and J.N. Vieira, *New Trends in Spectrum Management in Europe: How to deal with Transient Waveforms*, CETC 2011 – Conference on Electronics Telecommunications and Computers, Lisbon, Portugal, Nov. 2011.
- [7] G. J. Mazzaro, *Time-Frequency Effects in Wireless Communication Systems*, PhD. Thesis, North Carolina State University, Raleigh, NC, USA, 2009.
- [8] Tektronix, *Transient RF Signal Analysis in R&D Environments*, Technical Brief Notes, Nov. 2004.
- [9] R. Gómez-García, J. P. Magalhães, J.-M. Muñoz-Ferreras, J. M. N. Vieira, N. B. Carvalho, and J. Pawlan, *Filling the spectral holes*, IEEE Microwave Magazine., Mar./Apr. 2014.
- [10] H. Bezabih, B. Ellingsaeter, J. Noll, and T. Maseng, *Digital broadcasting: increasing the available White Space spectrum Using TV receiver information*, IEEE Vehicular Technology Magazine, pp. 24-30, vol. 7, no. 1, Mar. 2012.
- [11] U. Ladebusch and C. A. Liss, *Terrestrial DVB (DVB-T): A broadcast technology for stationary portable and mobile use*, Proceedings of IEEE, pp.183-193, vol. 94, no. 1, Jan. 2006.
- [12] ITU, *Final Acts of the World Radiocommunication Conference 2007*, 2007
- [13] ECC/CEPT, ECC Report 148, *Measurements on the Performance of DVB-T Receivers in the Presence of Interference from the Mobile Service (Especially from LTE)*, Jun. 2009.
- [14] European Commission, *Mandate to CEPT to develop least restrictive technical conditions for frequency bands addressed in the context of WAPECS*, Information Society and Media Directorate-General, Electronic Communications Policy, Radio Spectrum Policy, Jul. 5<sup>th</sup>, 2006.
- [15] CEPT, CEPT Report 19, *Report from CEPT to the European Commission in response to the Mandate to develop Least Restrictive Technical Conditions for frequency bands addressed in the context of WAPECS*, 2008.
- [16] CEPT, CEPT Report 31, *Technical considerations regarding harmonisation options for the digital dividend in the European Union, Frequency (channelling) arrangements for the 790-862 MHz band*, 2009.

- 
- [17] European Commission [web access: Sep. 2014], *Reorganising the EU's Spectrum*, [Available Online]: <https://ec.europa.eu/digital-agenda/en/reorganising-eus-spectrum>
- [18] European Commission [web access: Sep. 2014], *Radio Spectrum Policy Program: the roadmap for a wireless Europe*, [Available Online]: <https://ec.europa.eu/digital-agenda/radio-spectrum-policy-program-roadmap-wireless-europe>
- [19] European Commission [web access: Sep. 2014], *Spectrum Needs and Spectrum Availability*, [Available Online]: <https://ec.europa.eu/digital-agenda/en/spectrum-needs-and-spectrum-availability>
- [20] European Commission [web access: Sep. 2014], *EU's Spectrum Policy Framework*, [Available Online]: <https://ec.europa.eu/digital-agenda/node/118>
- [21] European Commission [web access: Sep. 2014], *Managing and monitoring the EU's radio spectrum*, [Available Online]: <http://ec.europa.eu/digital-agenda/en/managing-and-monitoring-eus-radio-spectrum>
- [22] European Commission [web access: Sep. 2014], *Public use of spectrum*, [Available Online]: <https://ec.europa.eu/digital-agenda/en/public-use-spectrum>
- [23] European Commission [web access: Sep. 2014], *Radio and Telecommunications Terminal Equipment (R&TTE)*, [Available Online]: [http://ec.europa.eu/enterprise/sectors/rtte/index\\_en.htm](http://ec.europa.eu/enterprise/sectors/rtte/index_en.htm)
- [24] European Commission [web access: Sep. 2014], *Electromagnetic Compatibility (EMC)*, [Available Online]: [http://ec.europa.eu/enterprise/sectors/electrical/emc/index\\_en.htm](http://ec.europa.eu/enterprise/sectors/electrical/emc/index_en.htm)
- [25] European Commission [web access: Sep. 2014], *Radio Spectrum: coordination, harmonisation and information*, [Available Online]: <http://ec.europa.eu/digital-agenda/en/radio-spectrum-coordination-harmonisation-and-information>
- [26] European Commission [web access: Sep. 2014], *Europe 2020 initiatives*, [Available Online]: <http://ec.europa.eu/social/main.jsp?catId=956>
- [27] European Commission [web access: Sep. 2014], *Europe 2020*, [Available Online]: [http://ec.europa.eu/europe2020/index\\_en.htm](http://ec.europa.eu/europe2020/index_en.htm)

- [28] European Commission [web access: Sep. 2014], *Digital Agenda for Europe*, [Available Online]: <http://ec.europa.eu/digital-agenda/digital-agenda-europe>
- [29] European Commission [web access: Sep. 2014], *Concrete actions on Radio Spectrum Policy Programme (RSPP)*, [Available Online]: <https://ec.europa.eu/digital-agenda/en/news/concrete-actions-radio-spectrum-policy-programme-rspp>
- [30] European Commission [web access: Sep. 2014], COM(2014) 228 final, *Report from the Commission to the European Parliament and the Council on the implementation of the Radio Spectrum Policy Programme*, Apr. 22<sup>th</sup>, 2014, [Available Online]: <http://eur-lex.europa.eu/legal-content/EN/TXT/PDF/?uri=CELEX:52014DC0228&from=EN>
- [31] European Commission [web access: Oct. 2014], *Decision 676/2002/EC of the European Parliament and of the Council of 7 March 2002 on a regulatory framework for radio spectrum policy in the European Community (Radio Spectrum Decision)*, OJ L 108, 24.4.2002, pp. 1-6, Apr. 24<sup>th</sup>, 2002, [Available Online]: <http://eur-lex.europa.eu/legal-content/EN/TXT/PDF/?uri=CELEX:32002D0676&from=EN>
- [32] European Commission [web access: Oct. 2014], *Regulatory framework for electronic communications in the European Union – Situation in December 2009* (put in place in 2002, revised in 2009), [Available Online]: <https://ec.europa.eu/digital-agenda/sites/digital-agenda/files/Copy%20of%20Regulatory%20Framework%20for%20Electronic%20Communications%202013%20NO%20CROPS.pdf>
- [33] European Commission [web access: Oct. 2014], *Telecoms Rules*, [Available Online]: <https://ec.europa.eu/digital-agenda/telecoms-rules>
- [34] European Commission [web access: Oct. 2014], *Easier access to radio spectrum: the EU's electronic communications framework*, [Available Online]: <https://ec.europa.eu/digital-agenda/en/easier-access-radio-spectrum-eus-electronic-communications-framework>
- [35] European Commission [web access: Oct. 2014], *Mandating Europe's spectrum experts*, [Available Online]: <https://ec.europa.eu/digital-agenda/en/mandating-europe%E2%80%99s-spectrum-experts>
- [36] European Commission [web access: Oct. 2014], *EU Coordination on Radio Spectrum*, [Available Online]: <http://ec.europa.eu/digital-agenda/en/eu-coordination-radio-spectrum>

- [37] European Commission [web access: Oct. 2014], *Radio Spectrum Policy Group (RSPG)*, [Available Online]: <http://ec.europa.eu/digital-agenda/en/radio-spectrum-policy-group-rspg>
- [38] European Commission [web access: Oct. 2014], *Decision 2002/622/EC: Commission Decision of 26 July 2002 establishing a Radio Spectrum Policy Group*, OJ L 198, 27.7.2002, pp. 49-51, Jul. 27<sup>th</sup>, 2002, [Available Online]: <http://eur-lex.europa.eu/legal-content/EN/TXT/PDF/?uri=CELEX:32002D0622&from=EN>
- [39] European Commission [web access: Oct. 2014], *Radio Spectrum Committee (RSC)*, [Available Online]: <http://ec.europa.eu/digital-agenda/en/radio-spectrum-committee-rsc>
- [40] European Conference of Postal and Telecommunications Administrations (CEPT) [web access: Oct. 2014], *About CEPT*, [Available Online]: <http://www.cept.org/cept/about-cept>
- [41] European Commission [web access: Oct. 2014], *Delivering the digital dividend*, [Available Online]: <http://ec.europa.eu/digital-agenda/en/delivering-digital-dividend>
- [42] European Commission [web access: Oct. 2014], *Commission Decision 2010/267/EU, of 6 May 2010, On harmonised technical conditions of use in the 790-862 MHz frequency band for terrestrial systems capable of providing electronic communications services in the European Union*, OJ EU L117, 11.5.2010, pp. 95–101, May 11<sup>th</sup>, 2010, [Available Online]: <http://eur-lex.europa.eu/legal-content/EN/TXT/PDF/?uri=CELEX:32010D0267&from=EN>
- [43] ITU-R [web access: Oct. 2014], *Resolution 232 [COM5/10] (WRC-12) – Use of the frequency band 694-790 MHz by the mobile, except aeronautical mobile, service in Region 1 and related studies*, The World Radiocommunication Conference, Geneva, 2012, [Available Online]: <http://www.itu.int/oth/R0A0600004B/en>
- [44] ETSI, ETSI TS 136 104 V9.4.0 (2010-07), *LTE; Evolved Universal Terrestrial Radio Access (E-UTRA); Base Station (BS) radio transmission and reception (3GPP TS 36.104 version 9.4.0 Release 9)*, Jul., 2010.
- [45] European Commission [web access: Oct. 2014], *Directive 2009/114/EC of the European Parliament and of the Council of 16 September 2009 amending Council Directive 87/372/EEC on the frequency bands to be reserved for the coordinated introduction of public pan-European cellular digital land-based mobile communications in the Community*, OJ EU L274, 20.10.2009, pp. 25–27, Oct. 20<sup>th</sup>,

- 2009, [Available Online]: <http://eur-lex.europa.eu/legal-content/EN/TXT/PDF/?uri=CELEX:32009L0114&from=EN>
- [46] European Commission [web access: Oct. 2014], *Council Directive 87/372/EEC of 25 June 1987 on the frequency bands to be reserved for the coordinated introduction of public pan-European cellular digital land-based mobile communications in the Community*, OJ EC L196, 17.7.87, pp. 85-86, Jul. 17<sup>th</sup>, 1987, [Available Online]: <http://eur-lex.europa.eu/legal-content/EN/TXT/PDF/?uri=CELEX:31987L0372&from=EN>
- [47] European Commission [web access: Oct. 2014], *Commission Decision 2009/766/EC of 16 October 2009 on the harmonisation of the 900 MHz and 1 800 MHz frequency bands for terrestrial systems capable of providing pan-European electronic communications services in the Community*, OJ EU L274, 20.10.2009, pp. 32-35, Oct. 20<sup>th</sup>, 2009, [Available Online]: <http://eur-lex.europa.eu/LexUriServ/LexUriServ.do?uri=OJ:L:2009:274:0032:0035:EN:PDF>
- [48] Analysis Consulting Ltd, DotEcom Ltd, and Hogan & Hartson LPP, *Study on the conditions and options in introducing secondary trading of radio spectrum in the European Community*, Information Society Directorate-General of the European Commission, May, 2004.
- [49] European Commission [web access: Oct. 2014], *Flexibility – the key to competition and innovation*, [Available Online]: <http://ec.europa.eu/digital-agenda/en/flexibility-key-competition-and-innovation>
- [50] European Commission [web access: Oct. 2014], *WAPECS – a flexible approach to spectrum use*, [Available Online]: <http://ec.europa.eu/digital-agenda/en/wapecs-%E2%80%93-flexible-approach-spectrum-use>
- [51] RSPG [web access: Oct. 2014], *Radio Spectrum Policy Group Opinion on Wireless Access Policy for Electronic Communications Services (WAPECS) (A more flexible spectrum management approach)*, RSPG 05-102final, Brussels, Nov. 23<sup>th</sup>, 2005, [Available Online]: [http://rspg-spectrum.eu/wp-content/uploads/2013/05/rspg05\\_102\\_op\\_wapecs.pdf](http://rspg-spectrum.eu/wp-content/uploads/2013/05/rspg05_102_op_wapecs.pdf)
- [52] European Commission [web access: Oct. 2014], *Directive 2002/21/EC of the European Parliament and of the Council of 7 March 2002 on a common regulatory framework for electronic communications networks and services (Framework Directive) as amended by Directive 2009/140/EC (OJ L 337, 18.12.2009, p. 37) and Regulation 544/2009 (OJ L 167, 18.6.2009, p. 12) (unofficially consolidated version)*, OJ L 108, 24.04.2002,



- pp. 33-50, Apr. 24<sup>th</sup>, 2002, [Available Online]: [http://ec.europa.eu/digital-agenda/sites/digital-agenda/files/140framework\\_5.pdf](http://ec.europa.eu/digital-agenda/sites/digital-agenda/files/140framework_5.pdf)
- [53] Vieira de Almeida & Associados, [web access: October 2014], *A nova política de gestão do espectro – Revisão do Pacote Regulamentar das Comunicações Electrónicas (“Revisão 2006”)*, APDC Master Class, Apr. 13<sup>th</sup>, 2010, [Available Online, in Portuguese]: [http://www.apdc.pt/filedownload.aspx?schema=f7664ca7-3a1a-4b25-9f46-2056eef44c33&channel=72F445D4-8E31-416A-BD01-D7B980134D0F&content\\_id=45605481-307B-4B82-AF29-2E7981794BD0&field=storage\\_image&lang=pt&ver=1](http://www.apdc.pt/filedownload.aspx?schema=f7664ca7-3a1a-4b25-9f46-2056eef44c33&channel=72F445D4-8E31-416A-BD01-D7B980134D0F&content_id=45605481-307B-4B82-AF29-2E7981794BD0&field=storage_image&lang=pt&ver=1)
- [54] European Commission [web access: Nov. 2014], *Promoting the shared use of Europe’s radio spectrum*, [Available Online]: <http://ec.europa.eu/digital-agenda/en/promoting-shared-use-europes-radio-spectrum>
- [55] European Commission [web access: Nov. 2014], *Short range, mass market*, [Available Online]: <http://ec.europa.eu/digital-agenda/en/short-range-mass-market>
- [56] European Commission [web access: Nov. 2014], *Communication from the Commission to the European Parliament, the Council, the European Economic and Social Committee and the Committee of the Regions: Promoting the shared use of radio spectrum resources in the internal market*, COM (2012) 478 final, Brussels, 3.9.2012, Sep. 3<sup>rd</sup>, 2012, [Available Online]: <https://ec.europa.eu/digital-agenda/sites/digital-agenda/files/com-ssa.pdf>
- [57] N. B. Carvalho, A. Cidronali, R. Gómez-García, *White Space Communications Technologies*, Cambridge University Press, Cambridge, UK, 2014.
- [58] CEPT, CEPT Report 24, *Report C from CEPT to the European Commission in response to the Mandate on: “Technical considerations regarding harmonisation options for the Digital Dividend” – “A preliminary assessment of the feasibility of fitting new/future applications/services into non-harmonised spectrum of the digital dividend (namely the so-called “white spaces” between allotments)”*, Jul. 2008.
- [59] ECC/CEPT, ECC Report 159, *Technical and Operational Requirements for the Possible Operation of Cognitive Radio Systems in the ‘White Spaces’ of the Frequency Band 470-790 MHz*, Jan. 2011.
- [60] ITU-R, Report SM.2152 (09/2009), *Definitions of Software Defined Radio (SDR) and Cognitive Radio System (CRS)*, Sep. 2009.

- [61] ECC/CEPT, ECC Report 185, *Complementary Report to ECC Report 159 Further definition of technical and operational requirements for the operation of white space devices in the band 470-790 MHz*, Jan. 2013.
- [62] ECC/CEPT, ECC Report 186, *Technical and operational requirements for the operation of white space devices under geo-location approach*, Jan. 2013.
- [63] W. A. Gardner, *Cyclostationarity in Communications and Signal Processing*, IEEE Press, New York, USA, 1994.
- [64] A. Basaure, V. Marianov, and R. Paredes, *Implications of dynamic spectrum management for regulations*, Telecommunications Policy (2014), DOI: 10.1016/j.telpol.2014.07.001, Aug. 2014.
- [65] ECC/CEPT, ECC Report 148, *Measurements on the Performance of DVB-T Receivers in the Presence of Interference from the Mobile Service (Especially from LTE)*, Jun. 2009.
- [66] Agilent [web access: Nov. 2014], *Agilent EEsof EDA - SystemVue 2013, Technical Overview*, Aug. 2013, [Available Online]: <http://cp.literature.agilent.com/litweb/pdf/5990-4731EN.pdf>
- [67] CEPT, CEPT Report 30, *The identification of common and minimal (least restrictive) technical conditions for 790-862 MHz for the digital dividend in the European Union*, 2009.
- [68] G. J. Mazzaro, M. B. Steer, K. G. Gard and A. L. Walker, *Response of RF Networks to Transient Waveforms: Interference in Frequency-Hopped Communications*, IEEE Transactions on Microwave Theory and Techniques, vol. 56, no. 12, pp. 2808-2814, Dec. 2008.
- [69] ECC/CEPT, ECC Recommendation 11(06), *Block Edge Mask Compliance Measurements for Base Stations*, Edition 4, Oct. 2013.
- [70] P. Cruz and N. B. Carvalho, *PAPR evaluation in multi-mode SDR receivers*, 38<sup>th</sup> European Microwave Conference, pp. 1354-1357, Amsterdam, The Netherlands, Oct. 27-31, 2008.
- [71] M. M. Vélez, P. Angueira, D. de la Vega, A. Arrinda, L. de Haro, and J. L. Ordiales, *DVB-T BER measurements in the presence of adjacent channel and co-channel analogue*

- television interference*, IEEE Transactions on Broadcasting, pp. 80-84, vol. 47, no. 1, Jan. 2001.
- [72] M. G. Sánchez, M. A. Acuña, I. Cuiñas, R. M. Martínez-Osorio, L. de Haro, and A. García-Pino, *Co-channel and adjacent channel interference in actual terrestrial TV scenarios—Part I: field measurements*, IEEE Transactions on Broadcasting, pp. 111-115, vol. 48, no. 2, Jun. 2002.
- [73] M. G. Sánchez, M. A. Acuña, I. Cuiñas, R. M. Martínez-Osorio, L. de Haro, and A. García-Pino, *Co-channel and adjacent channel interference in actual terrestrial TV scenarios—Part II: MATV systems laboratory tests*, IEEE Transactions on Broadcasting, pp. 116-122, vol. 48, no. 2, Jun. 2002.
- [74] G. Barrufa, M. Femminella, F. Mariani, and G. Reali, *Protection ratio and antenna separation for DVB-T/LTE coexistence issues*, IEEE Communications Letters, pp. 1588-1591, vol. 17, no. 8, Aug. 2013.
- [75] A. Martínez, D. Zabala, I. Peña, P. Angueira, M. M. Vélez, A. Arrinda, D. de la Vega, and J. L. Ordiales, *Analysis of the DVB-T signal variation for indoor portable reception*, IEEE Transactions on Broadcasting, pp. 11-19, vol. 55, no. 1, Jan. 2009.
- [76] M. García-Lozano, M. A. Lema, S. Ruiz, F. Minerva, *Metaheuristic procedure to optimize transmission delays in DVB-T single frequency networks*, IEEE Transactions on Broadcasting, pp. 876-887, vol. 57, no. 4, Dec. 2011.
- [77] ETSI, ETSI EN 300 744 V1.1.2 (1997-08), *Digital Video Broadcasting (DVB); Framing structure, channel coding and modulation for digital terrestrial television*, 1997.
- [78] W. Fischer, *Digital Video and Audio Broadcasting Technology – A Practical Engineering Guide*, Springer-Verlag, 3<sup>rd</sup> Ed., 2010.
- [79] S. O’Leary, *Understanding Digital Terrestrial Broadcasting*, Artech House Digital, Audio, and Video Technology Library, Artech House, 1999.
- [80] Infineon Technologies, *Application note of DVB-T (COFDM) tuner with broadband Multimedia IC, TUA6034*, version 2, 2002.
- [81] ETSI, ETSI TR 101 290 V1.2.1 (2001-05), *Digital Video Broadcasting (DVB); Measurement guidelines for DVB systems*, 2001.

- [82] D. Bernal, P. Closas, and J. Fernández-Rubio, *Digital I&Q demodulation in array processing: theory and implementation*, 16<sup>th</sup> European Signal Processing Conference, Lausanne, Switzerland, Aug. 25-29, 2008.
- [83] R. Brugger and D. Henningway, *OFDM Receivers – Impact on coverage of inter-symbol interference and FFT window positioning*, EBU – UER, EBU Technical Review, Jul. 2003.
- [84] ITU-R, Recommendation ITU-R SM.1875 (04/2010), *DVB-T Coverage Measurements and Verification of Planning Criteria*, 2010.
- [85] ITU-R, Report ITU-R BT.2035-2 (2003-2004-2008), *Guidelines and techniques for the evaluation of Digital Terrestrial Television Broadcasting systems including assessment of their coverage areas*, 2008.
- [86] ITU-R, Recommendation ITU-R BT.1735-1 (08/2012), *Methods for objective quality coverage assessment of Digital Terrestrial Television Broadcasting signals of system B specified in Recommendation ITU-R BT.1306*, 2012.
- [87] EBU – UER, *General issues to be considered when planning SFNs*, EBU Technical Media Technology & Innovation, Mar. 13<sup>th</sup>, 2009.
- [88] J.-S. Hong and M. J. Lancaster, *Microstrip Filters for RF/Microwave Applications*, New York, NY, USA: Wiley, 2001.
- [89] C. Rauscher, *Microwave active filters based on transversal and recursive principles*, IEEE Transactions on Microwave Theory and Techniques, vol. MTT-33, no. 12, pp. 1350-1360, Dec. 1985.
- [90] R. Gómez-García and J. I. Alonso, *Design of sharp-rejection and low-loss wide-band planar filters using signal-interference techniques*, IEEE Microwave Wireless Components Letters, vol. 15, no. 8, pp. 530-532, Aug. 2005.
- [91] Sonnet, [web access: Nov. 2014], Sonnet High Frequency Electromagnetic Software, [Available Online]: <https://www.sonnetsoftware.com>
- [92] D. Lee, M. Choi, and S. Choi, *Channel estimation and interference cancellation of feedback interference for DOCR in DVB-T system*, IEEE Transactions on Broadcasting, vol. 58, no. 4, pp. 87-97, Dec. 2012.

- [93] L. Angrisani, M. Farias, D. Fortin, and A. Sona, *Experimental analysis of in-channel interference effects on the performance of a DVB-T system*, IEEE Transactions on Instrumentation and Measurement, vol. 58, no. 8, pp. 2588-2596, Aug. 2009.
- [94] G. Baruffa, M. Femminella, F. Mariani, and G. Reali, *Protection ratio and antenna separation for DVB-T/LTE coexistence issues*, IEEE Communications Letters, vol. 17, no. 8, pp. 1588-1591, Aug. 2013.
- [95] P. Baracca, S. Tomasin, N. Benvenuto, and L. Vangelista, A. Morello, *Per sub-block equalization of very long OFDM blocks in mobile communications*, IEEE Transactions on Communications, vol. 59, no. 2, pp. 363-368, Feb. 2011.
- [96] B. Beidas, and R. I. Seshadri, *Analysis and compensation for nonlinear interference of two high-order modulation carriers over satellite link*, IEEE Transactions on Communications, vol. 58, no. 6, pp. 1824-1833, Jun. 2010.
- [97] M. G. Sanchez, M. A. Acuna, I. Cuinas, R. M. Rodriguez-Osorio, L. de Haro, and A. Garcia-Pino, *Cochannel and adjacent channel interference in actual terrestrial TV scenarios - part I: field measurements*, IEEE Transactions on Broadcasting, vol. 48, no. 2, pp. 111-115, Jun. 2002.
- [98] A. Chorti, and M. Brookes, *On the effects of memoryless nonlinearities on M-QAM and DQPSK OFDM signals*, IEEE Transactions on Microwave Theory Techniques, vol. 54, no. 8, pp. 3301-3315, Aug. 2006.
- [99] P. Varahram, B. M. Ali, S. Mohammady, and N. Sulaiman, *Power amplifier linearisation scheme to mitigate superfluous radiations and suppress adjacent channel interference*, IET Communications, vol. 8, no. 2, pp. 258-265, 2014.
- [100] M. Younes, and F. M. Ghannouchi, *Generalised twin-box model for compensation of transmitters radio frequency impairments*, IET Communications, vol. 8, no. 4, pp. 413-418, 2014.
- [101] L. Angrisani, A. Napolitano, and M. Vadursi, *Measuring I/Q impairments in WiMAX transmitters*, IEEE Transactions on Instrumentation and Measurement, vol. 58, no. 5, pp. 1299-1306, May 2009.
- [102] M. Li, L. Hoover, K. G. Gard, and M. B. Steer, *Behavioural modelling and impact analysis of physical impairments in quadrature modulators*, IET Microwaves, Antennas and Propagation, vol. 4, no. 12, pp. 2144-2154, Dec. 2010.

- [103] ITU-R, Report ITU-R SM.2022, *The Effect on Digital Communications Systems of Interference from other Modulation Schemes*, 2000.
- [104] D. Stoneback, R. Howald, and R. Brophy, *Distortion beat characterization and the impact on QAM BER performance*, 48<sup>th</sup> Annual NCTA Convention and International Exposition, Chicago, IL, Jun. 13-16, 1999.
- [105] G. Terreault, *QAM signal impairments and their effects on MER and BER*, Sunrise Telecom Broadband Corp., Norcross, GA, Tech. Rep. Version 1.04, Jan. 2003.
- [106] J. Walsh, *PathTrak QAMTrak analyzer functionality*, JDSU Corp., Application Note, Milpitas, CA, Mar. 2009.
- [107] ECC/CEPT, ECC/DEC/(09)03, *ECC Decision of 30 October 2009 on harmonised conditions for mobile/fixed communications networks (MFCN) operating in the band 790-862 MHz*, Oct. 2009.
- [108] W. L. Hatton, *Simplified FM Transient Response*, Technical Report No. 196, Massachusetts Institute of Technology, Research Laboratory of Electronics, Apr. 1951.
- [109] H. Salinger, *Transients in Frequency Modulation*, Proceedings of the I.R.E., vol. 30, Issue: 8, pp. 378-383, Aug. 1942.
- [110] R. E. McCoy, *FM Transient Response of Band-Pass Circuits*, Proceedings of the I.R.E., vol. 42, no. 3, pp. 574-579, Mar. 1954.
- [111] H. F. Hartley, *Transient Response of Narrow-Band Networks to Narrow-Band Signals with Applications to Frequency Shift Keying*, IEEE Transactions on Communications Technology, vol. Com-14, no. 4, pp. 470-477, Aug. 1966.
- [112] J. Yang and S. X. Tan, *Nonlinear Transient and Distortion Analysis via Frequency Domain Volterra Series*, Circuits Systems Signal Processing, vol. 25, no. 3, pp. 295-314, 2006.
- [113] ECC/CEPT, Project Team FM22, FM22(13)10, *BEM Compliance Measurements on a LTE Base Station at different traffic loads*, 39<sup>th</sup> Meeting of FM22, Copenhagen, Apr. 2013.

- 
- [114] ERA Technology, *Assessment of LTE 800 MHz Base Station Interference into DTT Receivers*, Ofcom PO 4100017570, Jul. 2011.
- [115] ETSI, ETSI EN 301 908-14 V5.2.1 (2011-05), *IMT cellular networks; Harmonized EN covering the essential requirements of article 3.2 of the R&TTE Directive; Part 14: Evolved Universal Terrestrial Radio Access (E-UTRA) Base Stations (BS)*, May, 2011.
- [116] ETSI, ETSI TS 136 141 V11.8.0 (2014-03), *LTE; Evolved Universal Terrestrial Radio Access (E-UTRA); Base Station (BS) conformance testing (3GPP TS 36.141 version 11.8.0 Release 11)*, Mar., 2014.
- [117] ITU-R, Recommendation ITU-R P.525-2 (1978-1982-1994), *Calculation of Free-Space Attenuation*, 1994.
- [118] E. Dahlman, S. Parkvall and J. Sköld, *4G LTE / LTE-Advanced for Mobile Broadband*, Academic Press – Elsevier, 2011.
- [119] S. J. Bae, Y. M. Kwon, M. Y. Lee, B. T. Koo and M. Y. Chung, *Femtocell interference analysis based on the development of system-level LTE simulator*, EURASIP Journal on Wireless Communications and Networking 2012, Springer Open Journal 2012:287, 2012.
- [120] L. Cohen, *Time-Frequency Distributions – A Review*, Proceedings of the IEEE, vol. 77, no. 7, pp. 941-981, Jul. 1989.
- [121] M. R. Portnoff, *Time-Frequency Representation of Digital Signals and Systems Based on Short-Time Fourier Analysis*, IEEE Transactions on Acoustics, Speech, and Signal Processing, vol. ASSP-28, no. 1, pp. 55-69, Feb. 1980.
- [122] R. L. Allen and D. W. Mills, *Signal Analysis – Time, Frequency, Scale and Structure*, IEEE Press / Wiley Inter-science, 2004.
- [123] M. Ojala and E. Leinonen, *The Theory of Transient Intermodulation Distortion*, IEEE Transactions on Acoustics, Speech, and Signal Processing, vol. ASSP-25, no. 1, pp. 2-8, Feb. 1977.
- [124] E. M. Cherry, *Transient Intermodulation Distortion – Part I: Hard Nonlinearity*, IEEE Transactions on Acoustics, Speech, and Signal Processing, vol. ASSP-29, no. 2, pp. 137-146, Apr. 1981.

- [125] T. J. Lynn and A. Z. bin Sha'ameri, *Comparison between the Performance of Spectrogram and Multi-Window Spectrogram in Digital Modulated Communication Signals*, Proceedings of the 2007 IEEE International Conference on Telecommunications and Malaysia Conference on Communications, pp. 97-101, May 2007.
- [126] B. N. Vo, A. Cantoni and K. L. Teo, *Filter Design With Time Domain Mask Constraints*, Theory and Applications, Kluwer Academic Press, 2001.
- [127] E. N. Bruce, *Biomedical Signal Processing and Signal Modeling*, John Wiley & Sons, 2001.
- [128] S. W. Smith, *The Scientist and Engineer's Guide to Digital Signal Processing*, California Technical Publishing, 1997.
- [129] A. Leon-Garcia, *Probability and Random Processes for Electrical Engineering*, Addison-Wesley Publishing Company, 1994.
- [130] N. B. Carvalho, *Statistical Analysis of RF Signals*, Sabbatical Research Notes, Instituto de Telecomunicações, 2009.
- [131] S. Mallat, *A Wavelet Tour of Signal Processing*, Academic Press, 3<sup>rd</sup> Edition, 2008.
- [132] N. B. Carvalho, K. A. Remley, D. Schreurs and K. G. Gard, *Multisine Signals for Wireless System Test and Design*, IEEE Microwave Magazine, vol. 9, pp. 122-138, Jun. 2008.
- [133] F. Auger, P. Flandrin, P. Gonçalves and O. Lemoine, *Time-Frequency Toolbox Tutorial for Use with MATLAB*, Centre National de la Recherche Scientifique (CNRS), France, Oct. 2005.
- [134] F. Auger, P. Flandrin, P. Gonçalves and O. Lemoine, *Reference Guide: Time-Frequency Toolbox Tutorial for Use with MATLAB*, Centre National de la Recherche Scientifique (CNRS), France, Oct. 2005.
- [135] P. Flandrin, *Time-Frequency and Chirps*, Proc. SPIE 4391, Wavelet Applications VIII, 161, Mar. 2001.
- [136] S. Mann and S. Haykin, *The Chirplet Transform: A Generalization of Gabor's Logon Transform*, Vision Interface '91, Canadian Image Processing and Pattern Recognition Society, Calgary, Alberta, Jun. 1991.



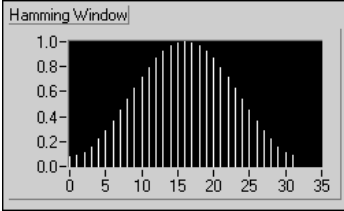
- 
- [137] S. Qian and D. Chen, *Joint Time-Frequency Analysis: Methods and Applications*, Prentice Hall, 1996.
- [138] National Instruments [web access: Nov. 2014], *Characteristics of Different Smoothing Windows*, Labview 2011 Help Manuals, [Available Online]: [http://zone.ni.com/reference/en-XX/help/371361H-01/vanlsconcepts/char\\_smoothing\\_windows/](http://zone.ni.com/reference/en-XX/help/371361H-01/vanlsconcepts/char_smoothing_windows/)
- [139] National Instruments [web access: Nov. 2014], *Choosing the Correct Smoothing Window*, Labview 2012 Help Manuals, [Available Online]: [http://zone.ni.com/reference/en-XX/help/371361J-01/vanlsconcepts/choosing\\_smoothing\\_window/](http://zone.ni.com/reference/en-XX/help/371361J-01/vanlsconcepts/choosing_smoothing_window/)
- [140] A. S. Wightman [web access: Nov. 2014], *Eugene Paul Wigner 1902-1995*, Notices of the AMS, vol. 42, no. 7, pp. 769-771, Jul. 1995, [Available Online]: <http://www.ams.org/notices/199507/wigner.pdf>
- [141] N. B. Carvalho and D. Schreurs, *Microwave and Wireless Measurement Technoques*, Cambridge University Press, 2013.
- [142] Rhode & Schwarz, *Implementation of Real-Time Spectrum Analysis*, R&S White Paper, Jan. 2011.
- [143] Tektronix, *Fundamentals of Real-Time Spectrum Analysis Primer*, 2005.
- [144] Tektronix, *Fundamentals of Real-Time Spectrum Analysis Primer*, 2008.
- [145] Tektronix, *DPX<sup>TM</sup> Acquisition Technology for Spectrum Analyzers Fundamentals Primer*, 2009.
- [146] National Instruments [web access: Nov. 2014], *Labview Reference Website*, [Available Online]: <http://www.ni.com/labview/>
- [147] National Instruments, *Labview 2014 Help* (Integrated “Help”, provided by Labview Professional Development System).

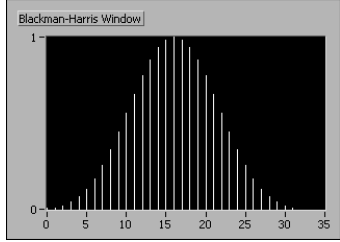
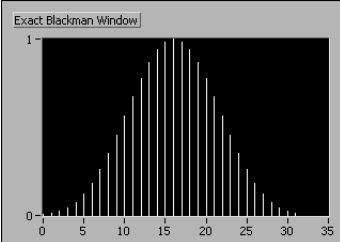
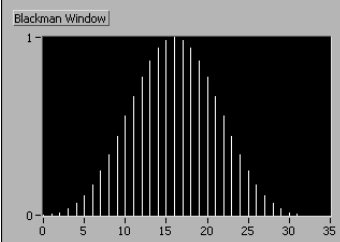
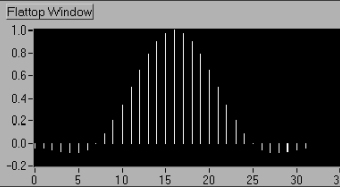
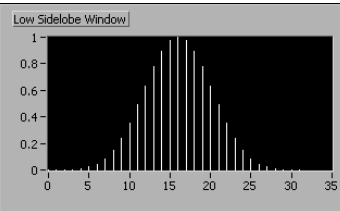


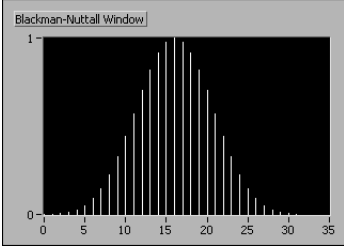
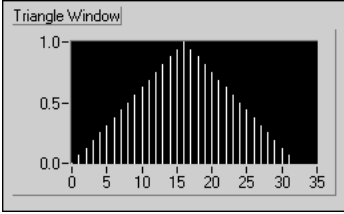
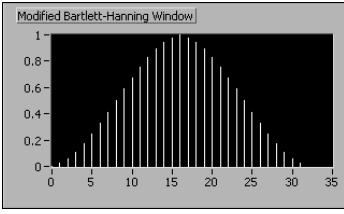
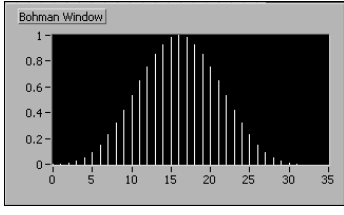
# Appendices

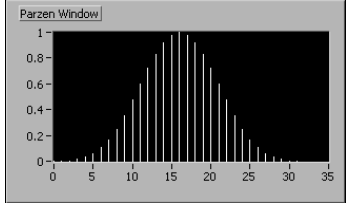
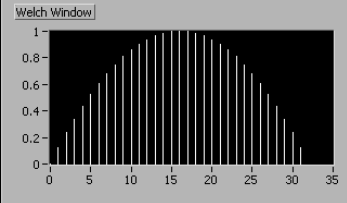
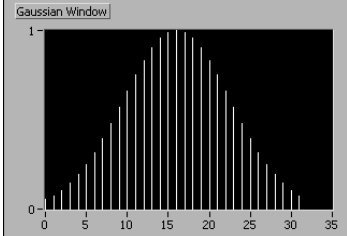
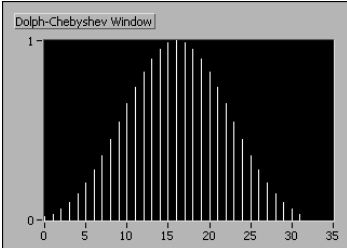
## Appendices

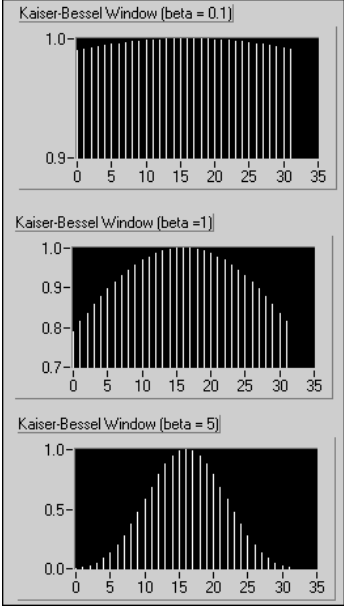
### Appendix A: Smoothing Windows implemented in the Software Tool and available in Labview

Window	Definition	Window Shape
Hamming	$w(n) = 0.54 - 0.46 \cos\left(\frac{2\pi n}{N}\right)$	

Window	Definition	Window Shape
<b>Blackman-Harris</b>	$w(n) = 0.422323 - 0.49755 \cos\left(\frac{2\pi n}{N}\right) + 0.07922 \cos\left(\frac{4\pi n}{N}\right)$	
<b>Exact Blackman</b>	$w(n) = a_0 - a_1 \cos\left(\frac{2\pi n}{N}\right) + a_2 \cos\left(\frac{4\pi n}{N}\right)$ $a_0 = \frac{7938}{18608}$ $a_1 = \frac{9240}{18608}$ $a_2 = \frac{1430}{18608}$	
<b>Blackman</b>	$w(n) = 0.42 - 0.50 \cos\left(\frac{2\pi n}{N}\right) + 0.08 \cos\left(\frac{4\pi n}{N}\right)$	
<b>Flat Top</b>	$w(n) = \sum_{k=0}^4 (-1)^k a_k \cos\left(k \frac{2\pi n}{N}\right)$ $a_0 = 0.215578948$ $a_1 = 0.416631580$ $a_2 = 0.277263158$ $a_3 = 0.083578947$ $a_4 = 0.006947368$	
<b>Low Sidelobe</b>	$w(n) = \sum_{k=0}^4 (-1)^k a_k \cos\left(k \frac{2\pi n}{N}\right)$ $a_0 = 0.471492057$ $a_2 = 0.17553428$ $a_3 = 0.028497078$ $a_4 = 0.001261367$	

Window	Definition	Window Shape
Blackman-Nuttall	$w(n) = a_0 - a_1 \cos\left(\frac{2\pi n}{N}\right) + a_2 \cos\left(\frac{4\pi n}{N}\right) + a_3 \cos\left(\frac{6\pi n}{N}\right)$ $a_0 = 0.3635819$ $a_1 = 0.4891775$ $a_2 = 0.1365995$ $a_3 = 0.0106411$	 <p>A plot titled 'Blackman-Nuttall Window' showing a smooth, bell-shaped curve. The x-axis ranges from 0 to 35 with major ticks every 5 units. The y-axis ranges from 0 to 1 with major ticks every 0.5 units. The curve starts at 0 at n=0, reaches a maximum of 1 at n=17.5, and returns to 0 at n=35.</p>
Bartlett (Triangle)	$w(n) = 1 - \left  \frac{2n - N}{N} \right $	 <p>A plot titled 'Triangle Window' showing a triangular shape. The x-axis ranges from 0 to 35 with major ticks every 5 units. The y-axis ranges from 0.0 to 1.0 with major ticks every 0.5 units. The curve starts at 0 at n=0, reaches a maximum of 1 at n=17.5, and returns to 0 at n=35.</p>
Bartlett-Hanning	$w(n) = 0.62 - 0.48 \left  \frac{n}{N} - 0.5 \right  + 0.38 \cos\left(2\pi \left(\frac{n}{N} - 0.5\right)\right)$	 <p>A plot titled 'Modified Bartlett-Hanning Window' showing a smooth, bell-shaped curve. The x-axis ranges from 0 to 35 with major ticks every 5 units. The y-axis ranges from 0 to 1 with major ticks every 0.2 units. The curve starts at 0 at n=0, reaches a maximum of 1 at n=17.5, and returns to 0 at n=35.</p>
Bohman	$w(n) = \left(1 - \frac{ n - \frac{N}{2} }{\frac{N}{2}}\right) \cos\left(\pi \frac{ n - \frac{N}{2} }{\frac{N}{2}}\right) + \frac{1}{\pi} \sin\left(\pi \frac{ n - \frac{N}{2} }{\frac{N}{2}}\right)$	 <p>A plot titled 'Bohman Window' showing a smooth, bell-shaped curve. The x-axis ranges from 0 to 35 with major ticks every 5 units. The y-axis ranges from 0 to 1 with major ticks every 0.2 units. The curve starts at 0 at n=0, reaches a maximum of 1 at n=17.5, and returns to 0 at n=35.</p>

Window	Definition	Window Shape
Parzen	$w(n) = \begin{cases} 1 - 6\left(\frac{n - \frac{N}{2}}{\frac{N}{2}}\right)^2 + 6\left(\frac{ n - \frac{N}{2} }{\frac{N}{2}}\right)^3, & 0 \leq  n - \frac{N}{2}  \leq \frac{N}{4} \\ 2\left(1 - \frac{ n - \frac{N}{2} }{\frac{N}{2}}\right)^3, & \frac{N}{4} <  n - \frac{N}{2}  \leq \frac{N}{2} \end{cases}$	 <p>A plot titled 'Parzen Window' showing a smooth, bell-shaped curve. The x-axis ranges from 0 to 35 with major ticks every 5 units. The y-axis ranges from 0 to 1 with major ticks every 0.2 units. The curve starts at 0 at x=0, reaches a maximum of 1 at x=15, and returns to 0 at x=35.</p>
Welch	$w(n) = 1 - \left(\frac{n - \frac{N}{2}}{\frac{N}{2}}\right)^2$	 <p>A plot titled 'Welch Window' showing a smooth, bell-shaped curve. The x-axis ranges from 0 to 35 with major ticks every 5 units. The y-axis ranges from 0 to 1 with major ticks every 0.2 units. The curve starts at 0 at x=0, reaches a maximum of 1 at x=15, and returns to 0 at x=35.</p>
Gaussian	$w(n) = e^{-\frac{(n-m)^2}{2(\sigma N)^2}}$	 <p>A plot titled 'Gaussian Window' showing a smooth, bell-shaped curve. The x-axis ranges from 0 to 35 with major ticks every 5 units. The y-axis ranges from 0 to 1 with major ticks every 0.2 units. The curve starts at 0 at x=0, reaches a maximum of 1 at x=15, and returns to 0 at x=35.</p>
Dolph-Chebyshev	$w(n) = \frac{1}{N} \left[ s + 2 \sum_{k=1}^{\lfloor \frac{N-1}{2} \rfloor} c_{N-1} \left( t_0 \cos\left(\frac{k\pi}{N}\right) \cos\left(\frac{2k\pi\left(n - \frac{N-1}{2}\right)}{N}\right) \right) \right]$ $c_m(x) = \begin{cases} \cos(m \cos^{-1}(x)), &  x  \leq 1 \\ \cosh(m \cosh^{-1}(x)), &  x  > 1 \end{cases}$ $t_0 = \cosh\left(\frac{1}{N-1} \cosh^{-1}(s)\right)$	 <p>A plot titled 'Dolph-Chebyshev Window' showing a smooth, bell-shaped curve. The x-axis ranges from 0 to 35 with major ticks every 5 units. The y-axis ranges from 0 to 1 with major ticks every 0.2 units. The curve starts at 0 at x=0, reaches a maximum of 1 at x=15, and returns to 0 at x=35.</p>

Window	Definition	Window Shape
<b>Kaiser-Bessel</b>	<p>The Kaiser-Bessel window is a flexible smoothing window whose shape can be modified by adjusting the beta input. Thus, depending on the application, the shape of the window can be changed, in order to control the amount of spectral leakage.</p> <p>For small values of beta, the shape is close to that of a rectangular window. For <math>\beta = 0.0</math>, a rectangular window is, actually, obtained. As beta increases, the window tapers off more to the sides.</p>	 <p>The figure consists of three vertically stacked plots, each showing the magnitude of a Kaiser-Bessel window over a range of 0 to 35. The top plot is titled 'Kaiser-Bessel Window (beta = 0.1)' and shows a nearly rectangular window with a magnitude of 1.0 across the entire range. The middle plot is titled 'Kaiser-Bessel Window (beta = 1)' and shows a window that tapers off slightly towards the edges, with a minimum magnitude of approximately 0.7. The bottom plot is titled 'Kaiser-Bessel Window (beta = 5)' and shows a window that tapers off significantly more, with a minimum magnitude of 0.0 at the edges. All plots have an x-axis from 0 to 35 and a y-axis from 0.0 to 1.0.</p>

Source: **National Instruments**, *Characteristics of Different Smoothing Windows*  
[Available Online]:

[http://zone.ni.com/reference/en-XX/help/371361H-01/lvanlsconcepts/char\\_smoothing\\_windows/](http://zone.ni.com/reference/en-XX/help/371361H-01/lvanlsconcepts/char_smoothing_windows/)

(Pictures: credits to National Instruments™)

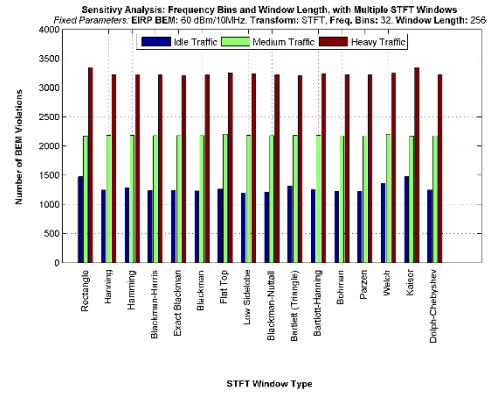
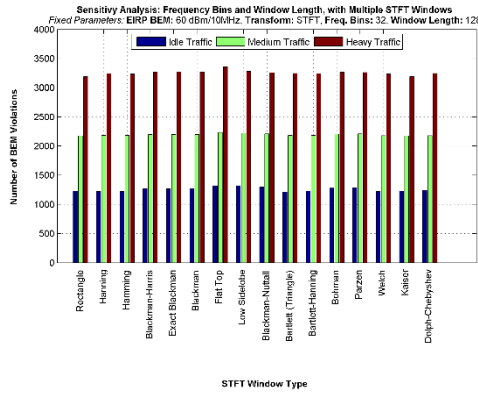
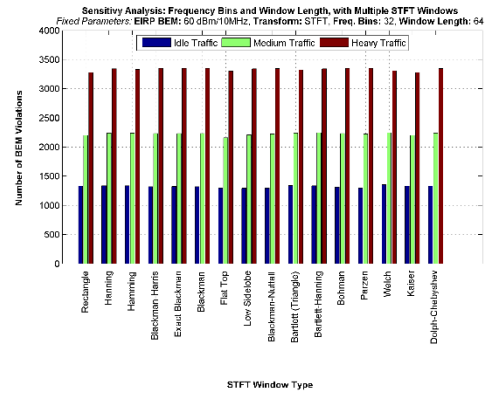
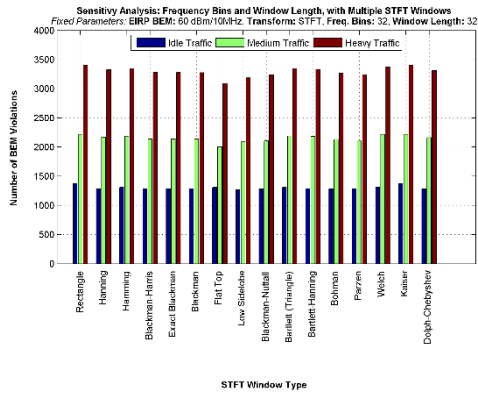




# Appendix B: Transient Waveform Validation, Sensitivity Analysis – Complete Results

## STFT Multiple Windows

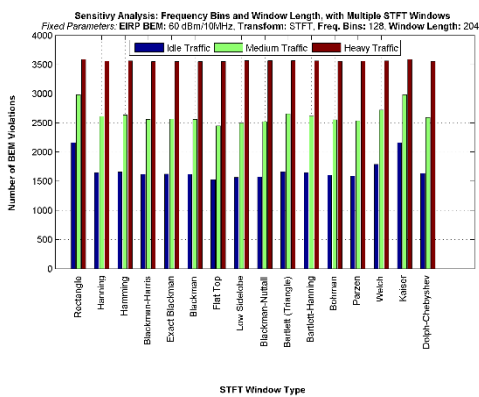
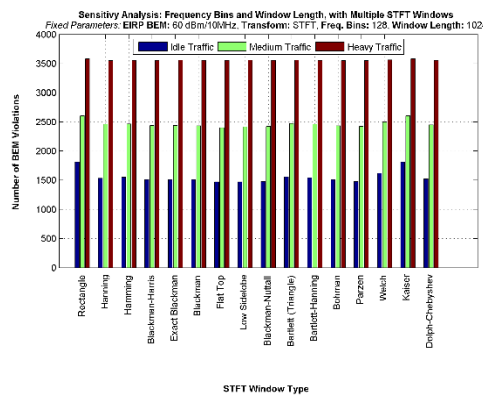
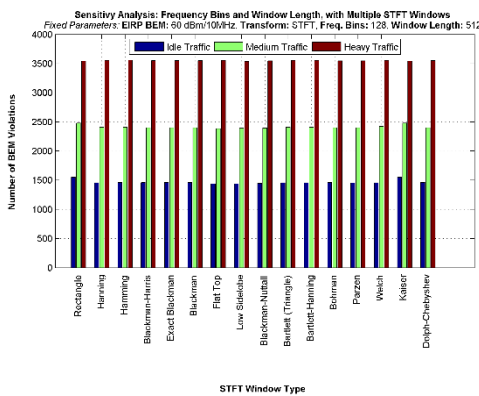
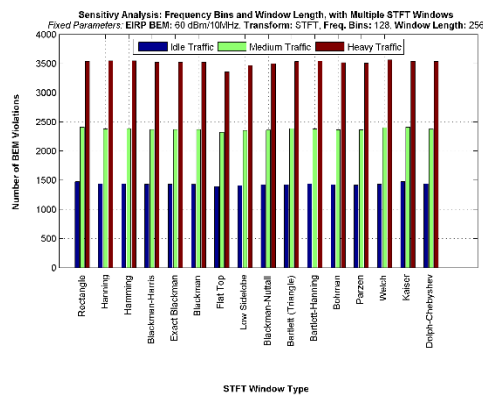
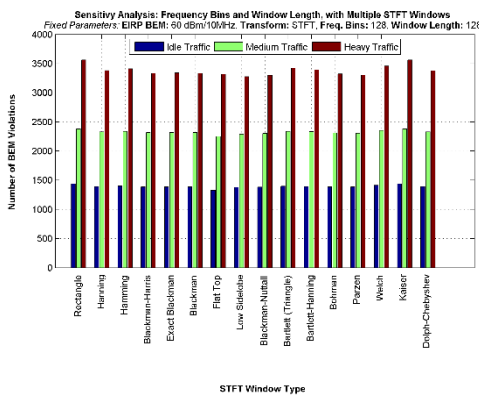
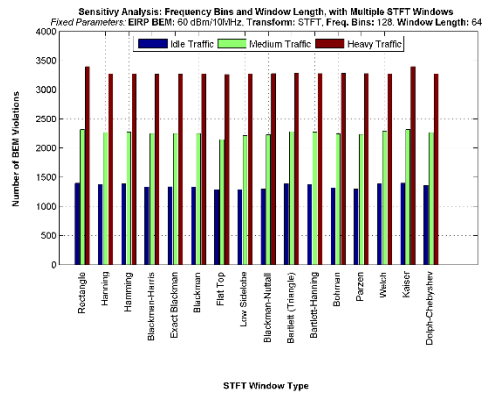
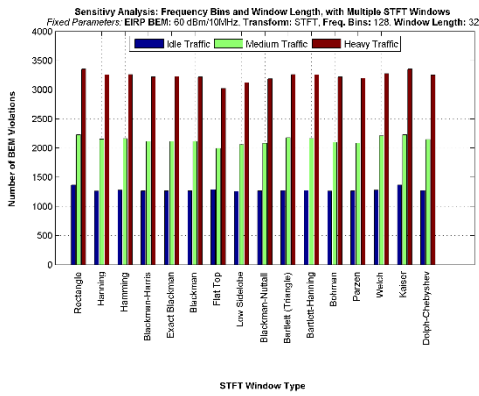
### Frequency Bins: 32, Variable Window Length





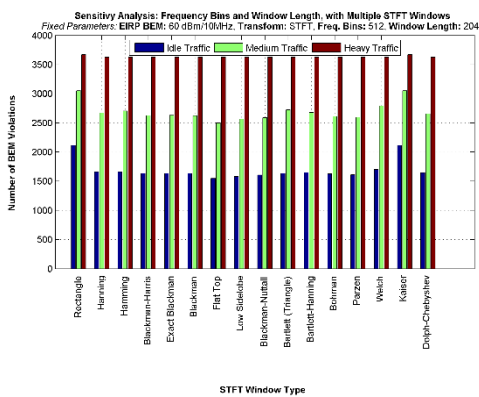
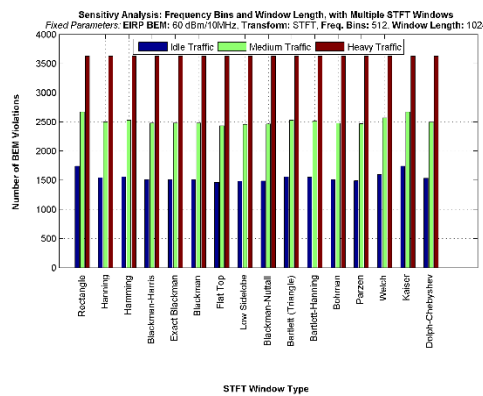
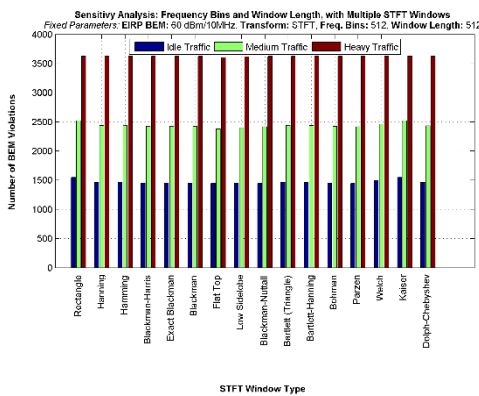
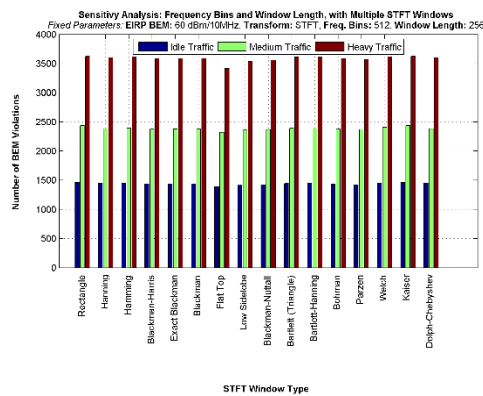
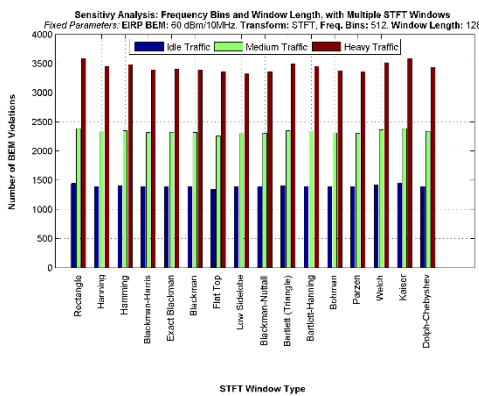
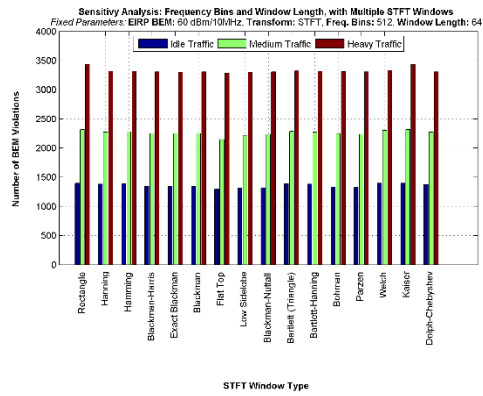
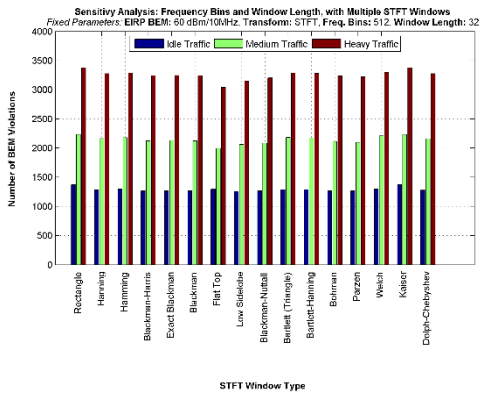


Frequency Bins: 128, Variable Window Length



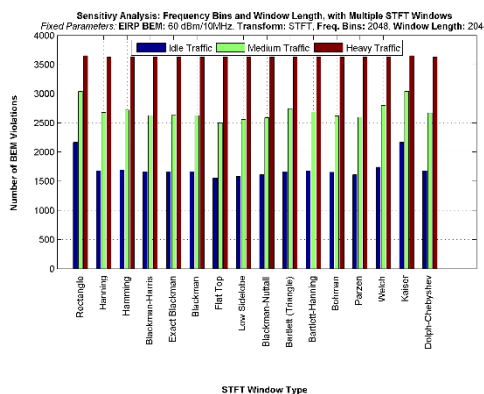
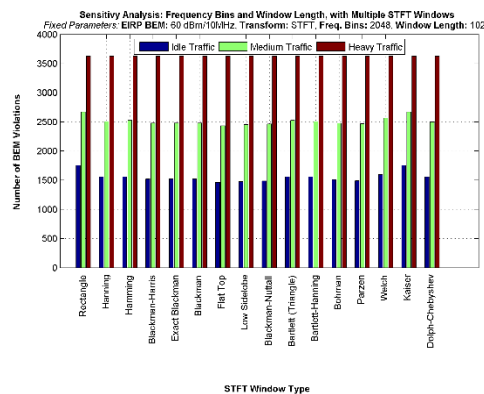
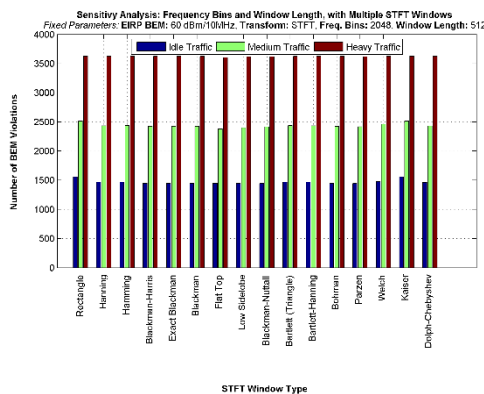
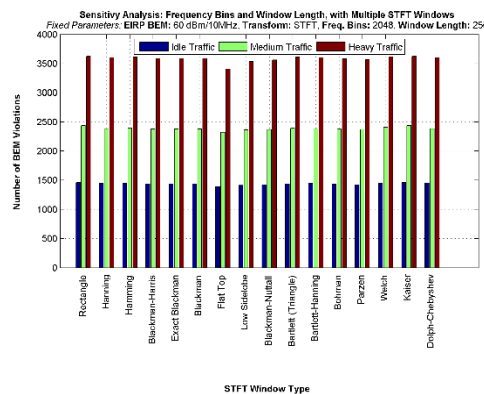
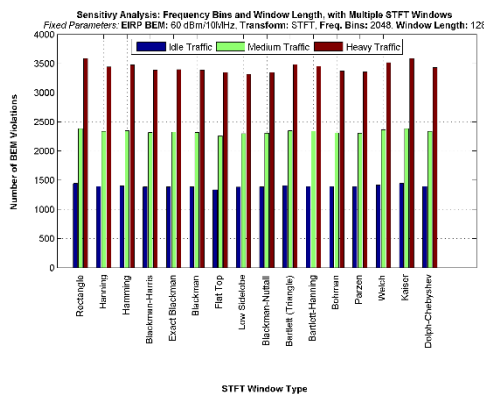
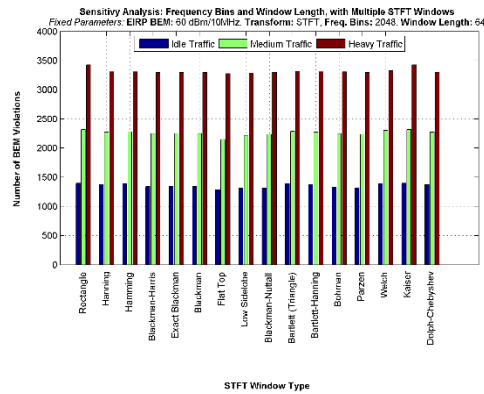
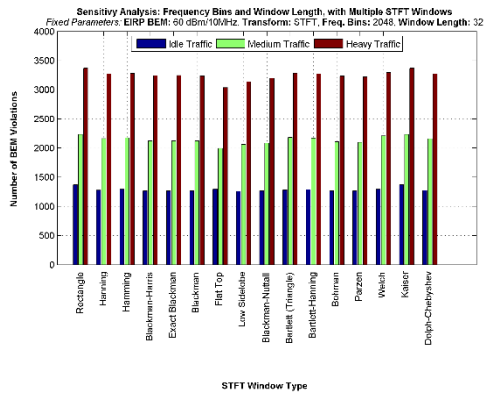


Frequency Bins: 512, Variable Window Length





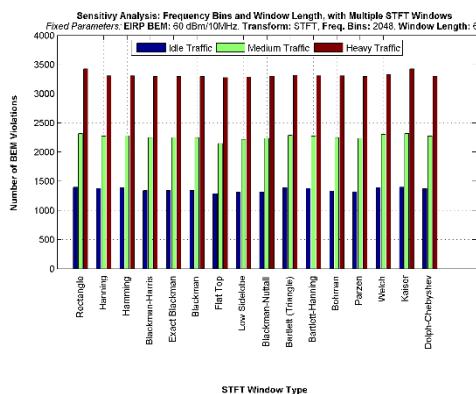
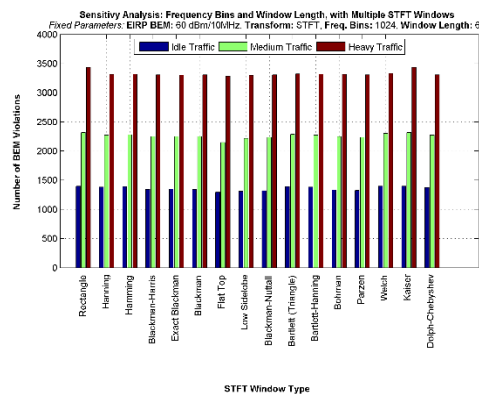
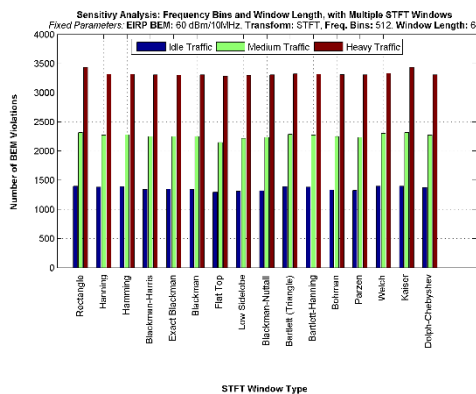
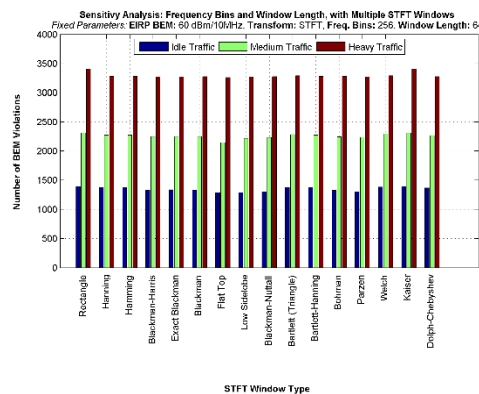
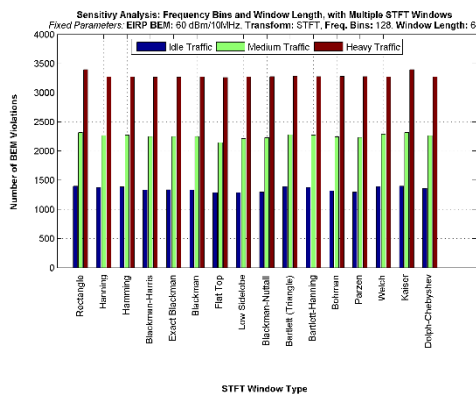
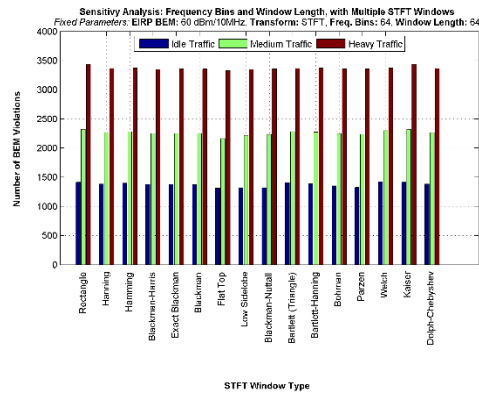
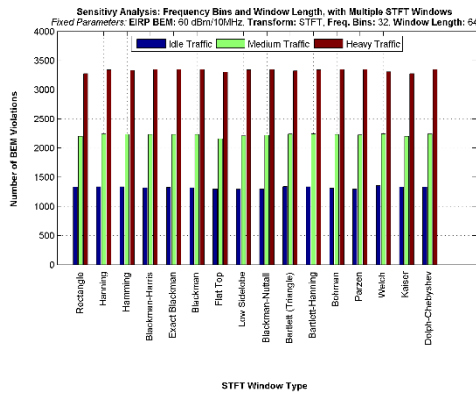
### Frequency Bins: 2048, Variable Window Length



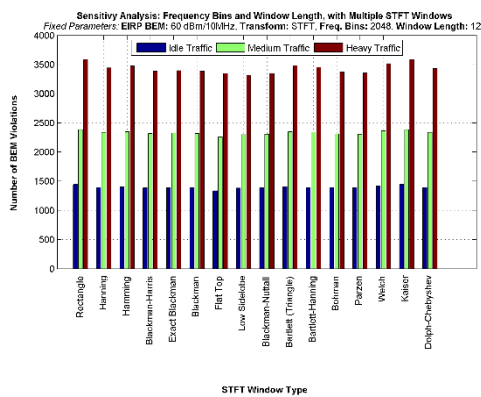
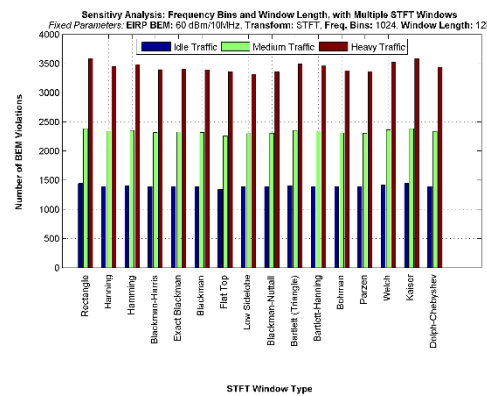
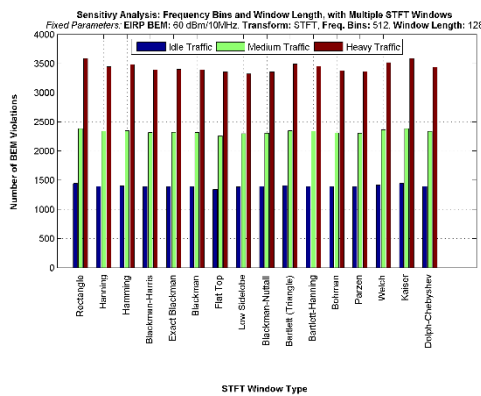
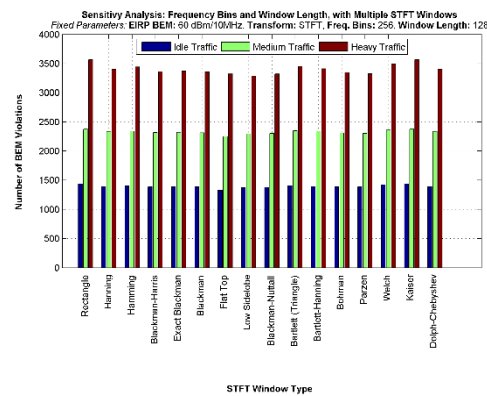
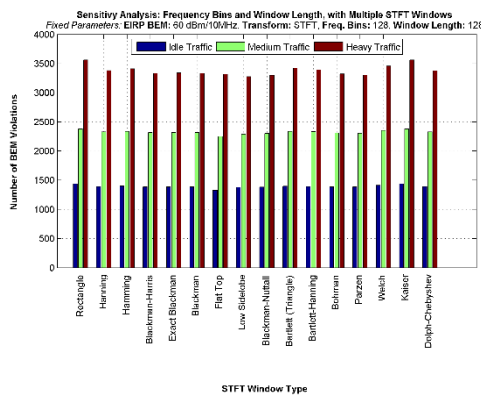
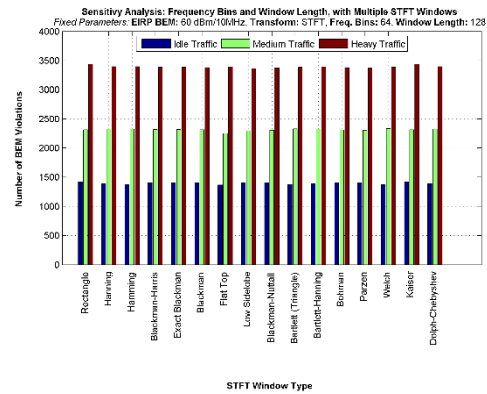
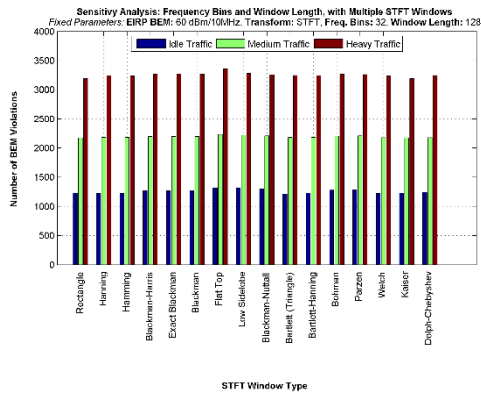




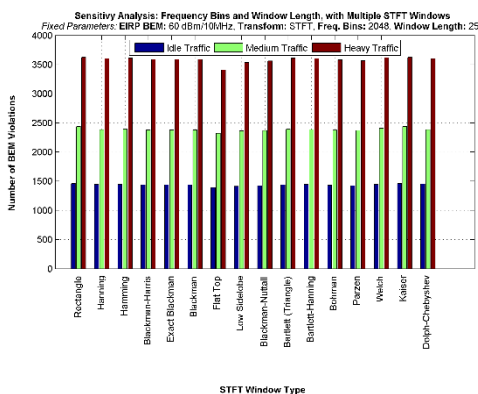
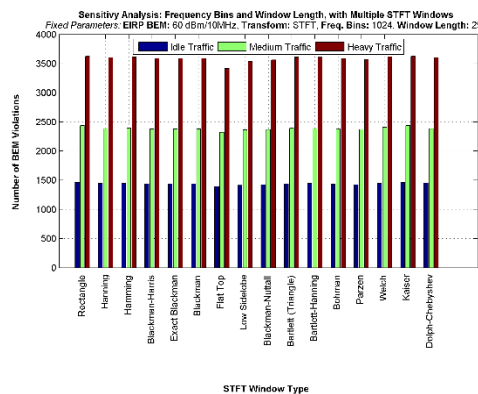
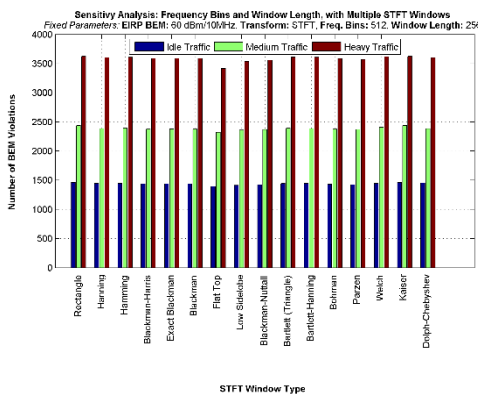
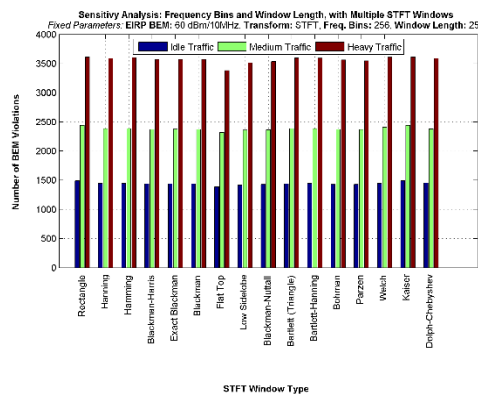
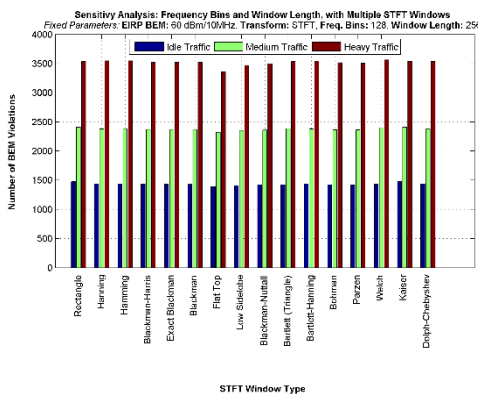
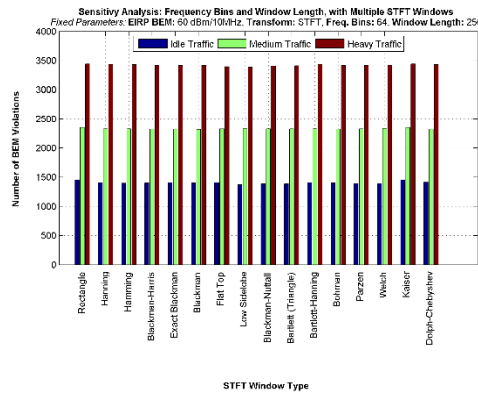
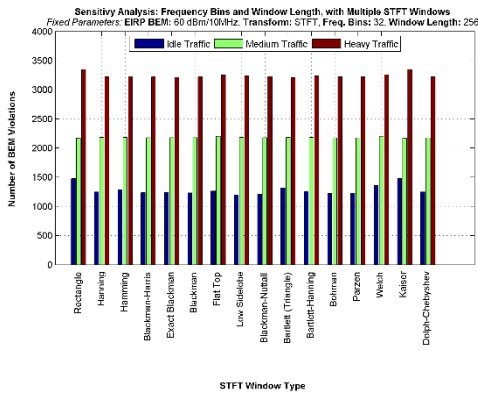
STFT Window Length: 64 samples, Variable Frequency Bins



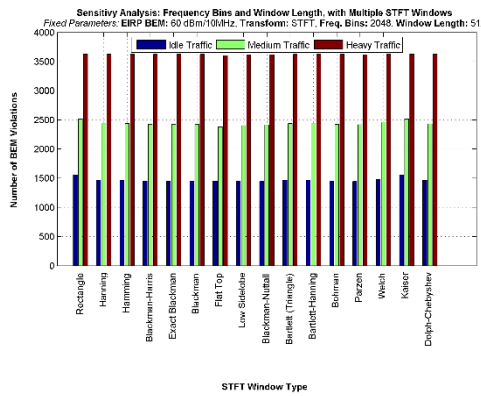
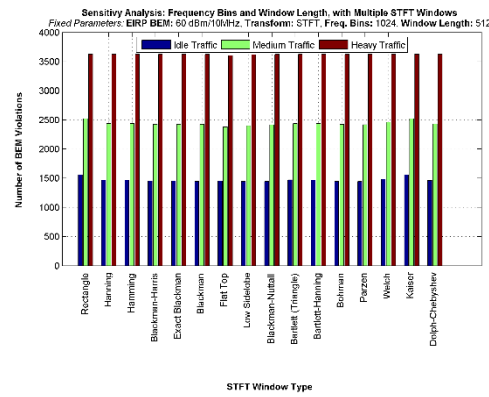
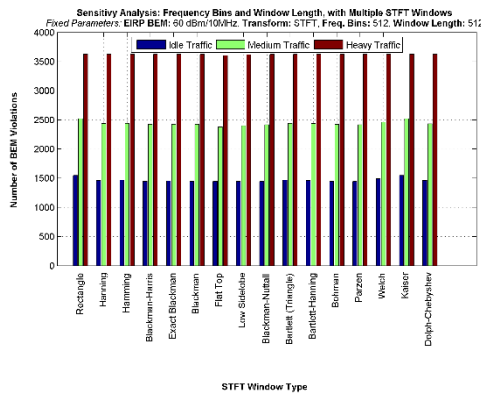
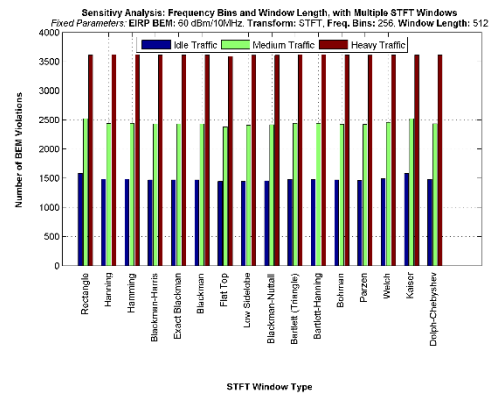
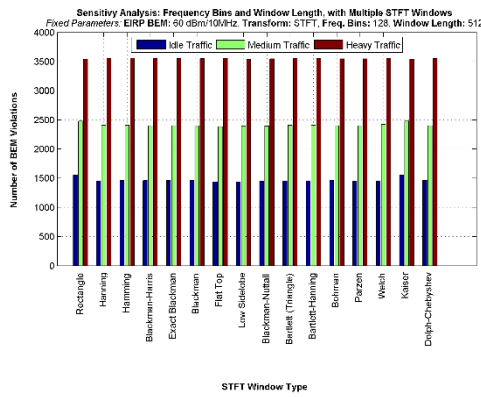
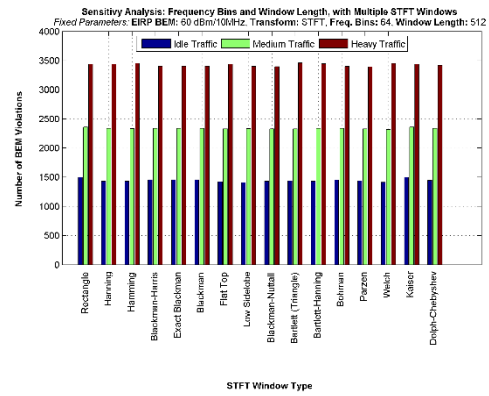
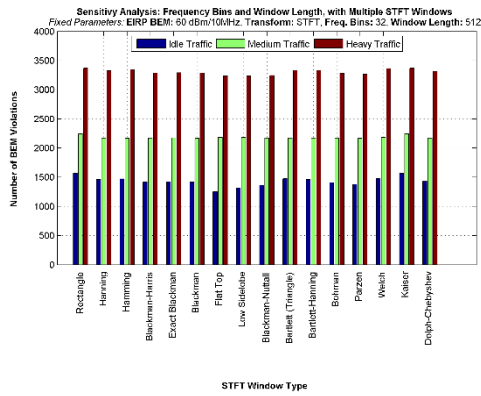
### STFT Window Length: 128 samples, Variable Frequency Bins



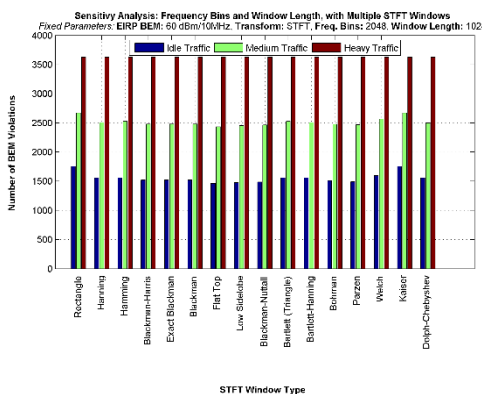
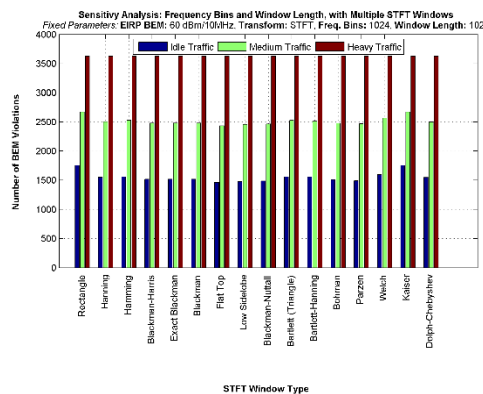
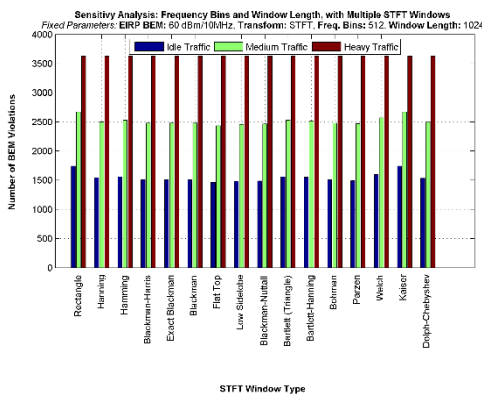
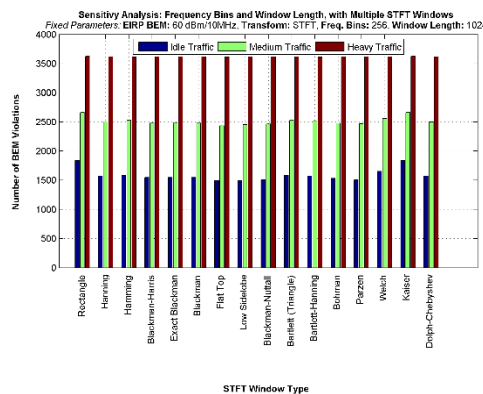
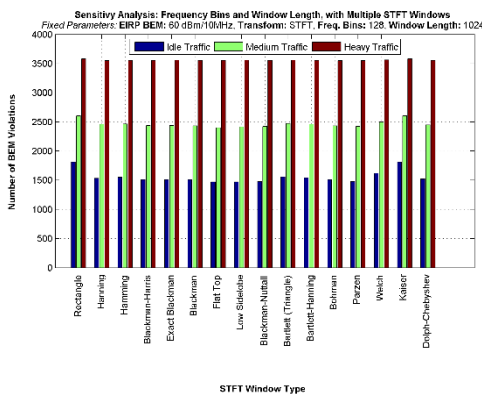
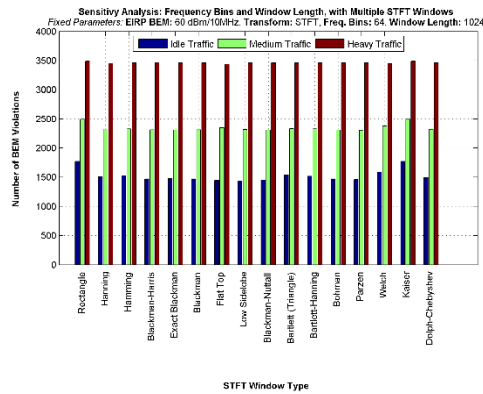
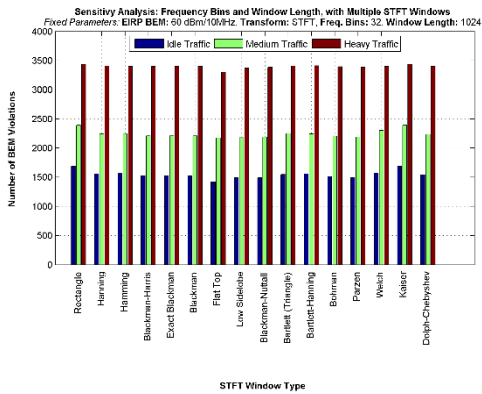
STFT Window Length: 256 samples, Variable Frequency Bins



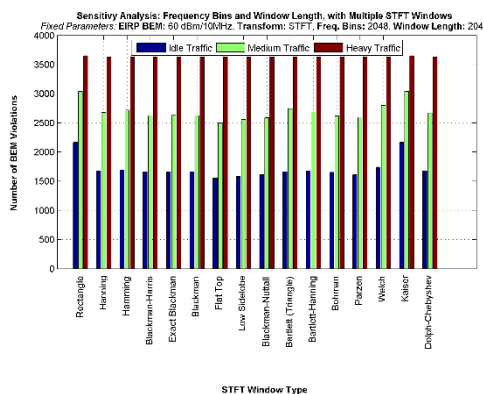
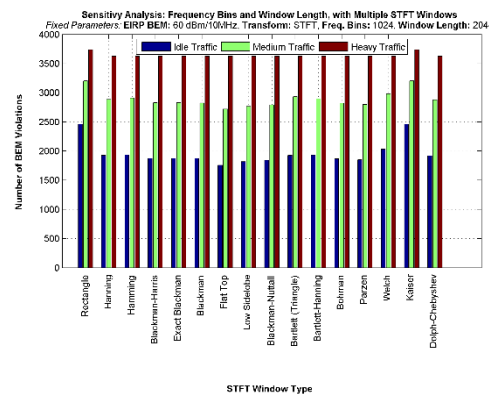
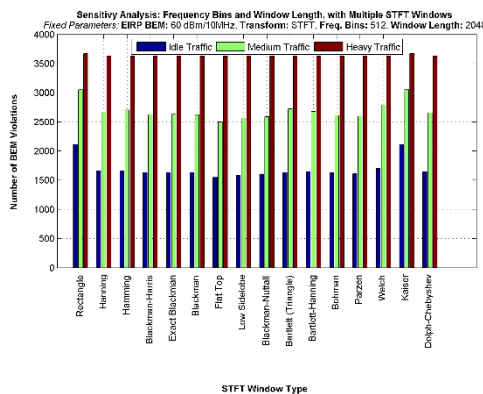
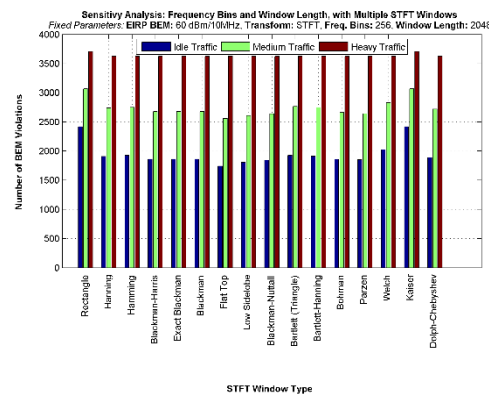
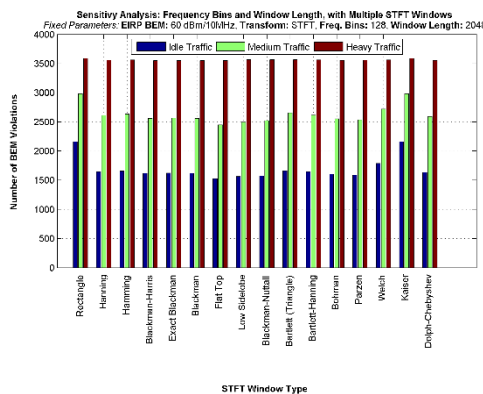
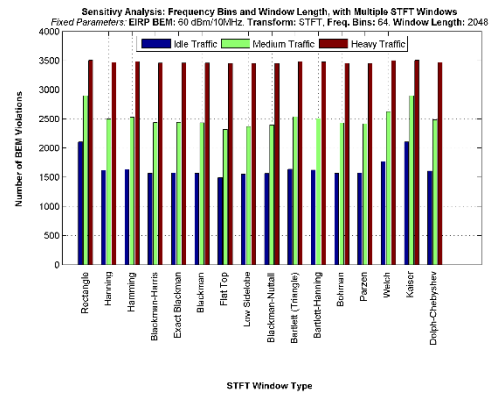
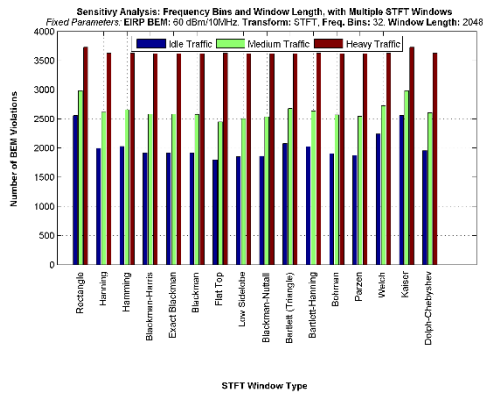
### STFT Window Length: 512 samples, Variable Frequency Bins



STFT Window Length: 1024 samples, Variable Frequency Bins



STFT Window Length: 2048 samples, Variable Frequency Bins



PAGE INTENTIONALLY LEFT BLANK